Calhoun: The NPS Institutional Archive

DSpace Repository

Theses and Dissertations | 1. Thesis and Dissertation Collection, all items

1957

Quasi-optimization of relay servomechanisms.

McDonald, Carlton Angus Klump

Monterey, California: Naval Postgraduate School, 1957.

http://hdl.handle.net/10945/14540

QUASI-OPTIMIZATION OF RELAY SERVOMECHANISMS

Carlton Angus Klump McDonald

72

QUASI-OPTIMIZATION

OF

RELAY SERVOMECHANISMS

* * * * * *

Carlton A. K. McDonald

QUASI-OPTIMIZATION

OF RELAY SERVOMECHANISMS

by

Carlton Angus Klump McDonald

Lieutenant, United States Navy

Submitted in partial fulfillment
of the requirements
for the degree of
MASTER OF SCIENCE
IN
ELECTRICAL ENGINEERING

United States Naval Postgraduate School
Monterey, California

1957

This work is accepted as fulfilling

the thesis requirements for the degree of

MASTER OF SCIENCE

IN

ELECTRICAL ENGINEERING

from the

United States Naval Postgraduate School

ABSTRACT

The DC shunt motor relay servomechanism offers a great deal of promise from the standpoint of a fast, inexpensive, accurate control system. The author has endeavored to develop means of improving the response characteristics of this type of control system. From investigations conducted at the Naval Postgraduate School, Monterey, California, it is the opinion of the author that a linear switching criteria, produced by a combination of error and error rate feedback, would prove highly desirable from the standpoint of cost, weight, and simplicity of design. If derivative feedback were to be combined with discontinuous damping in the dead zone provided by dynamic braking, it is indeed possible that a high degree of static accuracy may result. Investigations tend to show that the static accuracy, using this system, is dependent upon (1) the gear ratio between the motor and the error detector (2) the ratio of armature inductance to armature resistance of the motor (3) the ratio of coulomb friction to inertia of the motor load combination and (4) the delay time of the relay.

Preliminary calculations and computer studies on the use of an inductance and a resistance in a circuit in parallel with the motor armature tend to show that this form of dynamic braking would be of considerable value in improving the characteristics. Indeed, it is possible that this type of system would produce response characteristics that would be comparable to if not surpass the optimum relay servomechanism.

TABLE OF CONTENTS

LIST OF ILLUSTRATIONS

A — $\ddot{\Theta}_o$

A' — 1

a — $-\mathcal{f}\omega - \sqrt{\mathcal{f}^2\omega^2 - \omega^2}$

a' — $-\mathcal{f}\omega' - \sqrt{\mathcal{f}'^2\omega'^2 - \omega'^2}$

B — $\dfrac{RJ\ddot{\Theta}_o + LK_\tau \dot{\iota}_o}{LJ}$

B' — $f/_J$

b — $-\mathcal{f}\omega + \sqrt{\mathcal{f}^2\omega^2 - \omega^2}$

b' — $-\mathcal{f}'\omega' + \sqrt{\mathcal{f}'^2\omega'^2 - \omega'^2}$

C — Coulomb friction referred to output

$C_1, C_2,$ — Constants

D — $\dfrac{\vee K_\tau}{LJ}$

DC — Direct current

$E_R/_2$ — Energy loss at the relay at the instant of switching

e_1 — Voltage at which relay pulls in

e_2 — Voltage at which relay drops out

F — Figure of merit for the relay

G — $\dfrac{1}{\omega'^2}$

H — $\dfrac{2\mathcal{f}'\omega'}{\omega'^4}$

HP — Horsepower

I	LaPlace Transform of i
i	Instantaneous value of the current through the motor after relay drop-out
i_o	Value of the current through the motor at the instant of relay drop-out
i_1	Instantaneous value of current through the motor before relay drop-out
i_2	Instantaneous value of current through the braking circuit before relay drop-out
$i_{(\infty)}, i_{(ss)}$	Steady state value of current
J	System inertia referred to the output
K_1, K_2, K_3, K_4, K_4'	Constants
K_t	Motor torque constant
K_v	Motor electromotive force constant
k_e	$\dfrac{\dot{i}_o}{\dot{\theta}_o}$
k_m	$\dfrac{J}{K_t}$
L_a	Inductance of motor armature
L_b	Inductance in the braking circuit
L	$L_a + L_b$
M	Total output shaft rotation from point of origin until the relay servo has stopped
N	$\dfrac{d\ddot{\theta}}{d\dot{\theta}}$

P $4\gamma'^2\omega'^2 - \omega'^2$

P $\dfrac{\tau_{m2}}{\tau_m}$

Q $\dfrac{2f'\omega'}{\omega'^4}$

R_a Motor armature resistance

R_b Resistance of the braking circuit

R $R_a + R_b$

S Output shaft rotation during the delay time of the relay

T_b System torque

t Time

t_d Delay time of the relay

U $X + S$

V Voltage applied the d-c motor in the relay servo

X Output shaft rotation from point of reference until switching should theoretically take place

x $\dfrac{R_b}{R_a}$

α $\dfrac{B}{\omega^2}$ output shaft rotation from point of actual relay drop-out until system is at rest

α' $\dfrac{B'}{\omega'^2}$

γ $-\dfrac{B}{\omega^2}$

γ' $-\dfrac{B'}{\omega'^2}$

φ, E Error $\theta_R - \theta_c$

Θ, Θ_c — Position of output shaft

Θ_R — Position of command shaft

$\dot{\Theta}_o$ — Time rate of change of output shaft at instant of relay drop-out

$\Theta_{(\infty)} \Theta_{(ss)}$ — Steady state value of Θ

$\textcircled{H}$ — LaPlace Transform of Θ

ω — (math) $\sqrt{\dfrac{fR + K_v K_\tau}{JL}}$

ω — Measure of ramp input in radian/sec (exp)

ω' — $\sqrt{\dfrac{fR_a + K_v K_t}{JL}}$

$\mathcal{S}$ — $\dfrac{Lf - RJ}{2\sqrt{JL(fR + K_v K_c)}}$

$\mathcal{S}'$ — $\dfrac{Lf + R_a J}{2\sqrt{JL(fR_a + K_v K_t)}}$

δ — $\dfrac{A\omega^2 - 2BJ\omega}{\omega^2}$

δ' — $\dfrac{A'\omega'^2 - 2B'\mathcal{S}'\omega'}{\omega'^2}$

τ_{e_1} — $\dfrac{L_a}{R_a}$

τ_{e_2} — $\dfrac{L_b}{R_b}$

τ_m — $\dfrac{R_a J}{K_v K_t}$

τ_m' — $\dfrac{RJ}{K_v K_t}$

$$\tau_e' \qquad \frac{L_a + L_b}{R_a + R_o}$$

$$\tau_{ma} \qquad \text{Actual mechanical speed time constant}$$

$$(\; ^\circ \;) \qquad \frac{d}{dt} (\;) \qquad \qquad \text{first time derivative}$$

$$(\; ^{\circ \circ} \;) \qquad \frac{d^2}{dt^2} (\;) \qquad \qquad \text{second time derivative}$$

$$(\; ^{\circ \circ \circ} \;) \qquad \frac{d^3}{dt^3} (\;) \qquad \qquad \text{third time derivative}$$

$$\cong \qquad \qquad \text{approximately equal to}$$

CHAPTER I

INTRODUCTION

The relay servomechanism is an automatic control device that has tremendous possibilities. It is compact and relatively inexpensive, but to date there have been problems associated with it of stability, static accuracy, and speed of response. This paper is designed to outline some methods which may be adopted to improve its overall characteristics.

Chapter II presents a historical review of some of the basic concepts.

Chapter III is devoted to an investigation of the static accuracy of a relay servo in response to a step input using discontinuous damping in the dead zone. The nature of the damping is dynamic braking by means of resistances, and the servomotor was of a 1 HP variety.

Chapter IV outlines a detailed mathematical analysis of the system response to a step input with discontinuous damping incorporated in the system.

Chapter V presents an analysis of the relay servomechanism characteristics in response to a ramp input.

Chapter VI outlines the results obtained from an investigation of a servo system using a 1/125 HP motor.

Chapter VII affords a comparison of the transient response to a step input for a relay servo using optimum and quasi-optimum switching.

Chapter VIII includes a complete analysis of a relay servomechanism response to a step input, when discontinuous damping in the dead zone is supplied by an energy storage device.

1

HISTORICAL REVIEW

The relay servomechanism is essentially a means of automatic control wherein some device, similar in nature to a relay, is used to apply a large corrective signal to the servo system in response to an error signal. The system operates basically on an on-off basis. In other words, if the error signal is large enough to actuate the relay, full voltage will be applied to the servomotor to correct the error. The relay, in this sense, is a power amplifying device, which supplies large amounts of power to the system in response to a relatively small signal from the error detector.

Harris [1], McDonald [2], and Hopkin [3] have proposed an optimum relay servo having a very small dead zone. However, it is to be noted that the switching criteria, or locus of points of relay reversal, must be a curved line, and that it is assumed that the relay will operate instantaneously. These two considerations, when incorporated into an actual operating servo system, would add considerably to the complexity and cost. Therefore, the relay servomechanism in this case would tend to lose some of its inherent advantages. This paper does not include a consideration of the so-called optimum relay servo, except that in iso-lated instances it is referred to for comparison purposes.

One of the fundamentals of this consideration of relay servos is that the switching criteria shall be a straight line. This may be readily accomplished by making the signal to the relay a constant times the error and another constant times the error rate. Both constants may take on any value from zero to plus or minus infinity. A straight line

switching criteria is relatively simple to incorporate into an actual servomechanism, and inasmuch as it is possible to control the slope of the switching lines by adjusting the gain of the error rate signal relative to the error signal (or vice versa), the slope of the switching lines may be adjusted to any desired value. As has been explained previously, when the error signal is large enough, the relay closes and full voltage is applied to the servomotor. In order to obtain a short time of response and, in general, use the relay servo to best advantage, a major portion of the error (when a step input is applied to the system) should be corrected by the time the relay opens. If the initial error is appreciable, the servomotor will probably have obtained a considerable velocity by this time. It is at this point that certain problems arise which must be solved in order to realize the full potentialities of the relay servo.

Since the servomotor has a considerable amount of kinetic energy associated with the armature at the instant of relay opening or relay drop-out, if no damping forces were present the system would tend to coast at constant velocity until finally the error would be great enough to cause the relay to pull-in in the opposite direction. It is because of this that the concept of discontinuous damping was originated. The idea is to cause damping to exist while the relay is open, but not during the time that the relay is closed and power is being supplied to the system. If damping forces were to exist at all times, one of the real advantages of the relay servo would be lost, that of maximum corrective action during periods of relay closure. However, damping in the dead zone will have the effect of dissipating or countering the rotational kinetic energy of the

3

motor armature and load inertia, thereby causing deceleration and possi-
bly bringing the motor to a dead stop quickly and without oscillations.

It is reasonably well-known that a typical practical relay would be
expected to have characteristics shown in Figure 1.
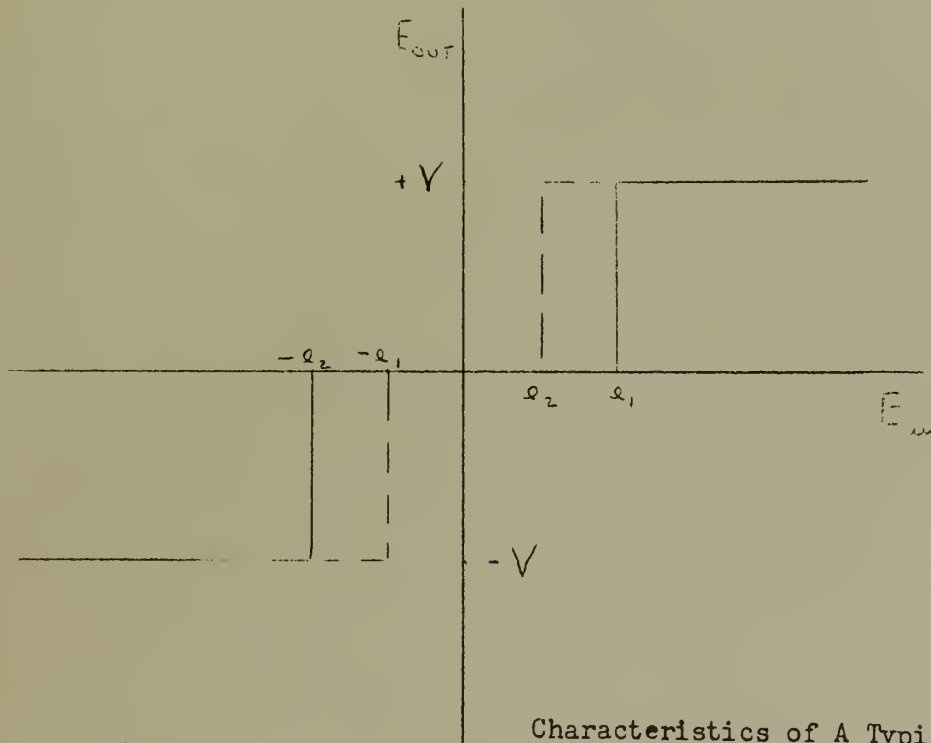
Characteristics of A Typical Relay

Figure 1

The relay would close, or pull-in at e_1, and the input voltage could
decrease to e_2 before the relay would drop out. In general, the relay
would display identical characteristics in both the forward and reverse
directions. If the relay was used in a relay servomechanism with the
error signal being the sole input to the relay, the dividing lines on
the phase plane would resemble those shown in Figure 2.
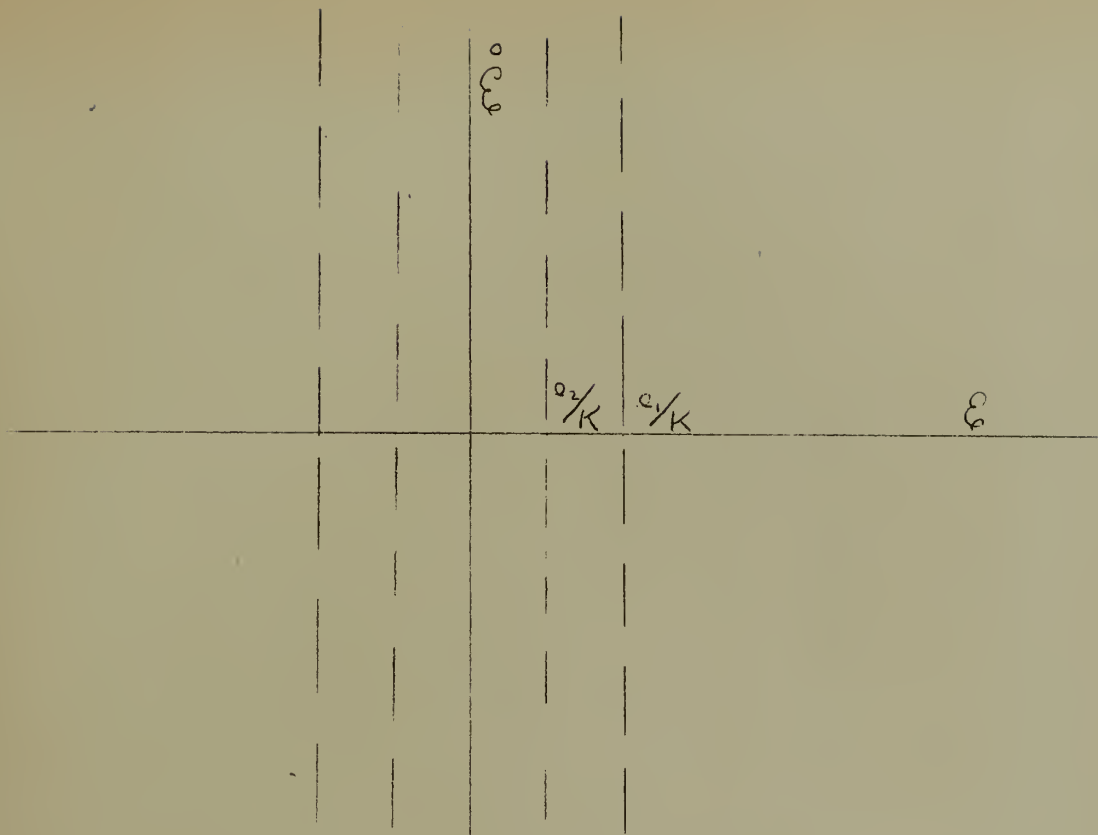
Dividing Lines of a Relay Servo on a Phase Plane Plot

Figure 2

For the conditions shown on Figure 2 the equations of the dividing
lines are $\mathcal{E} = \pm \dfrac{e_1}{K}$ & $\mathcal{E} = \pm \dfrac{e_2}{K}$ where e_1 and e_2 are the pull-in and
drop-out voltages of the particular relay and K_1 is the amplification
factor of the control system in volts per radian. Figure 2 shows that
as soon as the error reaches a certain magnitude the relay would pull-in.
As the servomotor drives the system towards correspondence, the relay would
stay closed until e_2 / K_1 was reached, at which point the relay would drop-
out. If a derivative signal was also applied to the relay in addition to
the error signal it would have the effect of rotating all switching lines
through the same angle about the intersection of the switching line with

5

the zero error rate line. This is shown in Figure 3. The amount of rota-
tion corresponds to the ratio of derivative signal to error signal.

Relay Servo Response to A Step
Input Showing No Damping (BC),
Some Damping (BD), and Optimum
Damping (BE) in the Dead Zone
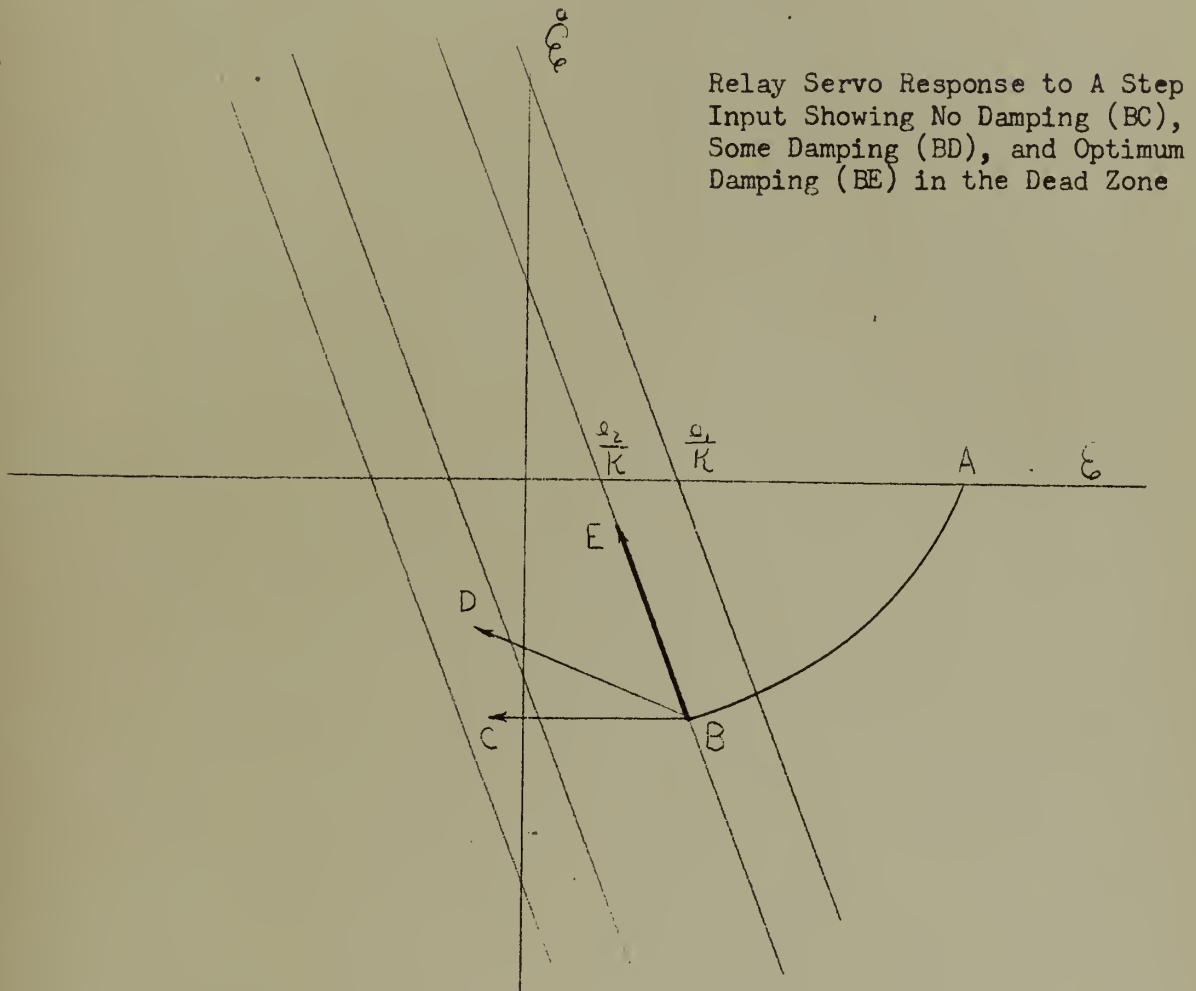
Figure 3

If, for some reason, a step input was applied to the system and this
step input could be represented by A in Figure 3, the relay would close
since $A > e_1 / K_1$ and the motor would accelerate to correct for the
error. The phase plane trajectory might typically be represented by AB.
Inasmuch as derivative feedback is incorporated into the system, the
relay would "anticipate" and drop out at B, since the error rate signal

6

subtracts from the error signal to give the resultant voltage at the relay of e_1.

If no damping was present in the system after the relay drops-out, the velocity of the motor would be expected to stay constant. Under these conditions, the phase plane trajectory in the dead zone would resemble BC. If a finite but arbitrary amount of damping is added to the system, the phase plane trajectory would logically expect to resemble, say, BD. HARRIS[*] has shown that if <u>discontinuous damping</u> added in the dead zone is (1) such as to produce a straight line for the dead zone trajectory and if (a) both the derivative feedback and the damping are correctly adjusted, the dead zone trajectory will be parallel to and super-imposed upon the drop-out switching line as in Figure 3, curve BE.

This is highly desirable, because, as shown in Figure 4, the dead zone width may be diminished by increasing the overall gain.
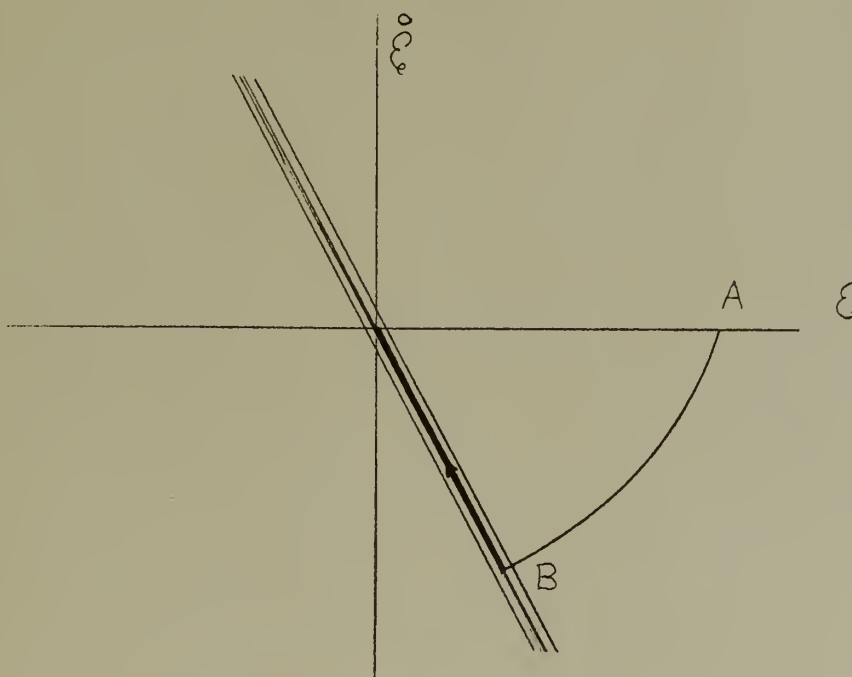
Figure 4.   Relay Servo Response to A Step Input
            Input Showing Optimum Discontinuous
            Damping

7

This greatly increases the static accuracy. In addition since the added damping is discontinuous, the time of response is short. The system is stable and no oscillations occur.

In the investigation of the relay servo characteristics when derivative feedback is incorporated into the control system and discontinuous damping is incorporated into the motor system, two basic ideas for discontinuous damping are analyzed. The first idea is to use a resistance across the motor armature in a relay servo that employs a DC Shunt Motor. For a sufficiently well-regulated power supply this has no effect on the overall characteristics of the relay servo system when the relay is closed, but after the relay opens the resistance provides for dissipation of the rotational kinetic energy of the motor armature. The dead zone trajectory for resistance braking has been predicted by phase plane analysis. The derivation of the isocline equation is contained in appendix I. HARRIS[*] has shown that the phase plane trajectory is a straight line until $\frac{\dot{\theta}}{\dot{c}}$ becomes small, and that the C/J ratio is important in determining when the trajectory departs appreciably from a straight line.

The second basic idea for discontinuous damping is to use an energy storage device across the terminals of the motor armature. For the relay servo that uses a DC shunt motor an ideal energy storage device is an inductance coil.

CHAPTER III

AN INVESTIGATION OF THE STATIC ACCURACY OF A RELAY SERVO USING DERIVATIVE FEEDBACK AND DISCONTINUOUS DAMPING

In Appendix 1, it is shown that the isocline equation for the phase plane analysis of the dead zone trajectory of a relay servo using a DC Shunt motor and discontinuous damping by means of a braking resistance is:

$$\frac{d\dot{\varepsilon}}{d\varepsilon} = -\frac{c/J}{\dot{\varepsilon}} - \frac{K_t K_v}{J(R_a + R_b)} \qquad (1)$$

provided that L_a and f are considered negligible.

If N is equal to $\frac{d\dot{\varepsilon}}{d\varepsilon}$ where N is the slope of the trajectory at its intersection with any isocline, equation (1) may be written

$$N = -\frac{c/J}{\dot{\varepsilon}} - \frac{K_t K_v}{J(R_a + R_b)} \qquad (2)$$

The phase plane trajectory may now be constructed using the isoclines and the slope markers as shown in Figure 5.

Phase Plane Showing Isoclines, Slope Markers, and Dead Zone Trajectory

Figure 5

9
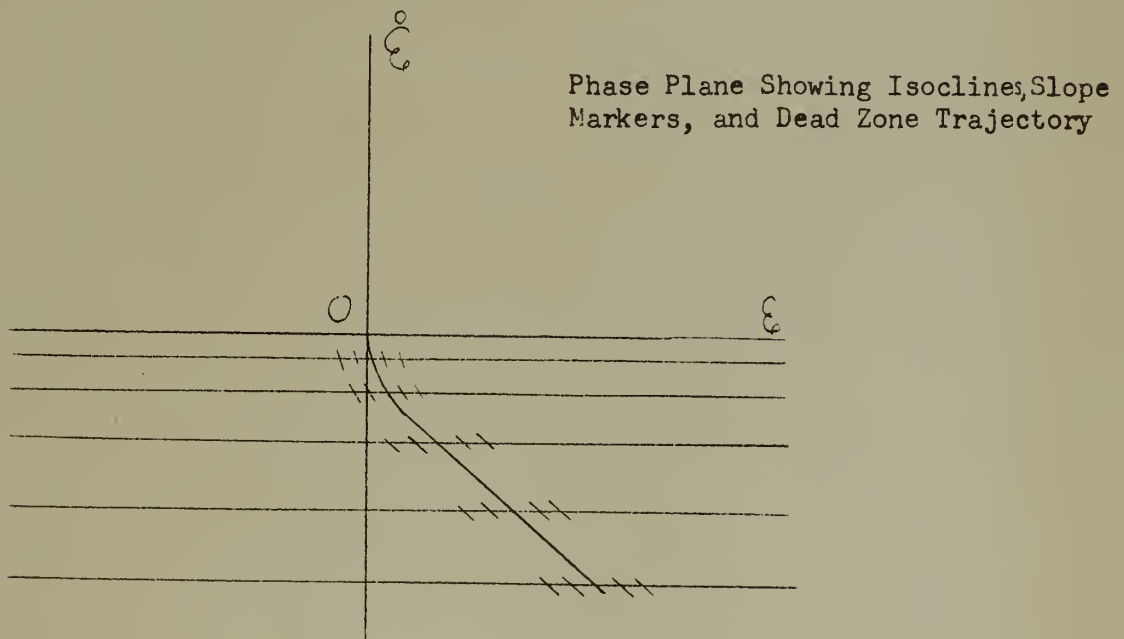
Once again considering equation (2) it is seen that in the case of a large motor which has a relatively small C/J ratio, the first term is important only when $\overset{\circ}{\underset{\circ}{\varepsilon}}$ is small. Therefore, the trajectory has a fixed negative slope in the dead zone except when $\overset{\circ}{\underset{\circ}{\varepsilon}}$ is very small, in which case the slope approaches infinity. It is seen that decreasing R_b increases the fixed negative slope and therefore the change in slope when $\overset{\circ}{\underset{\circ}{\varepsilon}}$ becomes small is less noticeable.

Accordingly, it was decided to use a 1 HP motor and a braking resistor of the same order of magnitude as the armature resistance. The original plan was to start with a dead zone of ten degrees and adjust the braking resistor to obtain a trajectory in the dead zone parallel to the dividing lines. This theoretically would be the optimum amount of damping and the dead zone could then be made extremely small, as shown in Figure 4, Chapter II. However, it was noted that as the step input signal was made small and saturation velocity was not reached during the period when the motor was being driven, the end of the dead zone trajectory tended to move away from the intersection of the drop-out line and the zero error rate line until finally the trajectory completely crossed the dead zone and oscillations occurred. This result is shown in Figure 6 as curves B, B', and B''

Phase Plane Plot of Relay Servo Responses to A Step Input
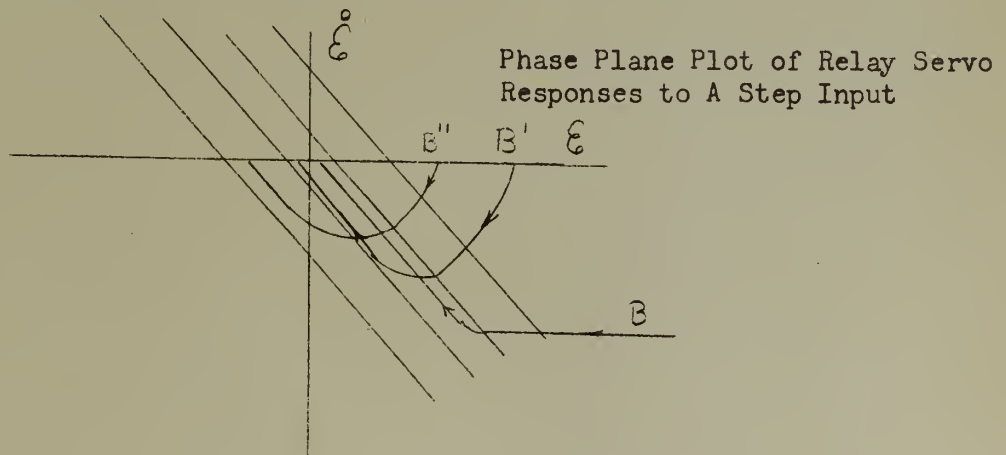
Figure 6.

Accordingly it was decided to
increase the dynamic braking in an
attempt to eliminate this over-
shooting effect. The new plan was
to increase the braking effect (de-
crease the braking resistor) until
the system was deadbeat just inside
the pull-in line. This behavior would
be shown as curve a in Figure 7.

After some experimentation it
decided to decrease the braking re-
sistor to four ohms. Inasmuch as the
resistance of the motor armature was
7.9 ohms, it is seen that considerable
dynamic braking was to be used. As
a matter of fact the use of four ohms
as a braking resistor caused the
trajectory in the dead zone to be
practically straight, since the
effect of coulomb friction was negli-
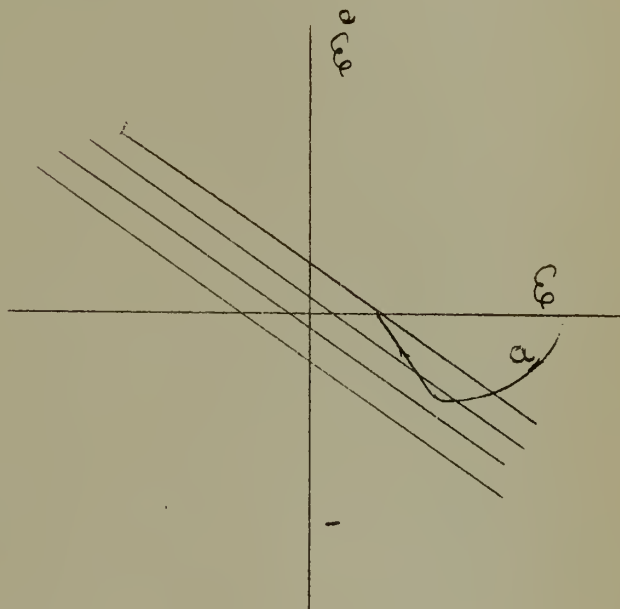
Relay Servo Response to A Step Input

Figure 7

gible. The procedure was to keep the dead zone width fixed at ten degrees
and make runs using step inputs of 40, 35, 30, 25, 20, 15, 10, 8, and 6
degrees. The schematic diagram of the physical layout used is shown as
Figure 8, and the phase plane diagram is shown as Figure 9. As may be
seen from Figure 9, in all of the runs in which the velocity reached
saturation, the trajectories in the dead zone were similar and according
to prediction. However, with the 15, 10 and 8 degree step inputs

11

SCHEMATIC DIAGRAM

FIGURE 8

12

Phase Plane Trajectories for Various Sizes of
Step Inputs, a Dead Zone of 10°, and Greater-
than-optimum Damping in the Dead Zone

Figure 9

13
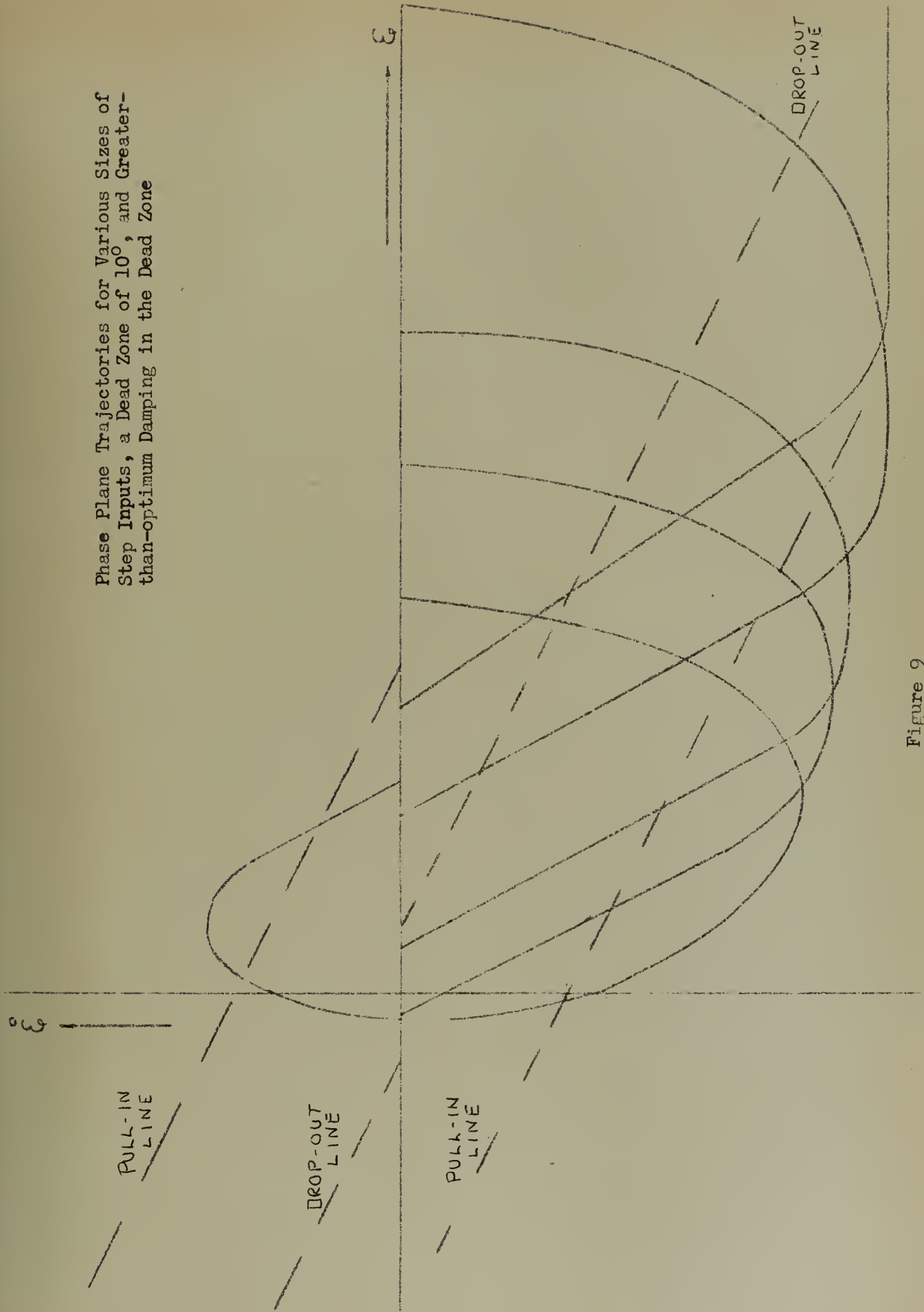
Phase Plane Trajectories for Large
and Small Step Inputs with a Four
Degree Dead Zone and Greater-than-
optimum Damping

Figure 10

14
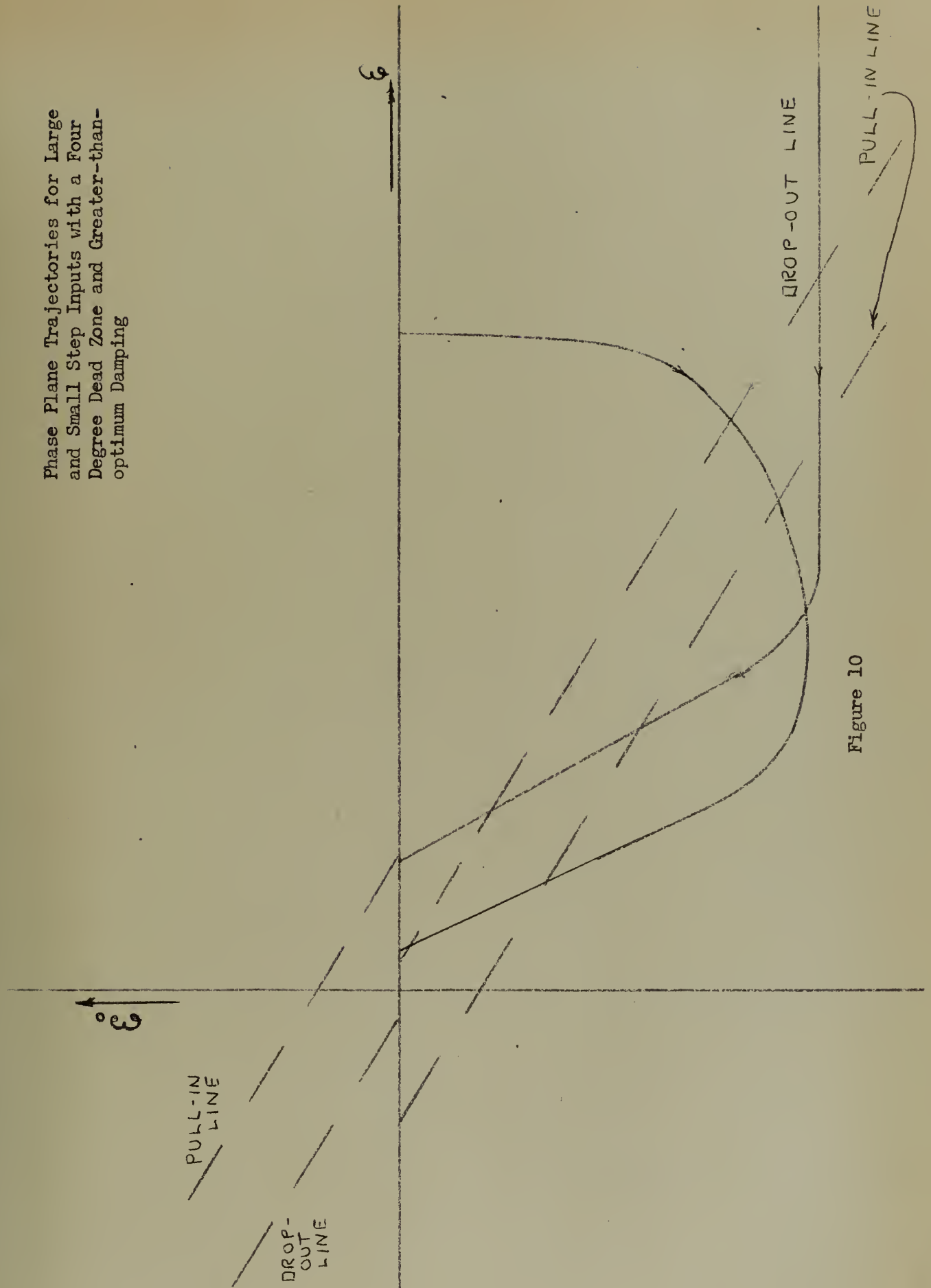
the rest point progressed across the phase plane to the left until finally with a 6 degree step input, the trajectory crossed the dead zone and the system went into oscillation.

As another interesting phenomenon, while the idealized dead zone trajectory predicts an instantaneous change in slope at the point of effective switching, notice that in the actual case there is a gradual curvature of the trajectory until finally it straightens out in the manner predicted by theory.

In order to obtain a better insight into the problem the dead zone was narrowed to four degrees. The results of this part of the procedure are shown in Figure 10. Again the trajectory of the run with a small step input went into oscillation whereas stable deadbeat performance had been obtained with a large step input.

A comparison of the two figures reveals another interesting item. The appearance of braking in the dead zone does not make itself known until after the drop-out line has been passed. Indeed, a comparison of the actual drop-out location with the expected drop-out point location indicates a time delay of about 0.048 seconds. Inasmuch as the physical design of the experimental device employed two relays in cascade, it is quite logical to attribute the time delay to the dead/time inherent in operation of the two relays. In order to show the existence of dead time more
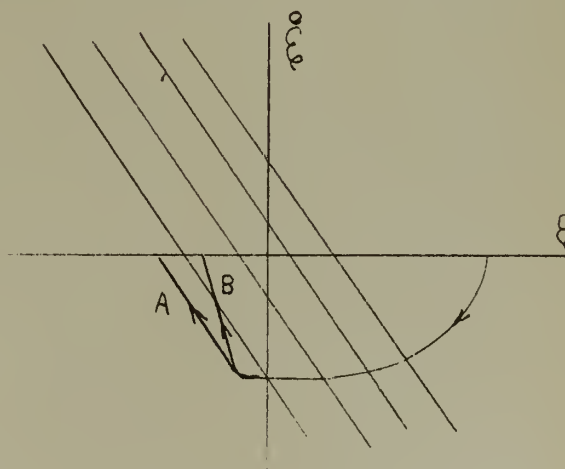
Figure 11. Relay Servo Response

concretely, it was decided to attempt to show what happened when the braking resistance was changed in the cases where the stability was marginal. As shown in Figure 11 the general idea was to obtain a trajectory just outside the more remote pull-in line as shown by curve A. Then if the resistance was decreased slightly, all other things being equal, the curve would be bent toward the vertical. Despite the fact that the trajectory crossed the pull-in line momentarily as shown by curve B, the system would deadbeat because the time delay would prevent operation of the relay during the short period that the trajectory was outside the pull-in line.

The first step was to obtain the dead zone trajectories for various values of R_b. These slopes are shown in Figure 12. As was expected, the smaller resistances are associated with the steeper slopes and for resistances of four and six ohms, the trajectory is essentially straight to the rest position. With higher values of resistance, however, the trajectory has a distinct change of slope when $\dot{x}$ becomes small, due to the effect of coulomb friction.

Having decided to use a resistance of ten ohms as a braking resistor, the settings of the various potentiometers, and the component and voltage magnitudes were calculated. The physical layout is shown schematically in Figure 13, and sample calculations are set forth in Appendix II. The slopes of the dividing lines were calculated to be parallel to the dead zone trajectory. By means of the potentiometer in the feedback path of the second amplifier, the dead zone width was decreased until the system went into oscillation. The phase plane trajectories were as shown in Figure 14. At this point the value of R_b was changed and the results were as predicted. Note that the ten ohm run is oscillatory, the nine ohm

16

Dead Zone Trajectories for Various
Values of Braking Resistance

a — R_b = 20
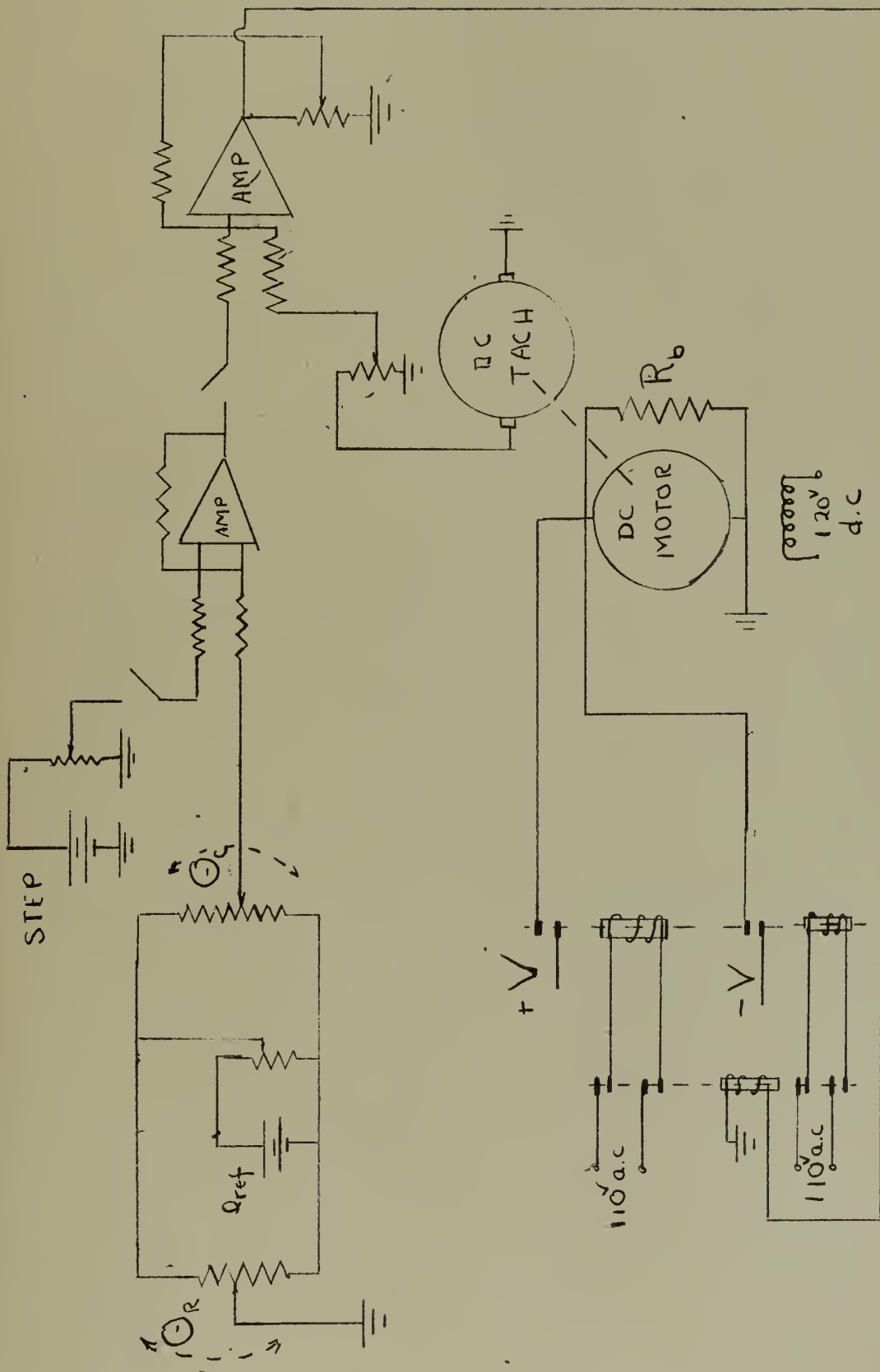
b — R_b = 10

c — R_b = 6

d — R_b = 4

Figure 12

SCHEMATIC DIAGRAM

FIGURE 13

18

Phase Plane Trajectories for Large Step Inputs and R_b "critical".

PULL-IN LINE

DROP-OUT LINE

DROP-OUT LINE

PULL-IN LINE

Run DEADBEAT

Run MARGINAL

Run OSCILLATORY

Run 61 $R_b = 8$

Run 62 $R_b = 9$

Run 63 $R_b = 10$

Figure 14

19
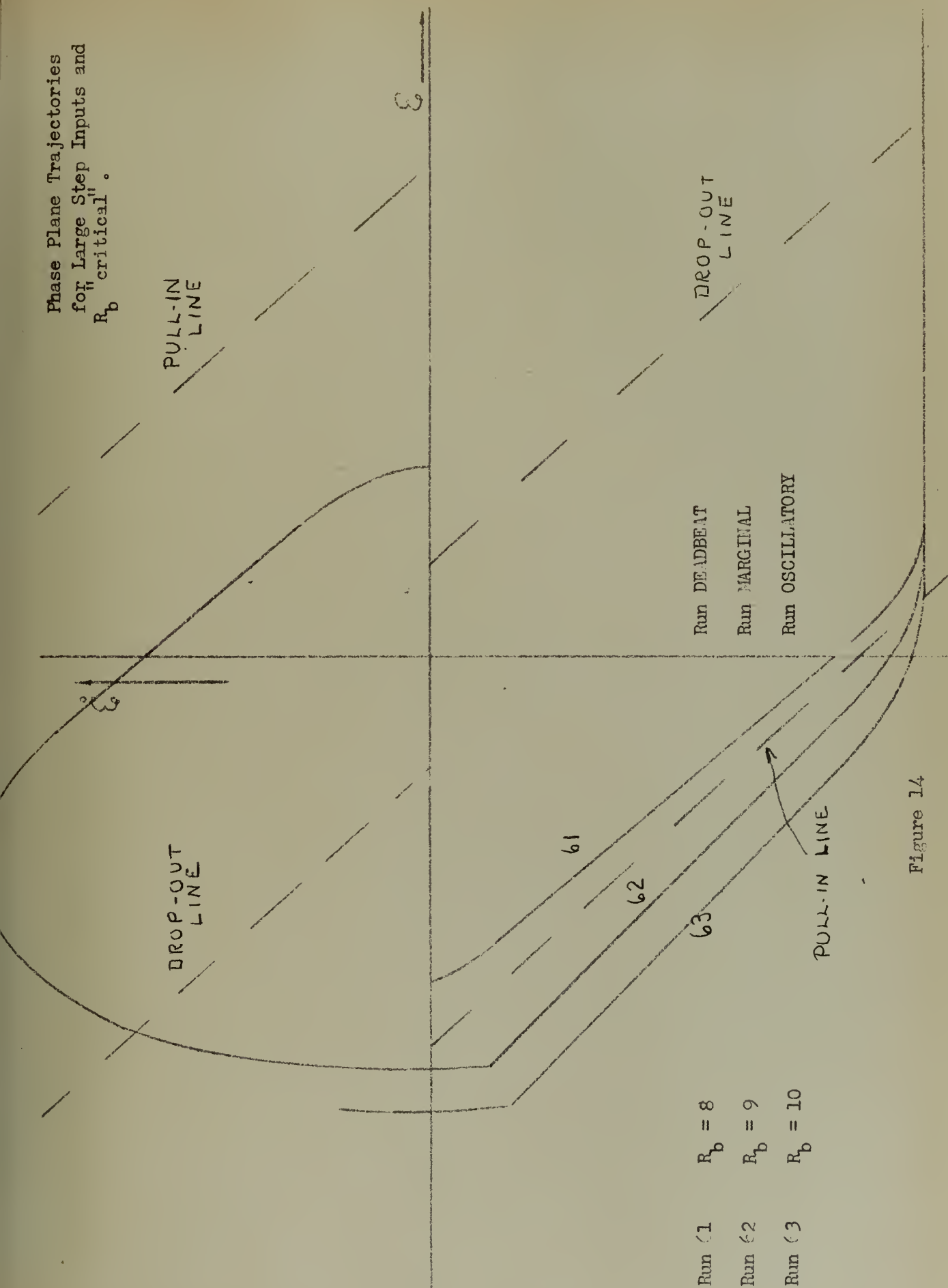
run deadbeats after a single oscillation, and the eight ohm run is dead-beat without oscillation.

In an effort to duplicate the general results, the dead zone was increased slightly as is shown in Figure 15. In this case the eight ohm run is deadbeat, the ten ohm run is marginal and the twelve ohm run is oscillatory.

During the latter runs no attempt was made to use step inputs that would be too small to effect velocity saturation. It was felt that this would have the effect of adding an additional unknown and would compli-cate the results.

While it is to be noted that in the preceding runs slight variances in the braking resistance caused completely different system behavior, the trajectories on the phase plane were quite similar. The runs that deadbeat had trajectories which had a sharper curvature in the transi-tion stage immediately after effective relay drop-out and therefore these runs never were in the region where the relay might be expected to pull-in.

In an effort to show the time delay associated with the relay more emphatically, it was decided to make runs with a dead zone much smaller and then drastically reduce the braking resistor in an effort to get dead-beat performance although the trajectory may actually have crossed the pull-in line for a short period of time. Accordingly, in runs 1, 2 and 3 the dead zone was narrowed, and braking resistances of ten, six, and two ohms were used. The phase plane diagrams for these runs are shown in Figure 16. The interesting part to be noted is that while the ten and six ohm runs were oscillatory, the two ohm run was deadbeat even though

Phase Plane Trajectories for Large Step Inputs and R_b "critical"

PULL-IN LINE

DROP-OUT LINE

DROP-OUT LINE

PULL-IN LINE

Run 64	$R_b = 8$	Run DEADBEAT
Run 65	$R_b = 10$	Run MARGINAL
Run 66	$R_b = 12$	Run OSCILLATORY

Figure 15

21
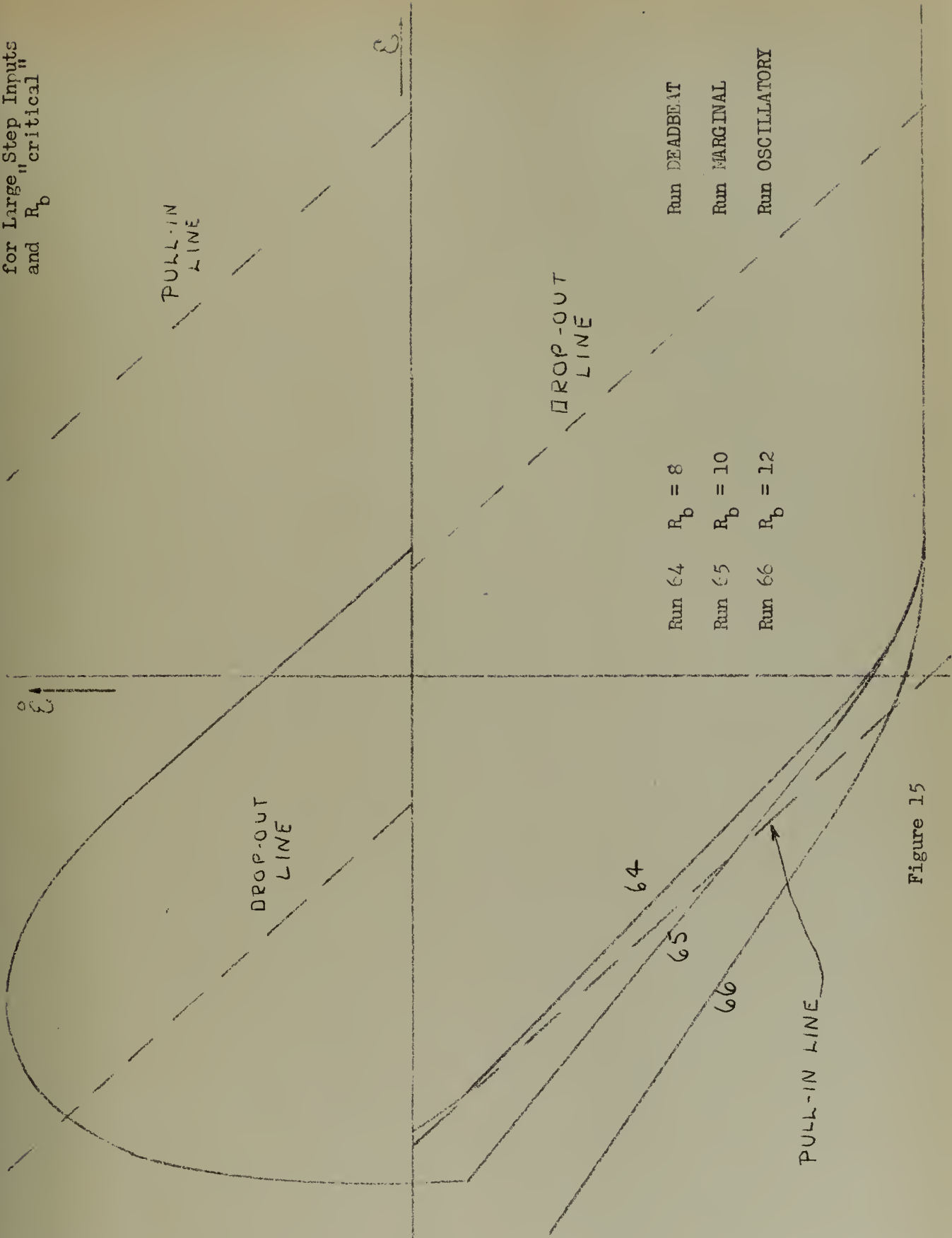
Phase Plane Trajectories for
Large Step Inputs and Various
Values of Braking Resistance

Figure 16

Run 1 R_b = 9   OSCILLATORY

Run 2 R_b = 6   MARGINAL

Run 3 R_b = 2   DEADBEAT
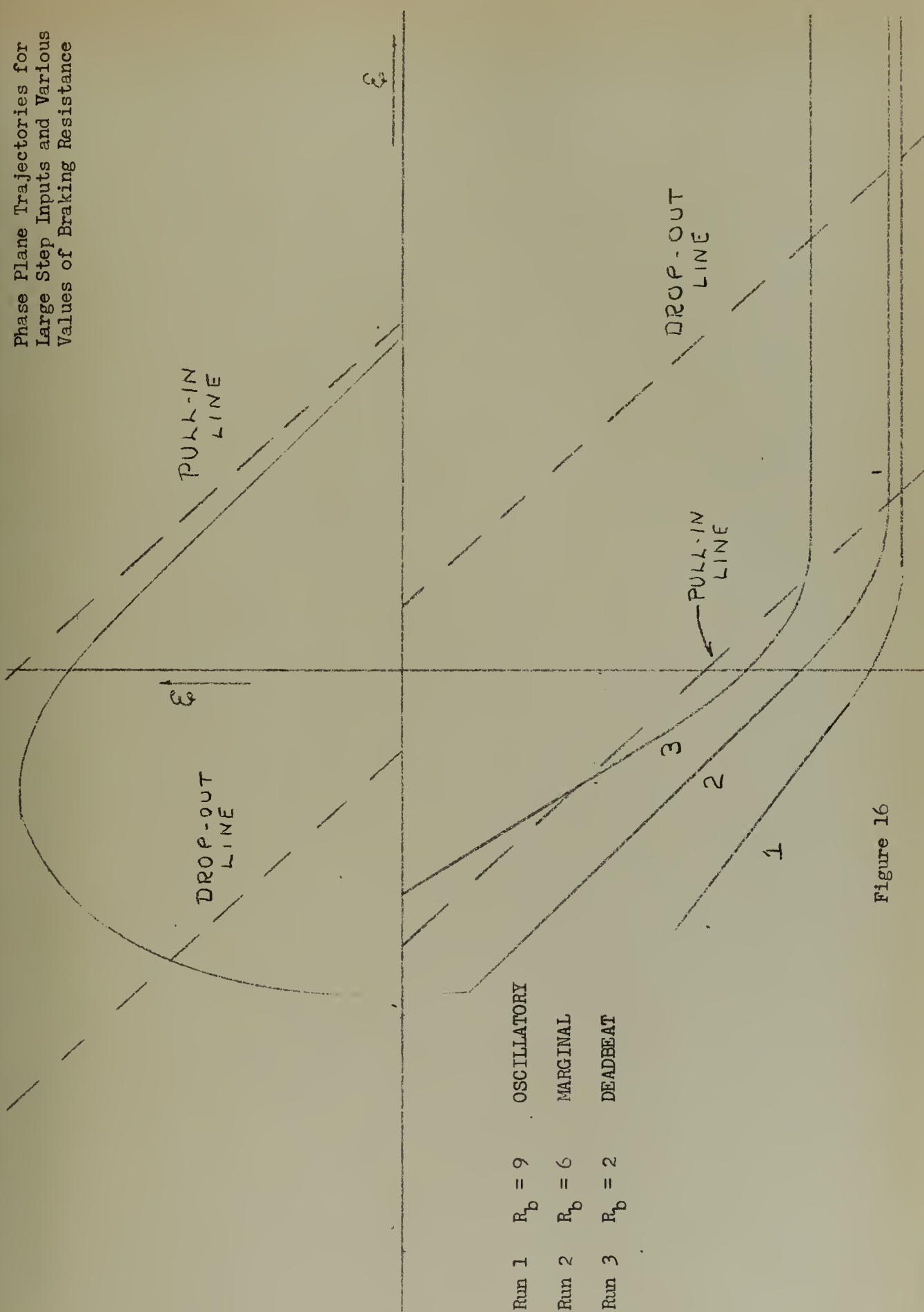
the trajectory actually crossed into the region where the relay might normally be expected to pull-in. This indicates that there is a time delay associated with the relay.

An illustration of the different trajectories in the dead zone caused by the size of the step input signal is shown in Figure 17. Notice the time delay associated with the relay and also that the run for a small step input is oscillatory while the run for a large step input deadbeats.

It is believed that the following conclusions are applicable:

(1) When the C/J ratio is small, the curvatures of the end of the trajectory in the dead zone can be eliminated for all practical purposes by making R_b small. The slope of the straight line portion of the trajectory increases with decreasing values of R_b. These conclusions fit the idealized phase plane equations perfectly.

(2) The dead time associated with the relay is quite disadvantageous because the dead zone must be quite large if dead beat performance for all sizes of signals is expected.

(3) With the use of a resistor only as a means of braking the dead zone trajectory is curved from the time the relay operates until the straight line portion is reached. This curvature depends upon the value of the braking resistance used. The curvature is sharper with lesser values of braking resistance.

Phase Plane Trajectories for Large and Small Steps and Optimum Damping

PULL-IN LINE

DROP-OUT LINE

PULL-IN LINE

DROP-OUT LINE

68

71

Run 68 R_b = 8.2   25° STEP DEADBEAT

Run 71 R_b = 8.2   10° STEP OSCILLATORY

Figure 17

24
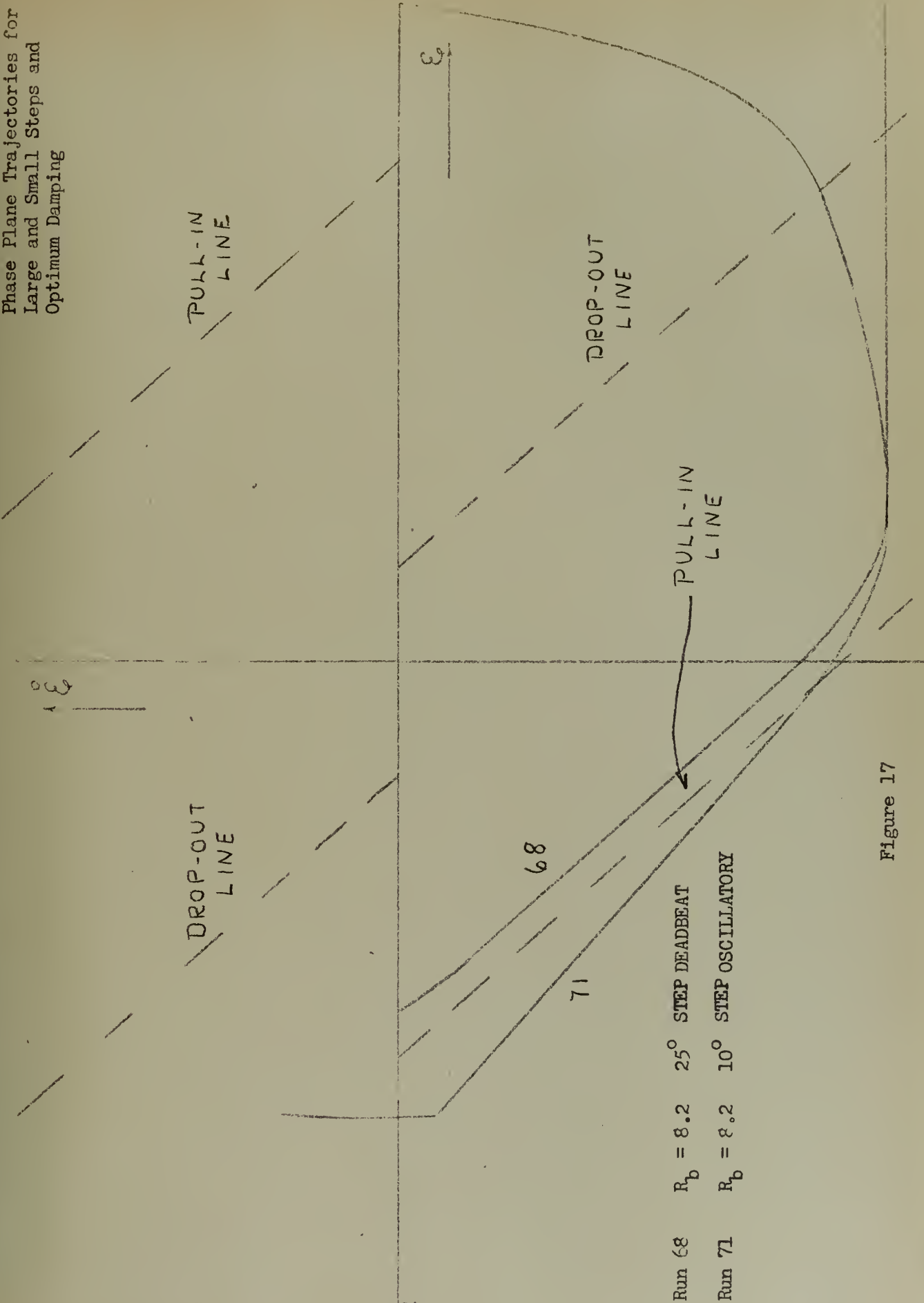
CHAPTER IV

MATHEMATIC ANALYSIS

In the previous chapter it was noted that the step input size seemed to effect the behavior of the dead zone trajectory. In order to explain this phenomenon the system is analyzed mathematically in this chapter, without resorting to some of the simplifying assumptions used in the previous chapters.

Accordingly it is proposed that the terms involving L and f be retained. The only fiction involved is that coulomb friction is assumed negligible. This of course is not entirely factual and at first glance it might appear that the complete analysis is worthless. However, it was shown in the previous chapter both mathematically and experimentally that the effect of coulomb friction was practically eliminated by making R_b small and using a 1HP motor. In addition the effect of coulomb friction is known qualitatively and therefore it is submitted that the following analysis is good for small values of R_b at the very least.

While the system is in the dead zone, the equations are as follows:

$$i(R_a + R_c) + L\frac{di}{dt} + K_v\frac{d\theta}{dt} = 0 \qquad (1)$$

$$- K_t i + J\frac{d^2\theta}{dt^2} + f\frac{d\theta}{dt} = 0 \qquad (2)$$

$$\text{Let } R_a + R_b = R$$

Let $\Theta = \Theta_0$ at $t = 0$

and $\dot{\Theta} = \dot{\Theta}_0$ at $t = 0$

and $i = i_0$ at $t = 0$

It is proposed that the analysis be made on a $\Theta - \ddot{\Theta}$ basis rather than on a $\dot{\varepsilon} - \ddot{\varepsilon}$ basis. It is further proposed that a conventional analysis on a time basis be made because of the complexities introduced when third order differential equations are depicted using the isocline techniques.

Using the LaPlace Transforms -

$$L\left[\rho I - i_0\right] + RI + K_v \rho \,(H) = 0 \qquad (3)$$

$$-K_t I + J\left(\rho^2 \,\Theta - \dot{\Theta}_0\right) + f\rho \,(H) = 0 \qquad (4)$$

$$I\left[\rho L + R\right] + K_v \rho \,(H) = L\, i_0 \qquad (5)$$

$$I\left[-K_t\right] + J\rho^2 \,(H) + f\rho \,(H) = J\, \ddot{\Theta}_0 \qquad (6)$$

From this it can be easily shown that -

$$\textcircled{H} = \dfrac{\wp\,\overset{\circ}{\Theta}_{o} + \dfrac{RJ\overset{\circ}{\Theta}_{o} + LK_{e}C_{o}}{LJ}}{\wp\left[\wp^{2} + \wp\left[\dfrac{Lf + RJ}{JL}\right] + \left[\dfrac{fR + K_{v}K_{e}}{JL}\right]\right]} \qquad (7)$$

Let $A = \overset{\circ}{\Theta}_{o}$

$$B = \dfrac{RJ\overset{\circ}{\Theta}_{o} + LK_{e}C_{o}}{LJ}$$

$$2J\omega = \dfrac{Lf + RJ}{JL}$$

$$\omega^{2} = \dfrac{fR + K_{v}K_{e}}{JL}$$

After some manipulation it develops that –

$$\textcircled{H} = \dfrac{B}{\omega^{2}\wp} + \dfrac{-\left(\dfrac{B}{\omega^{2}}\right)\wp + \left(\dfrac{A\omega^{2} - 2BJ\omega}{\omega^{2}}\right)}{\wp^{2} + 2J\omega\wp + \omega^{2}} \qquad (8)$$

Let $\alpha = \dfrac{B}{\omega^{2}}$

$$\gamma = -\dfrac{B}{\omega^{2}}$$

$$\delta = \dfrac{A\omega^{2} - 2BJ\omega}{\omega^{2}}$$

$$b = -J\omega + \sqrt{J^{2}\omega^{2} - \omega^{2}}$$

$$a = -J\omega - \sqrt{J^{2}\omega^{2} - \omega^{2}}$$

$$\Theta = \alpha + \dfrac{1}{b-a}\left[(\gamma b + \delta)e^{bt} - (\gamma a + \delta)e^{at}\right] \qquad (9)$$

27

It is seen that Θ at $t = \infty$ is the steady state value and the value of Θ at which the system comes to rest in the dead zone. Because of the obvious connection between this value and such crucial items as dead zone width and slope of the dividing lines it is suggested that this value be investigated to see upon what factors it depends.

$$\Theta_{(\infty)} = \alpha = \frac{B}{\omega}. \tag{10}$$

$$\Theta_{(\infty)} = \frac{\dfrac{R J \ddot{\Theta}_c + L K_t i_o}{J L}}{\dfrac{f R + K_v K_t}{J L}} \tag{11}$$

$$= \frac{R J \ddot{\Theta}_c + L K_t i_o}{f R + K_v K_t} \tag{12}$$

Here it is seen that the rest value of Θ depends not only linearly upon $\ddot{\Theta}_c$ but also upon i_o.

Now of course it would be of interest to see if at any time the term involving $i_o \left(L K_t i_o \right)$ is comparable in size to the term involving $\ddot{\Theta}_c \left(R J \ddot{\Theta}_c \right)$

In order to do this a solution is required for the differential

28

equations that describe the system at the moment full voltage is applied
to the terminals (the step input is introduced).

$$L \frac{di}{dt} + i R_a + K_v \frac{d\theta}{dt} = V \qquad (13)$$

$$-K_c i + J \ddot{\theta} + f \dot{\theta} = 0 \qquad (14)$$

$$\theta \dot{\theta} \quad = 0 \quad \text{at} \quad t = 0$$

$$L_s I + R_a I + K_v s \theta = \frac{V}{s} \qquad (15)$$

$$-K_c I + J s \theta + f s \theta = 0 \qquad (16)$$

$$I(sL + R_a) + K_v s \theta = \frac{V}{s} \qquad (17)$$

$$I(-K_c) - (Js + f_a)\theta = 0 \qquad (18)$$

$$I = \frac{\dfrac{V}{s}\left[s + \dfrac{f}{J}\right]}{s\left[s^2 + s\left[\dfrac{Lf + K_a J}{LJ}\right] + \left[\dfrac{R_a f + K_c K_v}{LJ}\right]\right]} \qquad (19)$$

Notice that the denominator in this case is similar to the denominator
in the case of the equation describing the dead zone behavior, the sole
difference being that R_a is substituted for R_a plus R_b.

29

Let $A' = 1$

$$B' = \pm \frac{}{}$$

$$2 \, \mathcal{J}' \omega' = \frac{L f + R_a \mathcal{J}}{L \mathcal{J}}$$

$$\omega'^2 = \frac{f R_a + K_v K_t}{L \mathcal{J}}$$

After some manipulation it turns out that

$$i = \frac{V}{L} \left\{ \alpha' + \frac{1}{b - a'} \left[\left(\mathcal{J}' b' - \delta' \right) \epsilon^{b't} - \left(\mathcal{J}' a' + \delta' \right) \epsilon^{a't} \right] \right\}$$

$$(20)$$

$$\alpha' = \frac{B'}{\omega'^2}$$

$$b' = -\mathcal{J}' \omega' + \sqrt{\mathcal{J}'^2 \omega'^2 - \omega'^2}$$

$$a' = -\mathcal{J}' \omega' - \sqrt{\mathcal{J}'^2 \omega'^2 - \omega'^2} \qquad -$$

$$b' - a' = 2\sqrt{\mathcal{J}'^2 \omega'^2 - \omega'^2}$$

$$\mathcal{J}' = -\frac{B}{\omega'^2}$$

$$\delta' = \frac{A' \omega'^2 - 2 B' \mathcal{J}' \omega'}{\omega'^2}$$

30

Notice that if $t \to \infty$, c approaches a steady state value of

$$c_{(\infty)} = \frac{V}{L} x = \frac{V}{L} \frac{f}{s} = \frac{V}{L} \frac{f}{J} \frac{LJ}{(f K_a + K_v K_t)} \tag{21}$$

$$c_{(\infty)} = \frac{Vf}{f K_a + K_v K_t} \tag{22}$$

By the same technique

$$\text{(H)} \qquad \frac{\dfrac{V K_t}{LJ}}{s\left[s^2 + s\left[\dfrac{L_1 + K_a J}{LJ} \right] + \left[\dfrac{R_a f + K_t K_v}{LJ} \right] \right]} \tag{23}$$

After some manipulation

$$\text{(H)} = D\left[\frac{G}{s^2} - \frac{H}{s} + \frac{G s + R}{s^2 + 2 J' \omega' s + \omega'^2} \right] \tag{24}$$

$$D = \frac{V K_t}{LJ}$$

$$G = \frac{1}{\omega'^2}$$

$$H = \frac{2 J' \omega'}{\omega'^2}$$

$$Q = \frac{2 J' \omega'}{\omega'^4}$$

$$P = \frac{4 J'^2 \omega'^2 - \omega'^2}{\omega'^4}$$

31

Solving for Θ and $\overset{\circ}{\Theta}$

$$\Theta = D\left\{ G\epsilon - H + \frac{1}{b'-a}\left[(Gb-P)\epsilon^{b'\epsilon} - (Ga+P)\epsilon^{a\epsilon} \right] \right\} \quad (25)$$

$$\overset{\circ}{\Theta} = D\left\{ G + \frac{1}{b'-a}\left[(Qb^2 + Pb')\epsilon^{b'-} - (Ga^2 + Pa)\epsilon^{a\epsilon} \right] \right\} \quad (26)$$

$$\overset{\circ}{\Theta}(\infty) = \frac{V K_+}{f R_a + K_v K_\epsilon} \quad (27)$$

Now assume that both i and $\overset{\circ}{\Theta}$ have reached steady state values
as they would to all intents and purposes if the step input was made
large enough.

Substituting $\overset{\circ}{\Theta}(\infty)$ and $i(\infty)$ in equation 12

$$\Theta(\infty) = \frac{RJ\overset{\circ}{\Theta}_0 + L K_\epsilon i_0}{f R + K_v K_\epsilon} \quad (12)$$

becomes

$$\Theta(\infty) = \frac{V K_\epsilon RJ}{(f R - K_v K_\epsilon)(f R_a + K_v K_v)}\left[1 + \frac{Lf}{RJ} \right] \quad (28)$$

Here it is seen that the effect of i_0 upon the steady state value
of Θ is quite small since $\frac{Lf}{RJ}$ is intuitively small compared to 1 in
any consistent system of units.

It was decided at this point to check into the transient current
that exists in the armature during the complete cycle of operations.
Accordingly a o.1 ohm resistor of high current capacity was placed in
the armature circuit and a Brush Recorder was used to obtain a scaled
representation of the current. Figure 17 on page 24 depicts the tra-
jectories on the phase plane for both a large and small step input.
Figures 18 A and B are the Brush Recorder traces for error, error rate,
and armature current for a large step input. Figures 19 A and B are the
Brush Recorder traces of the armature current, error and error rate for
a small step input. Notice that in Figures 18 B and 19 B the switching
points are clearly identified, as that is the point where the current
attempts to seek a maximum value in the opposite direction. Of interest
here is the fact that for small step inputs the current has not had a
chance to reach steady state in the direction that the current takes when
the motor is being driven to correct for the step error. Therefore, the
instantaneous value of current at the time of switching is much greater
in the case of the small step input than it is for a large step input.
This means that a greater change of current is required in order to obtain
the desired braking. Inasmuch as there is some inductance associated with
the armature, this change requires a finite amount of time and the time
involved in the change in the case of a small step input is greater than
that involved for a large step input. Since the velocity is high at this
particular point in the cycle, the output will move a trifle farther
during this transition stage and this explains the fact that the steady
state rest position is apt to be farther from the intersection of the
initial drop-out line and the zero error rate line on the phase plane in

33

Figure 18. Brush Recorder Traces Showing
A Relay Servo Response to A Large
Step Input
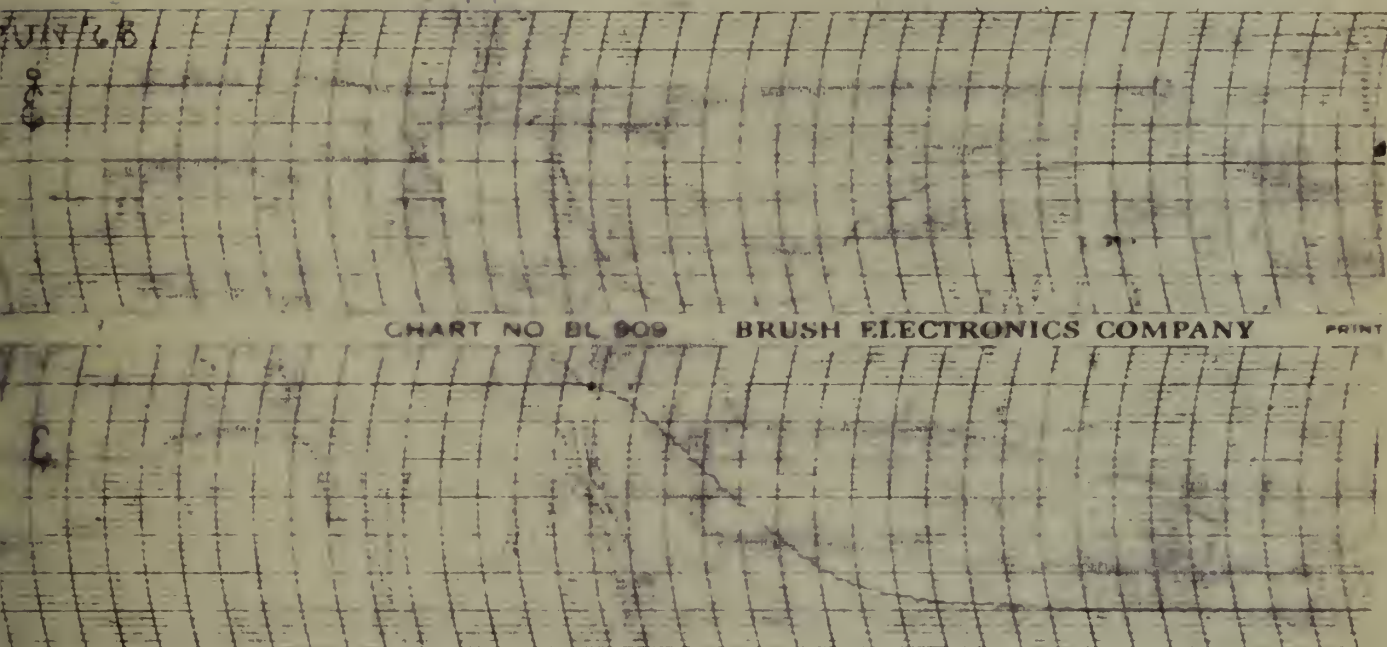
Figure 18A. Error and Error Rate
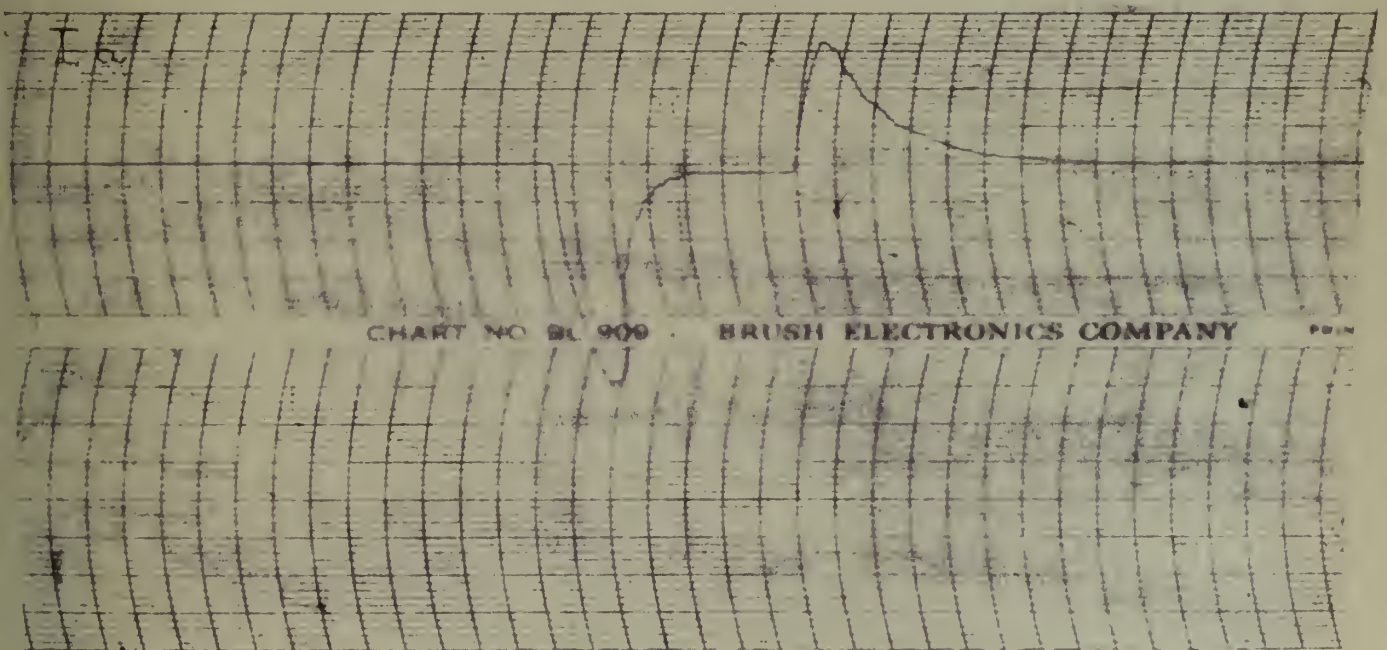
Figure 18B. Armature Current

34

Figure 19.   Brush Recorder Traces Showing Response of A
            Relay Servo to A Small Step Input
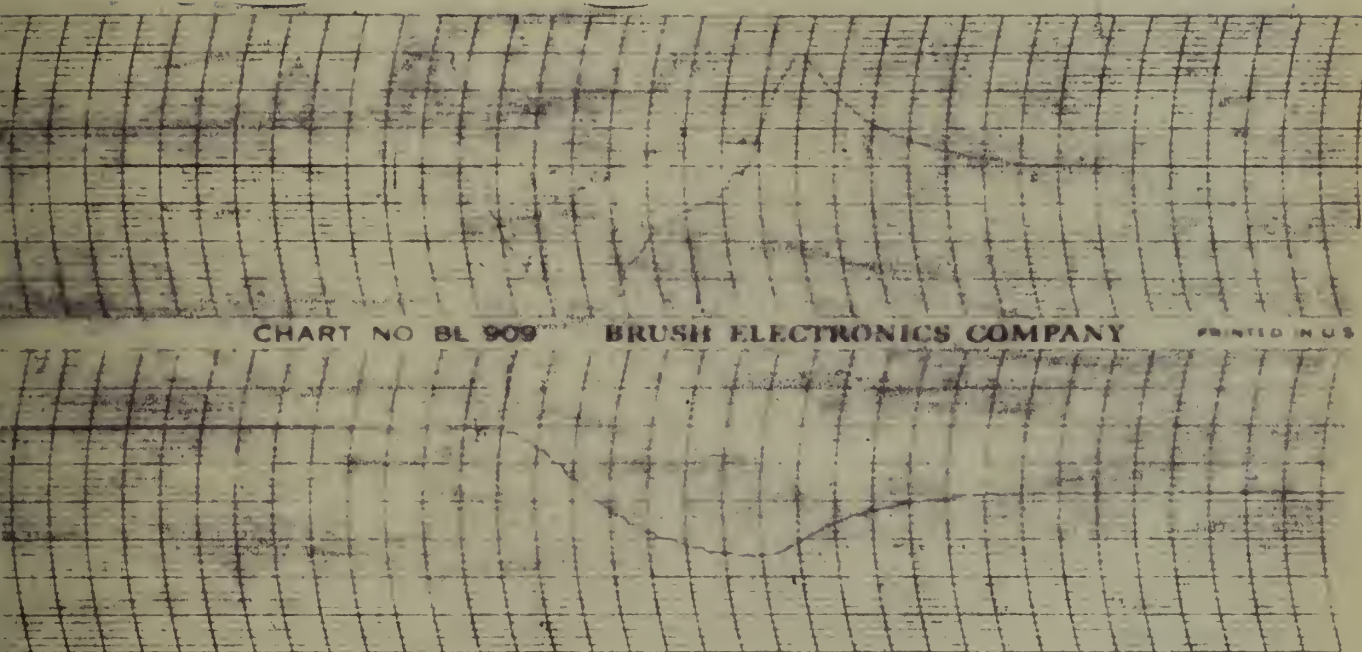
Figure 19A.   Error and Error Rate
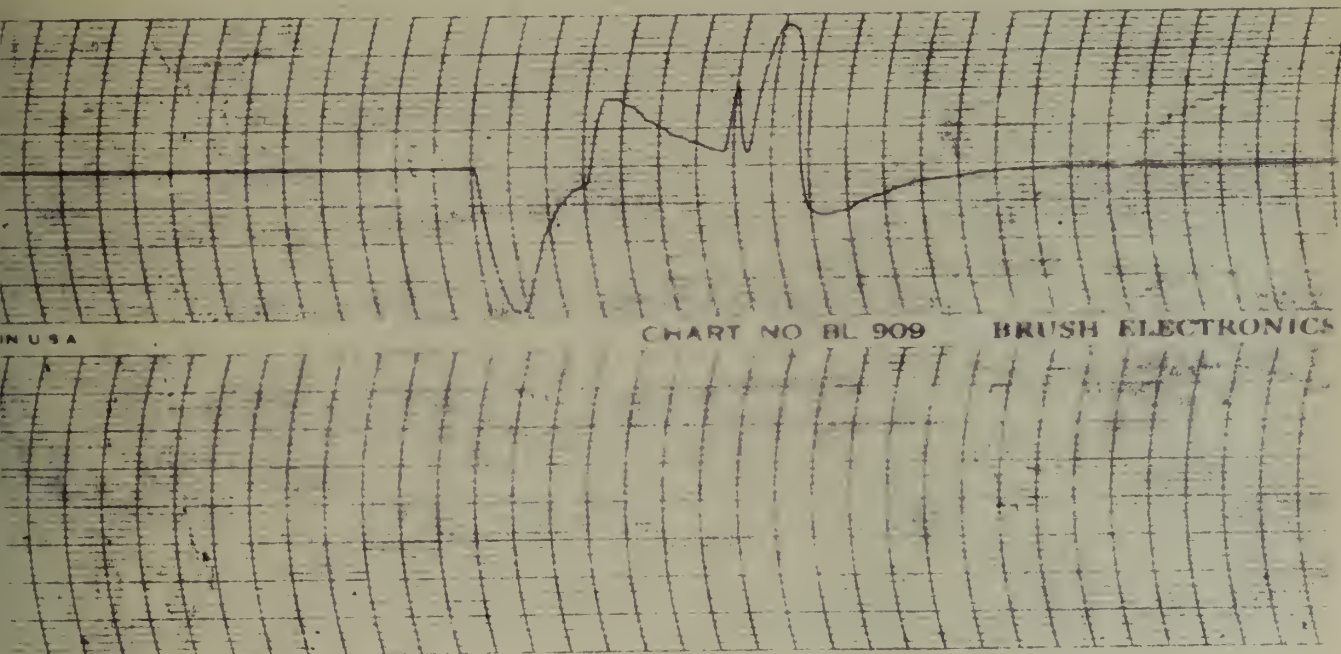
Figure 19B.   Armature Current

the case of the small step input.

It is to be noted in Figures 18B and 19B that i_{max} is at least
twenty times as great as i_{ss} and at that particular time the output
velocity is less than $\dot{\theta}_{(ss)}$. Therefore, it is not beyond the realm of
possibility that if the relay was to operate during the part of the run
when i is appreciably greater than i_{ss}, the steady state rest position
might depend to a great extent upon the term involving i_o.

Another interesting facet of this analytical solution is the deter-
mination of the slope on the phase plane at $t = 0$.

During the dead zone we know that -

$$\theta = \alpha + \frac{1}{b-a}\left[(\gamma b + \delta)e^{bt} - (\gamma a + \delta)e^{at}\right] \quad (9)$$

$$\dot{\theta} = \frac{1}{b-a}\left[(\gamma b^2 + \delta b)e^{bt} - (\gamma a^2 + \delta a)e^{at}\right] \quad (29)$$

$$\ddot{\theta} = \frac{1}{b-a}\left[(\gamma b^3 + \delta b^2)e^{bt} - (\gamma a^3 + \delta a^2)e^{at}\right] \quad (30)$$

$$at \quad t = 0$$

$$\frac{\ddot{\theta}}{\dot{\theta}} = \frac{d\dot{\theta}}{d\theta} = \frac{(b^3 - a^3)\gamma + \delta(b^2 - a^2)}{(b^2 - a^2)\gamma + \delta(b - a)} \quad (31)$$

36

After some substitution and manipulation

$$\frac{d\ddot{\theta}}{d\dot{\theta}} = \frac{1}{J}\left[\frac{K_t \, i_o}{\dot{\theta}_c} - f\right] \qquad (32)$$

Referring at this point to the basic equations describing the system when the step input is applied we see that at

$$t = \infty \qquad \ddot{\theta} = 0$$

$$\text{and} \quad \dot{\theta} = \frac{K_t \, i}{f}$$

Therefore if a step large enough to effect velocity saturation is applied –

$$\frac{\ddot{\theta}_c}{\ddot{\theta}} \approx \frac{d\ddot{\theta}}{d\dot{\theta}} = \frac{1}{J}\left[\frac{K_t \, i_o f}{K_t \, i_o} - f\right] = 0 \qquad (33)$$

This agrees with the experimental results. However, if velocity saturation had not been reached at the instant of effective switching

the term $\left[\dfrac{K_t \, i_o}{\dot{\theta}_c} - f\right]$

would be positive since i_o would be greater, $\dot{\theta}_c$ would be less.

This also agrees with the experimental results and also it indicates that the phase plane trajectory must undergo a greater change in slope before it reaches the straight line portion than does the trajectory for the velocity-saturated run.

The final mathematical analysis stems from the idea that knowing the $\theta_{(\infty)}$ for the velocity saturated run, it might be possible to predict

37

the maximum deviations from this rest position that might result from the
introduction of any size step input.

The performance of the entire system depends upon the operating
characteristics before and after switching. These characteristics are
readily shown on the phase plane diagram including conditions under which
transition takes place. Therefore, Figures 20 and 21 are constructed using
$\dot{\theta}$ and θ as ordinate and abscissa respectively in order to show the com-
plete system response to a step input.

From Figure 21 it is seen that (referred to the translated origin 0'),

$$M = X + S + \alpha$$

α — steady state position as referred to the point of effective
switching.

S — distance along abscissa traveled during the dead time of the
relay

X — distance traveled before the point of theoretical switching
should take place

$X = 0$ for the velocity saturated run

The idea in mind is to determine M as a function of the time before
actual switching takes place.
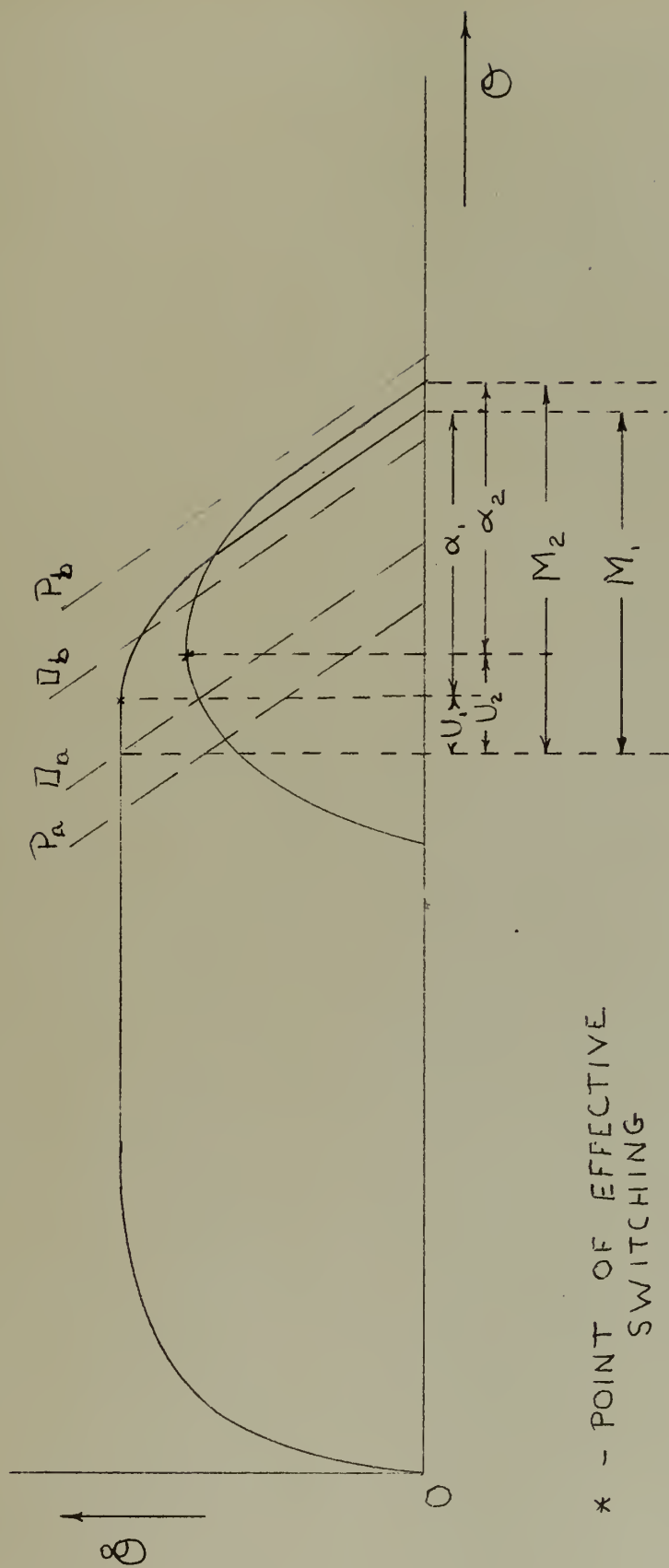
* - POINT OF EFFECTIVE
SWITCHING

—— — Dividing Lines

P_1, P_2 - PULL-IN LINES

D_1, D_2 - DROP-OUT LINES

$\overset{\circ}{\Theta}$ vs Θ For A Large and Small Step Input
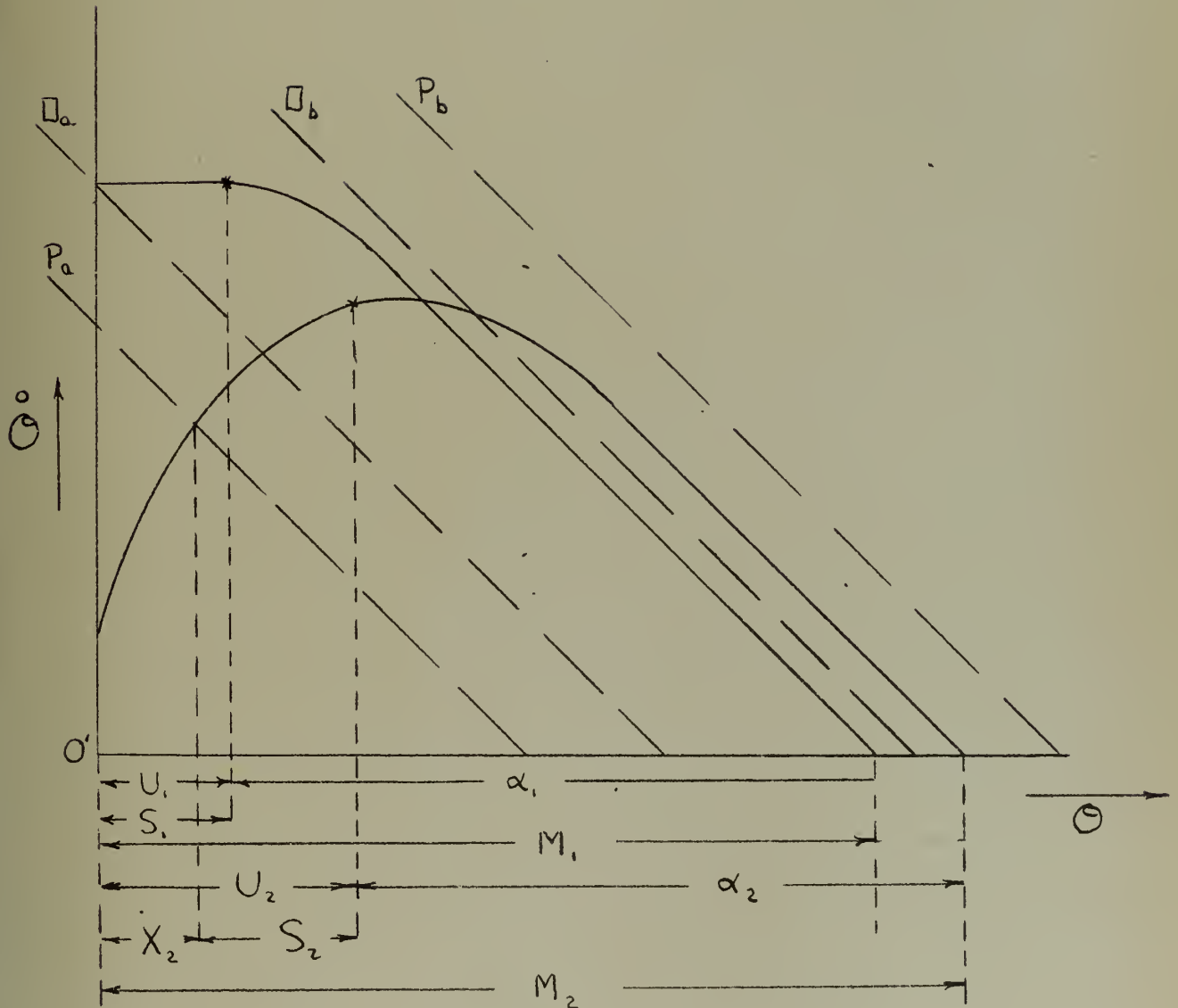
FIGURE 20

Figure 21

It has been shown previously that in the dead zone -

$$\Theta = \alpha + \frac{1}{b-a}\left[(\sigma b + \delta)\varepsilon^{bt} - (\sigma a + \delta)\varepsilon^{at}\right] \quad (9)$$

$$\Theta_{(\infty)} = \alpha = \frac{RJ\overset{\circ}{\Theta}_c + LK_t i_0}{fR + K_v K_t} \quad (12)$$

It remains to substitute function of t (before actual switching) for i_0 and $\overset{\circ}{\Theta}_0$. Then the size of the step input is related to t (the time from switch closure to effective drop out).

As has been shown previously -

$$i = \frac{V}{L}\left\{\sigma' + \frac{1}{b'-a'}\left[(\sigma b' + \delta')\varepsilon^{b't} - (\sigma a' + \delta')\varepsilon^{a't}\right]\right\} \quad (20)$$

$$\overset{\circ}{\Theta}_c = \frac{VK_t}{LJ}\left\{G + \frac{1}{b-a}\left[(Qb' + Pb)\varepsilon^{bt} - (Ga' - Pa')\varepsilon^{a't}\right]\right\} \quad (26)$$

$$\therefore \Theta_{(\infty)} \sim \alpha =$$

$$\frac{1}{fR - K_v K_t}\frac{RVK_t}{L}\left\{G + \frac{1}{b-a}\left[(Qb'' + Pb)\varepsilon^{bt} - (Ga' + Pa')\varepsilon^{a't}\right]\right\}$$

$$+ \frac{1}{fR + K_v K_t}K_t V\left\{\sigma' + \frac{1}{b'-a'}\left[(\sigma' b' + \delta')\varepsilon^{b't} - (\sigma' a' - \delta')\varepsilon^{a't}\right]\right\} \quad (34)$$

41

In order to determine X,   reference to the diagram is necessary –

$$K_1\Theta' + K_2\overset{o}{\Theta} = K_3$$ is equation of the drop out line where

the relay should actuate

$$\Theta = \left(\frac{K_3}{K_2} - \overset{o}{\Theta}\right)\frac{K_2}{K_1}$$

$$= \left(\overset{o}{\Theta}_{(\infty)} - \overset{o}{\Theta}\right)\frac{K_2}{K_1}$$

Here, this is precisely X,   the desired quantity.

$$\therefore \; X = \frac{K_2}{K_1}\left\{ -\frac{D}{b'-a'}\left[(Qb'^2 + Pb')e^{b't} - (Qa'^2 + Pa')e^{a't}\right]\right\} \quad (35)$$

However, in order to relate to the same time as used in the equations

for α , the time in this equation must be the time of effective switch-

ing. Since the time in this equation is for theoretical switching, we must

substitute $t-t_d$ for t where t_d is the time delay associated with the

relay. It is hereby assumed that t_d is a constant.

Therefore –

$$X = \frac{K_2}{K_1}\left\{ -\frac{D}{b'-a'}\left[(Qb'^2 + Pb')e^{b'(t-t_d)}\right.\right.$$

$$\left.\left. - (Qa'^2 + Pa')e^{a'(t-t_d)}\right]\right\} \quad (36)$$

with t of necessity larger than t_d.

42

The final problem is to write an equation for S where S is the
horizontal distance associated with the time delay of the relay

$$S = \Theta_{(t)} - \Theta_{(t-t_d)}$$

$$= D \left\{ G t_d + \frac{1}{b'-a} \left[(Q b' + P) \varepsilon^{b't} - (Q a' + P) \varepsilon^{a't} \right. \right.$$

$$- (Q b' + P) \varepsilon^{b(t-t_d)} + (Q a' + P) \varepsilon^{a'(t-t_d)}$$

$$\tag{37}$$

$$S = D \left\{ G t_d + \frac{1}{b'-a'} \left[(Q b' + P) \varepsilon^{b't} \left(1 - \varepsilon^{-b't_d} \right) \right. \right.$$

$$- (Q a' + P) \varepsilon^{a't} \left(1 - \varepsilon^{-a't_d} \right) \right] \right\} \tag{38}$$

Now M may be defined as -

$$M = \alpha + S + X$$

43

$$M = \left(\frac{1}{fR + K_v K_r}\right)\frac{RVK_r}{} \left\{ G + \frac{1}{b-a} \right.$$

$$\left[(Gb' + Pb')e^{b't} - (Qa'' + Pa)e^{a't} \right] \right\}$$

$$+ \frac{1}{fR + K_v K_r} K_r V \left\{ \alpha' + \frac{1}{b'-a'} \left[(\delta'b' + \delta)e^{b't} \right. \right.$$

$$\left. \left. - (\gamma'a' + \delta')e^{a't} \right] \right\}$$

$$- \frac{K_r}{K_r}\frac{\boxed{}}{(b'-a')} \left[(Gb'^2 + Pb')e^{b'(t-t_d)} \right.$$

$$- (Qa'' + Pa)e^{a'(t-t_d)}$$

$$+ \boxed{} \left\{ Gt_d + \frac{1}{b-a} \left[(Gb' + P)e^{b't}\left(1 - e^{-b't_d}\right) \right. \right.$$

$$\left. \left. - (Qa' + P)e^{a't}\left(1 - e^{-a't_d}\right) \right] \right\} \tag{39}$$

It now remains to define the range of values for which t is valid in the preceding expression for M. Referring to Figure 22, t can run from $t_1 \neq t_d$ to infinity where t_1 is the time required to traverse just the trajectory between the pull-in and drop-out line when a signal just large enough to actuate the relay is introduced and t_d is the time delay associated with the relay.
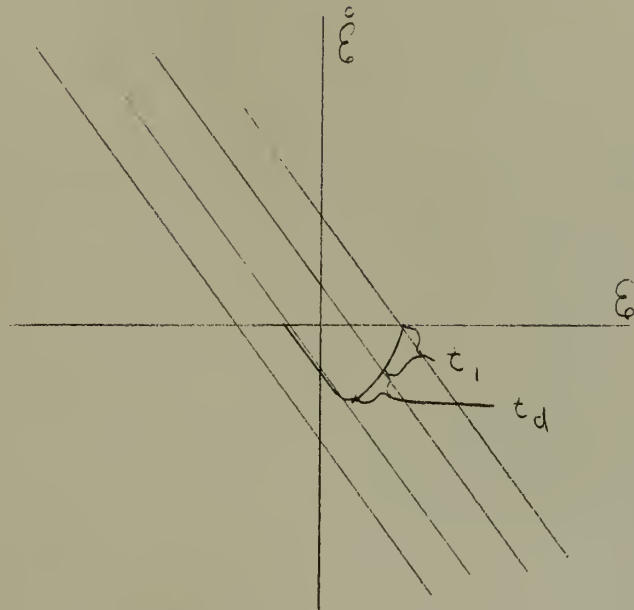
Relay Servo Response to A Step Input
Figure 22

It is desirable to define t_1 in terms of the physical constants of the system. At the time of switch closure,

$$\theta = \Pi \left\{ G t - H + \frac{1}{b' - a'} \left[(Q b' + P) \varrho^{b't} - (Q a' + P) \varrho^{a't} \right] \right.$$

$$(25)$$

$$\dot{\theta} = \Pi \left\{ G + \frac{1}{b' - a'} \left[(Q b'^2 + P b') \varrho^{b't} - (Q a'^2 + P a') \varrho^{a't} \right] \right\}$$

$$(26)$$

45

It is known that the equations of the pull-in and the drop-out lines

are

Pull-in $K_1 \theta + K_2 \overset{\circ}{\theta} = K_3$

Drop-out $K_1 \theta + K_2 \overset{\circ}{\theta} = K_4$

By appropriately translating the vertical axis the equations become

Pull-in $K_1 \theta + K_2 \overset{\circ}{\theta} = 0$

Drop-out $K_1 \theta + K_2 \overset{\circ}{\theta} = K_4'$

K_4' now represents the difference between the pull-in and drop-out

voltages.

It further remains to substitute equations (25) and (26) in

$K_1 \theta + K_2 \overset{\circ}{\theta} = K_4'$ and determine the value of t that satisfies

the equation. That is t_1. Therefore, in the expression for M, t can

take on all values of t from $t_1 + t_d$ to infinity.

In order to obtain maxima and minima from the expression for M

analytically, it is readily apparent that knowledge of all of the physical

constants of the system is required. It is quite probable that machine

methods could be used to advantage in solving for M over the complete

range of step inputs by successively substituting different values of t

in the equation for M, taking into account the limits imposed upon the

values that t can assume. Remember, however, that initially it was

assumed that R_b was small in order to eliminate for all practical

purposes the effect of coulomb friction.

Referring once again to the equation for M, it is highly unlikely

that for any physical system the value of M would be a constant for all
values of t. In order to compensate for the spread of values that M
must surely take on as t is varied, it is believed that the switching
criteria must certainly be a function of something besides error and error
'rate.

In order to develop something more adequate as a switching criteria,
a comparison of the actual experiments and the theory is perhaps in order.
It has been seen that in the actual experiments, the final steady state
resting point on the phase plane for runs that deadbeat is not a constant
for all values of step inputs. As soon as the step input is decreased in
size to the point where the armature current and the velocity do not have
a chance to build up to the steady state values prior to switching at the
drop-out line, there is a tendency for the system to come to rest farther
from the intersection of the drop-out line and the zero error rate line

than is the case when
the step input is large
enough for the armature
current and velocity to
ready steady state
values. This is shown
by curves a and b in
Figure 23.
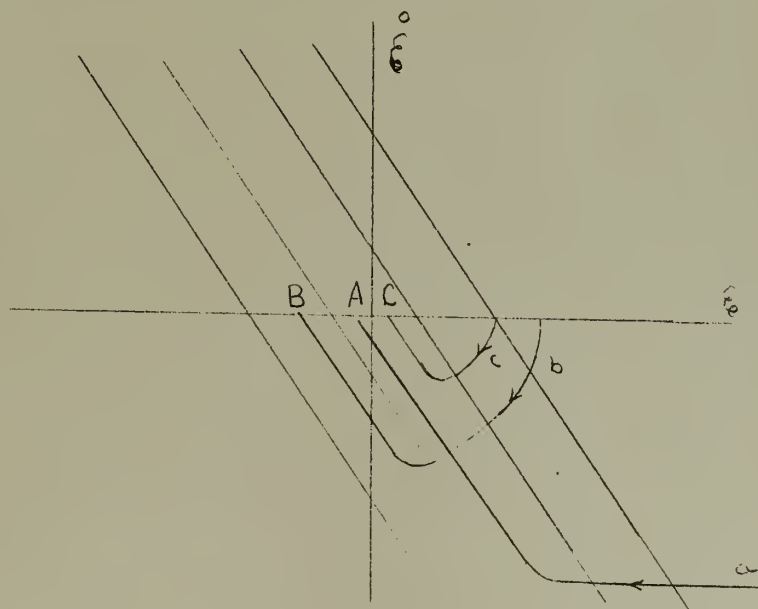
Figure 23. Relay Servo Response
to Step Inputs

In the mathematical analysis it has been shown that the resting point is a function of both armature current and velocity at the instant of switching.

It has been postulated that the reason for this behavior is due to the fact that it takes longer for effective braking to take place in the case of the small step input. This is because the current in the armature cannot change instantaneously due to the effect of inductance associated with the armature, but must take a finite amount of time. The amount of time involved is associated with the magnitude of change that the armature current is attempting to undergo. Since the armature reaches saturation velocity before the current reaches steady state, as shown in Figures 18 and 19, the Brush Recorder tapes for Θ , $\dot{\Theta}$ and i_a vs time, there is a period of time in the run when, if switching were to occur the current would tend to undergo a greater change than it would if switching were to take place when steady state and saturation conditions prevailed. The amount of change is dependent upon both the corresponding instantaneous values of current and velocity. Briefly the current seeks to change from i_o to $-\dfrac{K_v \dot{\Theta}}{R_a + R_b}$. As one examines the instantaneous values of current as t becomes smaller it becomes evident that a point is reached where the change that the current would attempt to undergo should switching occur at that point would once again be equal to the change that the current would attempt to undergo if steady state conditions prevailed. This is because the velocity has decreased from the steady state condition so that $K_v \dot{\Theta}$ is substantially smaller. If the comparison of instantaneous values is extended further toward zero time, it is seen that the

current tends to undergo a very small change, the inductance of the arma-
ture delays the effective braking to a very small extent, and the steady
state resting point lies closer to the intersection of the drop-out line
and the zero error rate line than is the case when a large step is used.
This is shown in Figure 23 as curve c.

Two factors enter the picture at this point to negate the idea that
switching may take place very near to zero time. First, in the practical
relay, there is a definite difference between the pull-in voltage and the
drop-out voltage. Therefore, a definite amount of time is necessary in
order for the motor to drive the system from the pull-in line to the drop-
out line. This time is equivalent to t_1 in the mathematical analysis.
Secondly, in addition to this time there is a delay time associated with
the relay. Although this time is undoubtedly not a constant, it is being
treated as such for the purposes of this paper. This time is t_d in the
mathematical analysis. It is easily conceivable that, due to the cumula-
tive effect of these two times, a step input just large enough to actuate
the relay will result in the system having a final resting point after
deadbeat operation on the phase plane farther from the intersection of the
drop-out line and the zero error rate line than is the case when steady
state conditions prevailed upon switching. In other words, curve c in
Figure 23 would not exist in a qualitative sense and the locus of points
where the system would come to rest would extend from point A to the left
on Figure 23, the exact extremity possibly but not necessarily occurring
at the culmination of a run in which a minimum step was used.

In the actual experiments this was the case. The time delay was large
enough so that the locus of points did extend from point A away from the

49

intersection of the drop-out line and the zero error rate line.

Therefore, it is hereby postulated that in order to get deadbeat performance from a relay servo with all sizes of step inputs and still have high static accuracy, something besides error and error rate must be involved in the switching criteria. It is believed that feeding back a signal dependent upon armature current might be an ideal stabilizing factor. It is known that the final resting point of the phase plane trajectory depends upon the instantaneous value of current as well as error rate at the instant of switching. Therefore, it is suggested that having the system switch early when the current is high relative to the steady state value would tend to compensate for the added displacement that takes place for relatively small step inputs. Since the current and velocity as a function of time resembles the curves shown in Figure 24, the phase plane switching lines could be made to resemble Figure 25 if a signal dependent upon armature current and properly amplified is fed back along with error and error rate. It would of course be necessary
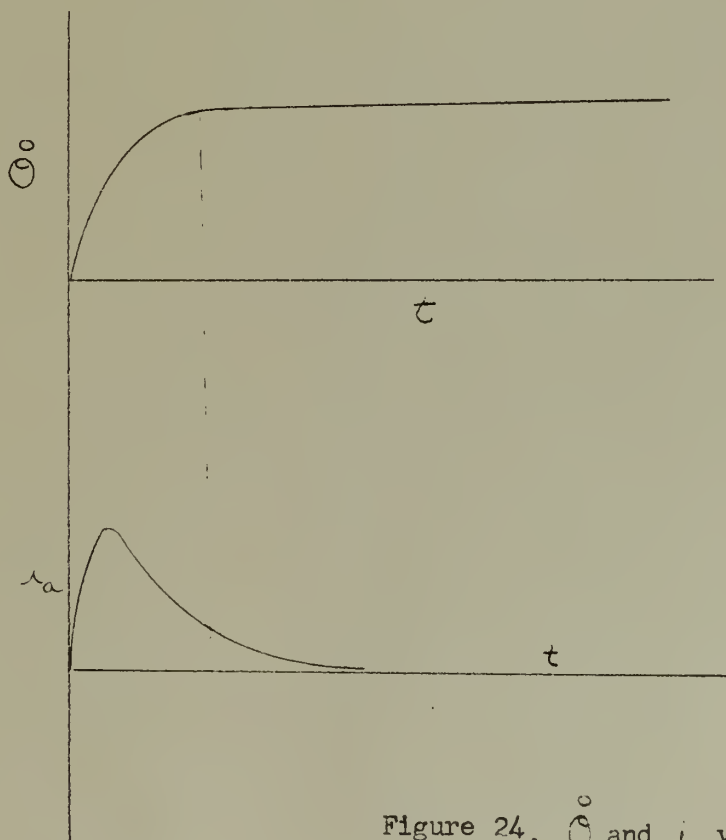
Figure 24. $\overset{\circ}{\theta}$ and i_a vs Time

50

Switching Criteria for
a Practical Relay Servo

P_b

D_b

D_a

P_a

P_a, P_b - Pull In Switching Lines with Error
and Error Rate Feedback

D_a, D_b - Drop Out Switching Lines with Error
and Error Rate Feedback

———·——— Drop Out Switching Lines with Error,
Error Rate and Armature Current
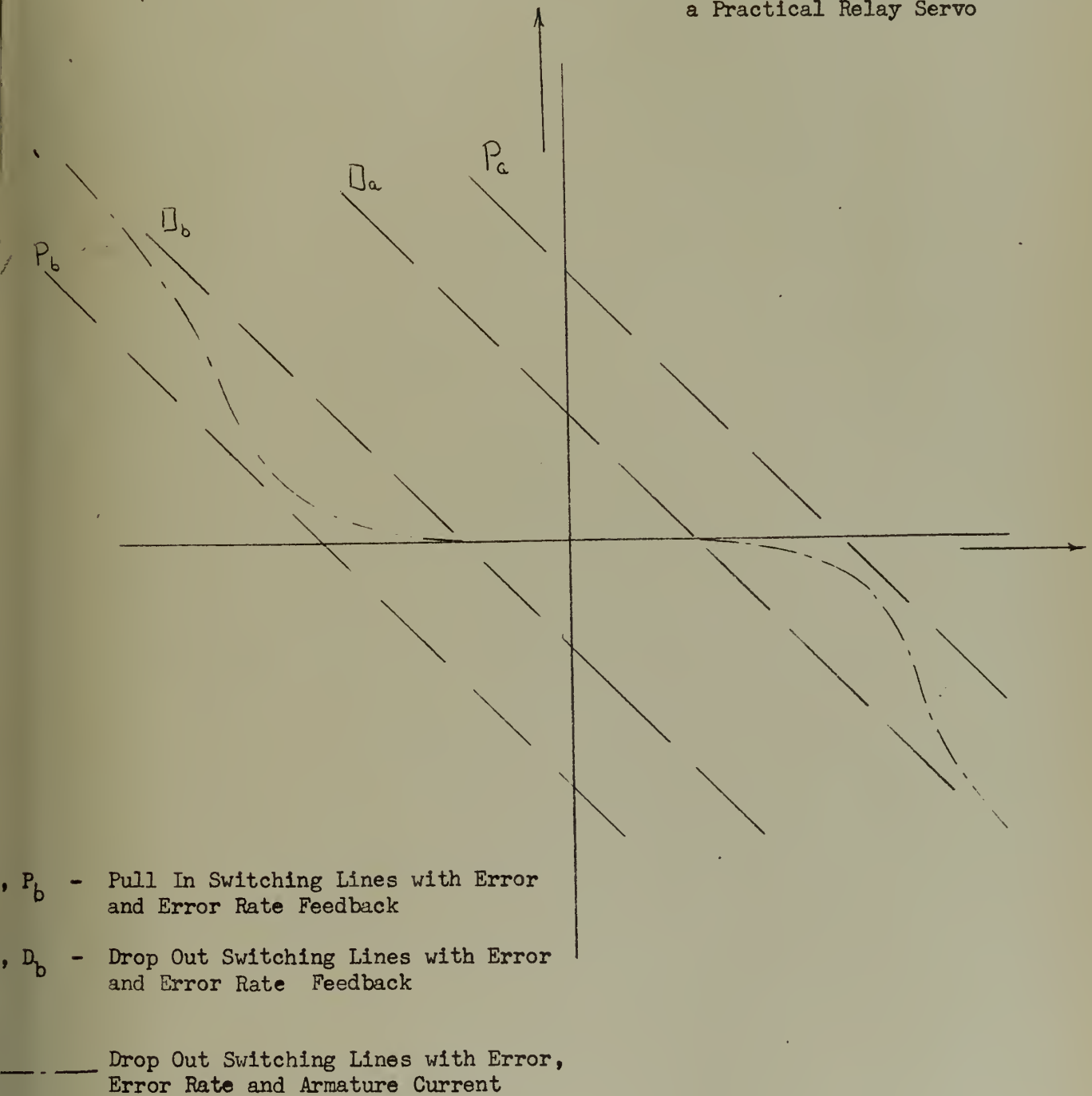
Figure 25

to arrange the physical layout so that the signal dependent upon armature current would not be fed back and affect the switching criteria while the system was in the dead zone, otherwise the pull-in lines would also be affected.

Accordingly the following conclusions should be drawn:

(1) It is possible to predict the locus of the ends of the dead zone trajectories in all cases where the system is deadbeat for all values of step inputs for a relay servo employing dynamic braking in the dead zone and derivative feedback provided (a) all of the physical quantities of the system are known and (b) the braking resistance is small enough so that the effect of coulomb friction is negligible.

(2) If the resistance in the braking circuit is correctly adjusted so that the straight line portion of the dead zone trajectory is parallel to the switching lines, the end of the dead zone trajectory will, in most cases, lie farther from the intersection of the zero error rate line and the drop-out line than will the end of the dead zone trajectory resulting from a large step input.

(3) In order to have deadbeat operation in a small dead zone for all sizes of step inputs when there is a considerable amount of armature inductance (the L/R ratio is great), the switching criteria must be a function of something besides error and error rate.

CHAPTER V

AN ANALYSIS OF THE RESPONSE OF A RELAY
SERVO TO A RAMP INPUT

There is naturally an interest in developing the relay servo system behavior analytically in the case of a ramp input to see to what extent the actual experimental behavior fits the predicted characteristics.

In the case of the ramp input,

$$\Theta_R = \omega t$$

$$\mathcal{E} = \Theta_R - \Theta_c$$

$$\dot{\mathcal{E}} = \omega - \dot{\Theta}_c$$

$$\dot{\Theta}_c = \omega - \dot{\mathcal{E}}$$

The first consideration is to establish the equations for the pull-in and drop-out lines.

With tachometer feedback we know that we are feeding back not $\dot{\mathcal{E}}$ as before but rather $\dot{\Theta}$.

$$K_1 \mathcal{E} \pm K_2 \dot{\Theta}_c = K_3$$

$$K_1 \mathcal{E} \pm K_2 \omega \mp K_1 \dot{\mathcal{E}} - K_3$$

53

In order for anticipation to occur –

$$K_1 \varepsilon + K_2 \overset{c}{\varepsilon} - K_2 \omega = K_3$$

$$K_1 \varepsilon + K_2 \overset{c}{\varepsilon} = K_3 + K_2 \omega$$

$$K_2 \overset{c}{\varepsilon} = K_3 + K_2 \omega - K_1 \varepsilon$$

$$\overset{c}{\varepsilon} = \frac{K_3 + K_2 \omega}{K_2} - \frac{K_1}{K_2} \varepsilon$$

This says that the slope of the dividing line is – $\dfrac{K_1}{K_2}$

and the ε-intercept is $\dfrac{K_3 + K_2 \omega}{K_1} = \dfrac{K_3}{K_1} + \dfrac{K_2}{K_1} \omega$

For the step input, recall that

$$K_1 \varepsilon + K_2 \overset{c}{\varepsilon} = K_3$$

$$\overset{c}{\varepsilon} = \frac{K_3 - K_1 \varepsilon}{K_2}$$

and that the slope of the dividing line is – $\dfrac{K_1}{K_2}$, with

an ε-intercept of $\dfrac{K_3}{K_1}$

54

Therefore, it is seen that in the two cases the slopes are the same, but that in the case of the ramp input all of the horizontal intercepts are advanced by the amount $\dfrac{K_v}{K_1} \omega$.

Inasmuch as the measured variable is $\overset{o}{\Theta}$ instead of $\overset{o}{\varepsilon}$ it is necessary to make a conversion. It is known that $\overset{o}{\varepsilon} = \omega - \overset{o}{\Theta}_c$

Therefore, for all values of $\overset{o}{\Theta}_c$, it is necessary to add a constant to portray the $\varepsilon - \overset{o}{\varepsilon}$ phase plane properly. This in effect means a translation of the axis as shown in Figure 26.

It would also be of interest to examine the dead zone trajectory.

Assuming the terms $\angle \dfrac{d_i}{dt}$ and $\oint \dfrac{d\,\Theta_c}{dt}$ to be negligible –
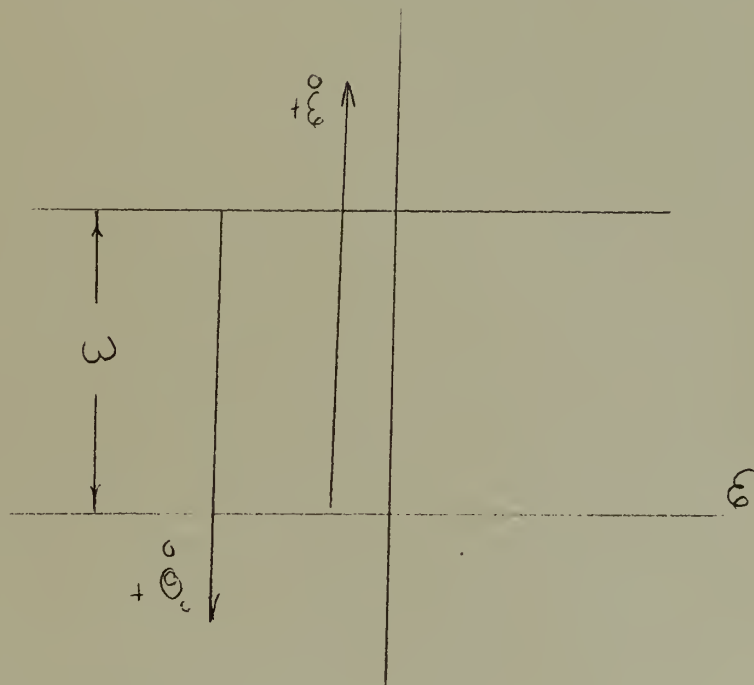
Figure 26. Error Rate and Velocity vs Error

$$K_v \, \overset{o}{\Theta}_c = i \, (R_a + R_b)$$

$$T_B = K_t \, i$$

$$J \, \overset{oo}{\Theta}_c = -T_B - C$$

55

Since $\quad \dot{\epsilon} = \omega - \dot{\theta}_c$

and $\quad \ddot{\epsilon} = -\ddot{\theta}_c$

$\dot{\theta}_c = \omega - \dot{\epsilon}$

$\ddot{\theta}_c = -\ddot{\epsilon}$

$K_v(\omega - \dot{\epsilon}) = i\,(R_a + R_b)$

$T = K_t\, i$

$J\ddot{\epsilon} = T_e - C$

$J\ddot{\epsilon} = K_t\left(\dfrac{K_v(\omega - \dot{\epsilon})}{R_a + R_b}\right) + C$

$\ddot{\epsilon} = \dfrac{K_t K_v \omega}{J(R_a + R_b)} - \dfrac{K_t K_v \dot{\epsilon}}{J(R_a + R_b)} + \dfrac{C}{J}$

$\dfrac{\ddot{\epsilon}}{\dot{\epsilon}} = \dfrac{d\dot{\epsilon}}{d\epsilon} = \dfrac{K_t K_v \omega}{J(R_a + R_b)} + \dfrac{C/J}{\dot{\epsilon}} - \dfrac{K_t K_v}{J(R_a + R_b)}$

In essence the meaning of this equation is as follows:
When $\overset{o}{\xi}$ is large and negative the trajectory should have a negative

slope. As $\overset{o}{\xi}$ decreases, still negative, the slope should increase

negatively to infinity as $\overset{o}{\xi}$ approaches zero. When $\overset{o}{\xi}$ is small and

positive, the slope should be large and positive, and, as $\overset{o}{\xi}$ increases

the slope should decrease, eventually reaching zero when $\overset{o}{\xi}$ is

large and positive.

The phase trajec-
tory should re-
semble Figure 27.

It was de-
cided to run some
actual tests with
a Low Frequency
Function Genera-
tor as a source
of a ramp input.
The schematic
diagram of the
system is as
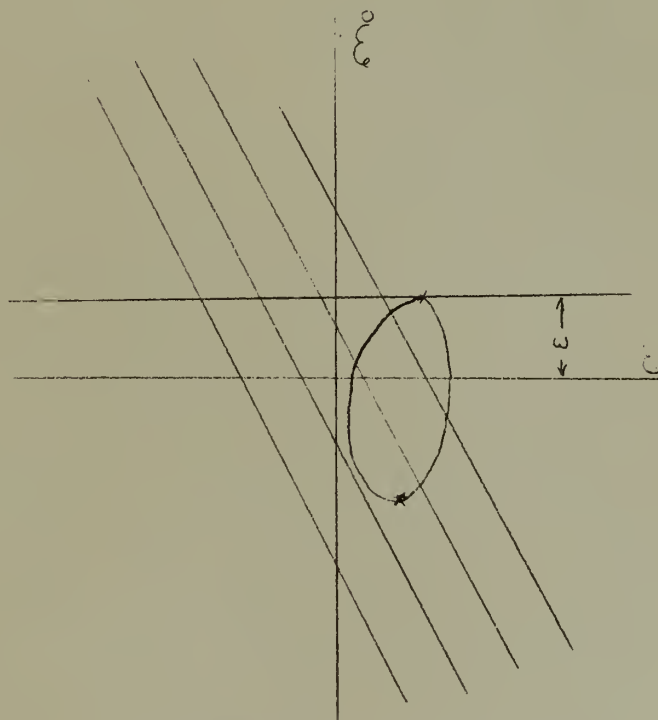
Relay Servo Response To A Ramp Input

Figure 27

shown in Figure 28. Figures 29 and 30 are the actual phase trajectories

for runs made with this system. Notice that there is a great deal of

similarity between the actual runs and the predictions made on theory.

57

Schmatic Diagram of a Relay Servo
System Using a Ramp Input

L.F.F.G. - Low Frequency Function Generator

Figure 28

58
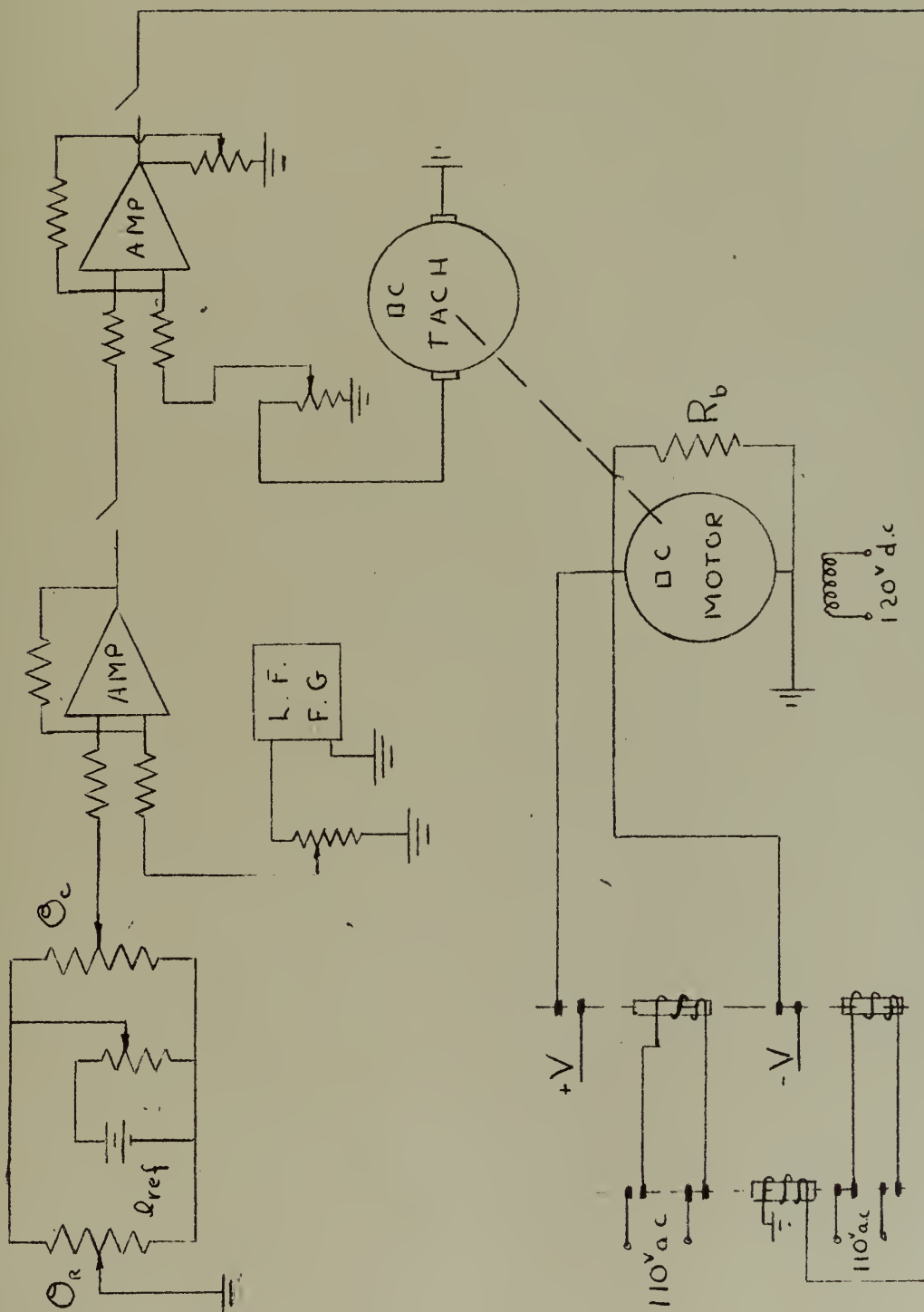
Phase Plane Trajectories of $\mathcal{E}$ vs $\overset{o}{\mathcal{E}}$
for a Ramp Input

$$\Theta_R = \omega t$$

Where $\omega = 1.2 \; rad/sec$

and t = time in seconds
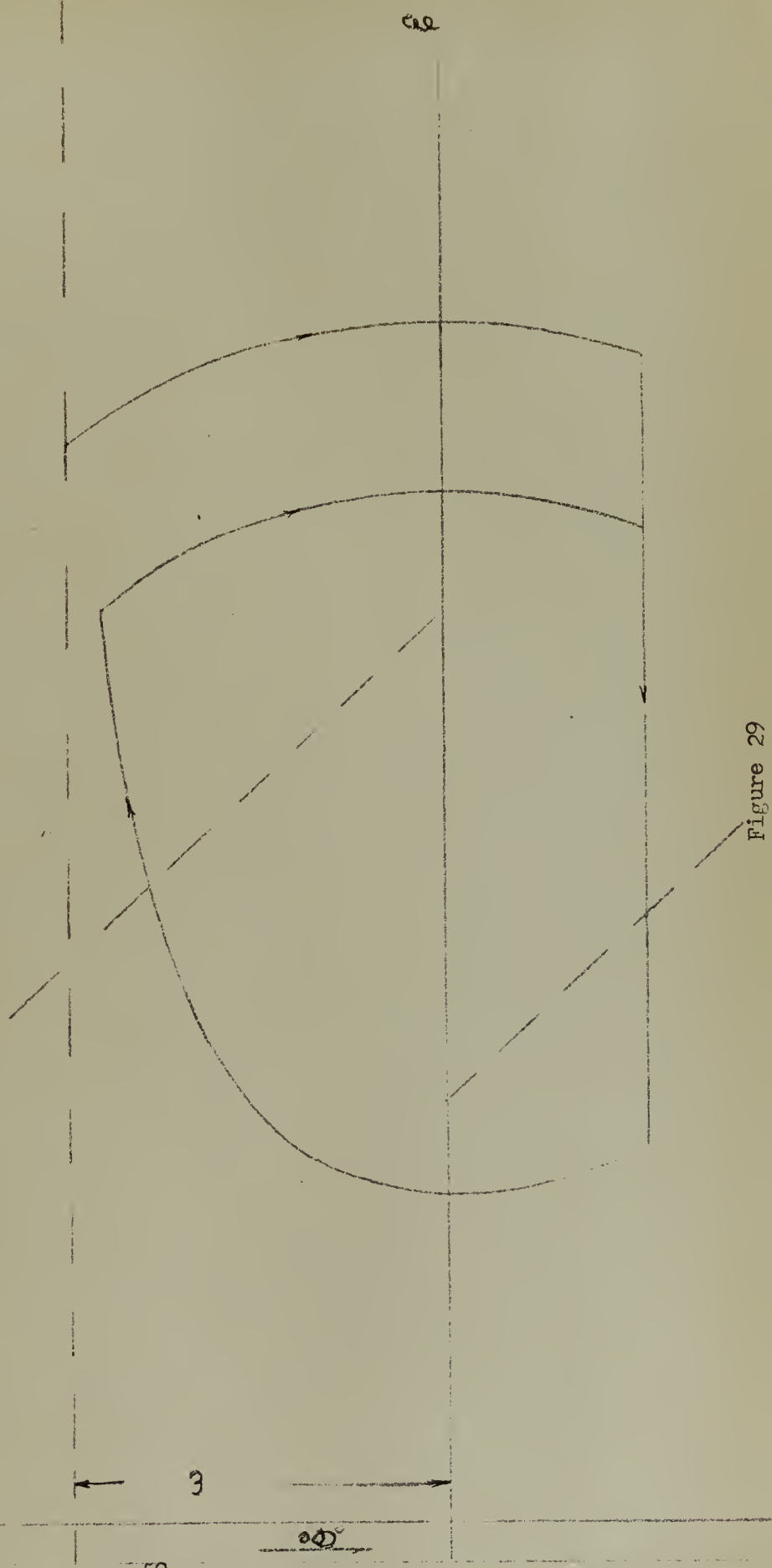
Figure 29

Phase Plane Trajectory for a
Ramp Input

$\Theta_R = \omega t$

Where $\omega = .046$ rad/sec

and t = time in seconds
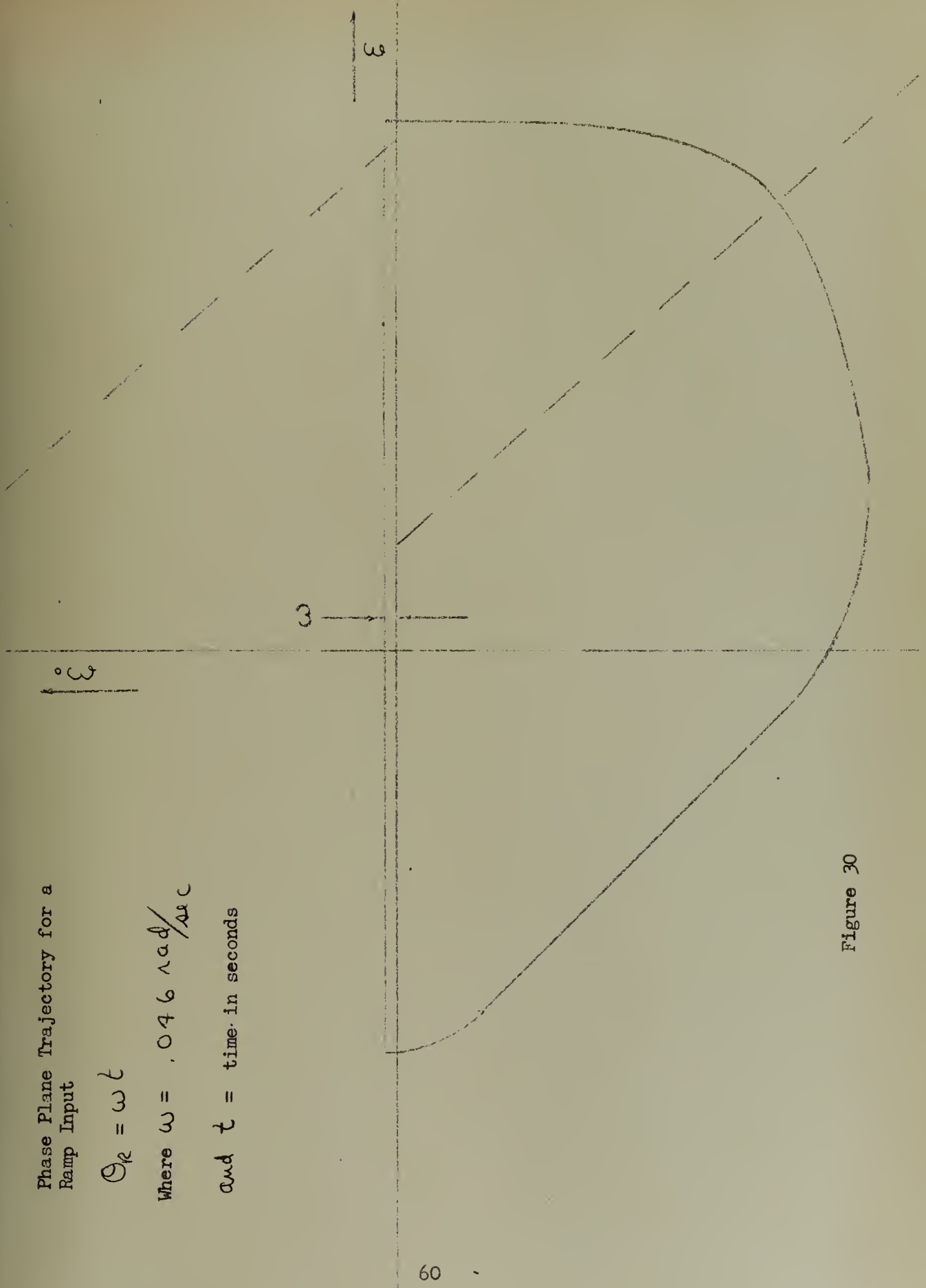
Figure 30

Inasmuch as the measurements for these runs consisted of tapes show-
ing $\dot{\epsilon}$ and $\dot{\theta}$, a conversion had to be made in order to portray ϵ_c
and $\dot{\epsilon}$. In order to do this first ϵ .was plotted against $\dot{\theta}$. Then a
horizontal line was drawn through the two points on the phase plane tra-
jectory where the slope was infinite. This line would be the zero error
rate line. The curve was replotted using ordinates to the zero error rate
line, thus effectively translating the horizontal axis. In both cases the
amount of translation necessary was equal to the scaled value of ω, which
fit the theory very well. In addition the ratio of the two translations
corresponded exactly with the ratio of the $\omega\dot{\epsilon}$ used, thus indicating that
the amount of translation of the zero error rate line varies linearly with
ω when a ramp input of ωt is introduced into a relay servo.

Another interesting point to be noted is the shifting of the dividing
lines in the positive error direction. While the dividing lines were
drawn according to theory, one can see that the lines are quite accurate
when one considers the time delay associated with the relay.

Another point in the analysis is the study to see whether a relay
servo system would operate satisfactorily when the tachometer was replaced
by an amplifier used as a differentiator. It is immediately obvious that
a system of this type would naturally be expected to have a great deal of
noise associated with it. Another disadvantage is that an amplifier with
a capacitor used as an input impedance would also probably produce a block-
ing effect in the event a large signal was introduced. The system finally
adopted included a small resistor in series with the input capacitor. The
schematic diagram is as shown in Figure 31. Figure 32 shows the phase

Schematic Diagram of the Relay Servo System with
both Error and Error Rate Feedback
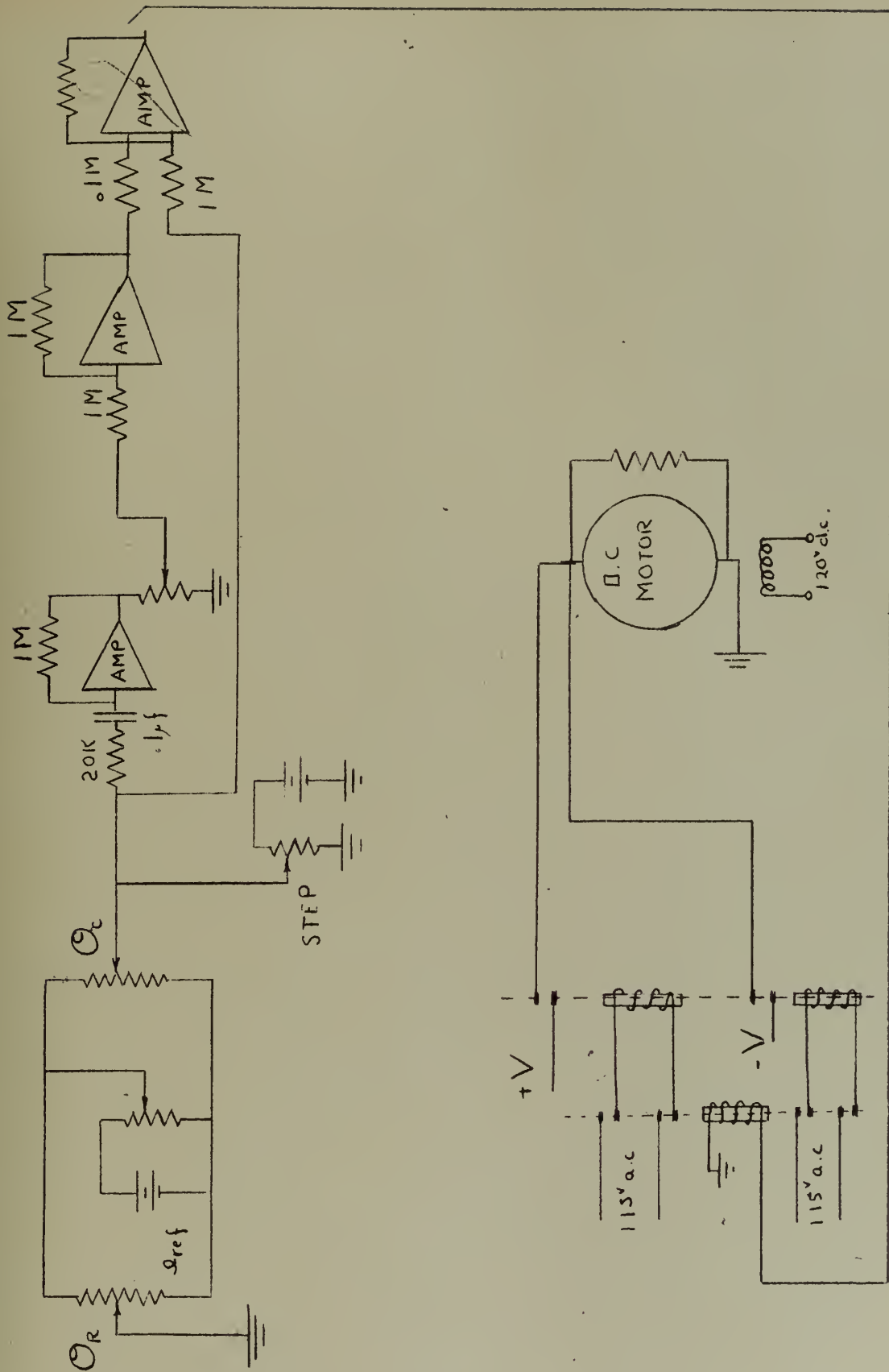
Figure 31

Figure 32. Phase Plane Trajectories For A Relay Servo System Response To A Step Input, and having Dynamic Braking in the Dead Zone, Error Feedback, and either Tachometer or Error Rate Feedback

Run 100   Large Step Input, Error and Error Rate Feedback

Run 101   Large Step Input, Error and Tachometer Feedback

Run 102   Small Step Input, Error and Tachometer Feedback

Run 103   Small Step Input, Error and Error Rate Feedback

63
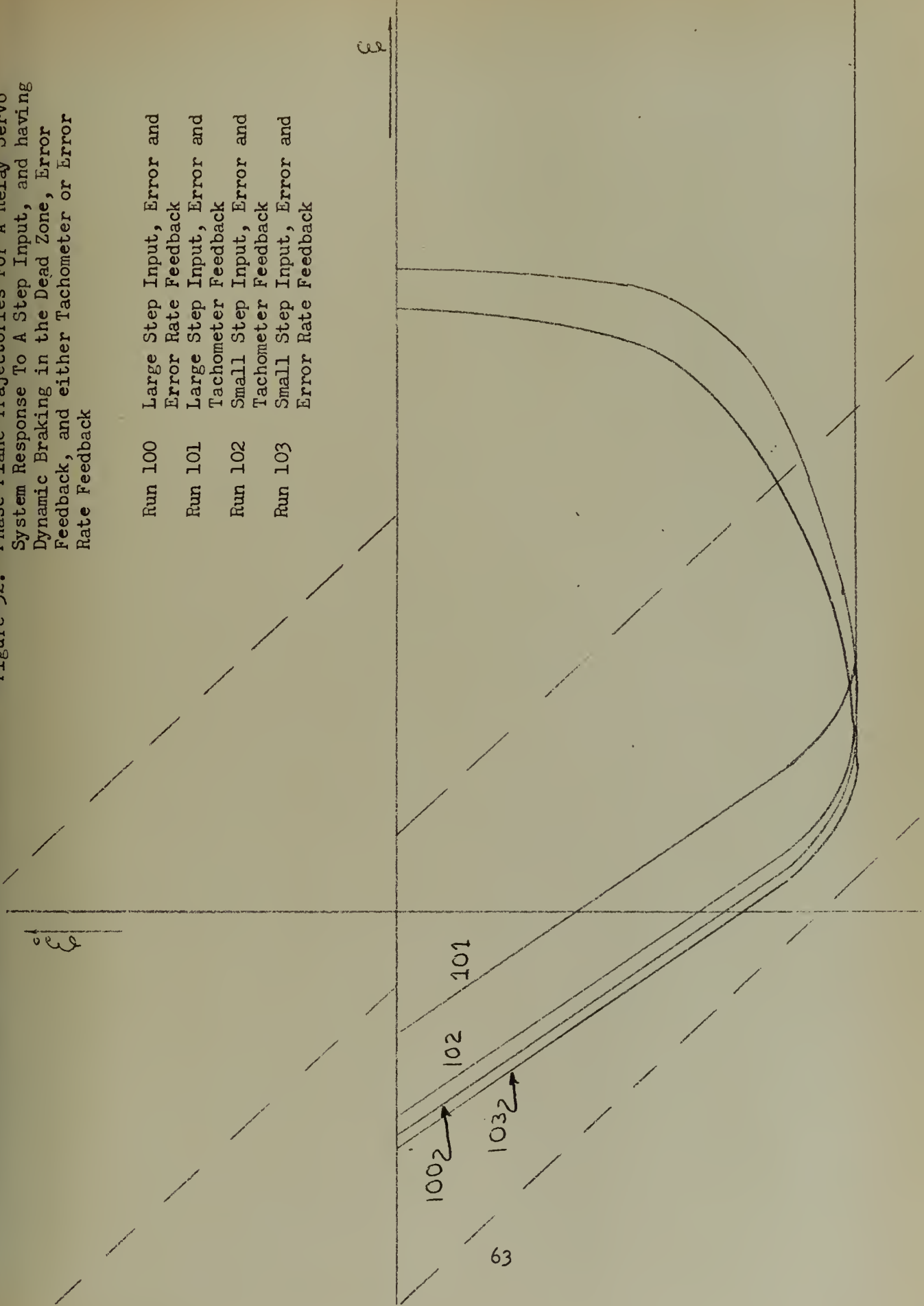
plane trajectories of runs made using this form of derivative feedback,
and with a step input. Also on this figure is portrayed to the same scale
runs made with the use of the tachometer. Figures 33 and 34 show the
Brush Recorder tapes of these runs. It is to be noted that while there is
quite a bit of noise associated with the runs using the derivative error
signal the characteristics of the two systems are remarkably similar. The
resistance used in series with the input capacitor to the derivative
amplifier was small enough so that the RC time constant was very small,
thus insuring fast action, and at the same time it was large enough to
prevent the noise from becoming too objectionable.

From these results the following conclusions may be drawn -

(1) If a positive ramp function is used for an input to a relay servo
having discontinuous damping furnished by a braking resistance and de-
rivative feedback furnished by a tachometer, all of the dividing (switch-
ing) lines will be displaced along the positive $\dot{\varphi}$ axis by an amount
$K_2/K_1 \omega$ where K_2 is the amplification of the error rate signal with
units of volt-sec per radian, K_1 is the amplification of the error signal
with units of volts per radian and ω is a measure of the input ramp in
radians per second. Since $\dot{\theta}_c$ is the measured quantity and not $\dot{\varphi}$,
it must be remembered that the zero $\dot{\varphi}$ axis is displaced from the zero
$\dot{\theta}_c$ axis by an amount ω .

(2) It is possible to use an error differentiator in a relay servo
in lieu of a tachometer provided precautions are taken to prevent ex-
cessive noise generation in the differentiator.

Brush Recorder Traces of Error and Error Rate with A
Relay Servo Subjected to a Large Step Input

Figure 33A. 25° Step Input, Error Rate Produced By An Error
Differentiator
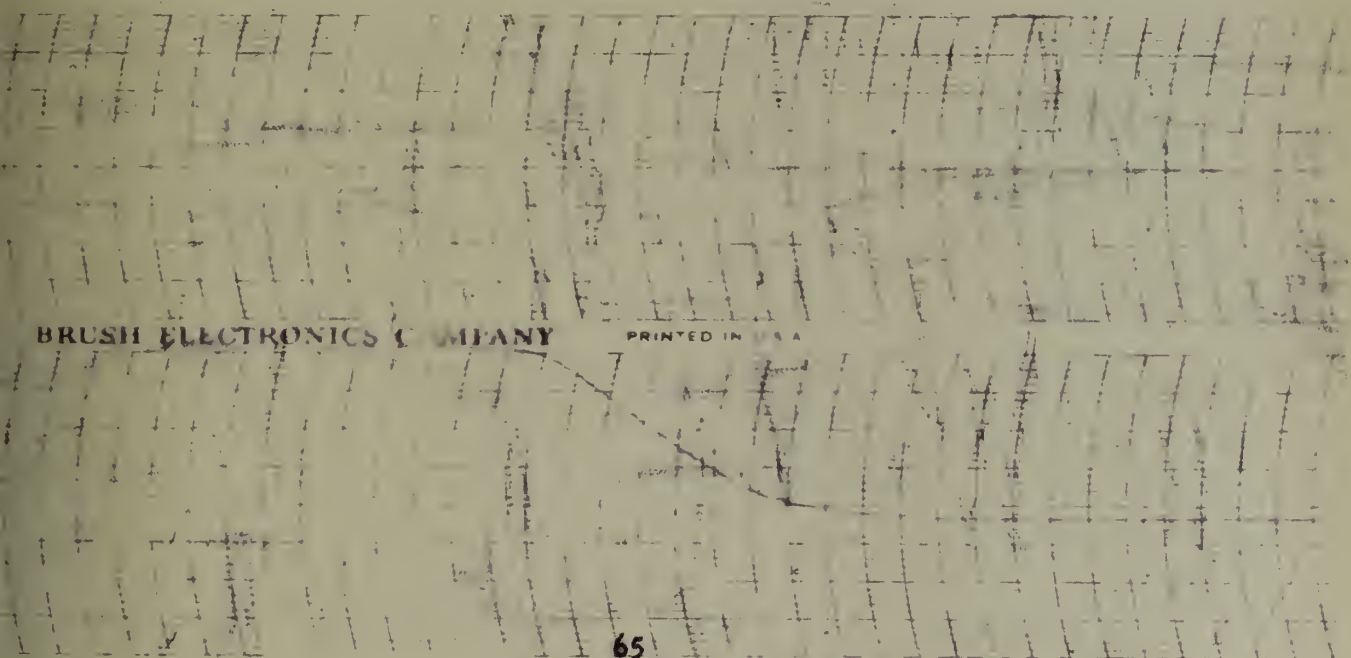
Figure 33B. 25° Step Input, Error Rate Produced By A
Tachometer

Brush Recorder Traces of Error and Error Rate
With A Relay Servo Subjected to a Small Step
Input

CHART NO BL 909   BRUSH ELECTRONICS COMPANY   PRINTED IN U
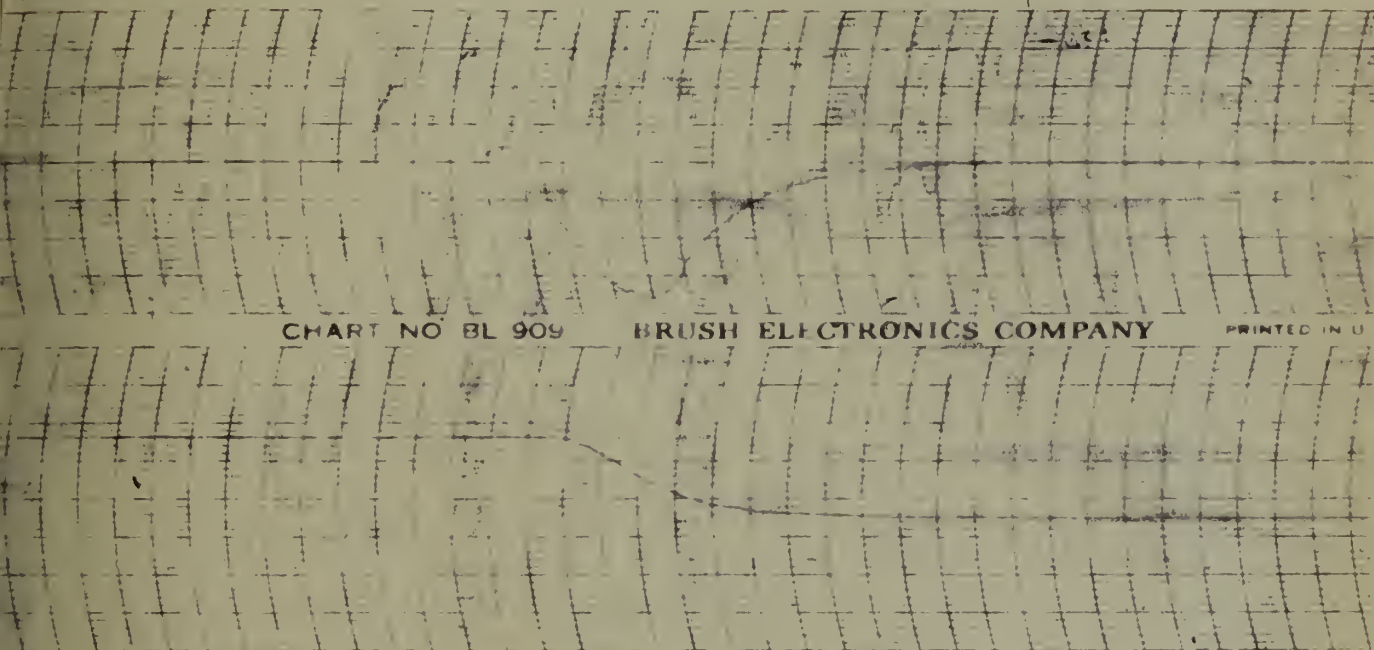
Figure 34A.   10° Step Input, Error Rate Produced
              by Tachometer

CHART NO BL 909   BRUSH ELECTRONICS COMPANY   PRINTE

66
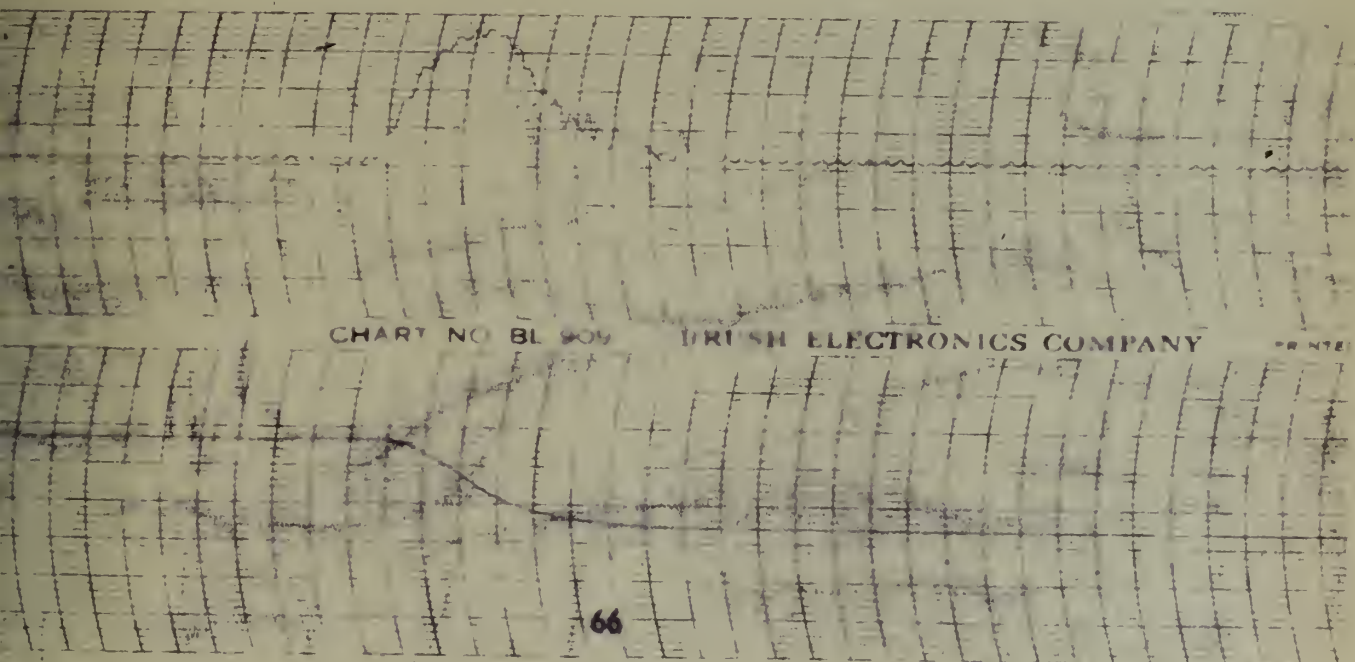
Figure 34B.   10° Step Input, Error Rate Produced by
              an Error Differentiator

CHAPTER VI

AN ANALYSIS OF A RELAY SERVO USING
USING A 1/125 HP MOTOR

In reviewing it is known from previous investigations that three effects cause the dead zone trajectory to depart from the ideal. These three factors are:

(1) the delay time associated with the relay,

(2) the inductance associated with the armature of the motor, which causes the dead zone trajectory to curve after relay drop-out and before ideal, (i.e. straight-line) braking becomes effective, and

(3) coulomb friction, which causes the dead zone trajectory to curve at small values of error rate.

In order to compare the relative effect of (2) and (3) among different relay servos, the L/R time constant of the braking circuit serves as a performance index of (2), and, as seen from the non-linear analysis, the performance index for (3) is the C/J ratio.

These three factors impose a practical limit upon the width of the dead zone wherein deadbeat performance can be expected for all sizes of step inputs.

In an effort to diminish the effect of some or perhaps all of these factors and also to investigate any similarities that exist between relay servos of various sizes, a relay servo using a 1/125 HP motor was selected to be investigated. This motor was modified such that the pressure of the brushes on the armature could be adjusted. It was hoped that lessening the pressure on the brushes to the point at which satisfactory commutation would still prevail would aid in reducing coulomb friction.

Several retardation runs were conducted using the system with a gear ratio of about 500:1 and the results were plotted in Figures 35 and 36. Figure 35 shows the results obtained when no braking was used, and it is interesting to note that the curves do not have the true straight line section that is the trademark of dynamically-braked retardation runs. Figure 36 portrays the results obtained when a braking resistor of 100 ohms was used. Notice that an appreciable part of the runs are straight indicating the effect of dynamic braking. In both figures the various curves are for different amounts of brush pressure.

In order to relate brush pressure, coulomb friction and the minimum dead zone width required because of coulomb friction, the straight line portion of the curve was extended until it intersected the zero velocity line. Then the difference between the value of error at this intersection and the value of error at which the motor actually stopped was taken as a measure of the minimum dead zone width required because of the effect of coulomb friction.

Retardation Curves

173 – Minimum Brush Pressure

174 ⎫
175 ⎬ Moderate Brush Pressure
    ⎭

176 – Excessive Brush Pressure

Figure 35

69
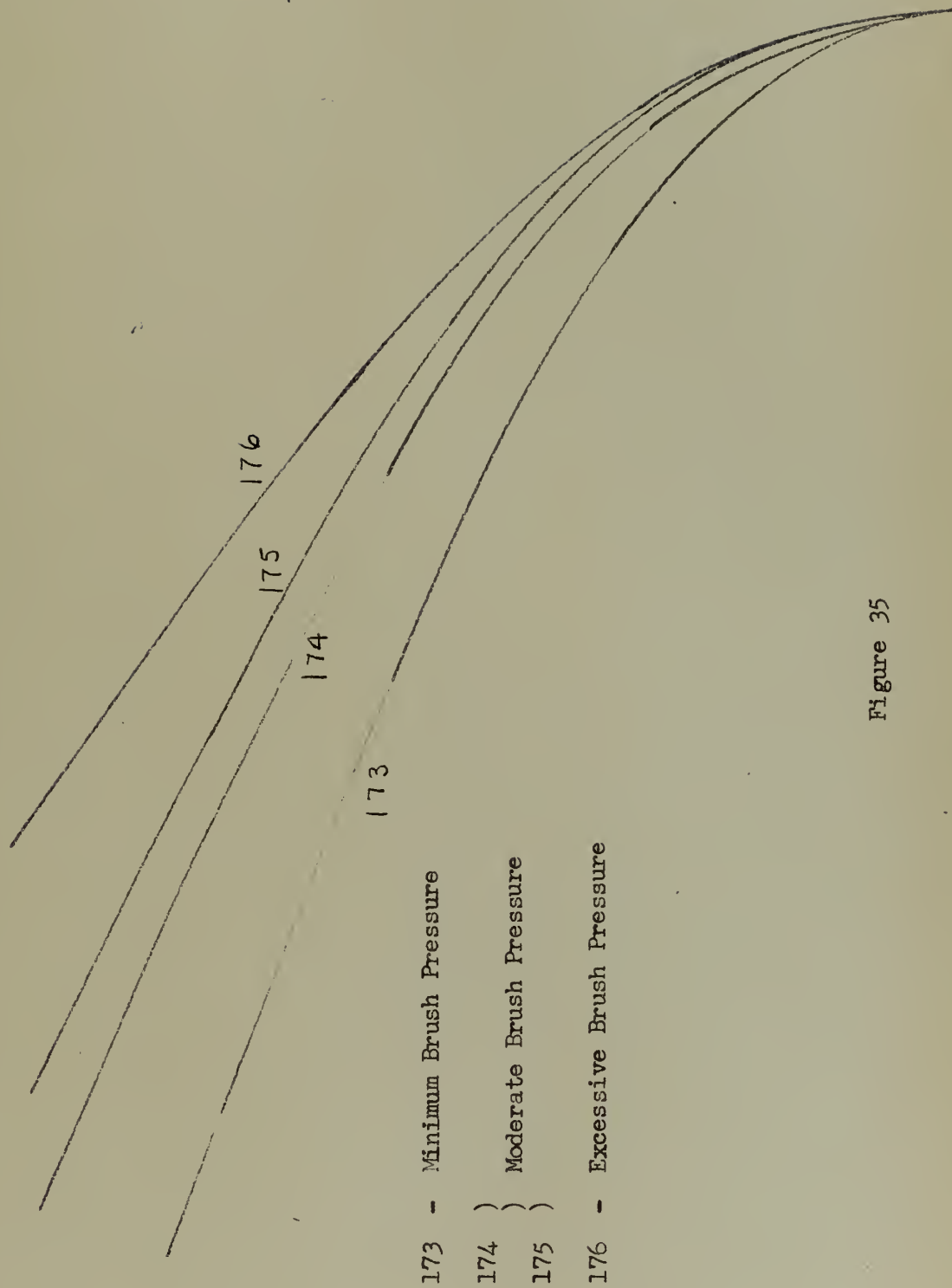
Retardation Curves

R_b = 100

201 — MINIMUM BRUSH PRESSURE

202 — MODERATE BRUSH PRESSURE

203 — EXCESSIVE BRUSH PRESSURE
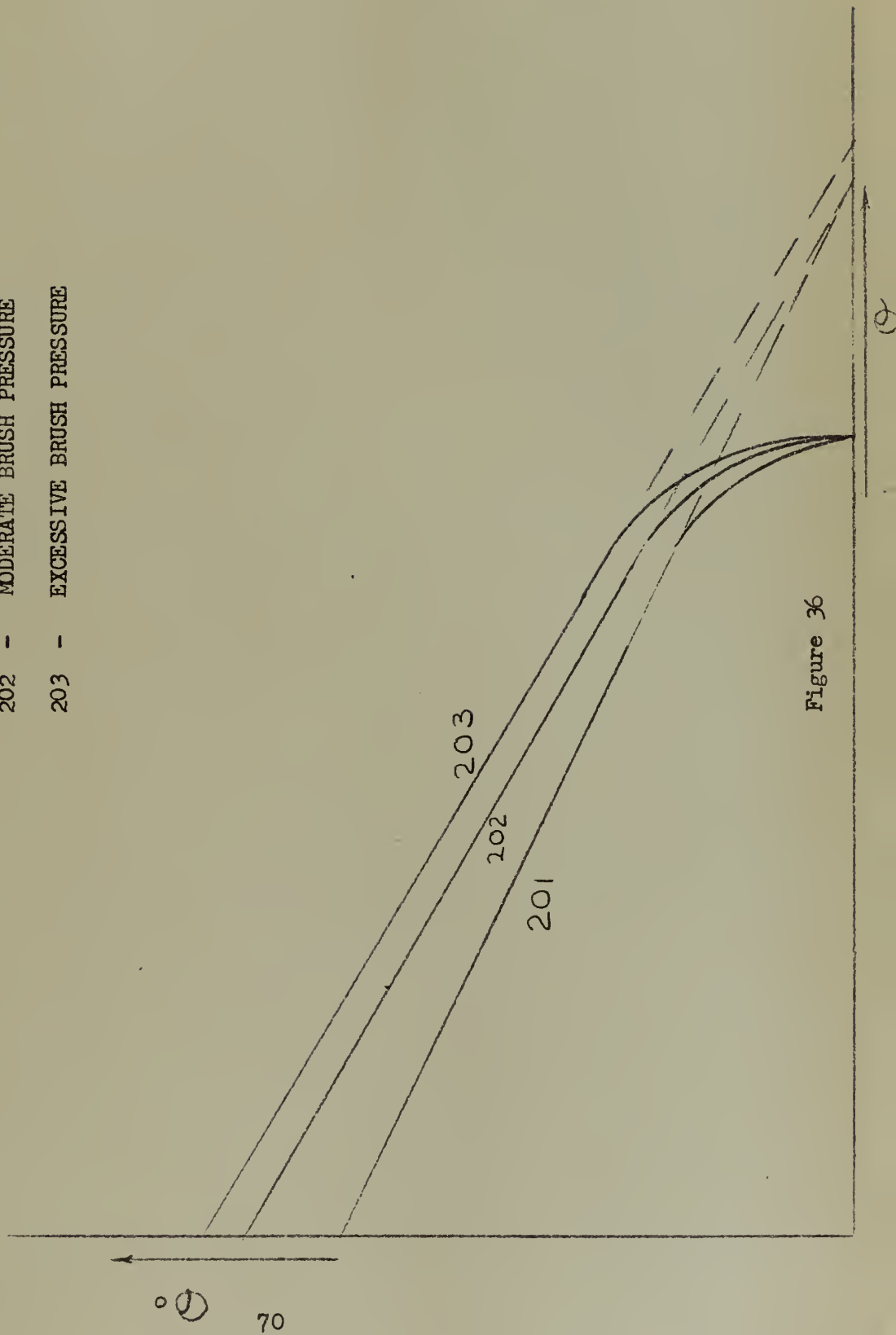
Figure 36

This idea is
shown in Figure
37 which shows a
dead zone and a
dead zone tra-
jectory. As can
be seen from the
illustration, the
following assump-
tions were made:

(1) that the
straight line sec-
tion of the dead
zone trajectory
is coincident with
a pull-in line.

(2) that the
trajectory brakes
to a stop just in-
side the opposite
pull-in line.
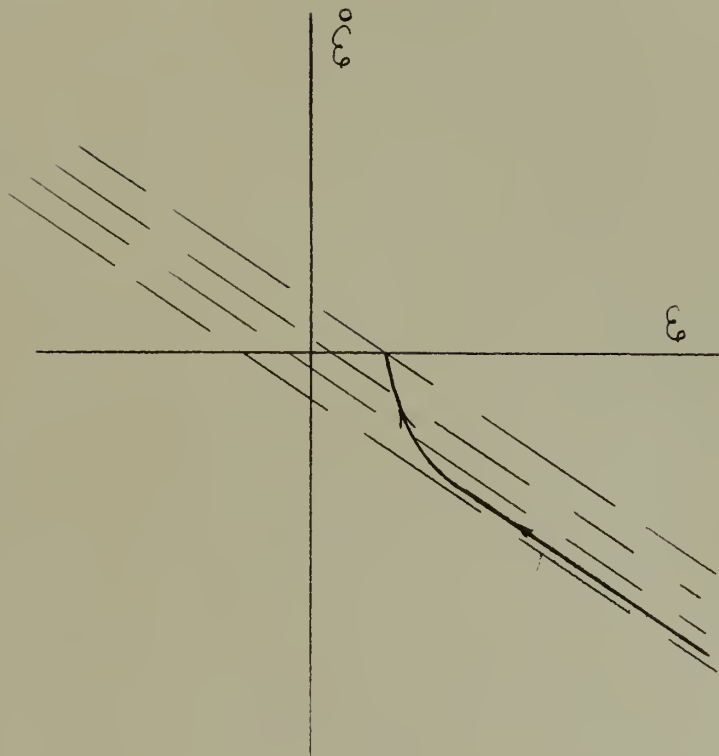
Figure 37. Phase Plane Showing the Effect
of Coulomb Friction on the Dead
Zone Trajectory

An analysis of several runs indicates that the dead zone width required
by moderate brush pressures is not appreciably greater than that required by
the minimum brush pressure that gives satisfactory operation. If the brush
pressure becomes great, however, the dead zone width must be appreciably
greater.

The reason for this phenomenon is shown in Figure 38.

1   MINIMUM BRUSH PRESSURE
2   MODERATE BRUSH PRESSURE
3   HIGH BRUSH PRESSURE
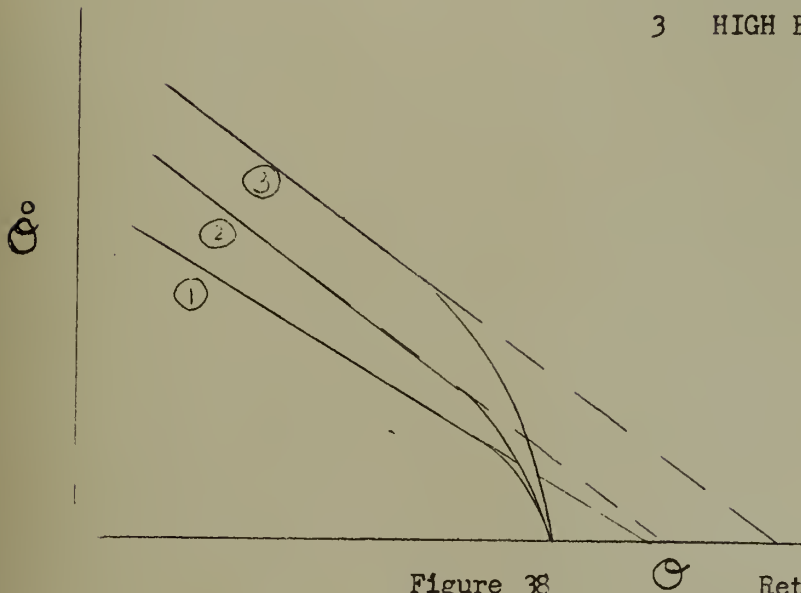
Figure 38.   Retardation Curves

As a general rule moderate brush pressures resulted in a retardation curve in which (1) the slope was greater than the retardation run in which minimum brush pressure was used because of an increased value of the dynamic friction coefficient, (2) the coulomb friction effect became appreciable at a higher value of velocity. The net effect was that the projections of the straight-line portion of the retardation curve intersected the zero velocity line at about the same point. With a large amount of brush pressure, however, the slope increased very slightly but the coulomb friction effect took place at a considerably greater velocity. The net effect of this was to cause the projection of the straight line portion to intersect the zero velocity line at a point which was farther from the point where the motor actually stopped than was the case for runs in which the brush pressure varied from minimum to moderate.

72

For the case of moderate brush pressure the slope of the switching lines must be increased from that used for minimum brush pressures which is simply a matter of decreasing the amount of derivative feedback, but the dead zone width need not be increased. For the case of heavy brush pressure, the dead zone width must be increased appreciably.

Inasmuch as a single relay could meet the current requirements, only one relay was used in this servo. The relay used was of the same type as the pilot relay used in the large (1HP motor) relay servo, and, therefore, the time delay associated with the main relays used in the large relay servo was eliminated. Therefore, it is entirely logical to expect that the delay time of the relay would be considerably smaller than was the case with the large relay servo.

It has been shown that the inductance of the armature or more properly the L/R time constant causes the dead zone trajectory to curve immediately after relay drop out instead of going abruptly to a straight line. For the small motor the L/R time constant was much smaller than in the case of the large 1 HP motor. The resistance of the armature was determined to be 285 ohms and a braking resistance of 100 ohms was used throughout the investigation. In order to show the time constant graphically, a small resistance was inserted in the armature circuit and a trace of armature current was obtained by means of a Brush Recorder. The trace of armature current is shown in Figure 40 and the trace for error is shown in Figure 39. Notice that the build-up of current in both directions is extremely rapid, since the paper speed is 125mm or 25 divisions per second. Therefore, it should develop that since the L/R time constant is small,

Error vs Time
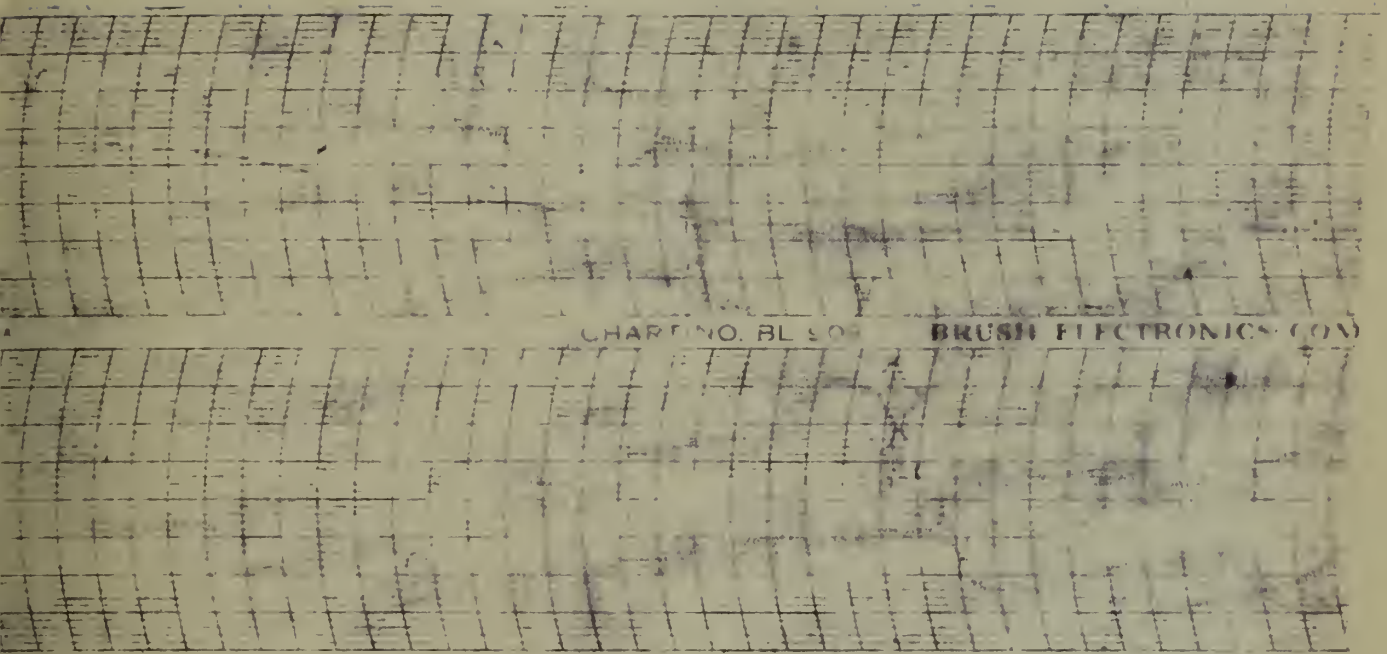
Figure 39

Armature Current vs Time

Figure 40

74
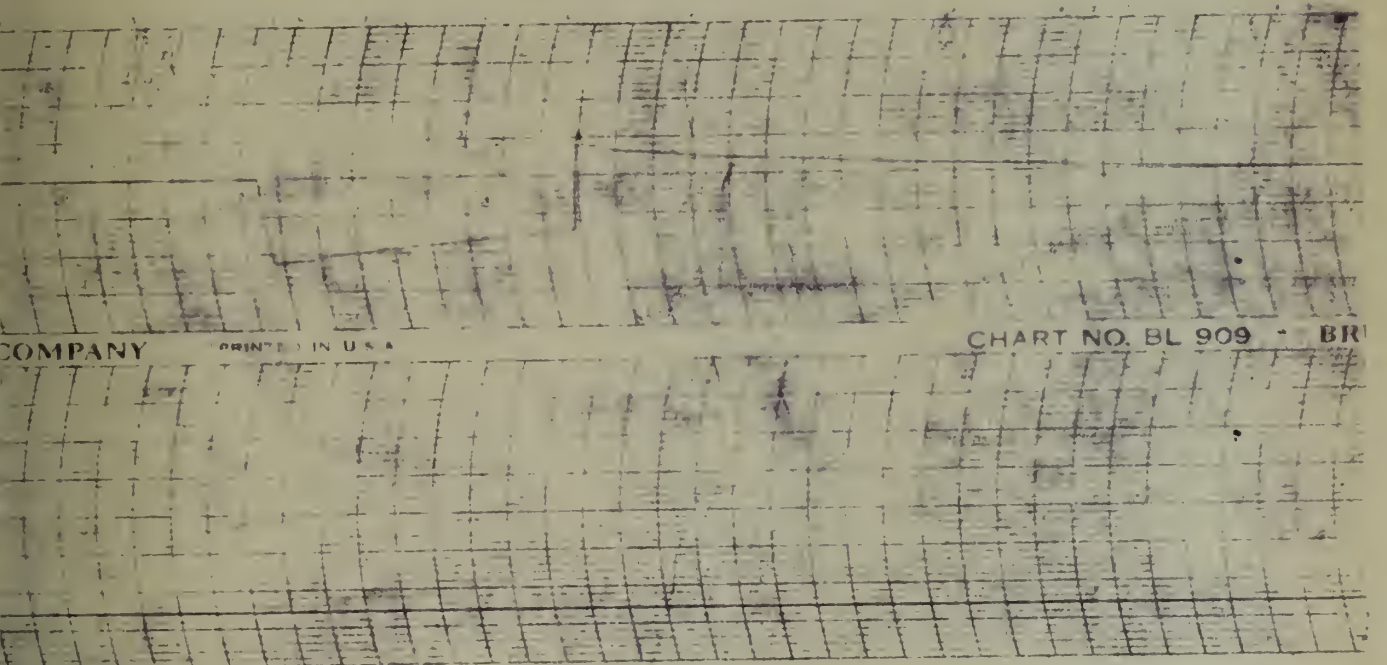
maximum braking should take place almost immediately after relay drop out. This means that the dead zone can be made small insofar as the allowance for the bending of the dead zone trajectory due to armature inductance is concerned.

In pursuing the investigation it was found that with rated voltage applied to the motor armature through the relay, an excessive time delay resulted at the point where the relay should have opened. It was noticed that the relay drew an appreciable arc after it opened. In fact, sometimes the arc persisted until the relay closed in the opposite direction and this meant that the dead zone did not exist at all for practical purposes. Hence, the armature supply voltage was reduced to 50 volts in order to obtain satisfactory operation. As a result of this, it may be said that the relay used in a servomechanism must be such that the arc is extinguished quickly or else the dead zone must be unreasonably wide.

During the initial phases of the investigation with the relay servo, a gear ratio of about 50:1 was employed between the motor, which had a rated speed of 4000 rpm, and the potentiometer. The phase plane trajectories for this system are as shown in Figure 41. The relay dead zone corresponded to a potentiometer rotation of thirty degrees and it is to be noted that while the dead zone could be made smaller, it is doubtful if the dead zone width could be made to approach any reasonable value if deadbeat operation for all sizes of step inputs is to be expected. Accordingly it was decided to increase the gear ratio to about 500:1 to see if improved performance would result.

After several preliminary adjustments it was immediately apparent that the dead zone could be made considerably smaller. Figure 42 shows

75

Phase Plane Trajectories for Dynamic Braking, Derivative
Feedback, and a Thirty Degree Dead Zone

Run 130   18 degree step input
Run 131   25 degree step input
Run 132   40 degree step input
Run 133   60 degree step input
Run 134   90 degree step input
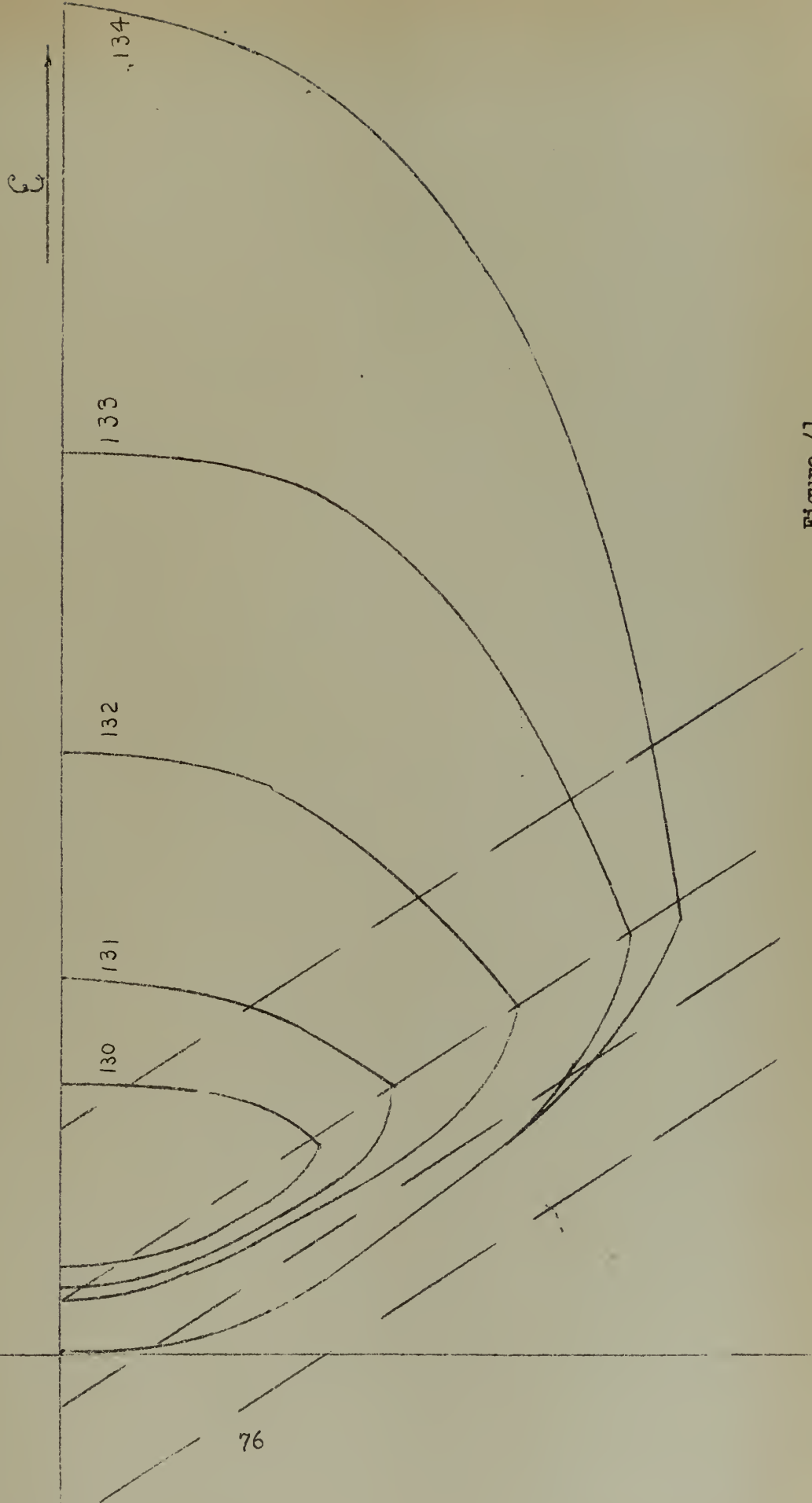
Figure 41

Phase Plane Trajectories for Derivative Feedback,
Dynamic Braking and a Four Degree Dead Zone

Run 150   Three degree step input
Run 151   Five degree step input
Run 152   Ten degree step input
Run 149   Fifteen degree step input

Figure 42

77
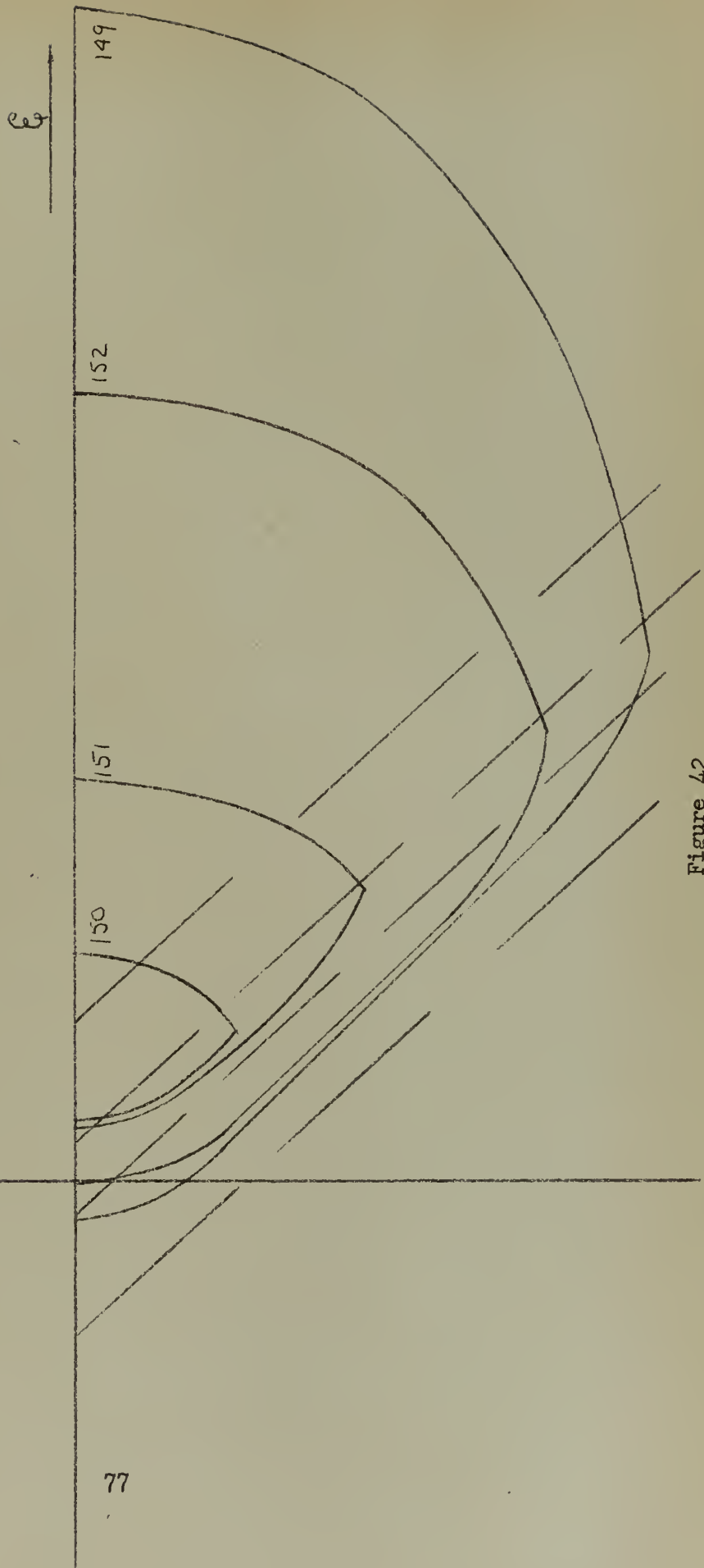
the results obtained when a four degree dead zone was used. Figure 43 portrays the dead zone trajectories for a dead zone width of three degrees. Figure 44 illustrates the results obtained for a dead zone width of two degrees and Figure 45 portrays the results obtained for a 1.5 degree dead zone. The dashed lines show the two pull-in lines and the two drop-out lines, while the solid lines show the dead zone trajectories. The maximum step input used in these investigations was roughly a factor of 3.5 times the dead zone width. The reason for this is that the amplifiers used would saturate at a value of voltage roughly seven times the voltage required to pull-in the relay, and, when the amplifier saturated at the beginning of the run, unsatisfactory results inevitably ensued. Notice that in all of the phase plane trajectories there is a small region immediately after relay drop-out where the dead zone trajectory is curved. This bending is not so marked as it was in the case of the 1 HP motor relay servo, but, nonetheless, it is present. This follows logically from the arguments advanced at the beginning of the chapter, namely, that the L/R time constant was small, and, therefore, the bending of the dead zone trajectory should be small. Notice also that the straight line is present until the error rate becomes small at which time the trajectory inclines toward the vertical. This again agrees with the theory that when error rate becomes small, the C/J ratio would cause the slope of the trajectory to approach negative infinity. Also due notice should be taken of the relatively small amount of delay time associated with the relay. The slope of the trajectory becomes discontinuous soon after relay drop-out should occur. The reason for this is that there is a much shorter time delay associated with the one relay as compared with the time delay associated with the double relay.

78

Figure 43. Phase Plane Trajectories Showing a Relay Servo Response to Step Inputs with Derivative Feedback, Discontinuous Damping, and A Dead Zone Width of Three Degrees

Figure 44. Phase Plane Trajectories Showing a Relay Servo Response to Step Inputs with Derivative Feedback, Discontinuous Damping and a Dead Zone Width of Two Degrees.

——— Switching Lines

——— Trajectories

Run 170   Two Degree Step

Run 169   Four Degree Step

Run 168   Six Degree Step
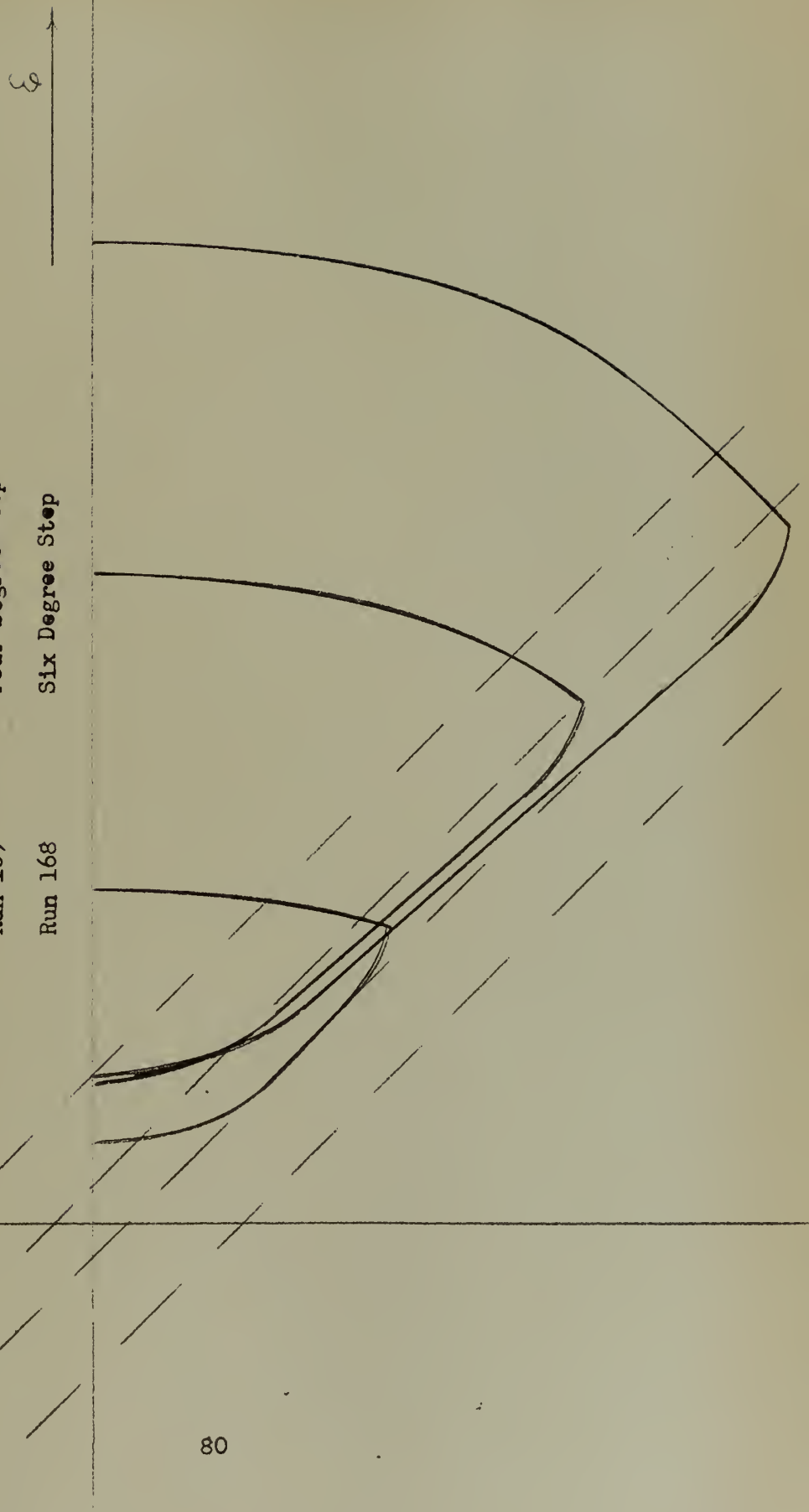
Phase Plane Trajectories for Dynamic Braking, Derivative Feedback, and a 1.5 degree dead zone
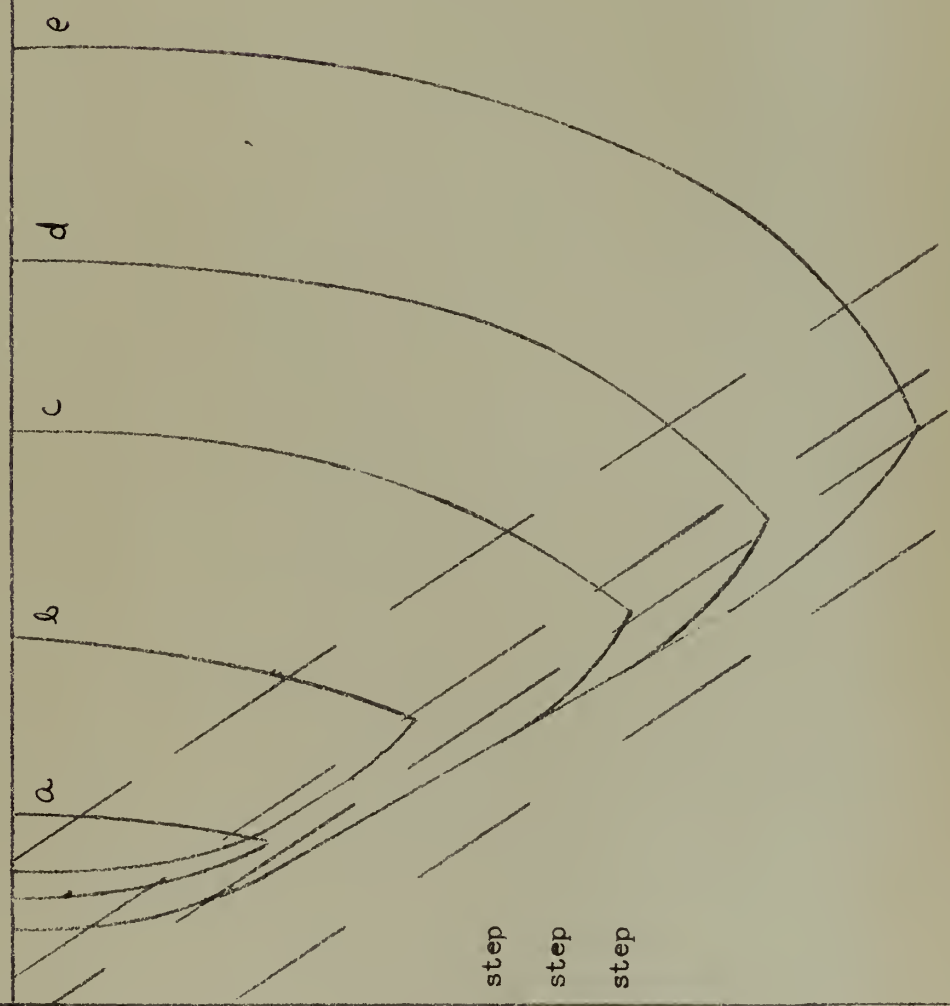
Figure 45.

a – one degree step
b – two degree step
c – three degree step
d – four degree step
e – five degree step

81

Conclusions:

(1) In any relay servomechanism using a DC shunt motor with dynamic braking in the dead zone, there will be a curvature of the dead zone trajectory immediately after relay drop-out due to the L/R time constant preventing maximum effective braking from transpiring until after about four time constants (t=4 L/R) have elapsed. There will also be a curvature at the end of the trajectory when error rate is small because of the C/J ratio. Any measure adopted to make these ratios small will inevitably result in improved performance from the standpoint of minimum dead zone width required to provide deadbeat performance for all sizes of step inputs. Of course, the two ratios should both be made small inasmuch as effects of each is such as to increase dead zone width.

(2) The relay used in a relay servomechanism should have two requirements:

(a) The delay time associated with the relay should be as small as possible, since this delay time will tend to increase the required dead zone width.

(b) The arcing over at the time the relay drops out should be all but eliminated if satisfactory operation is to result.

(3) Increasing the gear ratio aids materially in decreasing the dead zone width required to provide for deadbeat operation for all sizes of step inputs. One can reasonably expect that an increase in the gear ratio will result in a decrease of dead zone width in about the same proportion.

(4) Due to the effect upon the amount of coulomb friction present, attention should be given to insuring that the pressure upon the brushes of the motor and the tachometer is not excessive.

82

CHAPTER VII

A COMPARISON BETWEEN OPTIMUM AND
QUASI-OPTIMUM SWITCHING

In order to discuss optimum switching, it is first necessary to de-
fine explicitly the characteristics of a relay servo in which optimum
switching takes place. The characteristics are in general:

(1) The response to a step input shall consist of one period of
acceleration and one period of deceleration (as long as the servo is
second order to a good approximation). During both periods full voltage
is applied to the servo motor, and the voltage applied during acceleration
is exactly equal and opposite to the voltage applied during deceleration
for a direct current servo system.

(2) The dead zone is of infinitesimal width

(3) The relay servo always stops at precisely zero error.

In the quasi-optimum case, the acceleration period is precisely the
same as in the optimum case, but the deceleration period is characterized
not by power application but rather of an increased amount of damping over
the damping present during the acceleration period. This thesis is con-
cerned with the special case where the discontinuous damping is provided
by dynamic braking.

It was felt that it would be interesting to compare the transient
responses to a step input for the case in which optimum switching was
simulated and for the case in which quasi-optimum switching was actually
used. In order to accomplish this comparison, a response to a step input
was obtained with the system functioning normally; this is with dynamic
braking in the dead zone and a dead zone wide enough to insure deadbeat
performance. Then with all other things being equal, the normal operat-
ing mechanism was de-energized and the relay was operated manually. The

83

motor was allowed to accelerate until zero error had been reached and then
the relay was instantly reversed wherein a decelaration trajectory with
power application was obtained. The deceleration trajectory was trans-
lated in the positive error direction until the static error at zero error
rate agreed with the static error obtained with dynamic braking. The
intersection of the translated deceleration trajectory and the acceleration
trajectory would be the point where optimum switching would occur if the
system was constructed with that in mind.

The two trajectories were then plotted in Figure 46 and instants of
time in 1/25ths of a second were placed adjacent to corresponding points
on the trajectories. In order to afford a clearer understanding of the
transient response, the transient curves were drawn on a graph of error
vs time in Figure 47. Notice in Figure 47 that the curves do not separate
markedly at the point of actual relay drop-out with the quasi-optimum
system as one might be inclined to imagine, but rather the separation is
quite gradual, and that the time of response for the quasi-optimum system
is not too much greater than the time of response for the optimum system.

Phase Plane Trajectories for a Relay Servo Employing
Optimum Switching and Quasi-optimum SWITCHING with
Dynamic Braking

A - Point of Relay Drop-out for the Quasi-optimum Case
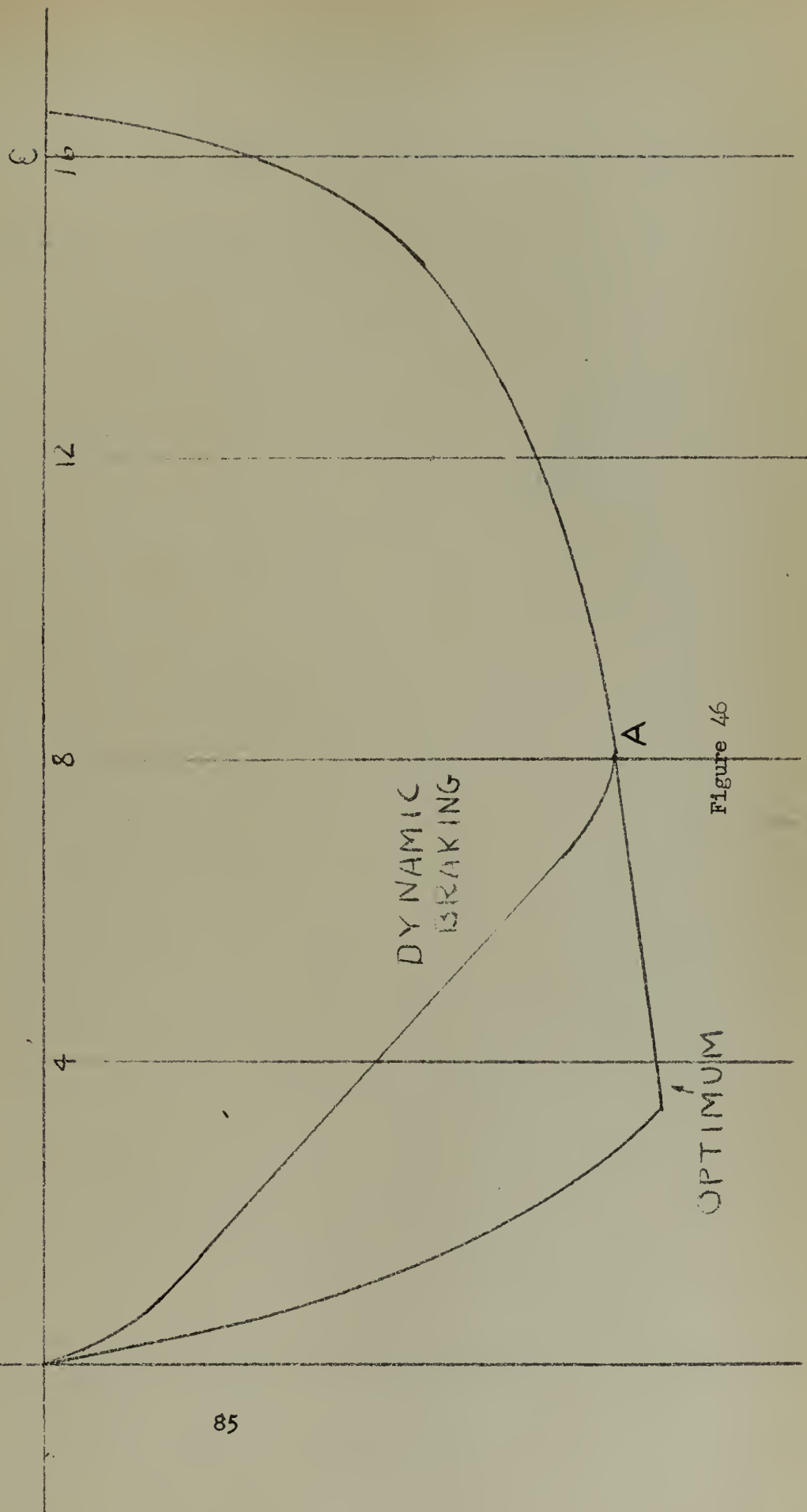
Figure 46

TRANSIENT RESPONSE CURVES FOR
A RELAY SERVO EMPLOYING Optimum
Switching and Quasi-Optimum
Switching with Dynamic Braking

A - POINT OF RELAY
DROP-OUT
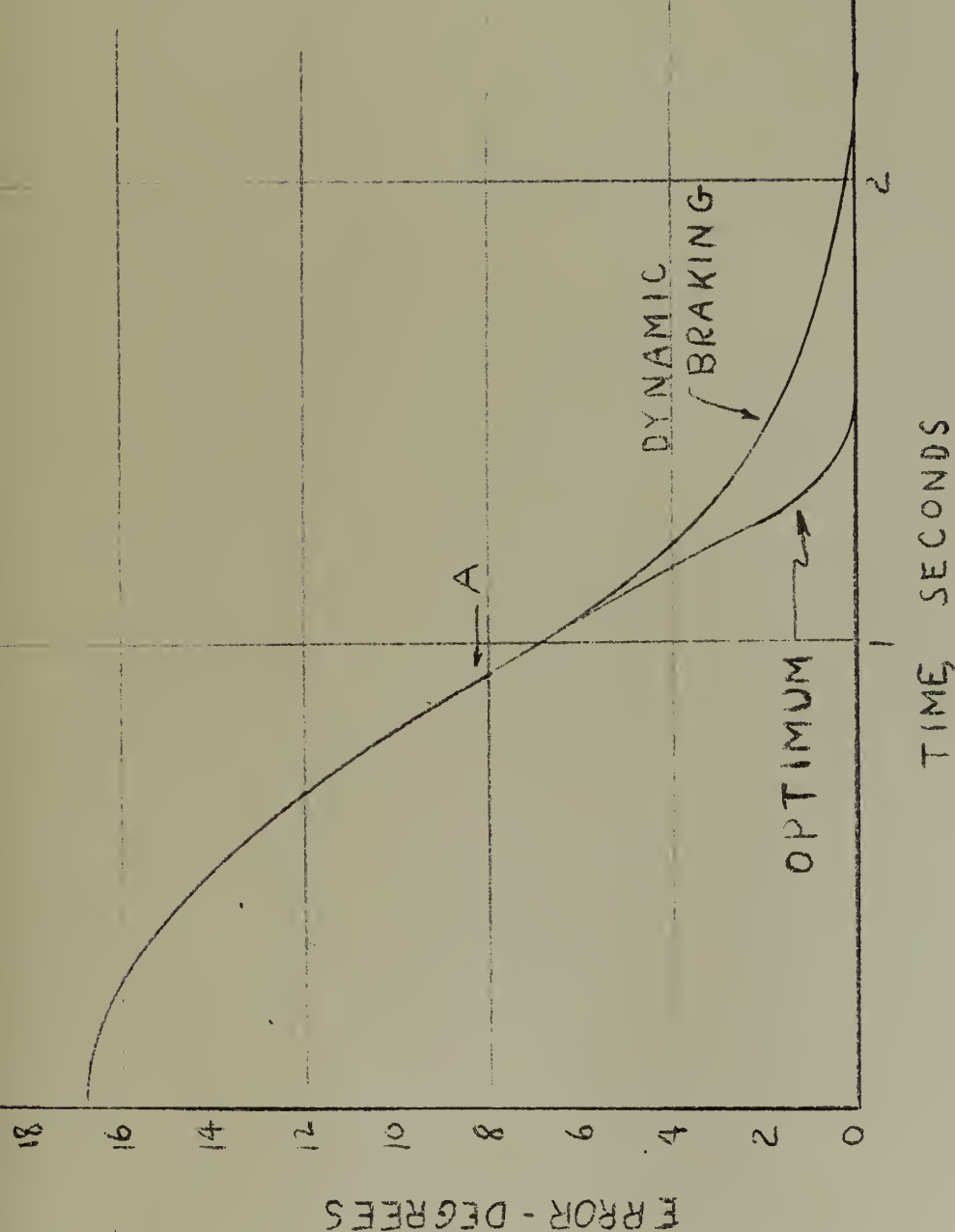
Figure 47

Conclusions:

In comparison with the optimum relay servo, the advantage of simplicity in the quasi-optimum relay servo employing derivative feedback and discontinuous damping far overshadows the small increase in response time to a step input.

CHAPTER VIII

AN INVESTIGATION OF INDUCTIVE
BRAKING

1. INTRODUCTION. The investigation of the effect of discontinuous damp-
ing of a relay servo using a DC shunt motor with resistance braking
indicates the value of a dissipative circuit which can be effectively
utilized to dissipate the stored kinetic energy of the motor armature.
This type of braking, however, is not as effective theoretically as the
optimum relay switching system wherein full reverse power is applied to
the motor. From the standpoint of overall speed of response and dead zone
width, the optimum servo is theoretically faster. This chapter is devoted
to the analysis of a system which will approach and possibly surpass the
optimum switching system in overall performance.

The principal difference between this system and the resistance braking
discontinuous damping system is that an energy storage device is incorpo-
rated into the braking circuit. The function of the energy storage device
is to release its energy at a controlled rate after the relay drops out and
the phase plane trajectory enters the dead zone. This release of energy if
correctly applied will act to counter the rotational kinetic energy of the
motor. In the relay servo using a DC shunt motor, the energy storage
device is an inductance and its associated resistance.
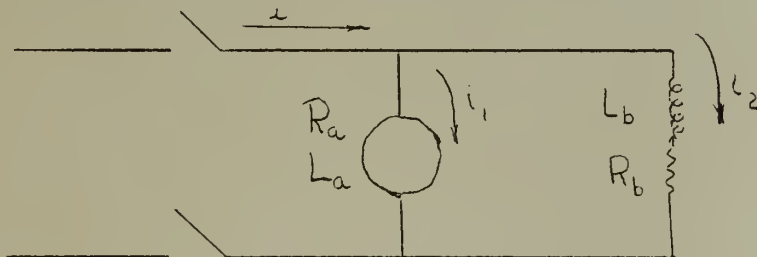
Figure 48. Schematic Diagram Showing DC Shunt Motor, Relay,
and Braking Circuit

88

In Figure 48 it is to be noted that if the braking resistance was not present, oscillations would occur if the armature resistance was small in comparison with the moment of inertia of the armature and the inductance of the braking circuit. This is not considered to be a good characteristic, and, indeed, would likely result in several relay reversals and perhaps a limit cycle. It is much more desirable to obtain a straight line for the dead zone trajectory in order that the dead zone may be made as narrow as possible. Therefore, both the resistance and the inductance in the braking circuit must enter into the calculations. Finally, it should be noted that the current in the braking circuit during the acceleration period is in such a direction that if it were to continue after relay drop-out, the current in the motor would reverse and be in such a direction as to increase deceleration.

In Figure 48 it is to be noted that the currents i_1 and i_2 are in the directions indicated when the relay drops out. At the instant of relay drop-out there will be a transient phenomenon which is somewhat difficult to analyze quantitatively. There is an inductance in the braking circuit, and an inductance associated with the armature. It is known that the current cannot change instantaneously in a circuit with an electrical inductance in it. Also, as soon as the relay opens to break the current in the relay, a single-valued current must flow in the loop which includes the braking inductance-resistance combination and the motor armature. How then to resolve the inconsistency of two currents of different magnitudes, changing instantaneously, one of them even reversing in direction, to two new currents which have the same magnitude? It is theoretically possible to open the relay contacts so quickly that no energy transfer will occur across the

contacts. However, it is believed that while the currents are undergoing a readjustment some arcing must transpire at the relay contacts. This analysis of the problem, however, does not solve the problem of the correct initial value of current to assume flowing through the motor at the start of the dead zone trajectory. This problem is difficult in that not only the inductance and the resistance of the armature and the braking circuit must be considered, but also the characteristics of the relay are involved.

Perhaps the best approach to the problem is to consider the energy relationships. At the instant of relay drop-out there is energy stored in the armature and braking inductance in the amount of $\frac{1}{2} L_a i_1^2$ and $\frac{1}{2} L_b i_2^2$ respectively. After equilibrium conditions prevail the back emf of the motor will produce a current i in the same direction as i_2, the opposite direction of i_1. Also since L_b is large with respect to L_a, it is plausible to believe that the resultant current after drop-out will be much closer to i_2 than i_1. If it is possible to associate direction with energy, it is seen that the energies in the two inductances tend to oppose one another and that the magnitude of the current after equilibrium conditions prevail should be somewhat less than the magnitude of either of the two currents. In order to attempt to sum electrical energies before and after relay drop-out, the equation which seems best suited would be:

$$\frac{1}{2} L_b i_2^2 - \frac{1}{2} L_a i_1^2 = \frac{1}{2} \left(L_a + L_b \right) i^2 + \frac{1}{2} E_R$$

E_r is a term used to account for twice the energy loss due to arcing at the relay.

$$i^2 = \frac{L_b i_2^2 - L_a i_1^2 - E_R}{L_a + L_b}$$

If no energy loss occurred at the relay

$$i'^2 = \frac{L_b i_2^2 - L_a i_1^2}{L_a + L_b}$$

where i' is the amount of current that would flow if no energy loss occurred at the relay.

Now define C_2 to be equal to $\sqrt{\dfrac{E_R}{L_b i_2^2 - L_a i_1^2}}$

Then
$$i^2 = i'^2 - C_2^2 i'^2$$

$$= i' \sqrt{1 - C_2^2}$$

The quantity $\sqrt{1 - C_2^2}$ is hereafter termed F, for figure of merit of the relay. This figure of merit is assumed to be a constant for any particular relay. Notice, however, that both intuitively and mathematically F must be less than one and if L_b is much greater than L_a, F must always be greater than zero.

In the ensuing analysis the effects of a change in F upon the dead zone trajectory shall be considered. Also an investigation will be made of the effect of changing L_b, while maintaining the L_b/R_b ratio constant.

91

PHASE PLANE ANALYSIS

The next step in the logical process of analyzing the behavior of
a relay servo with inductive braking is perhaps to graphically portray the
dead zone trajectory on the phase plane. The trajectory during acceleration
is assumed to be substantially the same as for the system in which resist-
ance braking was used. However, with an inductance in the braking circuit,
certain questions arise such as - for a given motor, what is the ideal
amount of inductance and resistance in the braking circuit? Is a straight
line possible for the trajectory on the phase plane? How will the time of
response compare with simple resistance braking and with the optimum case?
How does a change of both inductance and resistance affect the characteris-
tics? And what about the characteristics if the relay is not perfect and
energy transfer takes place across the relay? These and many more questions
should be answered in order to obtain a complete understanding of the subject.

In order to answer some of the questions that have been raised, it is
perhaps advisable to construct phase planes depicting the dead zone tra-
jectories if that is possible. Therefore, it seems logical to commence the
analysis by attempting to determine the equations of the isoclines so that
the dead zone trajectory under conditions of inductive braking may be con-
structed.

DETERMINATION OF THE ISOCLINE EQUATIONS

To begin with, it is assumed that (1) f, the coefficient of dynamic
friction, is zero, because under most operating conditions it is indeed
small and (2) C, the coulomb friction factor, is zero not because it is
necessarily small, but because it markedly complicates the analysis. How-

92

ever, from previous investigations, it is known that (1) it varies from
machine to machine and (2) if it is considerable it will affect the dead
zone trajectory only when $\dot{\Theta}$ ($\epsilon\epsilon$ $\dot{\iota}$) is small. Specifically, it causes
the steady state position to lie somewhat short of the position it would
otherwise have obtained if coulomb friction had not been present. If the
displacement caused by coulomb friction is small, it will affect the static
accuracy of the relay servo to some extent, but it will not cause the
system to step forward because of the separation of the drop-out and pull-in
lines that is associated with the practical relay.

Under these assumptions, it is known that the following two equations
are very good approximations of the system behavior in the dead zone—

$$\left(L_a + L_b\right)\dot{\iota} \cdot \iota\left(R_a + R_b\right) + K_v\,\dot{\Theta} = 0 \qquad (1)$$

$$K_t\,\iota = J\,\ddot{\Theta} \qquad (2)$$

Differentiating (2) with respect to time, the following results

$$K_t\,\dot{\iota} = J\,\dddot{\Theta} \qquad (3)$$

$$\text{Let} \quad L_a + L_b = L$$

$$\text{and} \quad R_a + R_b = R$$

$$L\,\dot{\iota} + \iota R + K_v\,\dot{\Theta} = 0 \qquad (4)$$

Then

$$L\,\dot{\iota} + \iota R + K_v\,\dot{\Theta} = 0 \qquad (4)$$

Substituting (2) and (3) in (4),

$$\frac{LJ\dddot{\Theta}}{K_t} + \frac{RJ}{K_t}\ddot{\Theta} + K_v\dot{\Theta} = 0 \qquad (5)$$

Simplifying

$$LJ\dddot{\Theta} + RJ\ddot{\Theta} + K_v K_t \dot{\Theta} = 0 \qquad (6)$$

Equation (6) may be integrated to obtain

$$LJ\ddot{\Theta} + RJ\dot{\Theta} + K_v K_t \Theta = C_1 \qquad (7)$$

The basic problem now is to evaluate C_1. When the system has reached its steady state point and $\ddot{\Theta} = \dot{\Theta} = 0$,

$$\Theta = \frac{C_1}{K_v K_t} \qquad \text{the steady state term assuming } \Theta = 0$$

at $t = 0$.

From the analytical solution in Chapter IV, it is known that if $\Theta = 0$ at $t = 0$

$$\Theta_{(ss)(t=\infty)} = \frac{RJ\dot{\Theta}_o + LK_t \dot{\iota}_o}{K_v K_t} \qquad (9)$$

Therefore

$$C_1 = RJ\dot{\Theta}_o + LK_t \dot{\iota}_o$$

or $$C_1 = LJ\left[\frac{R}{L}\dot{\Theta}_o + \frac{K_t}{J}\dot{\iota}_o\right] \qquad (10)$$

To continue, equation (7) may now be written -

$$\overset{\circ\circ}{\Theta} = -\frac{RJ}{LJ}\overset{\circ}{\Theta} - \frac{K_v K_t}{LJ}\Theta + \frac{R}{L}\overset{\circ}{\Theta}_0 + \frac{K_t}{J}i_0 \quad (11)$$

$$\frac{\dfrac{d^2\Theta}{dt^2}}{\dfrac{d\Theta}{dt}} = \frac{d\overset{\circ}{\Theta}}{d\Theta} = -\frac{R}{L} - \frac{K_v K_t}{LJ}\frac{\Theta}{\overset{\circ}{\Theta}} + \frac{\dfrac{R}{L}\overset{\circ}{\Theta}_0 + \dfrac{K_t}{J}i_0}{\overset{\circ}{\Theta}}$$
$$(12)$$

In order to obtain the isocline equations -

let $\quad N = \dfrac{d\overset{\circ}{\Theta}}{d\Theta}$

then $\quad N = -\dfrac{R}{L} - \dfrac{K_v K_t}{RJ}\left(\dfrac{R}{L}\right)\dfrac{\Theta}{\overset{\circ}{\Theta}} + \dfrac{\dfrac{R}{L}\overset{\circ}{\Theta}_0 + \dfrac{K_t}{J}i_0}{\overset{\circ}{\Theta}}$
$$(13)$$

At this point it would perhaps be wise to recognize that some widely-accepted abbreviations may be substituted.

Note particularly that -

$$\frac{L_a + L_b}{R_a + R_b} = \frac{L}{R}$$

is the electrical time constant, which will be denoted by τ_e'.

$$\frac{(R_a + R_b)J}{K_v K_t} = \frac{RJ}{K_v K_t}$$

is the mechanical speed time constant if L/R is small compared with

$\dfrac{RJ}{K_v K_t}$. It will be denoted by τ_m'. The derivation of the mechanical

speed time constant may be found in THALER and STEIN (4).

Also let

$$\frac{L_a}{R_a} = \tau_{e_1}$$

$$\frac{L_b}{R_b} = \tau_{e_2}$$

$$\frac{J}{K_t} = k_m$$

$$\frac{R_a J}{K_v K_t} = \tau_m$$

Let the closest approximation possible to the true mechanical speed time constant be τ_{m_a} and $p = \dfrac{\tau_{m_a}}{\tau_m}$

Substituting in (13),

$$N = -\frac{1}{\tau_e'} - \frac{1}{\tau_m'} \frac{1}{\tau_e'} \frac{\theta}{\dot{\theta}} + \frac{\frac{1}{\tau_e'}\ddot{\theta}_0 + \frac{1}{k_m}\dot{\iota}_0}{\dot{\theta}}$$

This then is the general equation of the isoclines for the dead zone portion of the phase plane for inductive braking assuming C and $f = 0$ At this point analytical methods become complex unless some definite rela- tionship is made to exist between ι_0 and $\ddot{\theta}_0$. It is known that $\ddot{\theta}_0$ is governed by the true mechanical speed time constant for the particular motor load combination. Also $\dot{\iota}_0$ is dependent upon L_a, L_b, R_a, R_b and F of the relay.

In order to proceed it will be assumed that for the particular motor- load combination under consideration, τ_{e_1} is small compared with τ_m and therefore $p \cong 1$; $\tau_m \cong \tau_{m_a}$. That being the case, L_b/R_b may be designed to be equal to τ_m. Under these conditions the current in the braking circuit during the acceleration period will at all times be pro-

96

portional to the velocity of the motor. The current in the braking circuit will increase similar to the increase in velocity.

Reference is made to the equations in the introduction to this chapter in order to obtain the initial value of current. There, it is to be noted that $i = F i'$ and

$$i' = \sqrt{\frac{L_b i_2{}^2 - L_a i_1{}^2}{L_a + L_b}}$$

If $L_a i_1{}^2$ is small in comparison with $L_b i_2{}^2$, and L_a is small in comparison with L_b, $i' \cong i_2$ in magnitude.

Then $\quad i_o \cong F i_2 \cong F k_e \dot{\theta}_o$

Where $\quad k_e = \dfrac{i_o}{\dot{\theta}_o} \cong \dfrac{K_v}{R_b}$

Before proceeding, the conditions imposed on the problem should be summarized so that the situation will be clearly understood.

1. $f, C = 0$

2. $L_a << L_b$

3. $L_a i_1{}^2 << L_b i_2{}^2$ at all times during acceleration

4. $\tau_{e_1} << \tau_m \quad$ or $\quad \dfrac{L_a}{R_a} << \dfrac{J R_a}{K_v K_t}$

5. $\tau_{e_2} = \tau_{ma} \quad$ or $\quad \dfrac{L_b}{R_a} = P \dfrac{J R_a}{K_v K_t} \cong \tau_m$

6. $F = \sqrt{1 - C_2{}^2}$

Where $C^2 = \dfrac{E_R}{L_b i_2^2 - L_a i_1^2}$

and F is a constant for all τ during acceleration and has a value
between 0 and 1.

Simplifying equation (14)

$$N \tau_m' \tau_e' \overset{\circ\circ}{\Theta} = - \tau_m' \overset{\circ}{\Theta} - \Theta + \tau_m' \overset{\circ\circ}{\Theta}_{\circ} + \frac{\tau_m' \tau_e'}{k_m} i_{\circ}$$

$$(15)$$

Substituting $F k_e \overset{\circ}{\Theta}_{\circ}$ for $i_{\circ}$

$$N \tau_m' \tau_e' \overset{\circ\circ}{\Theta} = - \tau_m' \overset{\circ}{\Theta} - \Theta + \tau_m' \overset{\circ\circ}{\Theta}_{\circ} + \tau_m' \tau_e' F \frac{k_e}{k_m} \overset{\circ}{\Theta}_{\circ}$$

$$(16)$$

$$\overset{\circ\circ}{\Theta} = \left[\frac{-1}{\tau_m'(N \tau_e' + 1)} \right] \Theta + \overset{\circ\circ}{\Theta}_{\circ} \left[\frac{1 + \tau_e' F \frac{k_e}{k_m}}{N \tau_e' + 1} \right] (17)$$

CONSIDERATION OF THE BEST CONDITIONS

The foregoing indicates that the isoclines are straight lines and for
any given N, the slope is $\dfrac{-1}{\tau_m'(N \tau_e' + 1)}$

and the $\overset{\circ\circ}{\Theta}$-intercept is $\overset{\circ\circ}{\Theta}_{\circ} \left[\dfrac{1 + \frac{k_e}{k_m} F \tau_e'}{N \tau_e' + 1} \right]$.

All of the straight lines intersect at $\overset{\circ\circ}{\Theta}_{\circ} \tau_m' \left[1 + \dfrac{k_e}{k_m} F \tau_e' \right], 0.$

Is may be observed there is a characteristic of the isocline equations that is rather unusual, namely a dependence upon $\overset{o}{\Theta}_o$ for the $\overset{o}{\Theta}$-intercept. This indicates that perhaps not one but a series of phase planes should be constructed in order to obtain the dead zone trajectory for any size of step input. In general this is true, but for many cases one phase plane will suffice as will be seen later.

As observed in the introduction, it would be most desirable if a relay servo could be constructed, such that when the dead zone trajectory is plotted on the phase plane, the trajectory would be a straight line. This means that if the slope of the switching lines is made parallel to the dead zone trajectory, it would be possible to obtain a high degree of static accuracy. Now inasmuch as this result is a desired one, it may be obtained in the case of inductive braking, subject to the restrictions imposed this far upon the problem, if it may be shown that (1) there is a value of N, such that, when it is substituted in the isocline equation, the equation describes a straight line having a slope of N. In other words, the slope markers will be coincident with the isocline and (2) the $\overset{o}{\Theta}$-intercept of the straight line in (1) is equal to $\overset{o}{\Theta}_o$.
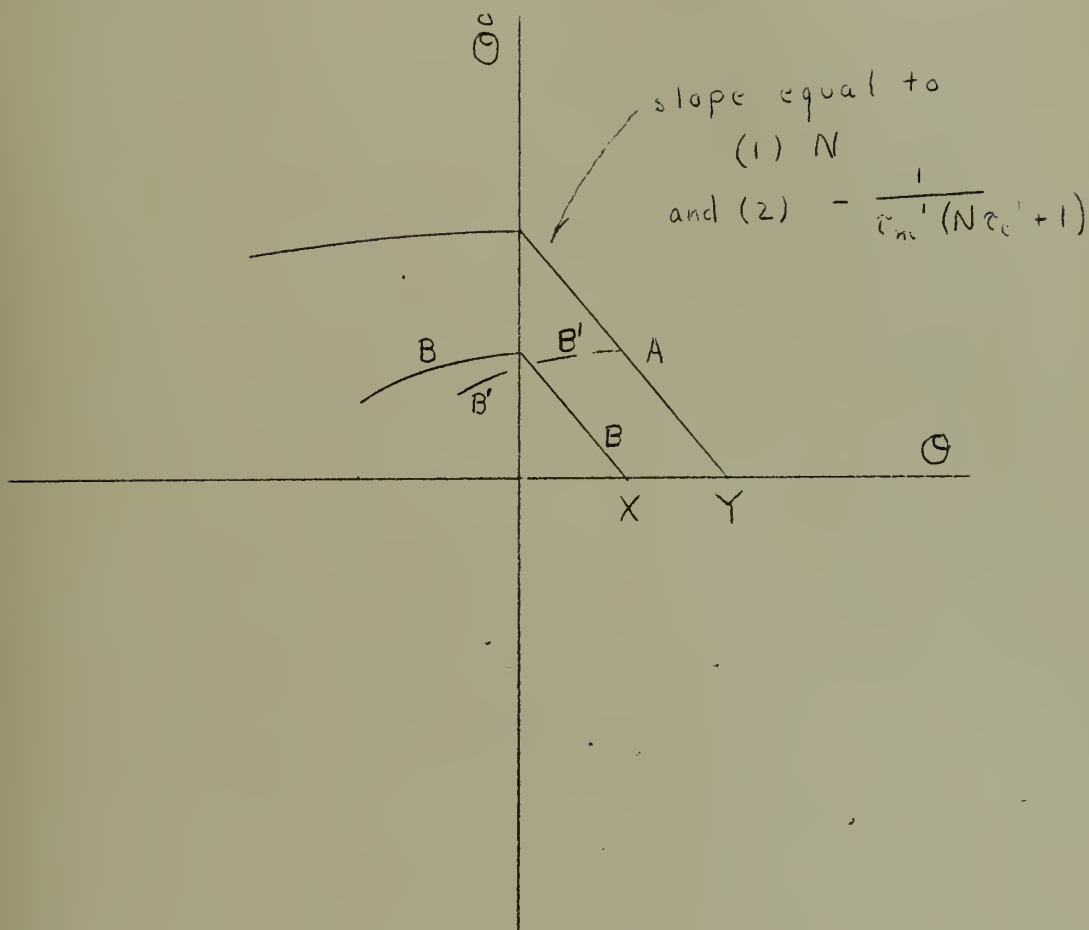
Figure 49   A Phase Plane Plot of $\overset{\circ}{\Theta}$ vs Θ showing Trajectories as a Result of Two Different-Sized Step Inputs

Pictorially in Figure 49, curve A displays this characteristic. Notice that in curve B, the $\overset{\circ}{\Theta}$-intercept is much less and since all Θ is measured from zero the trajectory will apparently come to rest at X vice Y. Upon closer inspection, however, it is seen that if the switching criteria is such that the drop-out line lies along curve A, the trajectory cannot be B but rather B$'$. Notice that the slope of the isocline is independent of $\overset{\circ}{\Theta}_o$. The significance of this is that if there is an isocline whose actual slope

is equal to N and if the $\overset{o}{\theta}$-intercept of this isocline is equal to $\overset{\circ}{\Theta}_o$,
the basic problem is solved and one phase plane will portray the dead zone
characteristics for all sizes of step inputs. Close examination of the
ensuing phase planes will reveal something else which is quite interesting.
If the switching (drop-out) line is straight and connects the nodal point
or the point of intersection of all isoclines with the point at which the
dead zone phase trajectory commences, then the dead zone trajectory for any
size of step input (all values of $\overset{\circ}{\Theta}_o$) may be drawn on one diagram. In
the event that the dead zone trajectories curve, it would be necessary to
construct the trajectory for the velocity-saturated case in order to determine
the appropriate dead zone width required in order to expect dead beat per-
formance for all sizes of step inputs. However, this investigation is
primarily concerned with straight dead zone trajectories, although curved
dead zone trajectories will be constructed for comparison purposes.

It is now desired to ascertain whether or not it is possible to achieve
a system which will produce dead beat performance for all sizes of step
inputs.

First, equate N to the generalized slope of the isocline equation -

$$N = - \frac{1}{\tau_m' \left(\tau_e' N + 1 \right)}$$

$$\tau_e' \tau_m' N^2 + \tau_m' N + 1 = 0$$

$$N = \frac{-\tau_m' \pm \sqrt{\tau_m'^2 - 4 \tau_e' \tau_m}}{2 \tau_e' \tau_m'}$$

or

$$N = -\frac{1}{2\tau_e'} \pm \frac{\sqrt{\tau_m'^2 - 4\tau_t'\tau_m'}}{2\tau_e'\tau_m'}$$

Considering the definition of N, it is difficult to envisage the meaning of imaginary values of N. However, it is seen that certainly the slope of an isocline may be made equal to the corresponding value of N if the radical is real or $\tau_m' \geq 4\tau_e'$.

As will be seen later, if $\tau_m' < 4\tau_e'$ damped oscillations may be expected, and if $\tau_m' \geq 4\tau_e'$ the dead zone trajectory will ultimately become asymptotic to a straight line.

The next step is to adjust the $\overset{o}{\theta}$-intercept to be equal to $\overset{o}{\theta}_o$. This will result if –

$$\frac{1 + \tau_e' \frac{k_e}{k_m} F}{N\tau_e' + 1} = 1$$

$$\text{or} \quad N = \frac{k_e}{k_m} F$$

$$\text{where} \quad k_c = \frac{c_o}{\theta_o} \cong \frac{K_v}{R_o}$$

$$\text{and} \quad k_m = \frac{J}{K_t}$$

There have now been established three conditions whereby if all are fulfilled simultaneously, the dead zone trajectory will be a straight line for all sizes of step inputs.

These conditions are:

$$(1) \quad \tau_m{}' \geq 4 \tau_e{}'$$

$$(2) \quad N = \frac{k_e}{k_m} F$$

$$(3) \quad N = -\frac{1}{2\tau_e{}'} \pm \frac{\sqrt{\tau_m{}'^2 - 4\tau_e{}' \tau_m{}'}}{2 \tau_e{}' \tau_m{}'}$$

A PRACTICAL PROBLEM

It is now desired to construct a typical problem to see if it is possible to attain the desired objectives with a typical relay servo and reasonable circuit parameters. The relay servo chosen is one similar to the relay servo using a 1/125 HP DC shunt motor that was utilized in investigating the effect of dynamic braking.

$$\tau_m = \frac{J R_a}{K_v K_t} = .5 = \tau_{ma}$$

$$R_a = 300 \ \Omega$$

$$L_a = .5 \ henry$$

$$K_v = .25 \ \frac{volt \cdot sec}{rad}$$

$$\frac{J}{K_t} = \frac{.125}{300} \ \frac{amp-sec^2}{rad}$$

103.

For the initial examination τ_m' is chosen equal to $4 \tau_e'$
The problem is illustrated in detail in Appendix III. As developed in the
Appendix III R_b = 300 ohms, L_b = 150 henries.

$$\tau_e' = \frac{L_a + L_b}{R_a + R_b} = \frac{150.5}{600} \cong 0.25$$

$$\tau_m' = \frac{J(R_a + R_b)}{K_v K_t} = \frac{J R_a}{K_v K_t}\left[1 + \frac{R_b}{R_a}\right] = 10$$

$$\frac{k_e}{k_m} = -\frac{K_v K_t}{J R_b} = -\frac{1}{\frac{J R_b}{K_v K_t}} = -\frac{1}{\frac{J R_a}{K_v K_t}\left(\frac{R_b}{R_a}\right)}$$

$$= -2$$

$$N_{crit} = -\frac{1}{2 \tau_e'} = -\frac{1}{2(.25)} = -2$$

$$N_{crit} = F \frac{k_e}{k_m} = -2 F$$

$$F = 1$$

For this case (Case A) it is apparent that 100% effectiveness is
required of the relay. For comparison purposes the slope of the dead
zone trajectory (assuming that the coulomb friction effect is negligible)
for the case in which 300 ohms only is in the braking circuit would be -

$$slope = -\frac{K_e K_t}{J(R_a + R_b)} = -\frac{1}{\frac{J R_a}{K_v K_t}\left(1 + \frac{R_b}{R_a}\right)} = -1$$

Hence, it is seen that the use of 150 henries in the braking circuit not only produces a straight line for the dead zone trajectory, but that this line has a greater negative slope in the case of the inductive braking, thereby implying at least a shorter response time. That the response time is indeed shorter in the case of inductive braking will be shown later.

The following five figures are phase planes showing the effect of the initial value of current upon the dead zone trajectory. Case A1 is an impractical case at best, and it is difficult to imagine a relay servo operating under the conditions stated in case A1. The reason for this is that the initial value of current in the motor as it enters the dead zone is twice the value of current that existed in the braking circuit at the moment of switching. The only reason that this case is shown at all is that it illustrates the fact that the trajectory may cross the zero error rate line (overshoot) and still oscillations will not occur. From the phase plane analysis it is seen that the trajectory becomes asymtotic to an isocline after a single overshoot. Case A2 may be said to represent the ideal case. Here, $F = 1$ or 100% of the braking current passes through the motor at time equal to zero. The dead zone trajectory has a greater negative slope than that for simple dynamic braking. In case A3, $F = .5$ or only one-half of the ideal initial value of current is present in the motor at time equal to zero. Note that the trajectory curves slightly, eventually becomes asymtotic to a straight line which does not pass through $\overset{\circ}{\Theta}_{0}$. In case A4, $F = 0$ or the initial value of current in the motor is zero. Note that the slope of the beginning of the dead zone trajectory is zero, and that the trajectory "bows out" even more than the case wherein $F = .5$.
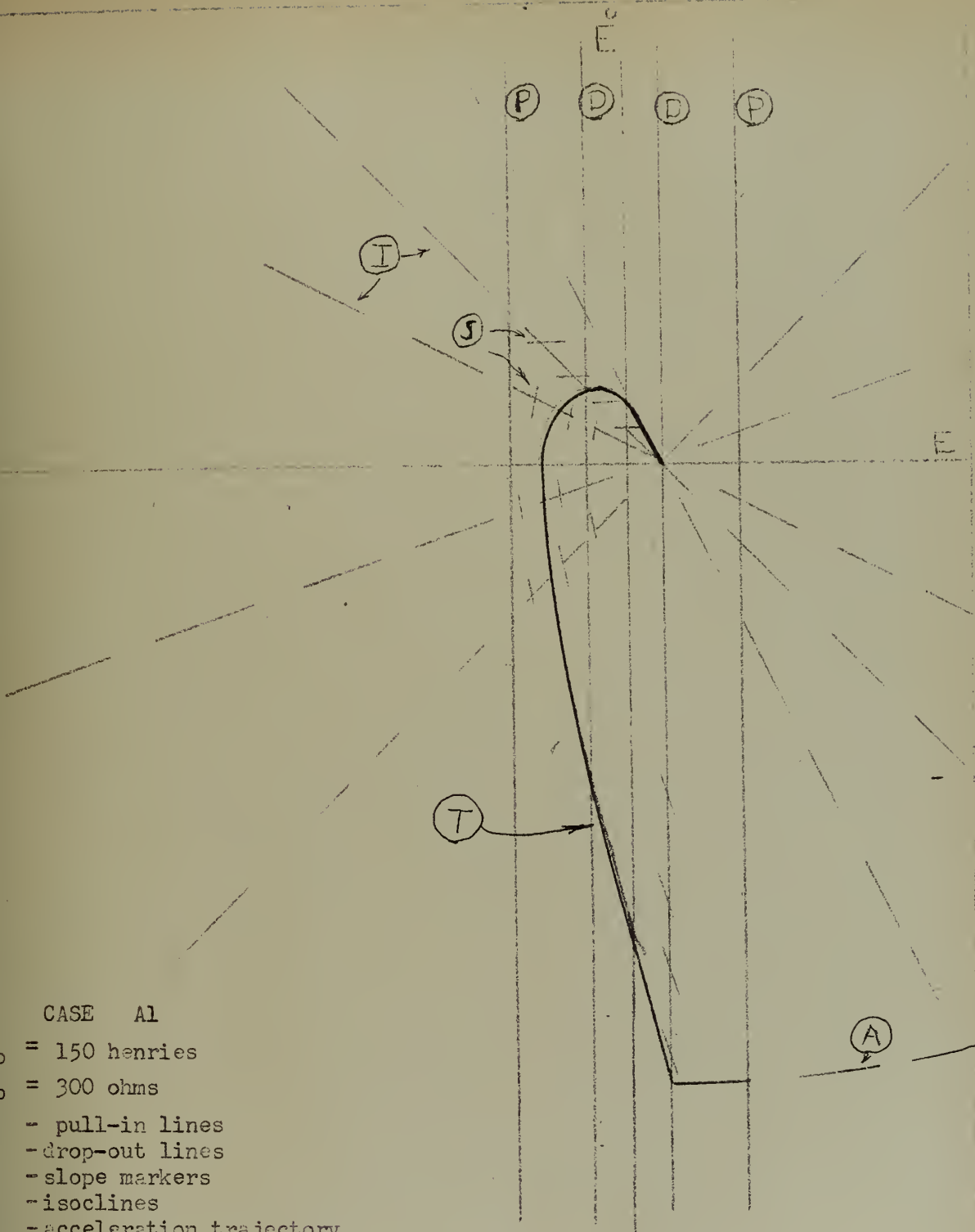
CASE   A1

L_b = 150 henries

R_b = 300 ohms

P - pull-in lines
D - drop-out lines
S - slope markers
I - isoclines
A - acceleration trajectory
T - deceleration trajectory

F = 2.0

Figure 50. Theoretical Dead Zone Trajectory for a Relay Servo
            Employing a DC Shunt Motor and Inductive Braking in
            the Dead Zone

106

Theoretical Dead Zone Trajectory
for a Relay Servo Employing a DC
Shunt Motor and Inductive Braking
in the Dead Zone

CASE A2

L_b = 150 henries

R_b = 300 ohms

F = 1

P - pull-in lines

D - drop-out lines

A - acceleration trajectory

T - deceleration trajectory

Figure 51
107

Theoretical Dead Zone Trajectory for
a Relay Servo Employing a DC Shunt
Motor and Inductive Braking in the
Dead Zone

CASE A3

b = 150 henries

b = 300 ohms

= .5

- pull in lines
- drop out lines
- acceleration trajectory
- isoclines
- slope markers
- deceleration trajectory

Figure 52

Theoretical Dead Zone Trajectory for a Relay Servo
Employing a DC SHUNT Motor and Inductive Braking
in the Dead Zone

CASE A4

L_b = 150 henries

R_b = 300 ohms

F = 0

P - pull-in lines
D - drop-out lines
S - slope markers
I - isoclines
A - acceleration trajectory
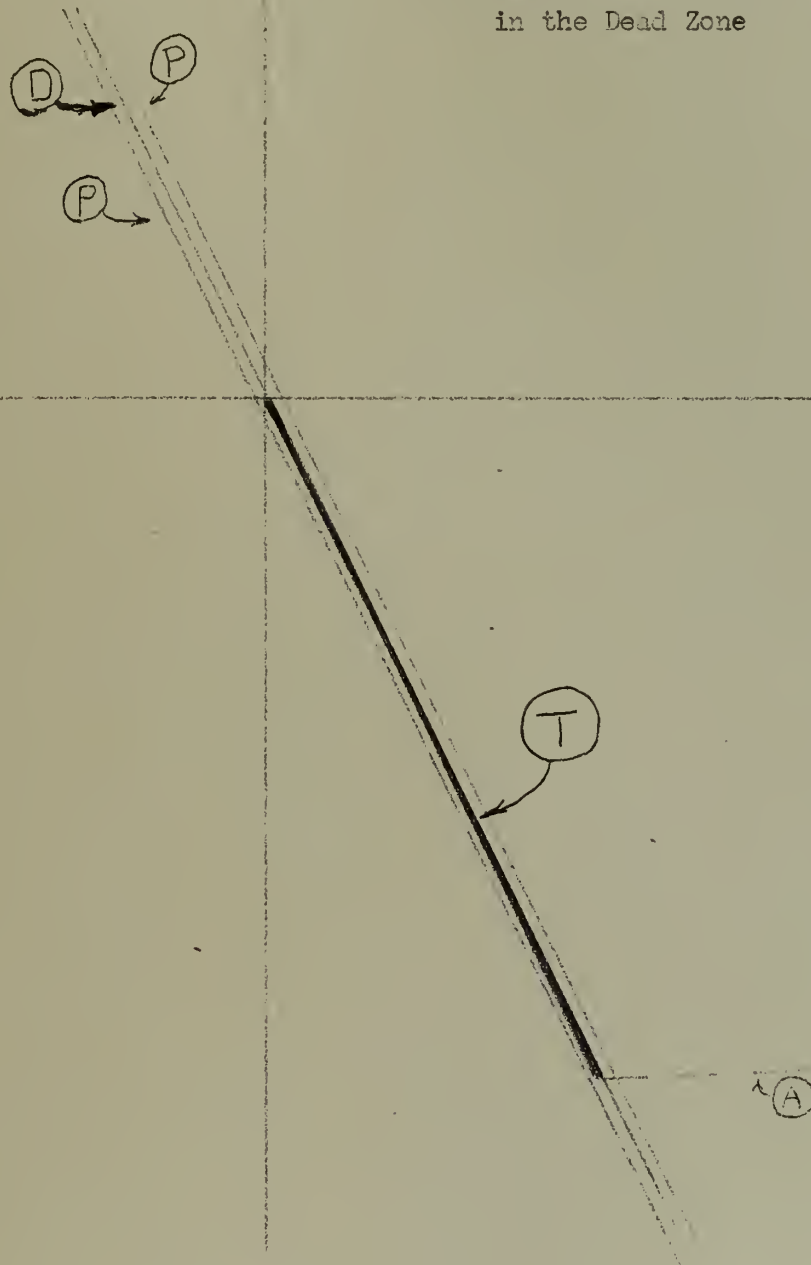T - deceleration trajectory

Figure 53

Theoretical Dead Zone Trajectory for a Relay
Servo Employing a DC SHUNT Motor and Inductive
Braking in the Dead Zone

CASE A5

L_b = 150 henries

R_b = 300 ohms

F = -.5

P - pull-in lines
D - drop-out lines
S - slope markers
I - isoclines
A - acceleration trajectory
T - deceleration trajectory

Figure 54

110
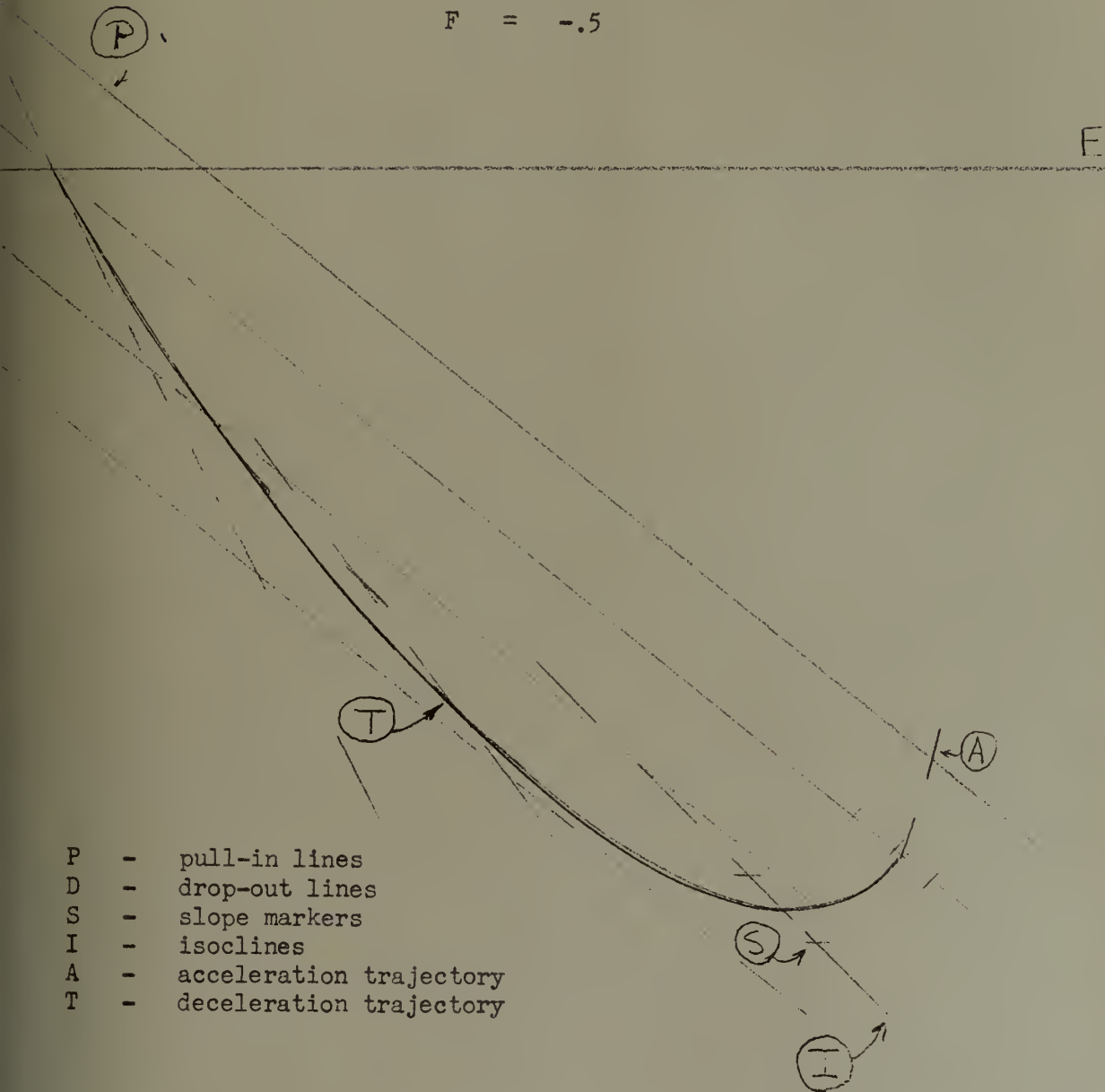
Since the case where $\tau_m' = 4\,\tau_e'$ has been investigated, it would perhaps be of interest to analyze the expected dead zone behavior when $\tau_m' > 4\,\tau_e'$ say $8\,\tau_e'$. As shown in Appendix IV the relationship between the time constants would exist if $L_b = 25$, $R_b = 50$ henries.

$$\tau_e' = \frac{L_a + L_b}{R_a + R_o} - .073$$

$$\tau_m' = .5\left[1 + \frac{50}{300}\right] = 1.167(.5) = 583$$

$$\frac{k_e}{k_m} = -\frac{1}{\tau_m\left(\frac{R_o}{R_a}\right)} = \frac{-1}{(.5)(.167)} = -12$$

$$N = -\frac{1}{2\,\tau_e'} \pm \frac{\sqrt{\tau_m'^2 - 4\,\tau_e'\,\tau_m}}{2\,\tau_e'\,\tau_m'}$$

$$= -11.7, -2.0$$

$$N = F\,\frac{k_e}{k_m}$$

$$F = \frac{N}{k_e/k_m} = \frac{-11.7}{-12} = .975$$

$$F = \frac{-2}{-12} = .167$$

In this particular case a straight line will be obtained for the dead zone trajectory in two instances. If the relay is 97.5% efficient, a straight line having a slope of -11.7 will be obtained. If, however, the relay is

only 16.7% efficient, the resulting slope of the straight line will be -2.
Again, for comparison purposes, the slope of the dead zone trajectory if
dynamic braking is employed would be $-\dfrac{K_v K_t}{J(R_a - R_a)} = -1.72$

For a complete representation of the possible trajectories using these
parameters, phase planes have been constructed with a value of F = 1,
.975, .9, .75, .333, .167 and 0. Notice that there is a small tendency
to overshoot when F = 1, the trajectory is straight with a slope of
-11.7 when F = .975, the trajectories "bow in" for F = .9, .75, .5,
.333, .2, a straight line results when F = .167 and the trajectory
characteristically "bows out" for F = 0.

The significance of this is that even though the relay is quite in-
efficient a straight line may be obtained for a dead zone trajectory pro-
vided that R_b and L_b have correct values. This straight line will have a
slope that is greater than it would be if no inductance was present in the
braking circuit.

Case C represents the expected behavior when the other combination of
braking inductance and resistance that would make $\tau_m' = 8\tau_e'$ was chosen.
$L_b = 875$ henries, $R_b = 1750$ ohms.

$$\tau_e' = \frac{875 + 5}{1750 + 300} = .425$$

$$\tau_m' = .5\left[1 + \frac{1750}{300}\right] = 3.42$$

$$\frac{k_e}{k_m} = -\frac{1}{\tau_m\left(\frac{K_e}{\tau_a}\right)} = -\frac{1}{(.5)(5.33)} = -.343$$

$$N = -.343, -2.0$$

112

Theoretical Dead Zone Trajectory
for a Relay Servo Employing a DC
SHUNT Motor and Inductive Braking
in the Dead Zone

CASE B2

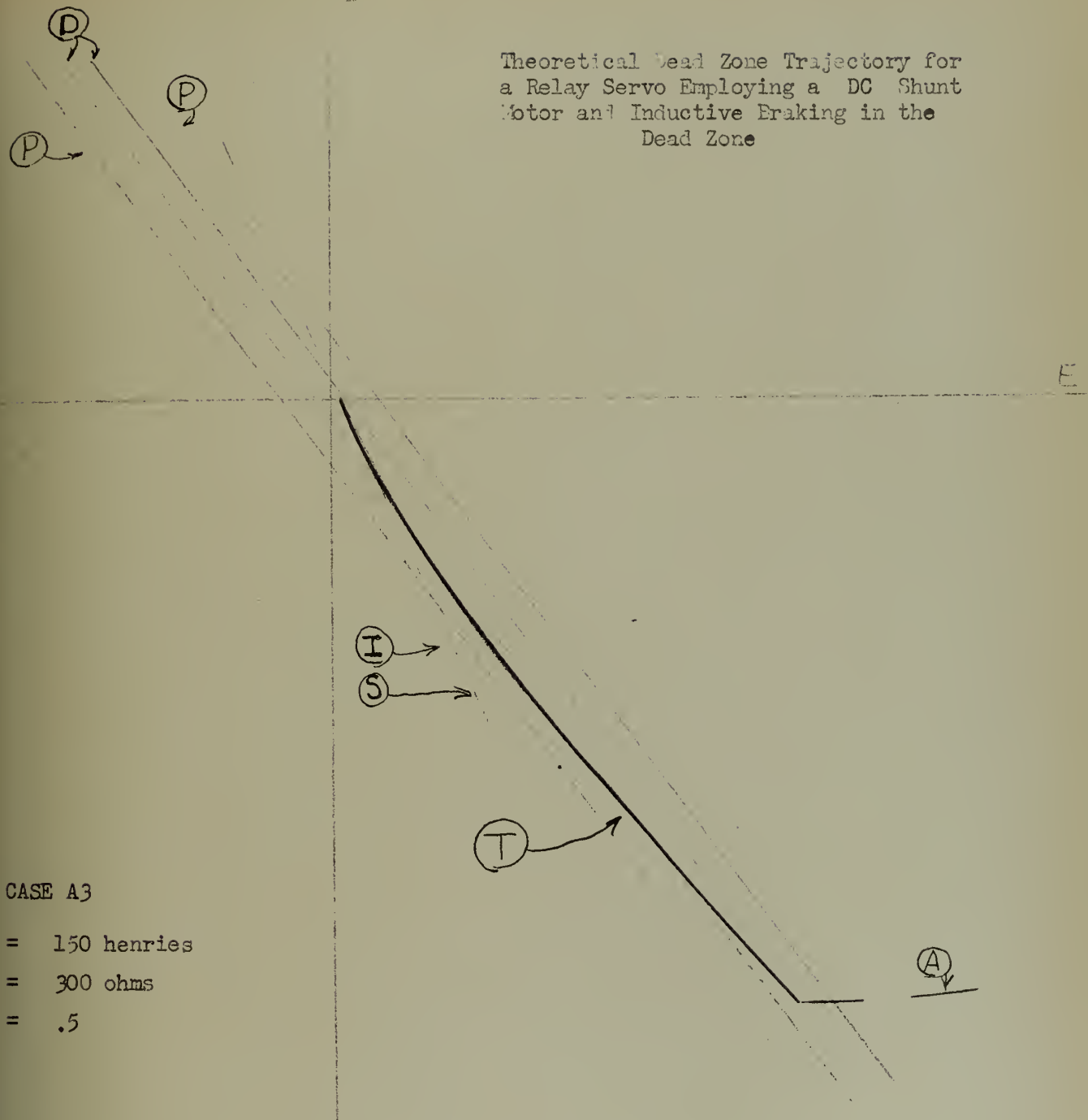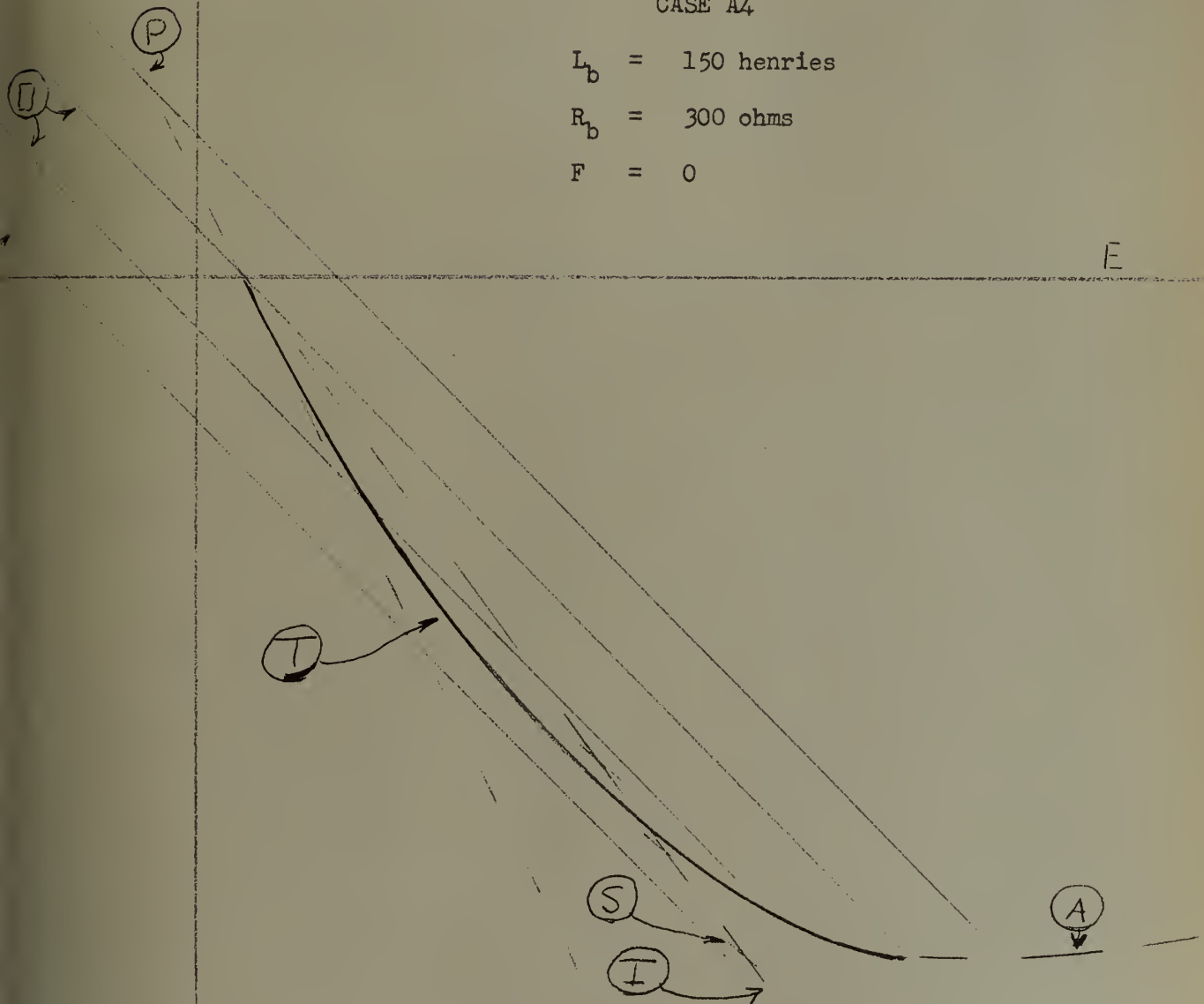L_b = 25 henries

R_b = 50 ohms

F = 1

P - pull-in lines
D - drop-out lines
A - acceleration trajectory
T - deceleration trajectory

Figure 55

113

Theoretical Dead Zone Trajectory for
a Relay Servo Employing a DC SHUNT
Motor and Inductive Braking in the
Dead Zone

CASE B3A

L_b = 25 henries

R_b = 50 henries

F = .975

P - pull-in lines
D - drop-out lines
A - acceleration trajectory
T - deceleration trajectory

Figure 56

114

Theoretical Dead Zone Trajectory
for a Relay Servo Employing a DC
SHUNT Motor and Inductive Braking
in the Dead Zone

CASE B2A

L_b = 25 henries

R_b = 50 ohms

F = .9

P - pull-in lines
D - drop-out lines
A - acceleration trajectory
T - deceleration trajectory

Figure 57

115

Theoretical Dead Zone Trajectory
for a Relay Servo Employing a DC
SHUNT Motor and Inductive Braking
in the Dead Zone

CASE B

L_b = 25 henries

R_b = 50 ohms

F = .75

P - pull-in lines
D - drop-out lines
A - acceleration trajectory
T - deceleration trajectory

Figure 58

116

Theoretical Dead Zone Trajectory
for a Relay Servo Employing a DC
SHUNT Motor and Inductive Braking
in the Dead Zone

CASE B3

L_b = 25 henries

R_b = 50 ohms

F = .333

P - pull-in lines
D - drop-out lines
A - acceleration trajectory
T - deceleration trajectory

Figure 59

117

Theoretical Dead Zone Trajectory
for a Relay Servo Employing a DC
SHUNT Motor and Inductive Braking
in the Dead Zone

CASE B

L_b = 25 henries

R_b = 50 ohms

F = .167

P — pull-in lines
D — drop-out lines
A — acceleration trajectory
T — deceleration trajectory

Figure 60

118
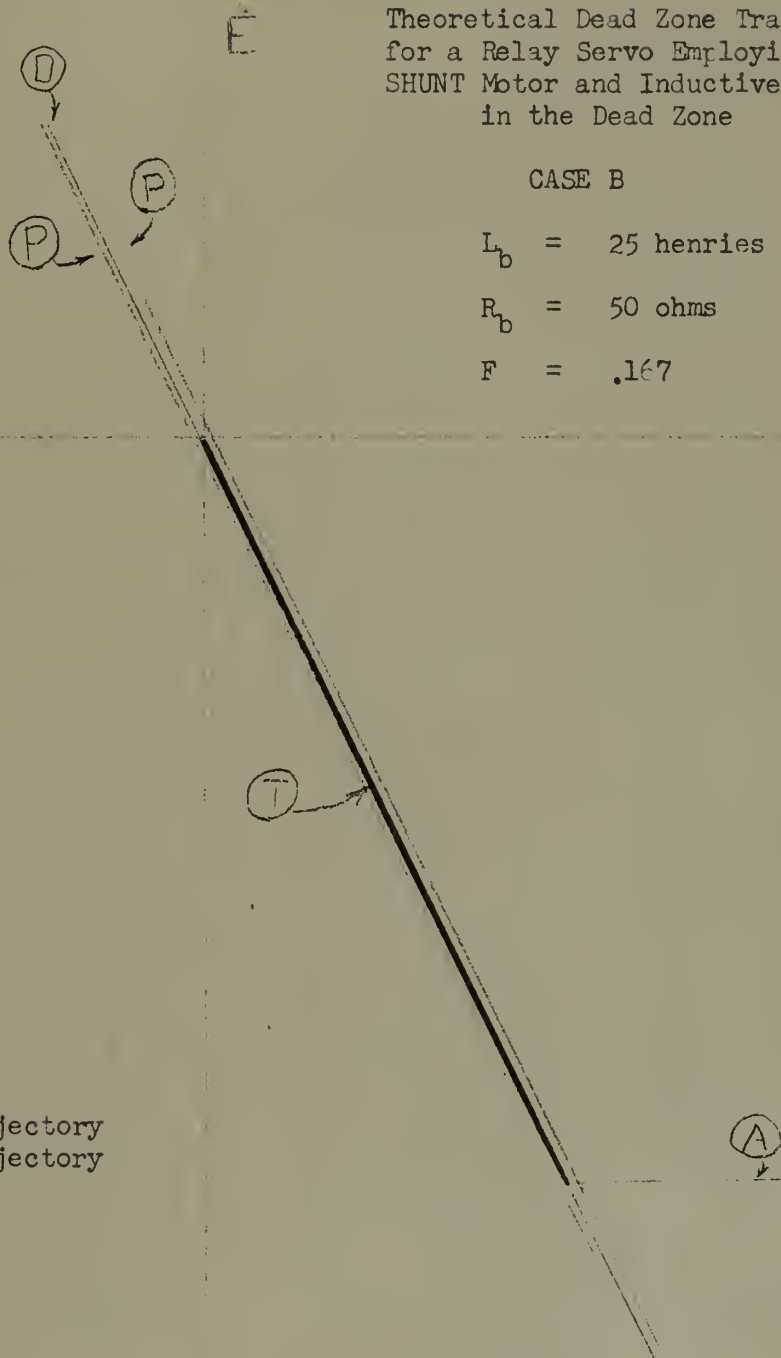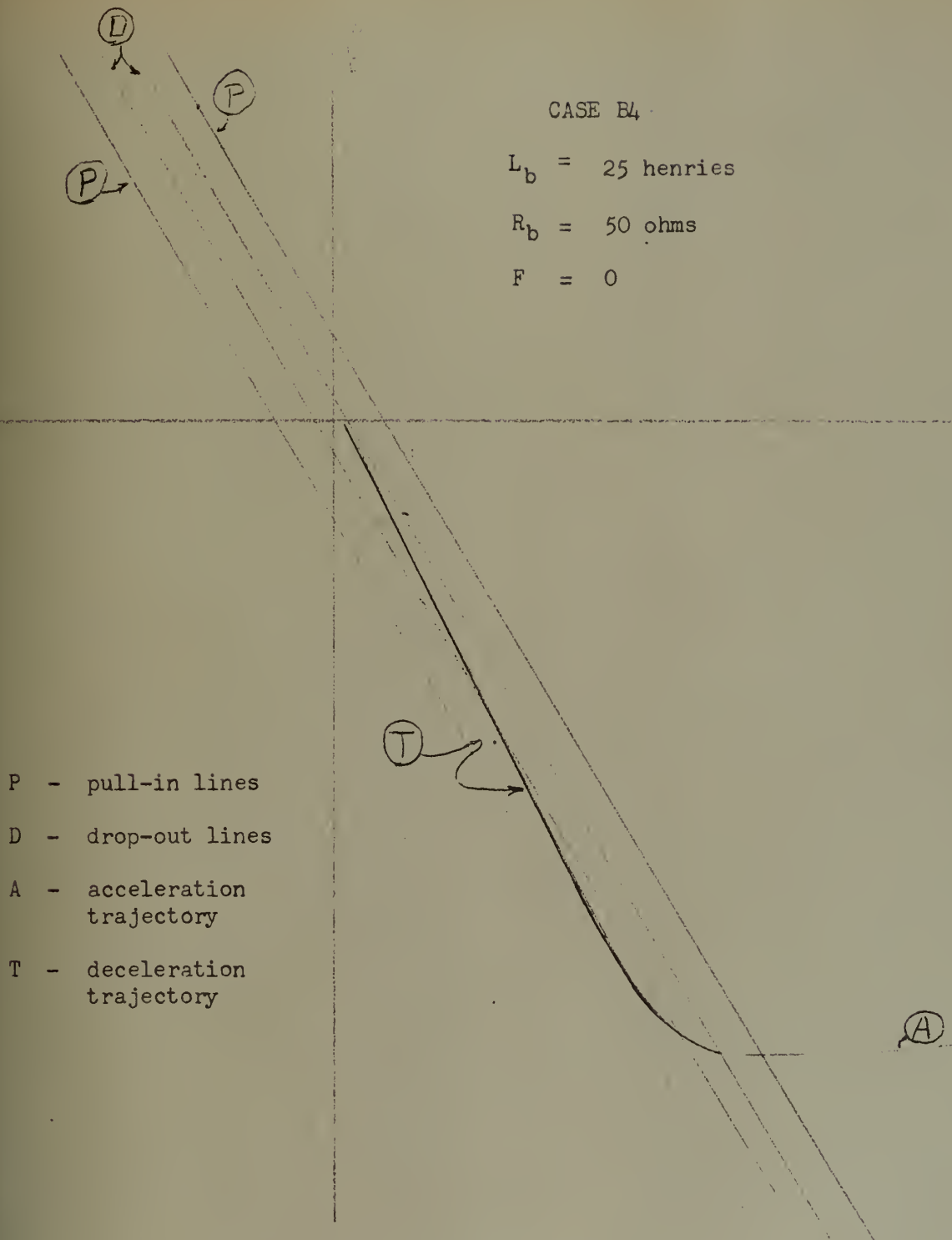
CASE B4

L_b = 25 henries

R_b = 50 ohms

F = 0

P - pull-in lines

D - drop-out lines

A - acceleration
    trajectory

T - deceleration
    trajectory

Figure 61. Theoretical Dead Zone Trajectory for a Relay
Servo Employing a DC Shunt Motor and Inductive
Braking in the Dead Zone

119

CASE C1

L_b = 875 henries

R_b = 1750 ohms

F = 1

P − pull-in lines

D − drop-out lines

A − acceleration trajectory

T − deceleration trajectory
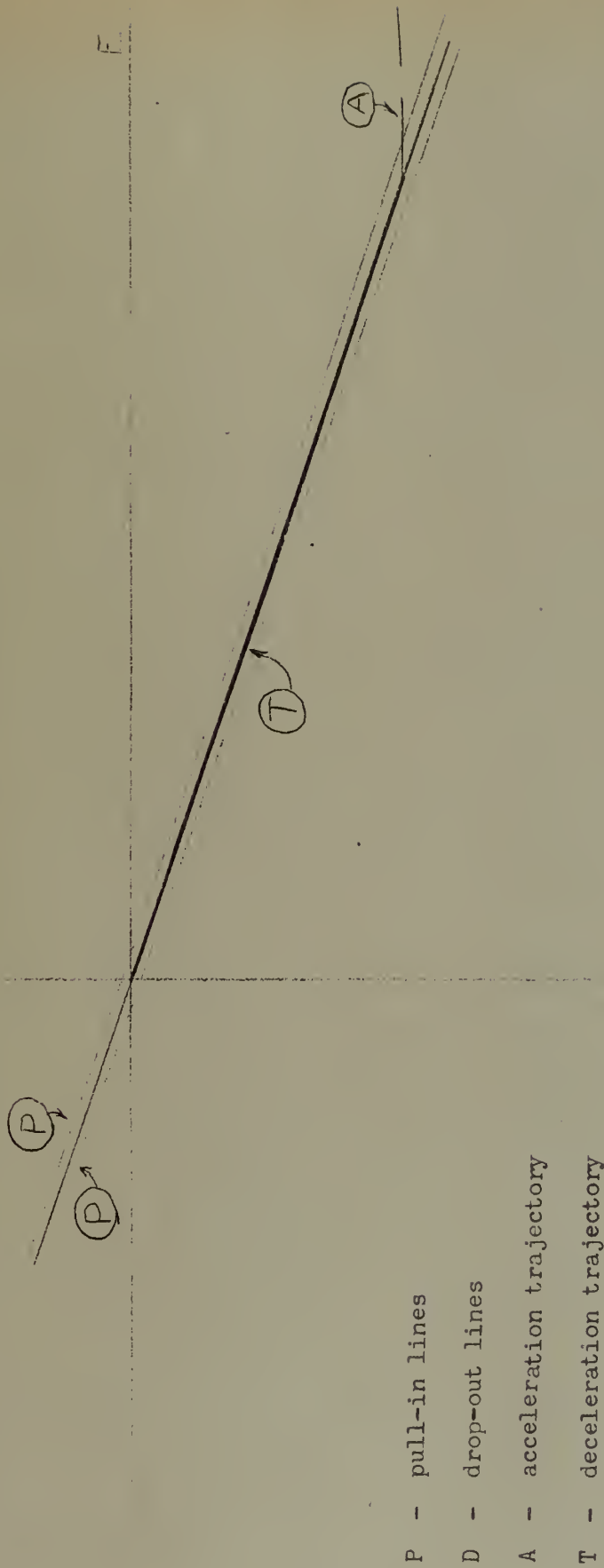
Figure 62. Theoretical Dead Zone Trajectory for a Relay Servo Employing a DC Shunt Motor and Inductive Braking in the Dead Zone

120

CASE C2

L_b = 875 henries

R_b = 1750 ohms

F = .5
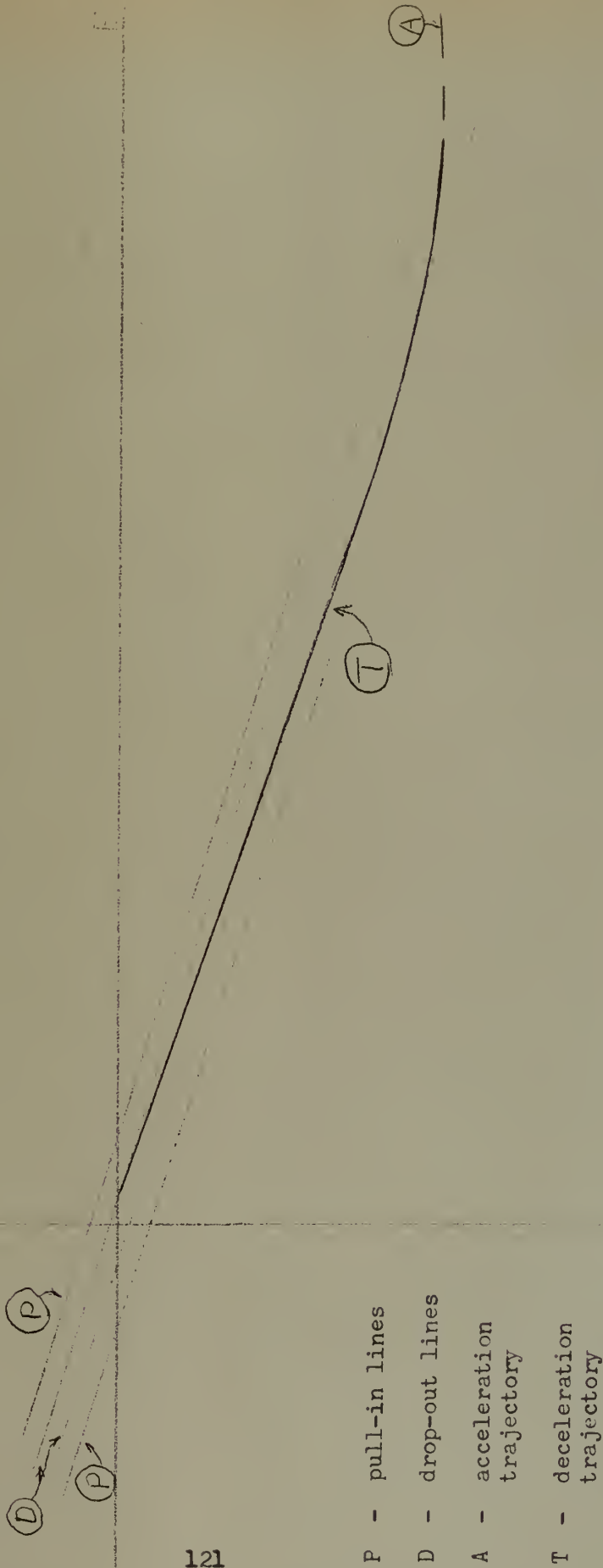
Figure 63. Theoretical Dead Zone Trajectory for a Relay Servo
Employing a DC Shunt Motor and Inductive Braking in the
Dead Zone

P – pull-in lines

D – drop-out lines

A – acceleration
      trajectory

T – deceleration
      trajectory
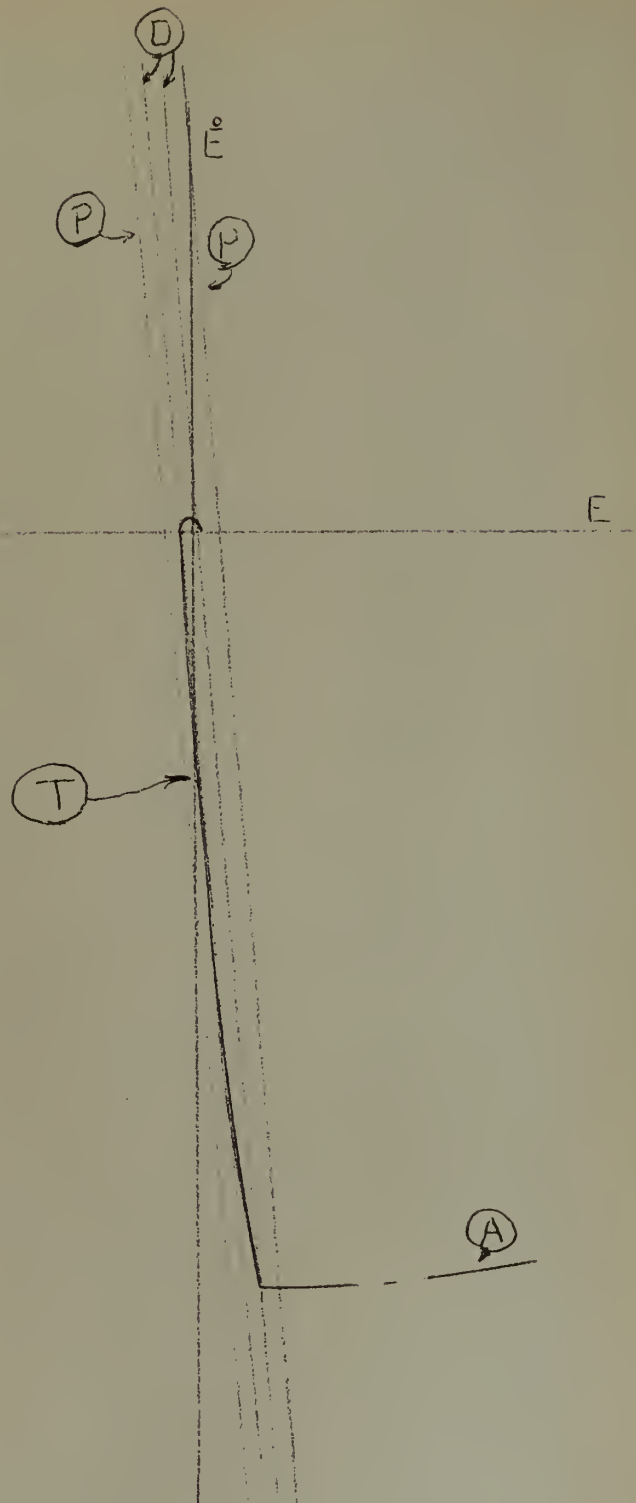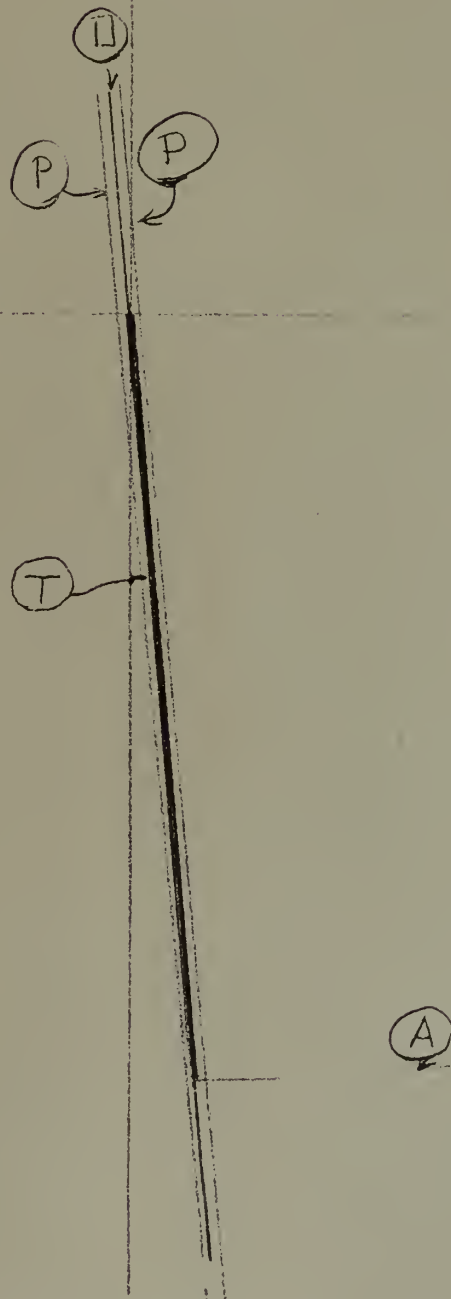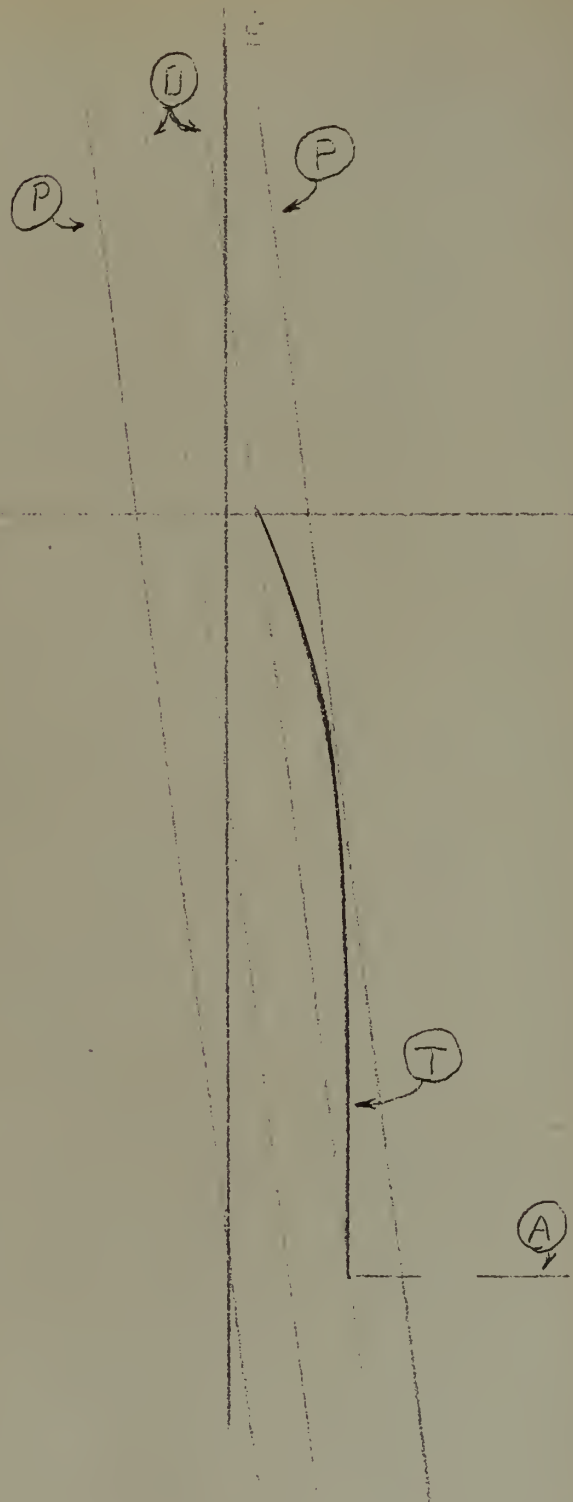
121

CASE C3

L_b = 875 henries

R_b = 1750 henries

F = 0

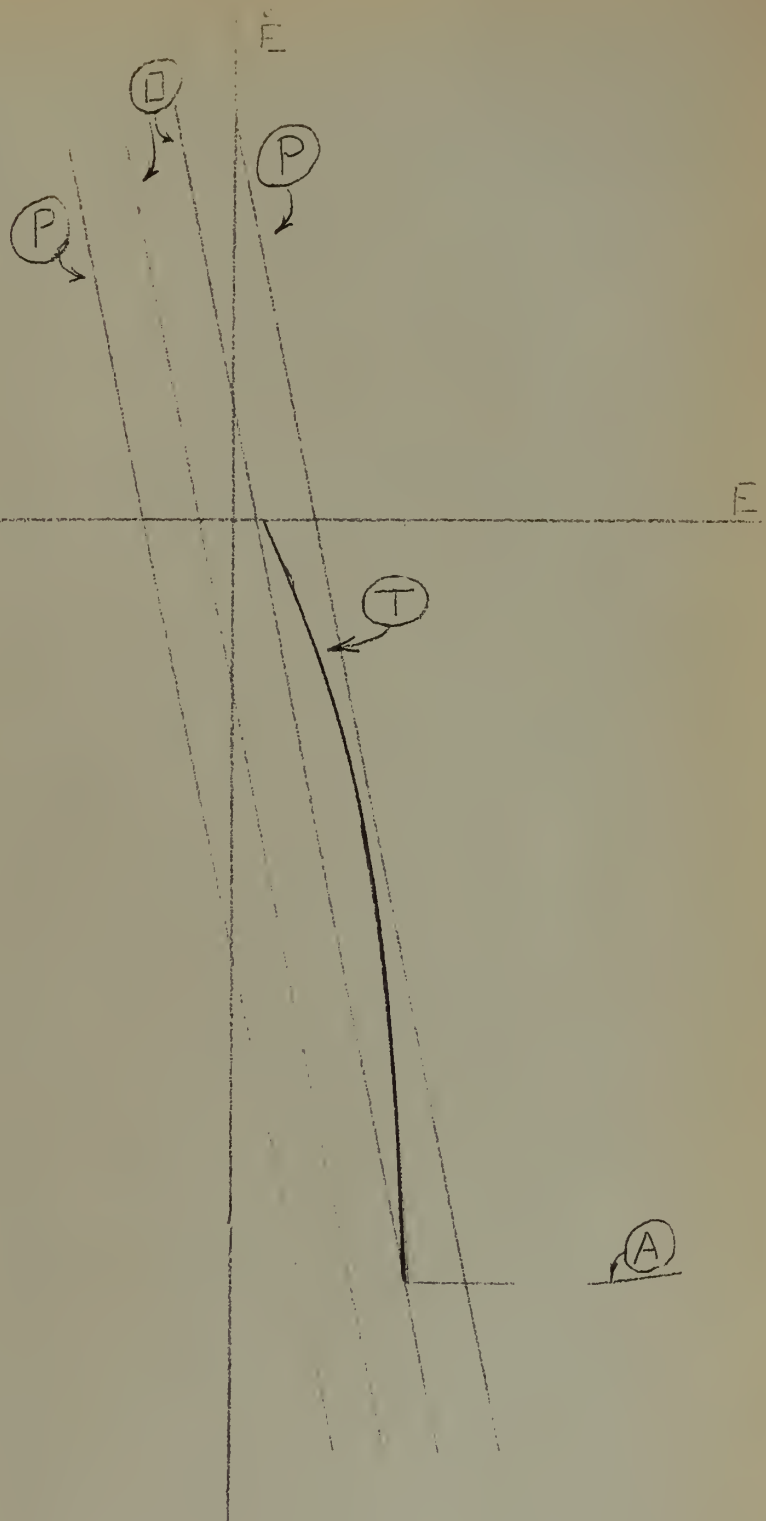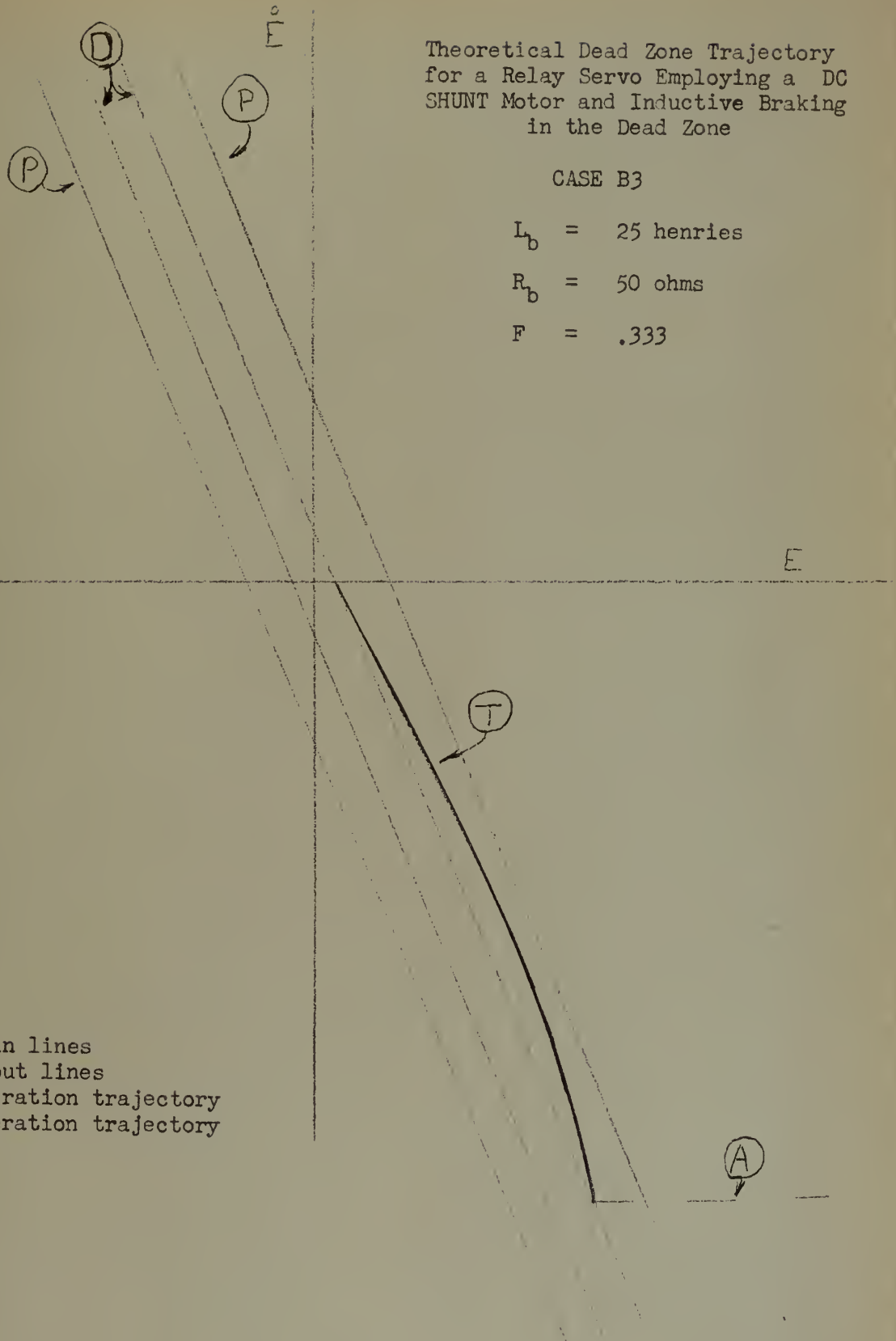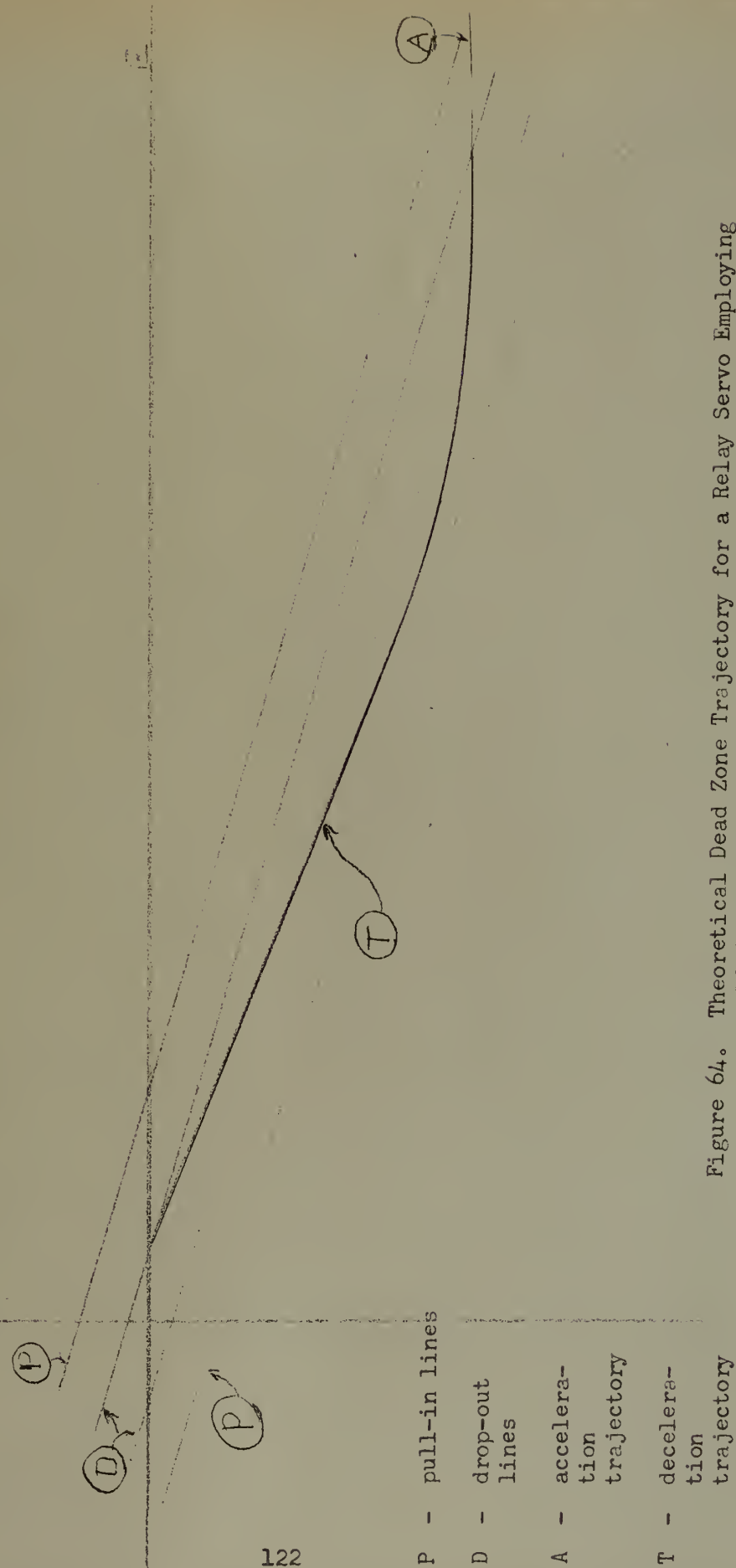Figure 64. Theoretical Dead Zone Trajectory for a Relay Servo Employing a DC Shunt Motor and Inductive Braking in the Dead Zone

P – pull-in lines

D – drop-out lines

A – acceleration trajectory

T – deceleration trajectory

122

For $N = -343$

$F = 10$

For $N = -2$

$F = 5.83$

It is manifestly impossible for $F = 5.83$ inasmuch as it can never be greater than one. Therefore, a straight line trajectory with a slope of -2 will not occur. Notice, however, that in all cases it has been a mathematical result that for some specific value of F, the dead zone trajectory would be straight and have a value of -2, even though it would not be realized in the last case (Case C) for physical reasons. Notice that the ratio $\left(R_b/R_a \right) = 5.83$ which is the identical value that F would have to take on if the dead zone trajectory was to have a slope of -2. The importance of this parameter will be shown later.

In case C2, $F = 1.0$, $\tau_m' = \delta \tau_e'$ and a straight line is obtained for the dead zone trajectory. In case C3 and C4, with $F = .5$ and 0 respectively the dead zone trajectory is "bowed out". The trajectory is straight only for the case in which $F = 1.0$.

A MATHEMATICAL REVIEW OF THE FUNDAMENTALS

From the phase planes and the analytical results certain relationships have now been found to exist between F, N, and the ratio of R_b/R_a for the specific relay servo under consideration. In an attempt to generalize the results the following mathematical analysis is presented.

A. The first requirement is to insure that no oscillations will occur (that the dead zone trajectory will ultimately become asymptotic to a straight line).

123

For this to occur –

$$\tau_m \geq 4 \tau_e{}'$$

$$\frac{(R_a + R_b) J}{K_v K_t} \geq 4 \left[\frac{L_a + L_b}{R_a + R_b} \right]$$

$$\frac{R_a J}{K_v K_t} \left[1 + \frac{K_b}{R_a} \right] \geq 4 \left[\frac{L_a}{R_a (1 - \frac{R_b}{R_a})} + \frac{L_b}{R_a (1 + \frac{R_b}{R_a})} \right]$$

Let $\dfrac{R_b}{R_a} = X$

If it is demanded that

$$\tau_{e_2} = \tau_{ma}$$

Then $\dfrac{L_b}{R_b} = \tau_{ma} = p \tau_m$

$$L_b = p \tau_m R_b = p \tau_m R_a \left(\frac{R_b}{R_a} \right)$$

Then

$$\tau_m (1 + x) \geq 4 \left[\frac{L_a}{R_a (1 + x)} + \frac{p \tau_m x}{1 + x} \right]$$

$$(1 + x)^2 \geq \frac{4}{\tau_m} \left[\tau_{e_1} + p \tau_m x \right]$$

$$(x + 1)^2 \geq \frac{4 \tau_e}{\tau_m} + 4 p x$$

$$x^2 + 2x (1 - 2p) - 1 \geq \frac{4 \tau_{e_1}}{\tau_m}$$

124

If $\quad \tau_{e_1} << \tau_m \qquad\qquad p \cong 1$

and

$$(x-1)^2 \geq \frac{4\,\tau_{v_1}}{\tau_m}$$

B.   In order for the dead zone trajectory to be a perfect straight line, not only must the previous result be satisfied, but also

$$N = F \frac{k_e}{k_m} = \frac{-F}{\tau_m X}$$

and

$$N = -\frac{1}{2\tau_e'} \pm \frac{\sqrt{\tau_m'^2 - 4\,\tau_e'\,\tau_m}}{2\,\tau_e'\,\tau_m'}$$

$$= -\frac{(1+x)}{2(\tau_{e_1} + p\,\tau_m X)} \pm \frac{\sqrt{\tau_m^2(1+x)^2 - 4\,\tau_m(\tau_{e_1} + p\,\tau_m X)}}{2\tau_m(\tau_{e_1} + p\,\tau_m X)}$$

If it may again be assumed that $\tau_{e_1} << \tau_m$ and therefore that

$$p \cong 1$$

$$N = \frac{-(1+x)}{2\,\tau_m X} \pm \frac{\sqrt{\tau_m^2(1+x)^2 - 4\,\tau_m^2 X}}{2\,\tau_m^2 X}$$

$$N = \frac{-(1+x)}{2\,\tau_m X} \pm \frac{(1-x)}{2\,\tau_m X}$$

or

$$N = -\frac{(1+x) - (1-x)}{2\,\tau_m X} = -\frac{1}{\tau_m}$$

and

$$N = \frac{-(1+x) - (1-x)}{2\tau_m X} = \frac{-2}{2\tau_m X} = -\frac{1}{\tau_m X}$$

In the case where

$$N = -\frac{1}{\tau_m}$$

Since

$$N = -\frac{F}{\tau_m X}$$

$$F = X$$

Notice that if x (or R_b/R_a) is between 0 and 1, then a straight line will be obtained for the dead zone trajectory when $F = x$, and this straight line will have a slope of $-\frac{1}{\tau_m}$.

In the case where —

$$N = -\frac{1}{\tau_m X}$$

$$F = 1$$

Therefore, when F is 100, a straight line will be obtained for the dead zone trajectory with a slope of $-\frac{1}{\tau_m X}$.

Briefly, subject to the conditions that —

1. $f, C = 0$

2. $L_a \ll L_b$

3. $L_{c c_1}{}^a \ll L_b {i_-}^a$

4. $\tau_{e_1} \ll \tau_{m a}$

5. $\tau_{e_2} = \tau_{m a}$

126

6. $F = \sqrt{1 - C^2}$

7. $x^2 + 2x(1 - 2\rho) + 1 > \dfrac{4\tau_{ei}}{\tau_m}$

A straight line for the dead zone trajectory will be obtained when

(1) $F = 1$, the slope being $-\dfrac{1}{\tau_m x}$.

(2) If $0 < x < 1$, when $F = x$, the slope being $-\dfrac{1}{\tau_m}$.

The results thus far have been encouraging. While it is highly un-
li ely that a relay can be made to operate such that $F = 1$, it is quite
probable that a value for F considerably less than one may be established
for a relay. Subject to the restrictions that $x^2 + 2x(1 - 2\rho) + x$

$\geq 4\tau_{ei}/\tau_m$

it remains to adjust $x = F$, and a straight line will be obtained for the
dead zone trajectory for all sizes of step inputs. The straight line will
have a slope of $-\dfrac{1}{\tau_m}$. Notice that the straight line will have a slope
that is greater negatively than for the case of pure dynamic braking, since
pure dynamic bra ing will result in the dead zone trajectory being a straight
line and having a slope of $-\dfrac{K_v K_T}{J(R_a + r_n)} = -\dfrac{1}{\tau_m(1+x)}$.

COMPUTER STUDIES

It would be difficult to analyze all of the various facets of the subject
of inductive braking solely by means of analytical phase planes. Also it
would require a large supply of high Q, high current, linear inductances for
proper investigation of the characteristics of a relay servo using inductive
braking. Therefore, it would appear that the next logical step would be to

use an analogue computer to simulate various conditions and obtain both
transients and phase planes for several combinations of resistances and
inductances.

A major contribution of the computer would be to eliminate combina-
tions of inductances and resistances which are unsatisfactory. Also, the
computer may be of value in estimating the amount of tolerance from the ideal
values of inductances and resistances that would be acceptable. The com-
puter solutions may or may not verify what was done analytically and also
may produce some favorable results which could not have been foreseen
analytically.

It was decided that the computer part of the problem could best be
accomplished by splitting the problem into two phases, an acceleration phase
and a deceleration phase. The reason for this is that at the instant of
braking, two parameters R and L, must be changed instantaneously, and some
means of varying i_o must be incorporated in order to examine the effect of
F, or the ratio of the current through the motor at time equal to zero to
the ideal amount of current through the motor.

Accordingly, acceleration trajectories were drawn using an x-y coordi-
nate plotter and a computer problem based upon the differential equations
holding true during the acceleration phase. A different computer problem
based upon the differential equations describing the situation during the
deceleration phase was then utilized to obtain deceleration trajectories.
For the deceleration trajectory the initial value of $\overset{\circ}{\Theta}\left(\overset{\circ}{\Theta_o}\right)$ was always
identical with the value of $\overset{\circ}{\Theta}$ for the acceleration phase at the instant
of switching. The initial value of i, however, as computed from the value

128

of i_1 and i_2 at the instant of switching coupled with the value of F for the particular run.

For the computer problem basic characteristics were chosen that were similar to the problem worked out by means of phase planes and analytical methods. The computer was extremely valuable in that it permitted investigations to be made of the system behavior for any ratio of L_b/R_b and for any value of F. It was necessary to record $\overset{o}{\Theta}$, i_1, and i_2 vs time on Brush Recorder charts for the acceleration phase in order to determine the initial conditions that should be set into the problem for the deceleration phase. Naturally, the computer problem used to determine the value of $\overset{o}{\Theta}$, i_1, and i_2 was also used to construct acceleration trajectories on the phase plane by means of the x-y coordinate plotter. The initial condition of i could be obtained by noting the value of $\overset{o}{\Theta}$ at the instant of braking, and referring to the transient curves to obtain values of i_1 and i_2 with which to compute i_o. The computer solution for the acceleration trajectory is shown in Appendix V. The other analogue computer solutions were derived by similar well-known techniques and will not be presented because it would be repetitious. Using the analogue computer for the acceleration phases, transients were obtained by means of a Brush Recorder and a family of portraits was obtained on phase planes by means of the x-y coordinate plotter.

The preliminary program for investigation envisaged some fifteen runs. However, only the runs listed below will be mentioned in the preliminary discussion.

129

RUN	L_b	R_b	i_o
1	150	300	$-i_b$
3	0	300	i_a
7	300	300	$-i_b$
11	75	300	$-i_b$
15	25	50	$-i_b$
19	0	50	i_a
21	50	50	$-i_b$
25	12.5	50	$-i_b$
29	Optimum Relay Servo		

For i_o, the value $-i_b$ in all instances was a very close approximation

of $-\sqrt{\dfrac{L_b i_1{}^2 - L_a i_1}{L_b + L_a}}$ due to the fact that either $L_b \gg L_a$ or

that $\left| i_2 \right| \gg \left| i_1 \right|$ or both.

In run 1 notice that the computer solution is identical with the ana-
lytical solution as portrayed by case A2. We obtain a straight line for a
dead zone trajectory with a slope of -2 for all sizes of step inputs.

In run 3 the trajectory is straight with a slope of -1, which is
identical with what was predicted by the term $-\dfrac{K_v K_t}{J(R_a + R_n)}$
derived in the isocline equation for resistance braking.

Run 7 is a special case. Note that

$$\tau_n{}' = \tau_m(1 + x) = \zeta(i) = 10$$
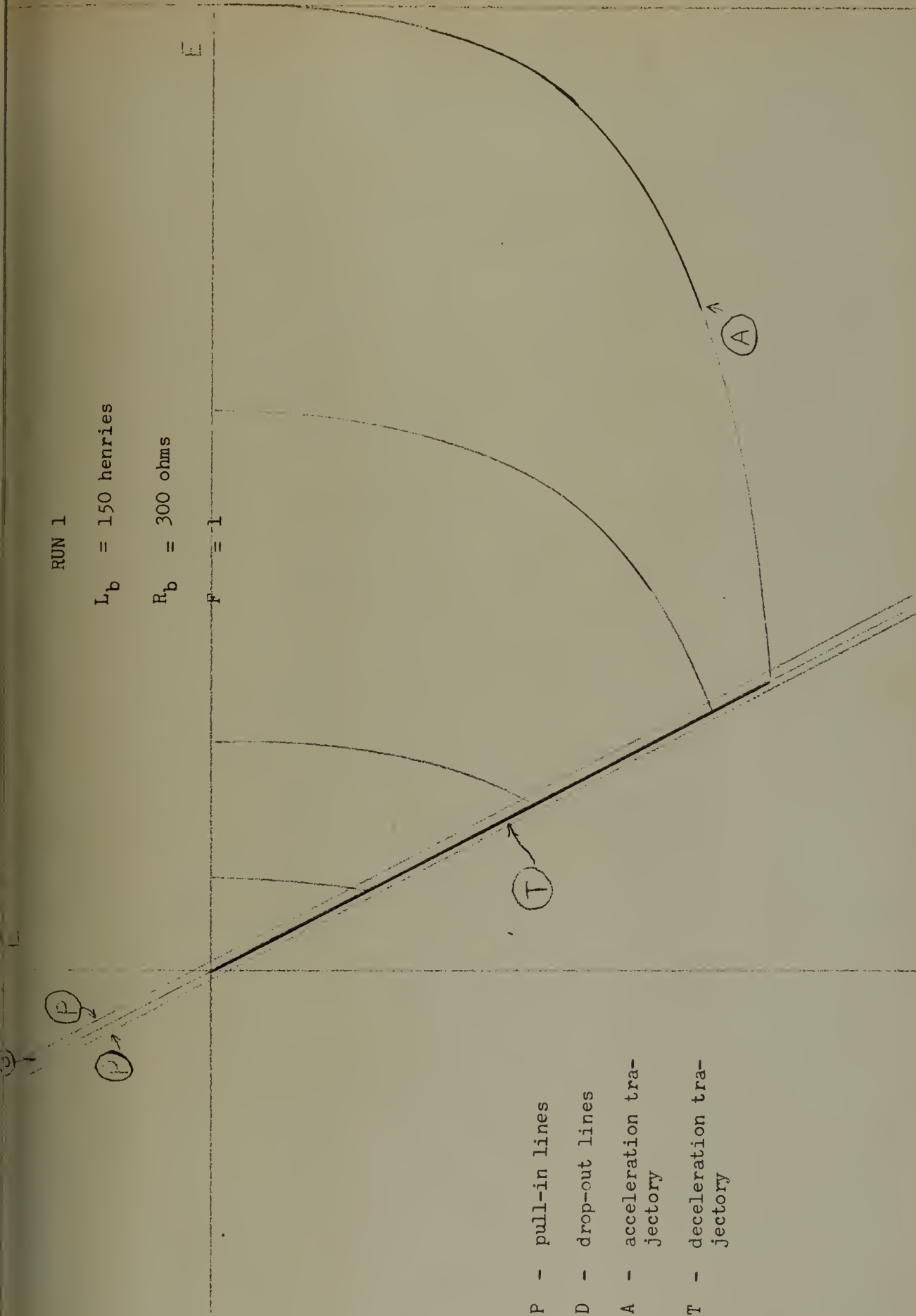
$$\tau_e{}' = \frac{300}{600} = \frac{1}{2}$$

$$\tau_n{}' < 4\tau_e{}'$$

130

Figure 65. Computer-derived Phase Plane Trajectories for a Relay Servo Employing a DC Shunt Motor and Inductive Braking in the Dead Zone

RUN 1

L_b = 150 henries

R_b = 300 ohms

P - pull-in lines

D - drop-out lines

A - acceleration tra-
    jectory

T - deceleration tra-
    jectory

131

RUN 3

$L_b = 0$

$R_b = 300$ ohms

$F = 1$

Figure 66. Computer-derived Phase Plane Trajectories for a Relay Servo Employing a DC Shunt Motor and In-ductive Braking in the Dead Zone.

P — pull-in lines

D — drop-out lines

A — acceleration trajectory

T — deceleration trajectory

RUN 7

L_b = 300 henries

R_b = 300 ohms

F = 1

Figure 67. Computer-derived Phase Plane Trajectories for a Relay Servo Employing a DC Shunt Motor and Inductive Braking in the Dead Zone.

P — pull-in line

D — drop-out line

A — acceleration trajectory

T — deceleration trajectory

133

Although the trajectories on the phase plane do not show it too well, this is an oscillatory, albeit highly-damped, case. There is simply too much energy stored in the inductance to produce desirable characteristics. Stated mathematically, there is no isocline for which N is equal to the actual slope of the isocline. This lends credence to the theory that whenever the radical $\sqrt{\zeta_m'^2 - 4\tau_\zeta'\tau_m'}$ is imaginary, there is no isocline for which the N that is associated with it is equal to the actual slope of the isocline, the dead zone trajectory will never become asymptotic to a straight line, and the system behavior in the dead zone will be oscillatory.

Run 11 depicts the case where the value of inductance is one-half of the desirable value. The slope of the dead zone trajectory is somewhat steeper at the initial part of the trajectory than it is at the final part.

In run 15 a trajectory is obtained which is straight for all practical purposes. It is the case when L_b = 25 and R_b = 50. It has been shown in theory a straight line should result when F = .975 rather than when F = 1.0. However, in practice the difference is very small and may be considered insignificant. For all intents and purposes the dead zone trajectory may be considered straight for F = 1.0. Notice also that the slope is very steep and equal to about -11.7 as predicted. From a velocity of 187 radians per second, the system will brake to a complete stop in about 15.5 radians, and, from the transient analysis, about 0.4 seconds under these conditions.

Run 19 shows the trajectory for 50 ohms resistance only in the braking circuit. The slope of the trajectory is not as steep as it is in the case where both 50 ohms resistance and 25 henries inductance is included in the braking circuit. The actual slope of the trajectory for run 19 is very close

to $- \dfrac{1}{\tau_m (1 + x)} = - 1 72.$

In run 21 the inductance was made equal to 50 henries and the resistance held constant at 50 ohms. Note that just as in the case where R_b was equal to 300 ohms and L_b equal to 300 henries, there is an overshoot. In this case, however, the trajectory appears to ultimately become asymtotic to a straight line, whereas in the 300 ohm-300 henry case, the trajectory continued to curve until steady state conditions prevailed. This gives rise
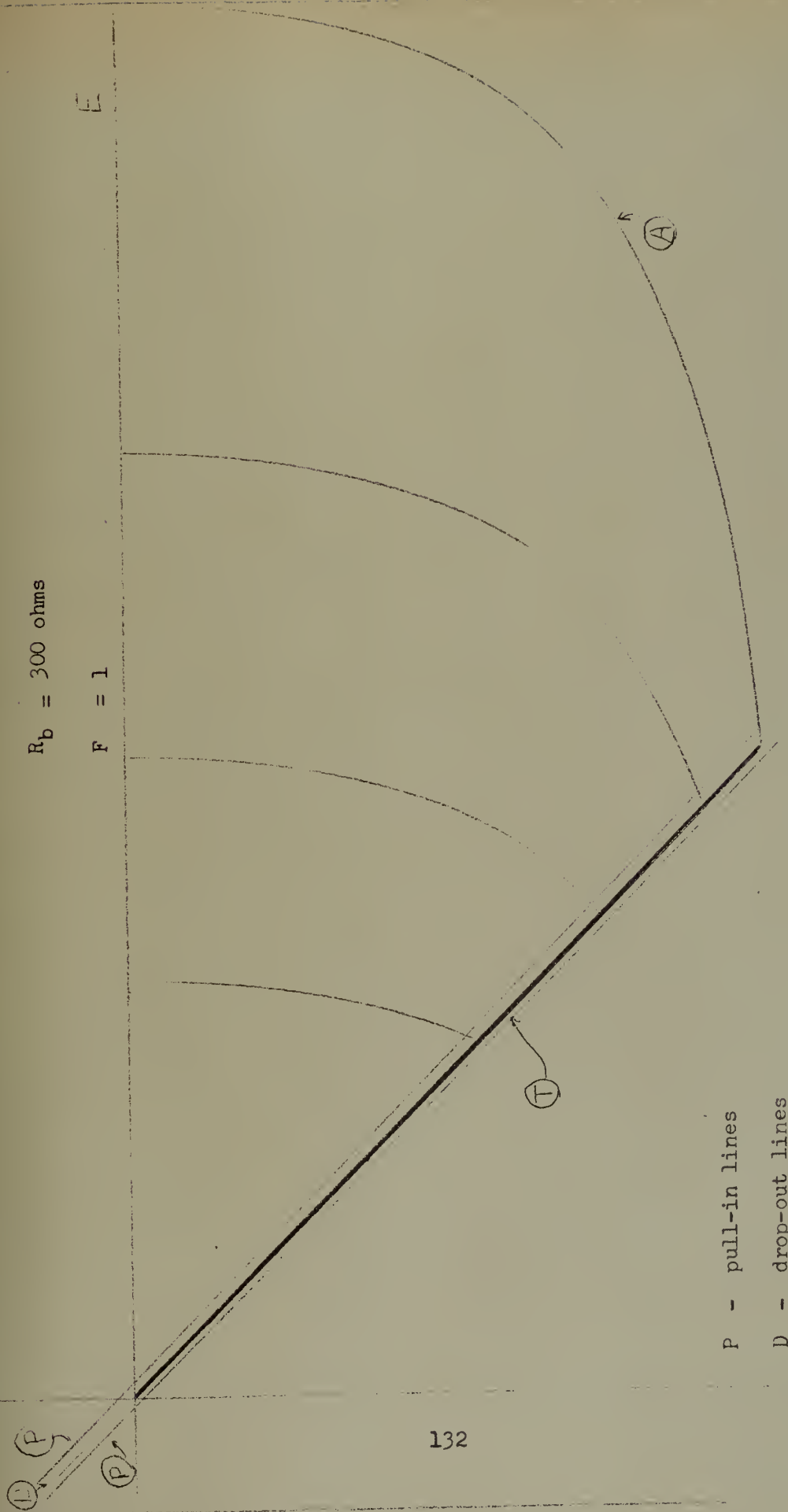
135

RUN 11

L_b = 75 henries

R_b = 300 ohms
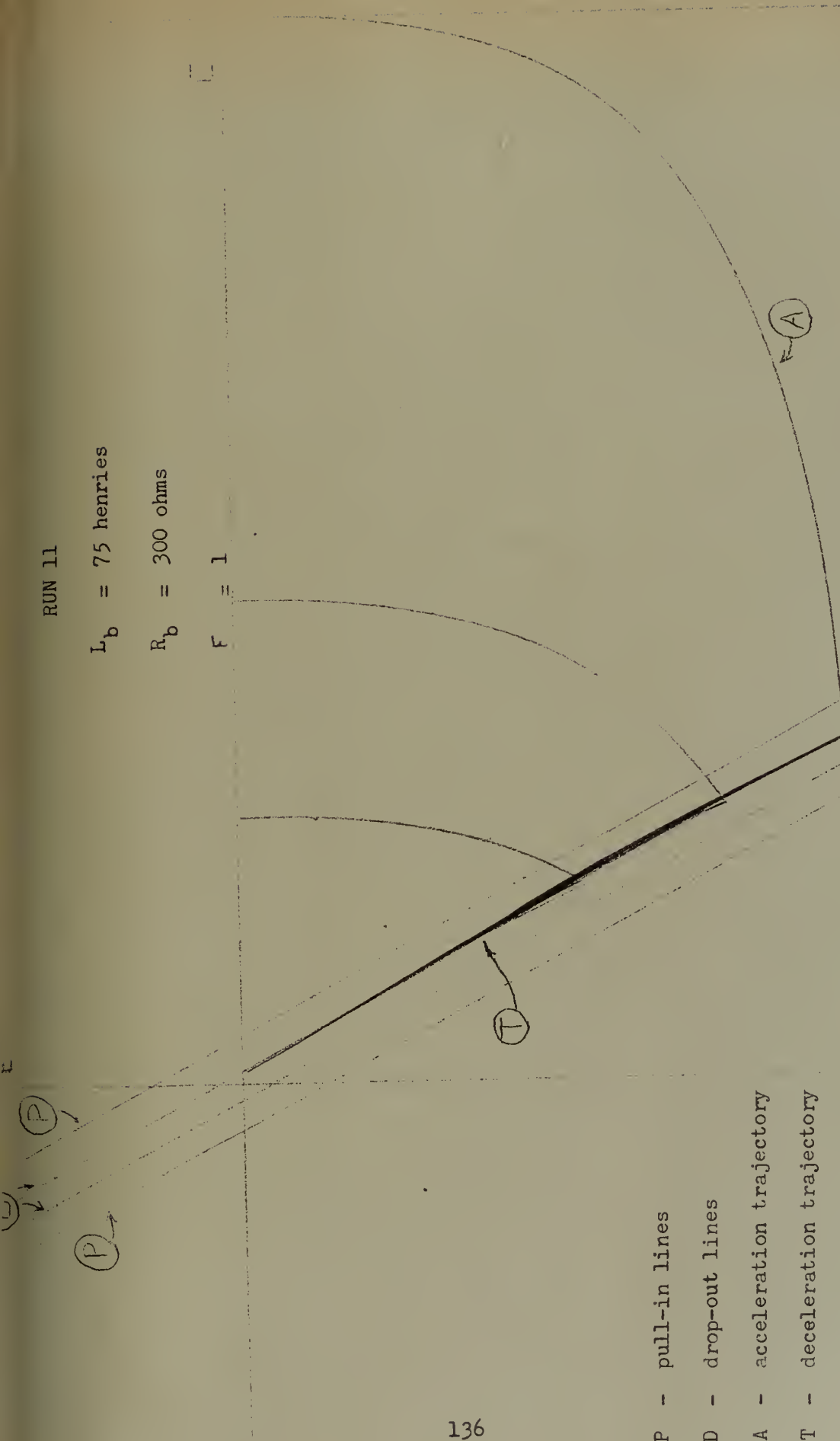
F = 1

Figure 68. Computer-derived Phase Plane Trajectories for a Relay Servo Employing a DC Shunt Motor and Inductive Braking in the Dead Zone.

P — pull-in lines

D — drop-out lines

A — acceleration trajectory

T — deceleration trajectory

136

RUN 15

L_b = 25 henries

R_b = 50 ohms

F = 1

Figure 69. Computer-derived Phase Plane Trajectories for a Relay Servo Employing a DC Shunt Motor and Inductive Braking in the Dead Zone.

P - pull-in lines

D - drop-out lines

A - acceleration trajectory

T - deceleration trajectory

137

RUN 19

$L_b = 0$

$R_b = 50$ ohms

$F = 1$

Figure 70. Computer-derived Phase Plane Trajectories for a Relay Servo Employing a DC Shunt Motor and Inductive Braking in the Dead Zone.

P — pull-in lines

D — drop-out lines

A — acceleration trajectory

T — deceleration trajectory

138

RUN 21

L_b = 50 henries

R_b = 50 ohms

F = 1

Figure 71. Computer-derived Phase Plane
Trajectories for a Relay Servo Employing
a DC Shunt Motor and Inductive Braking
in the Dead Zone.

P - pull-in lines

D - drop-out lines

A - acceleration trajectory

T - deceleration trajectory

139

to the concept that perhaps $\tau_n' \geq 4\tau_e'$ in run 21.

$$\tau_m' = (.5)(1.167) = .583$$

$$\tau_e' = \frac{505}{350} = .144$$

$$\tau_n' = 4.05\,\tau_e'$$

Therefore, it is seen that $\tau_n' > 4\tau_e'$ and the concept that the trajectory will ultimately become asymptotic to a straight line when $\tau_n' \geq 4\tau_e'$ is still valid. From the practical viewpoint, however, this type of behavior would be unacceptable.

In run 25 there is a situation wherein the trajectory has a steep slope in the initial phases and then the slope decreases until it is considerably less in the final phases. The slope of the switching line may be adjusted to make the trajectories corresponding to any step input end at the same place, but note that the intersection of the switching line and the zero error rate line is considerably removed from the point at which the trajectories end. Use of this R-L combination presumably would result in a wide dead zone and would be unacceptable from a practical standpoint.

Run 29 is offered for comparison purposes only. It shows the so-called optimum system which calls for full reverse voltage to be applied at the instant of switching. Note that the switching line must be curved in this case.

After the first thirty runs were completed it was decided to investigate (1) how small changes in the value of inductance from the ideal would affect the dead zone trajectory and (2) how a change in F would affect the dead zone trajectory. In order to consider all possibilities it was

140

RUN 25

L_b = 12.5 henries

R_b = 50 ohms

F = 1

P – pull-in lines
D – drop-out lines
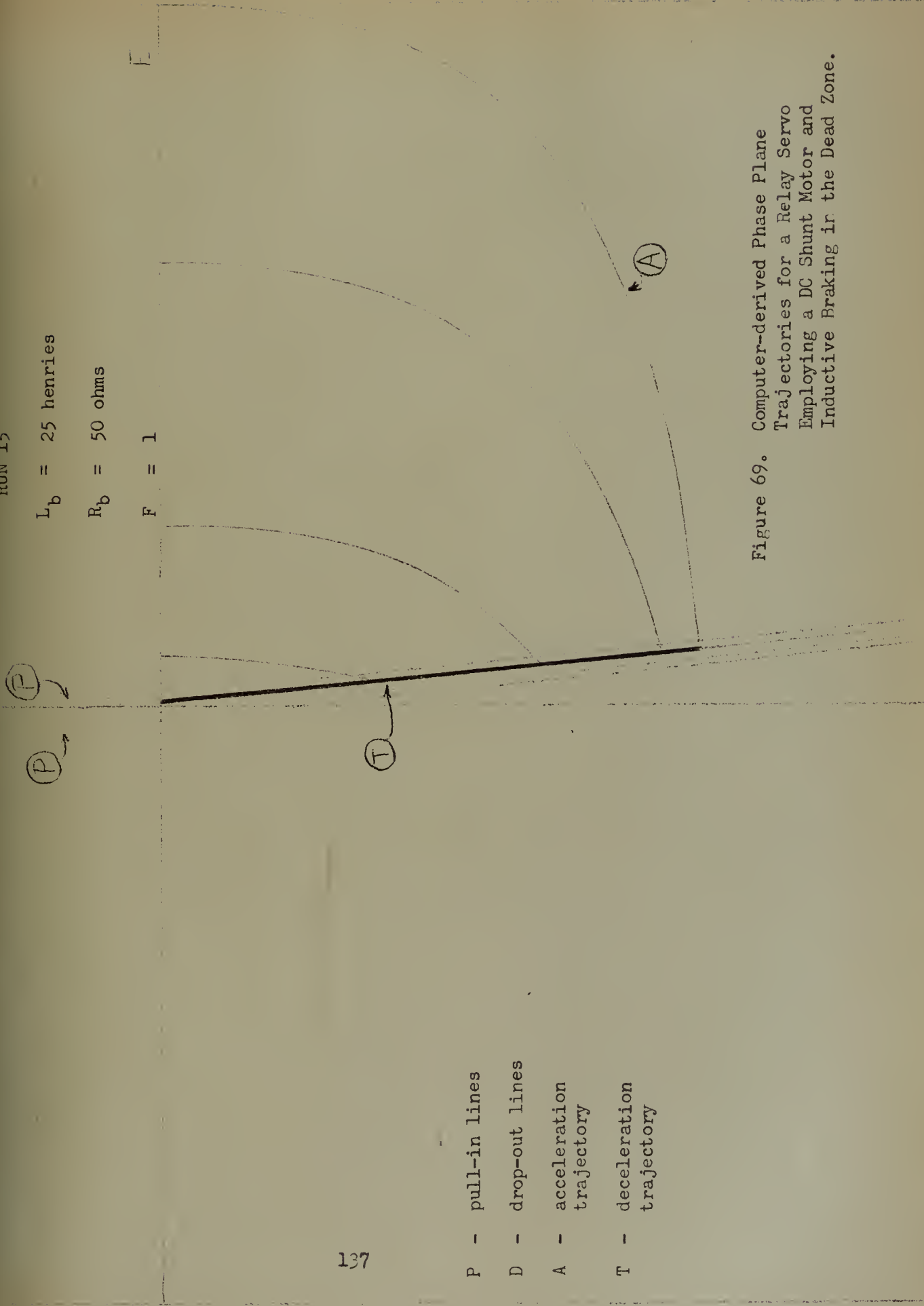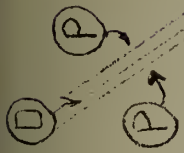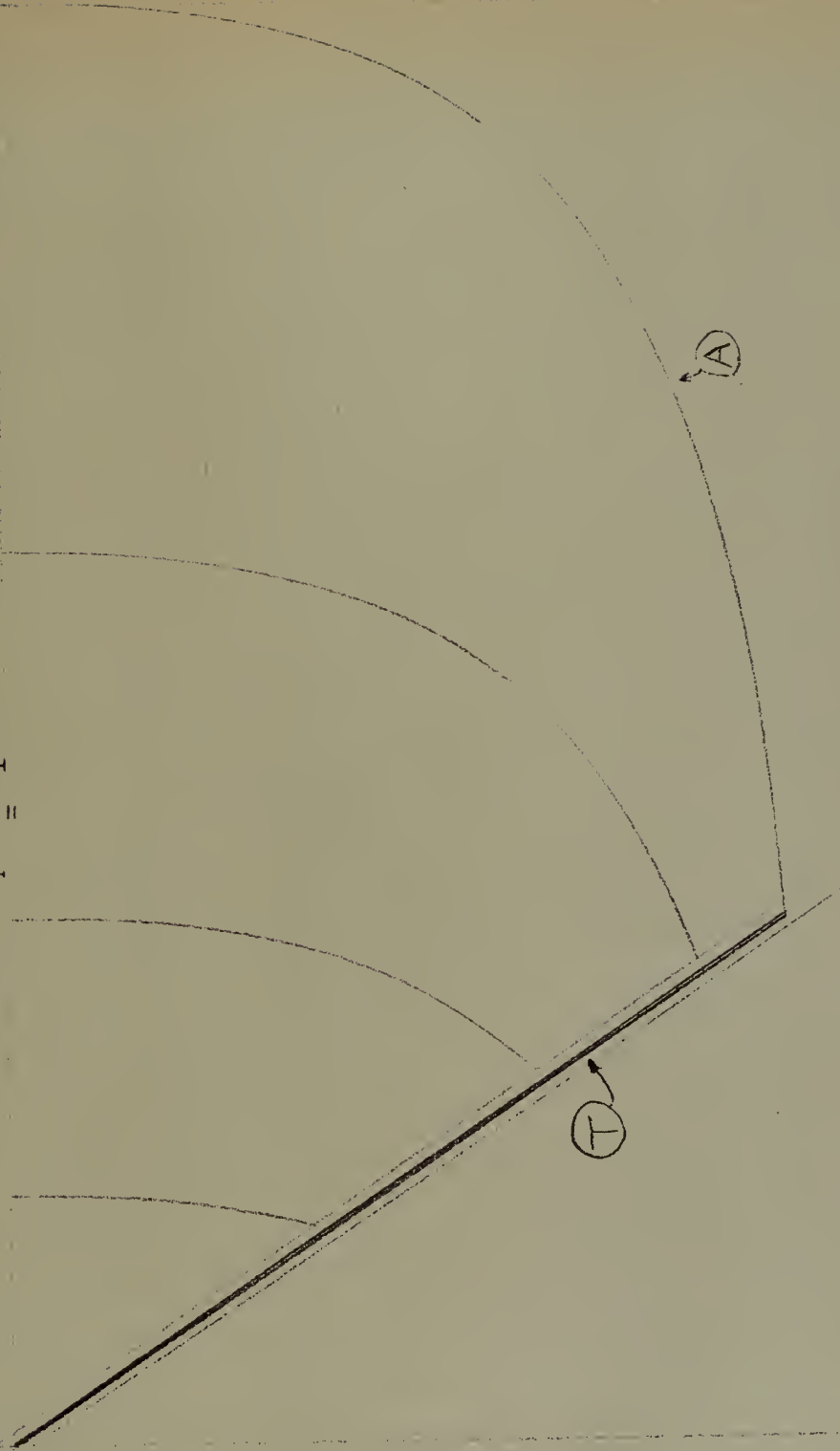A – acceleration
    trajectory
T – deceleration
    trajectory

141

Figure 72. Computer-derived Phase Plane Trajectories for a Relay Servo Employing a DC Shunt Motor and Inductive Braking in the Dead Zone.
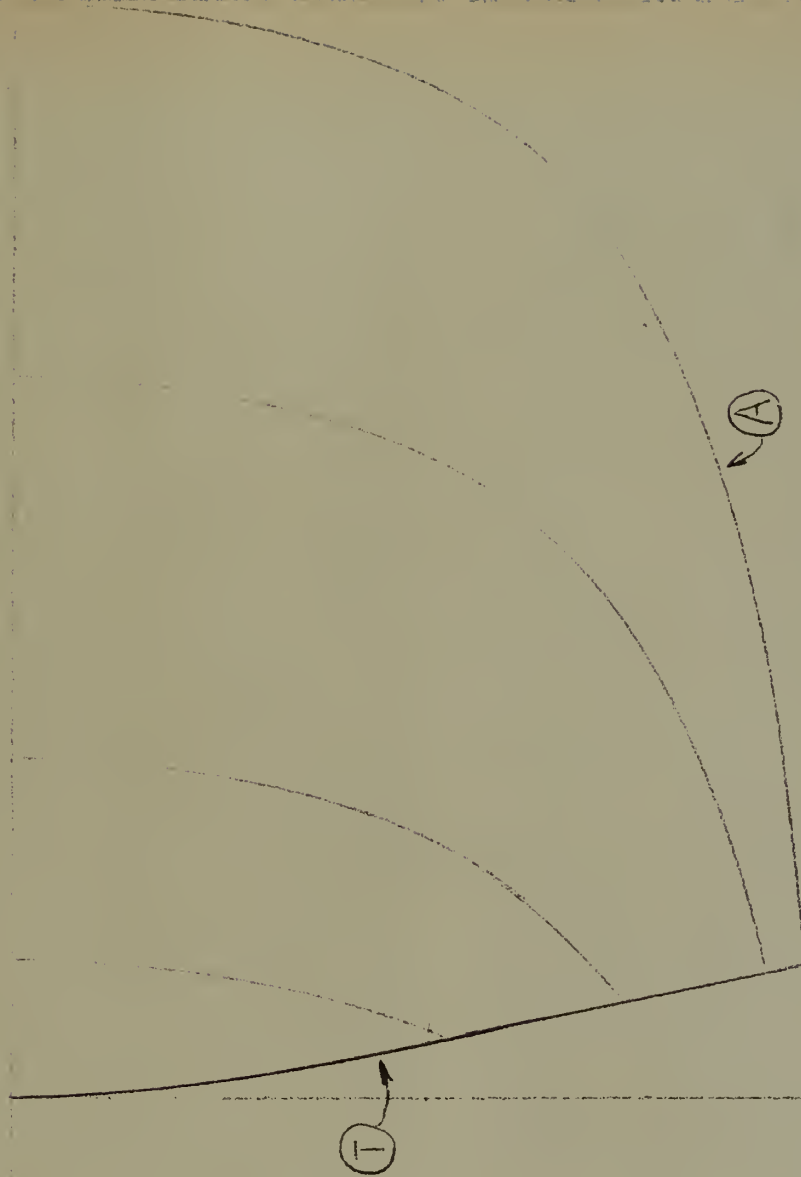
Figure 73. Computer-derived Phase Plane Trajectories for a Optimum Relay Servo System Employing a DC Shunt Motor. RUN 29

A - acceleration trajectory

T - deceleration trajectory

142

decided to simulate inductances of 30, 27.5 25, 22.5, and 20 henries with
a resistance of fifty ohms. It was also decided that for each value of
inductance, an F of 1.0, .9, .75, 12, and 0 would be simulated.

Run	L_b	R_b
31	25	50
32	30	50
33	27.5	50
34	22.5	50
35	20	50

In order to designate the F used for each run the value of F was
added after the basic run designation as a decimal.

Example:

For a run in which L_b = 22.5, R_b = 50, F = .5, the run would
be labeled 34.5.

Run 31 is essentially an enlargement of run 15. However, there are
several interesting results of the 31 series. First, for an F of 1.0, a
trajectory is obtained which is essentially straight and has a slope of
about -11.7. The switching line could be made to parallel the dead zone tra-
jectory and hence deadbeat performance and a small steady state error would
result for any size of step input. The second interesting phenomenon is
that just as the analysis predicted, a straight line results for the dead
zone trajectory when F = x = .167, although its slope is not anywhere
near as steep (about -2) as the slope when F = 1.0. The third interest-
ing point is that the trajectories tend to "bow in" for an F between 1.0
and .167, and "bow out" for F less than .167. Fourth and finally, for the
entire 31 series, which is, incidentally, the ideal case from a mathematical

FIG. 31.10

L_b = 25 henries

R_b = 50 ohms

F = 1

Ⓐ

Ⓣ

Ⓟ

Figure 74. Computer-Derived Phase Plane Trajectories for a Relay Servo Employing a DC Shunt Motor and Inductive Braking in the Dead Zone.

P - pull-in lines

D - drop-out lines

A - acceleration trajectory

T - deceleration trajectory

144

RUN 31.9

L_b = 25 henries

R_b = 50 ohms

F = .9

Figure 75. Computer-derived Phase Plane Trajectories for a Relay Servo Employing a DC Shunt Motor and Inductive Braking in the Dead Zone.

P — pull-in lines

D — drop-out lines

A — acceleration trajectory

T — deceleration trajectory

RUN 31.75

L_b = 25 henries

R_b = 50 ohms

F = .75

P - pull-in lines

D - drop-out lines

A - acceleration trajectory

T - deceleration trajectory

Figure 76. Computer-derived Phase Plane Trajectories for a Relay Servo Employing a DC Shunt Motor and Inductive Braking in the Dead Zone.

146

RUN 31.5

L_b = 25 henries

R_b = 50 ohms

F = .5

Figure 77. Computer-derived Phase Plane Trajectories for a Relay Servo Employing a DC Shunt Motor and Inductive Braking in the Dead Zone.

P – pull-in lines

D – drop-out lines

A – acceleration trajectory

T – deceleration trajectory

147

RUN 31.333

L_b = 25 henries

R_b = 50 ohms

F = .333

Figure 78. Computer-derived Phase Plane Trajectories for a Relay Servo Employing a DC Shunt Motor and Inductive Braking in the Dead Zone.

P - pull-in line

D - drop-out line

A - acceleration trajectory

T - deceleration trajectory
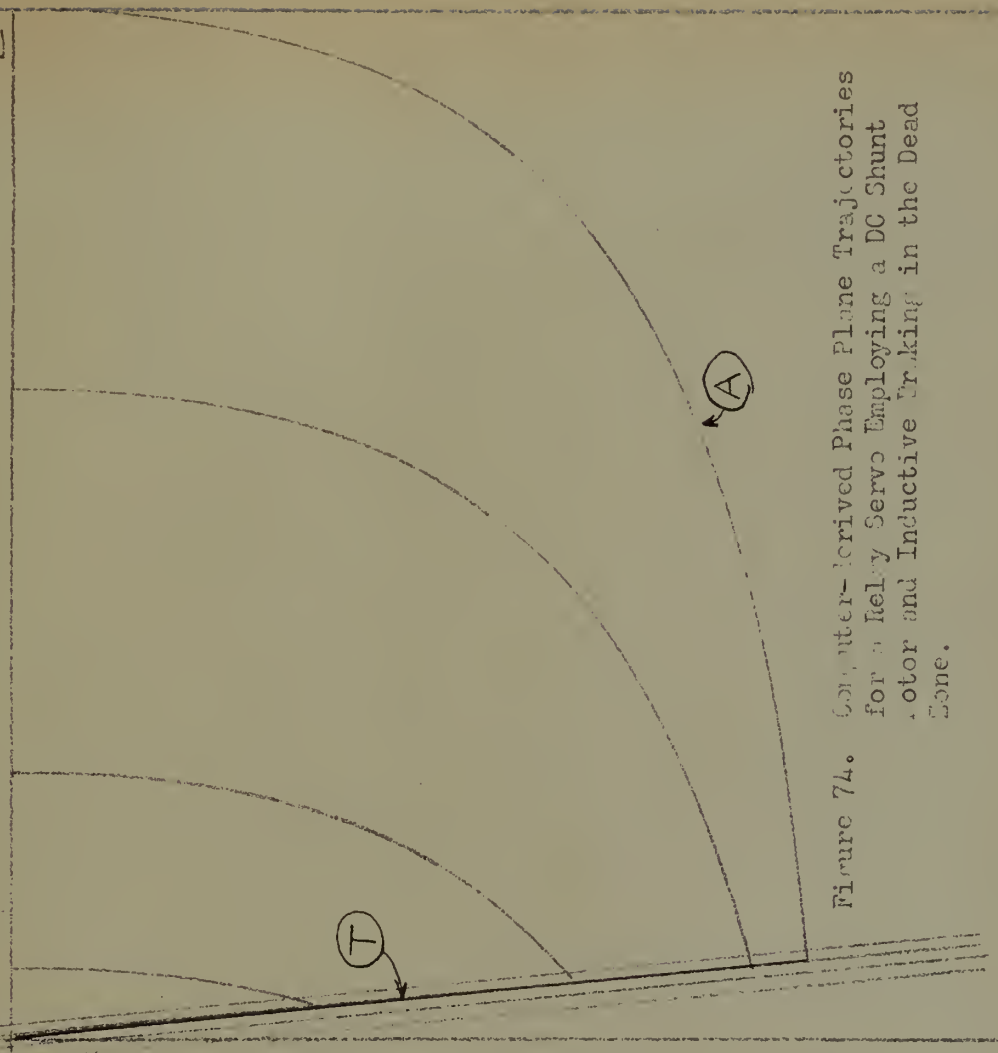
148

RUN 31.20

L_b = 25 henries

R_b = 50 ohms

F = .2

Figure 79. Computer-derived Phase Plane Trajectories for a Relay Servo Employing a DC Shunt Motor and Inductive Braking in the Dead Zone.

P - pull-in lines

D - drop-out lines

A - acceleration trajectory

T - deceleration trajectory

149

RUN 31.167

L_b = 25 henries

R_b = 50 henries

F = .167

Figure 80. Computer-derived Phase Plane Trajectories for a Relay Servo Employing a DC Shunt Motor and Inductive Braking in the Dead Zone.

150

P – pull-in lines

D – drop-out lines

A – acceleration trajectory

T – deceleration trajectory

RUN 31.0

L_b = 25 henries

R_b = 50 ohms

$F = c$

151

P — pull-in line

D — drop-out line
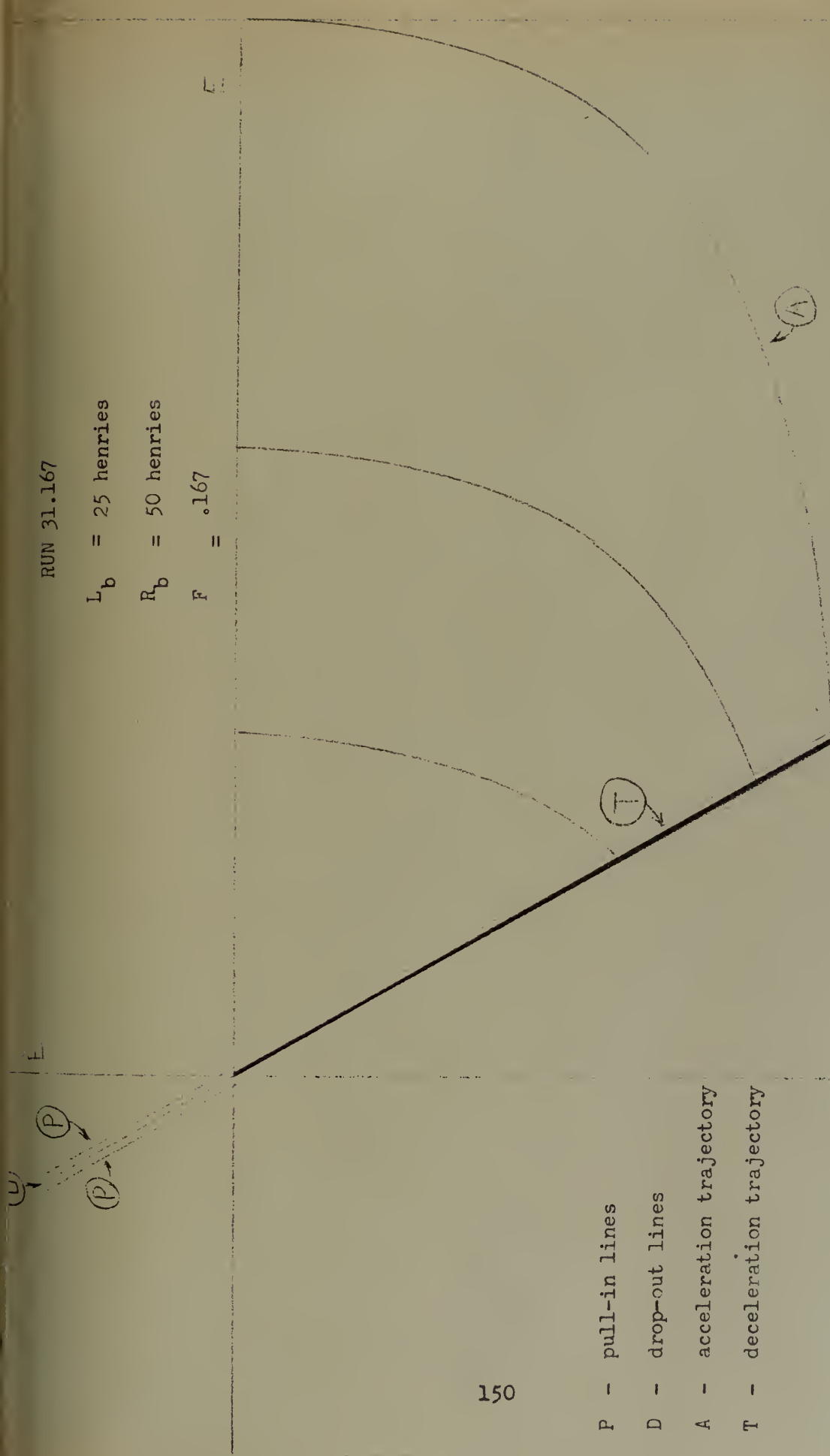
A — acceleration trajectory

T — deceleration trajectory

Figure 81. Computer-derived Phase Plane Trajectories for a Relay Servo Employing a DC Shunt Motor and Inductive Braking in the Dead Zone.

standpoint, the intersection of the drop-out switching line with the zero error rate line occurs at a point at which all trajectories, curved or straight, end. Therefore, if the difference between the pull-in and drop-out lines is appreciable, a high degree of static accuracy may be obtained even though the trajectories curve in the dead zone. If, on the other hand, the effects of coulomb friction are considered, a straight line condition would be preferred with the amount and effect of the coulomb friction determining the difference between the pull-in and drop-out lines that would be required.

The 32 and 33 series also produce an interesting result. Notice that when $F = 1.0$, an overshoot is obtained if $\overset{\cup}{\theta}_o$ is large. However, as F decreases slightly, a point is reached where the trajectory in the dead zone is straight for all sizes of step inputs. This effect is best illustrated in run 33.9. This effect was not predicted by the mathematics due to the difficulty in handling i_o and L_b when $\tau_{e_L} \neq \tau_{ma}$. It can be explained physically, however, from the standpoint that originally too much energy existed in the braking inductance at the time of relay drop-out. If some of this energy, however, is allowed to "bleed" or dissipate across the relay contacts, the amount of energy fed back to the motor after relay drop-out becomes the ideal amount and at about the ideal rate once again. As the value of inductance in the braking circuit is increased slightly from the ideal amount a straight line will be obtained for the dead zone trajectory as the value of F is decreased from 1.0. If inductance is increased too much, however, a straight line will not be obtained since the L_b/R_b ratio is nowhere near the ideal one. This was exemplified in run 21 when, with R_b equal to 50 ohms and L_b equal to 50 henries a straight line was not obtained although F was varied from 1.0 (figure 70) to 0 (not shown).

152

RUN 32.10

L_b = 30 henries

R_b = 50 ohms
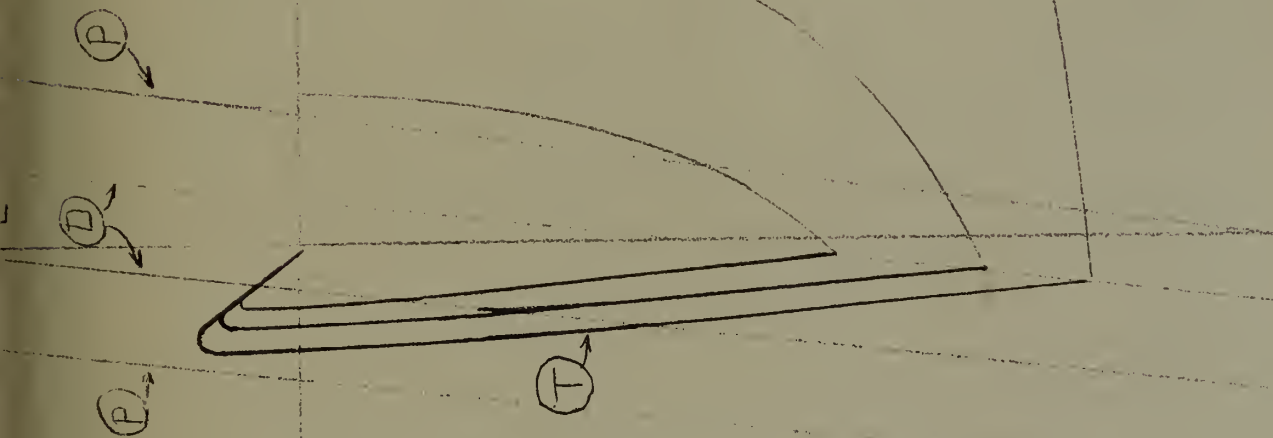
F = 1.0

P - pull-in lines

D - drop-out lines

A - acceleration trajectory

T - deceleration trajectory

153

Figure 82. Computer-derived Phase Plane Trajectories for a Relay Servo
Employing a DC Shunt Motor and Inductive Braking in the Dead Zone.

RUN 32.9

L_b = 30 henries

R_b = 50 ohms

F = .9

Figure 83. Computer-derived Phase Plane Trajectories for a Relay Servo Employing a DC Shunt Motor and Inductive Braking in the Dead Zone.

154

P - pull-in line

D - drop-out line

A - acceleration trajectory

T - deceleration trajectory

RUN 32.75

L_b = 30 henries

R_b = 50 ohms

F = .75

Figure 84. Computer-derived Phase Plane Trajectories for a Relay Servo Employing a DC Shunt Motor and Inductive Braking in the Dead Zone.

P - pull-in line

D - drop-out line

A - acceleration trajectory

T - deceleration trajectory

155

RUN 32.5

L_b = 30 henries

R_b = 50 ohms

F = .5

Figure 85. Computer-derived Phase Plane Tra-
jectories for a Relay Servo
Employing a DC Shunt Motor and
Inductive Braking in the Dead Zone.

156

P — pull-in lines

D — drop-out lines

A — acceleration trajectory

T — deceleration trajectory

RUN 32.2

L_b = 30 henries

R_b = 50 ohms

F = .2

Figure 86 Computer-derived Phase Plane Trajectories
for a Relay Servo Employing a DC Shunt
motor and Inductive Braking in the
Dead Zone.

157

P – pull-in line

D – drop-out line

A – acceleration
    trajectory

T – deceleration
    trajectory
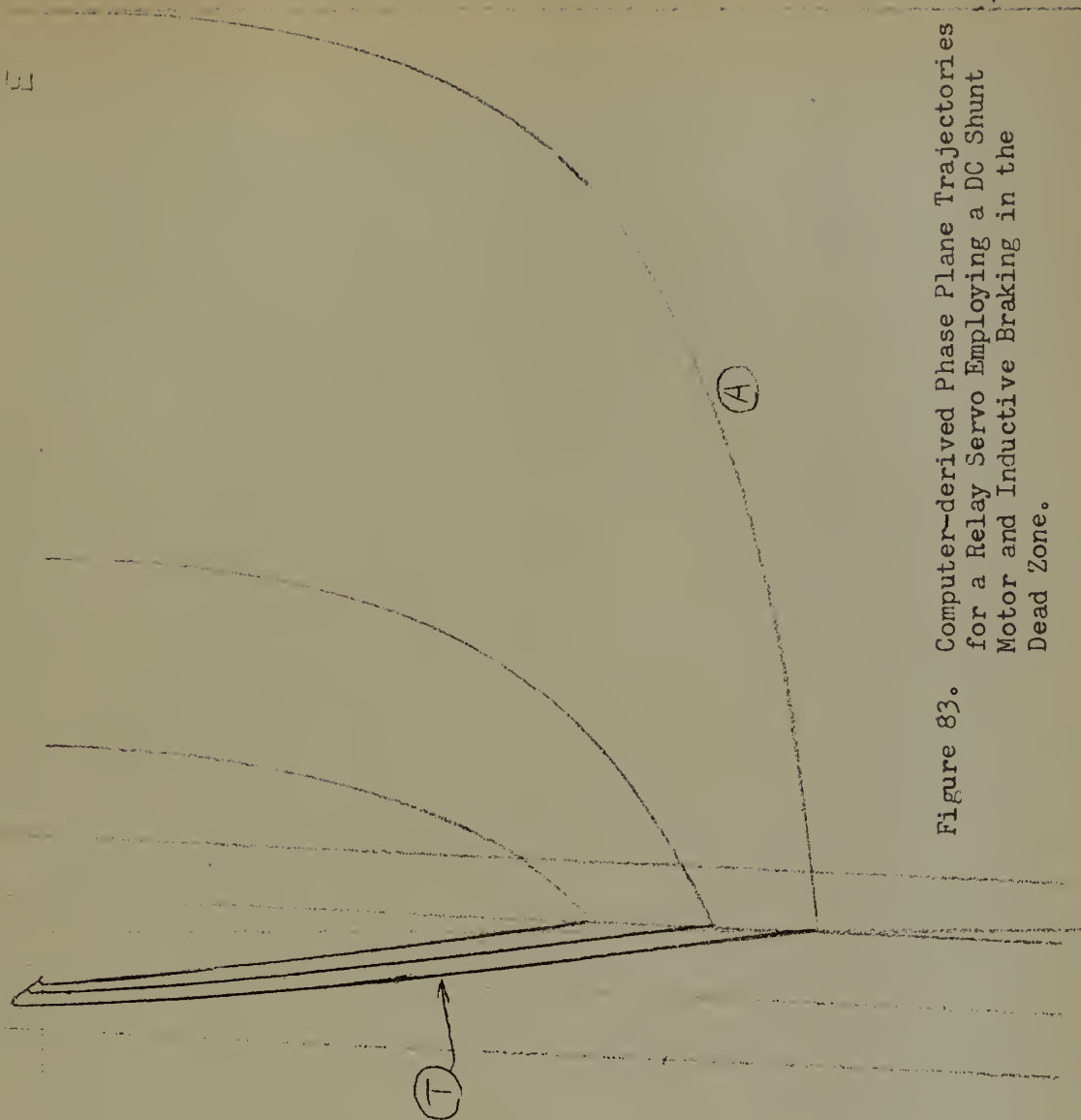
RUN 32.0

L_b = 30 henries

R_b = 50 ohms

F = 0

Figure 87. Computer-derived Phase Plane Trajectories for a Relay Servo Employing a DC Shunt Motor and Inductive Braking in the Dead Zone.

P - pull-in line

D - drop-out line

A - acceleration trajectory

T - deceleration trajectory

158

RUN 33.10

L_b = 27.5 henries

R_b = 50 ohms

F = 1.0

Figure 88. Computer-derived Phase Plane Trajectories for a Relay Servo Employing a DC Shunt Motor and Inductive Braking in the Dead Zone.

P   -   pull-in line

D   -   drop-out line

A   -   acceleration trajectory

T   -   deceleration trajectory

159

RUN 33.9

$L_b = 27.5$ henries

$R_b = 50$ ohms

$F = .9$
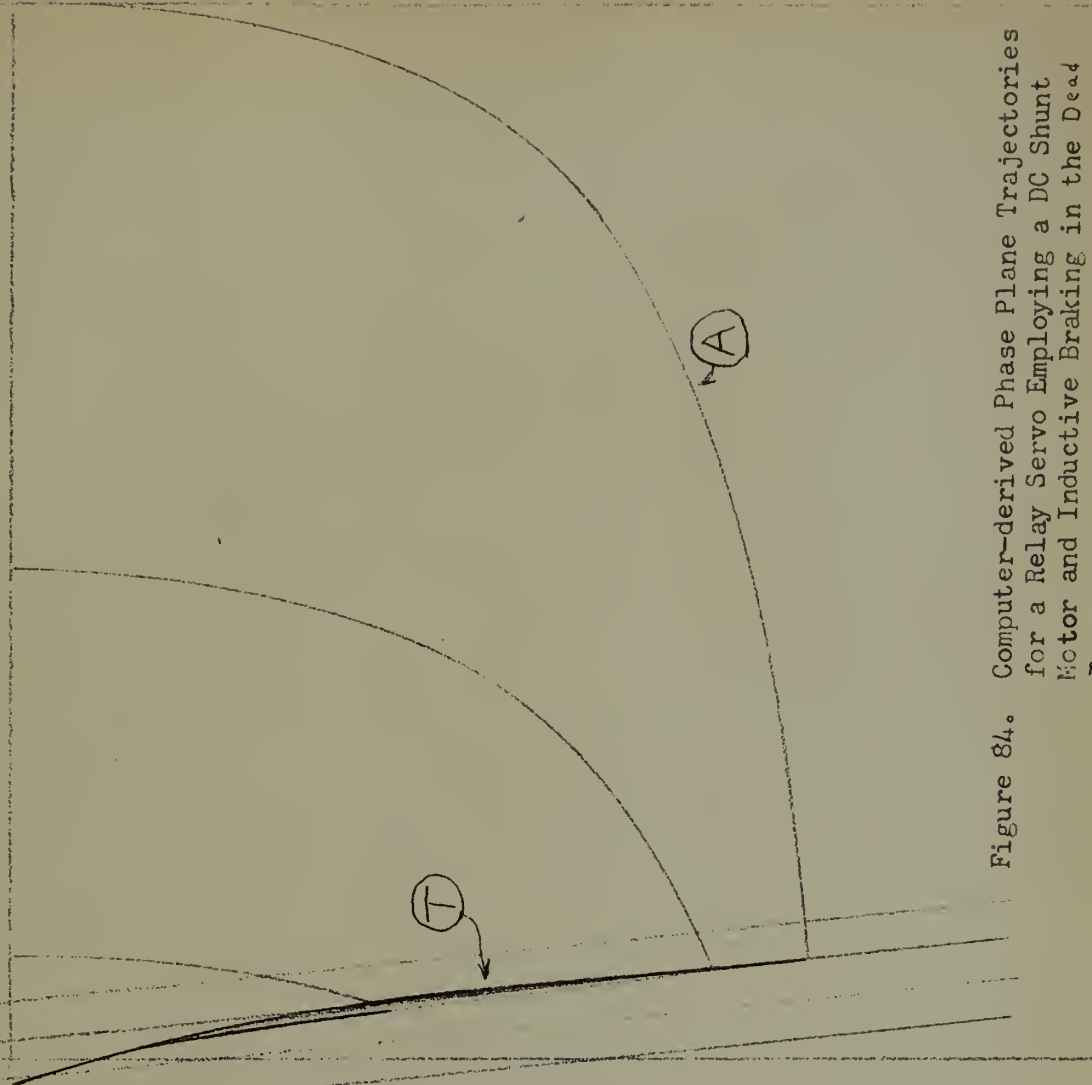
Figure 89. Computer-derived Phase Plane Trajectories for a Relay Servo Employing a DC Shunt Motor and Inductive Braking in the Dead Zone.

P — pull-in line

D — drop-out line

A — acceleration trajectory

T — deceleration trajectory

160

RUN 33.75

L_b = 27.5 henries

R_b = 50 ohms

F = .75

Figure 90. Computer-derived Phase Plane Trajectories for a Relay Servo Employing a DC Shunt Motor and Inductive Braking in the Dead Zone.
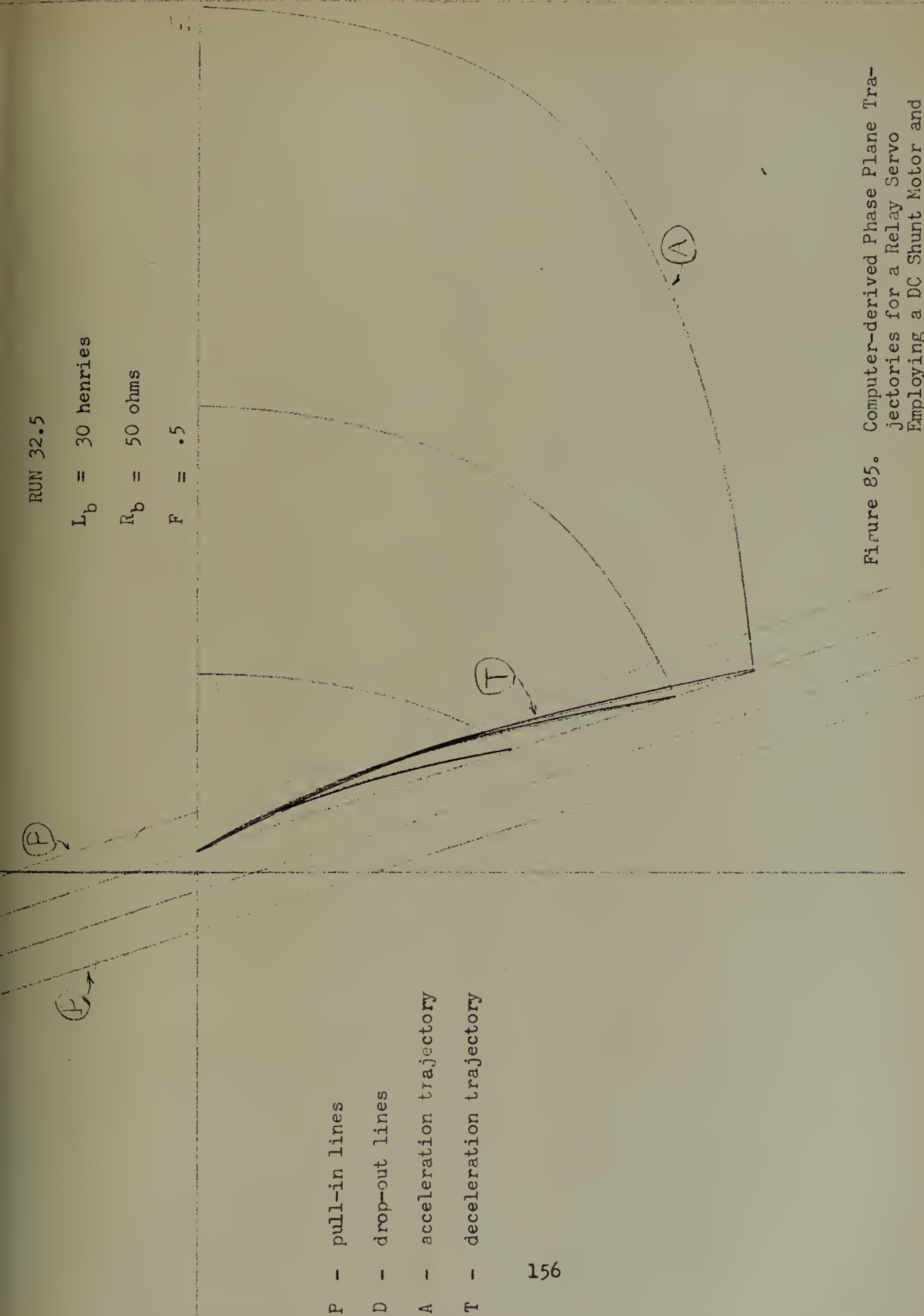
P - pull-in lines

D - drop-out lines

A - acceleration trajectory

T - deceleration trajectory
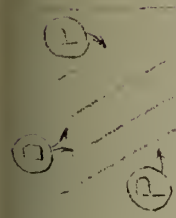
161

RUN 33.5

L_b = 27.5 henries

R_b = 50 ohms

F = .5

Figure 91. Computer-derived Phase Plane Trajectories for a Relay Servo Employing a DC Shunt Motor and Inductive Braking in the Dead Zone.

P – pull-in lines

D – drop-out lines

A – acceleration trajectory

T – deceleration trajectory
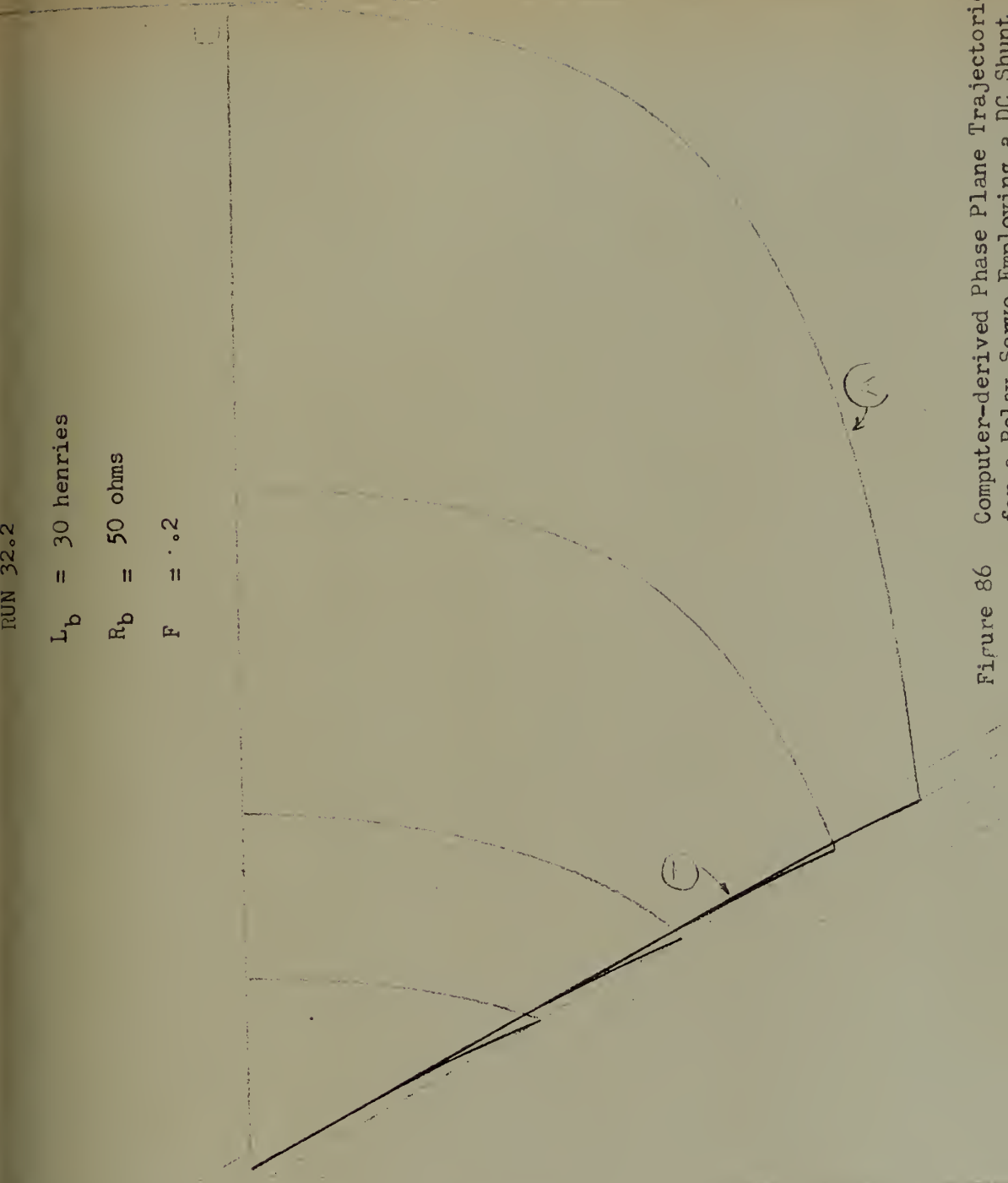
162

RUN 33.2

L_b = 27.5 henries

R_b = 50 ohms

F = .2

Figure 92. Computer-derived Phase Plane Trajectories for a Relay Servo
Employing a DC Shunt Motor and Inductive Braking in the
Dead Zone.

163

P - pull-in lines

D - drop-out lines
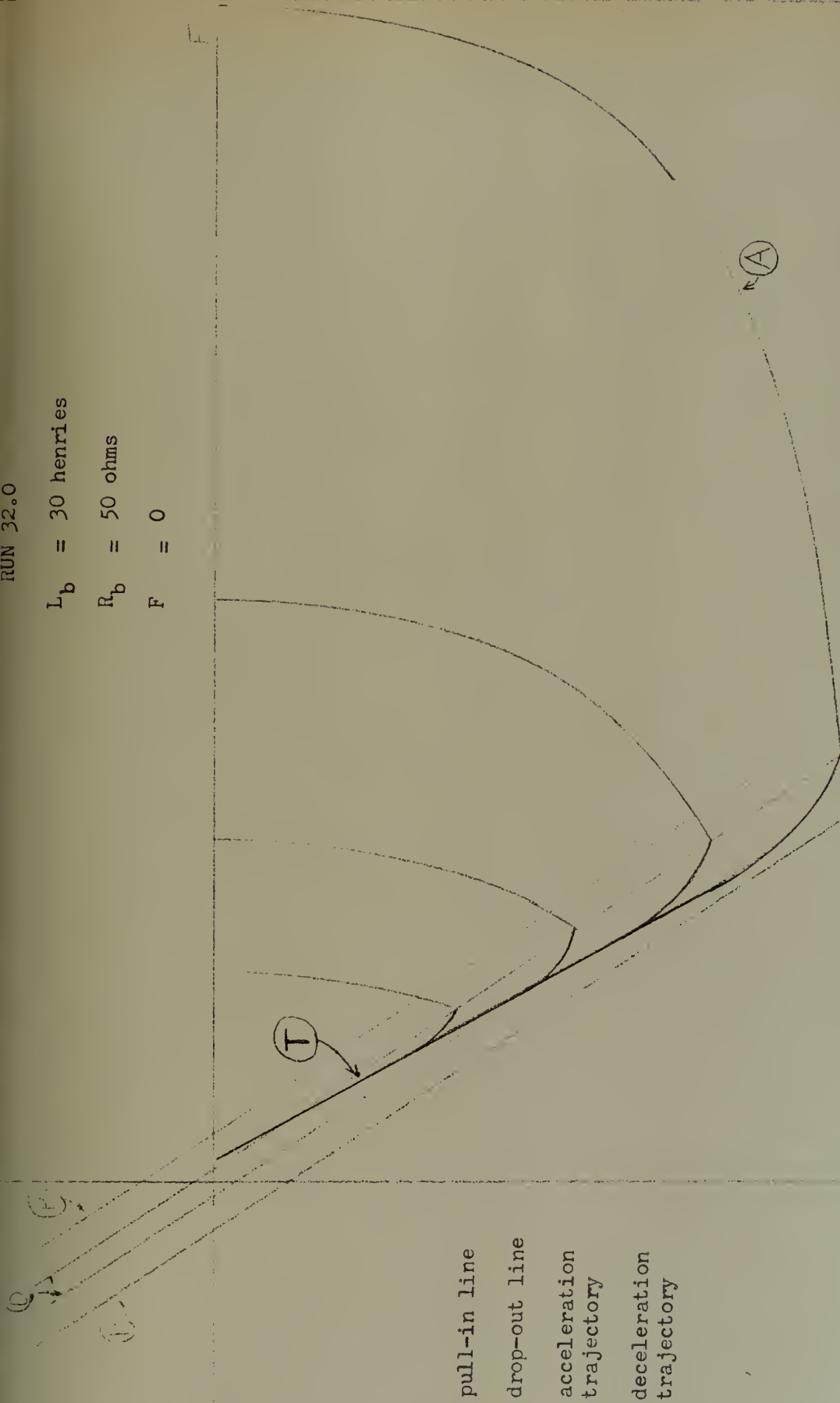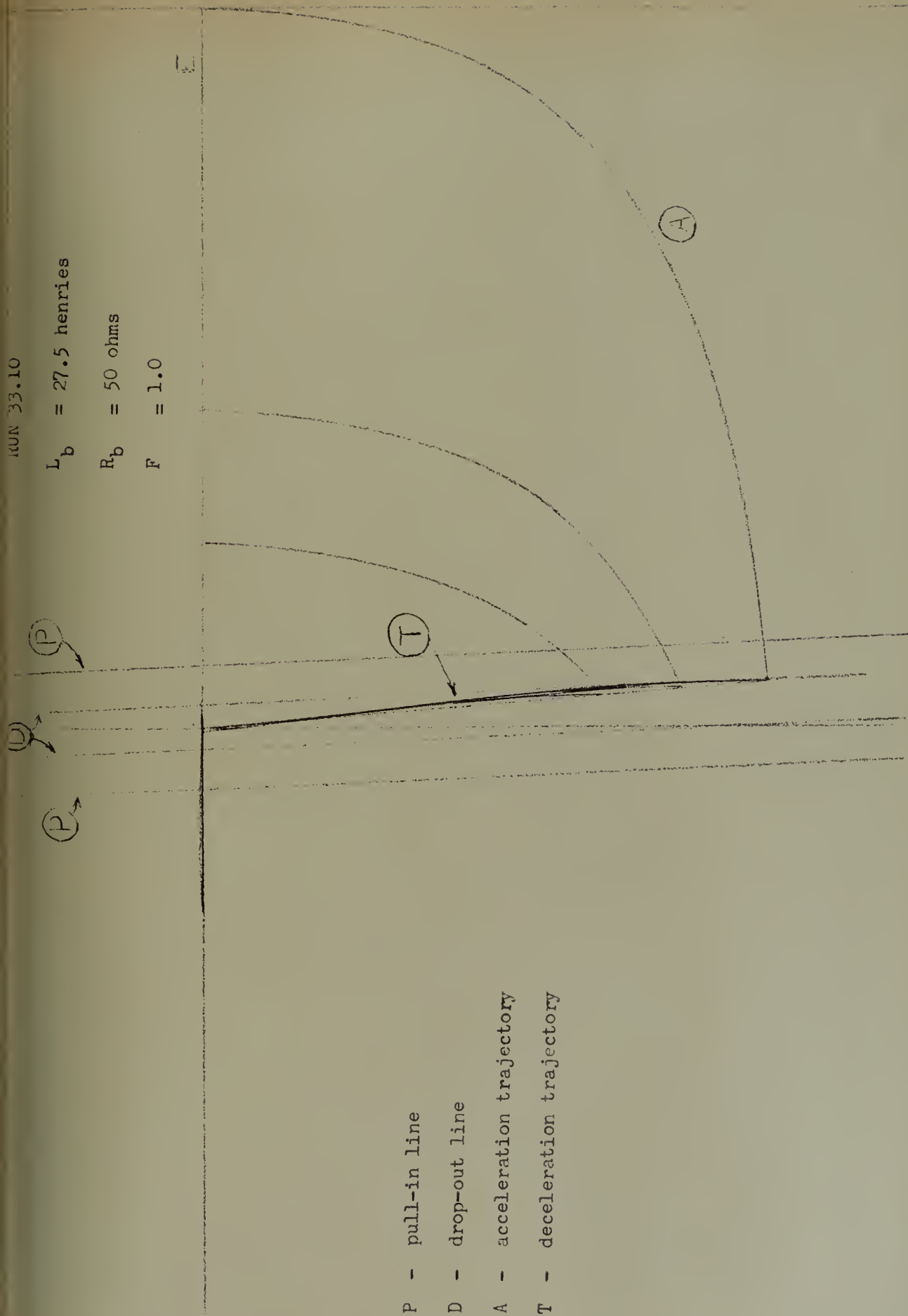
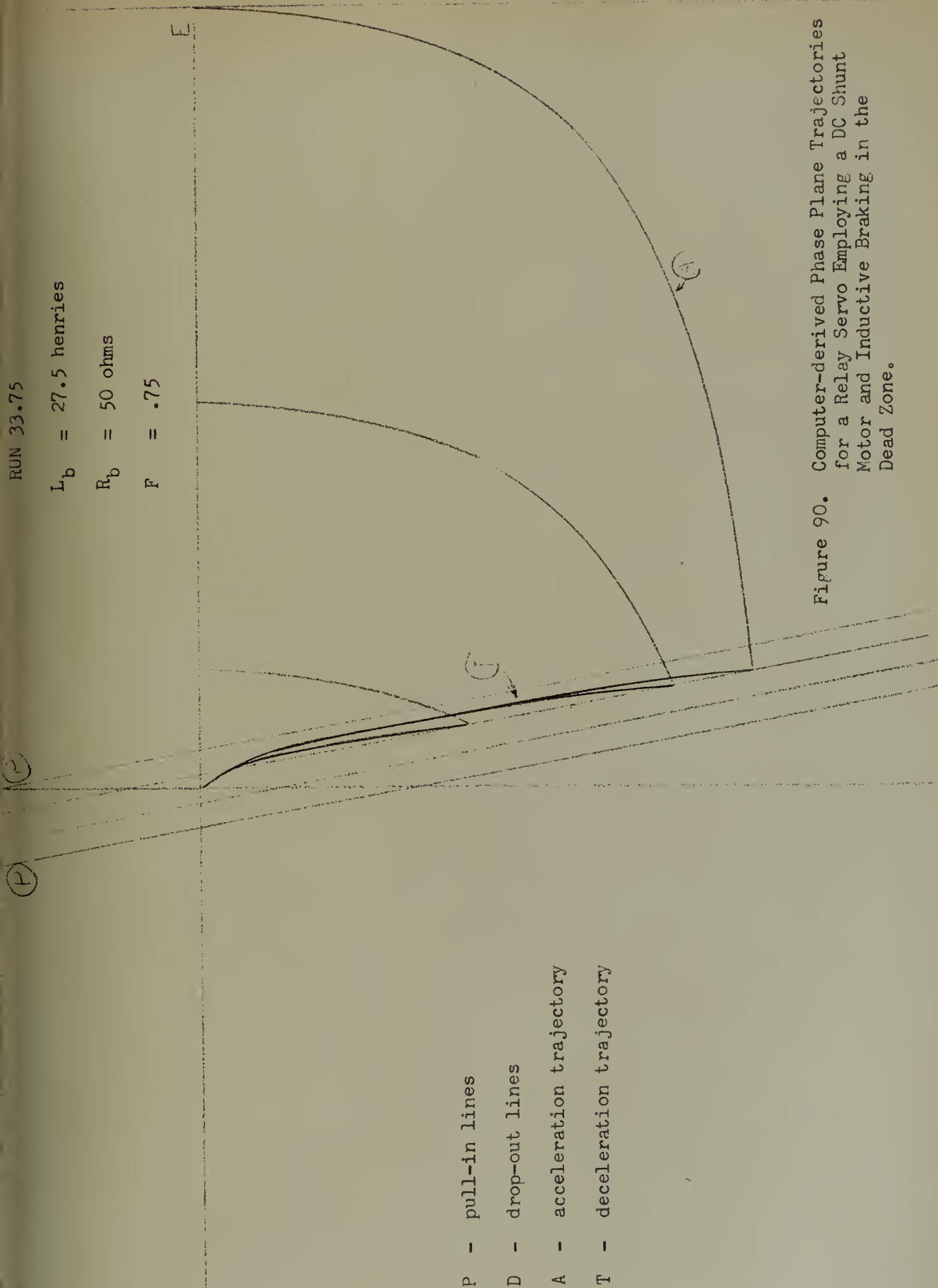A - acceleration
    trajectory

T - deceleration
    trajectory

Figure 93. Computer-derived Phase Plane Trajectories for a Relay Servo Employing a DC Shunt Motor and Inductive Braking in the Dead Zone.

RUN 33.0

L_b = 27.5 henries

R_b = 50 ohms

F = 0

P - pull-in lines

D - drop-out lines

A - acceleration trajectory

T - deceleration trajectory

164

The significance of this phenomenon is rather important. It is difficult to conceive of a relay-motor-load combination where F = 1.0. This would mean that the relay would open so quickly that energy loss at the relay contacts would not occur to any extent. However, it is conceivable that a relay might have a characteristic F of say .7 - .9. If it should, then it would remain to simply install an inductance in the braking circuit with a value of inductance that is slightly greater than the ideal value. Experimental evidence indicates that the actual value of inductance inserted in the braking circuit should be about $\frac{1}{F}$ times the ideal value of inductance. Note that a straight line could also be obtained by making F = x, but in this case the slope of the dead zone trajectory would be much less (negatively) than in the case where the inductance is adjusted to take into account the difference between the actual value of F and one. A straight line with a steep slope for the dead zone trajectory will be linked to a small time of response later.

Runs 34 and 35 depict the situation wherein the inductance used in the braking circuit is too small. Notice that even when F = 1.0. the trajectory is curved. Regarding case 34.10 it might appear that this type of behavior might be ideal if there was a considerable amount of coulomb friction present in the system. In other words, coulomb friction might be effectively utilized to "straighten out" the dead zone trajectory when the error rate became small. However, it must be pointed out that the intersection of the drop-out line and the zero error rate line occurs at a considerable distance from the point at which all of the trajectories end. Coulomb friction would act to _increase_ this separation and it is felt that the dead zone width would be excessive. Note that when F = .2, a close

RUN 34.10

L_b = 22.5 henries

R_b = 50 ohms
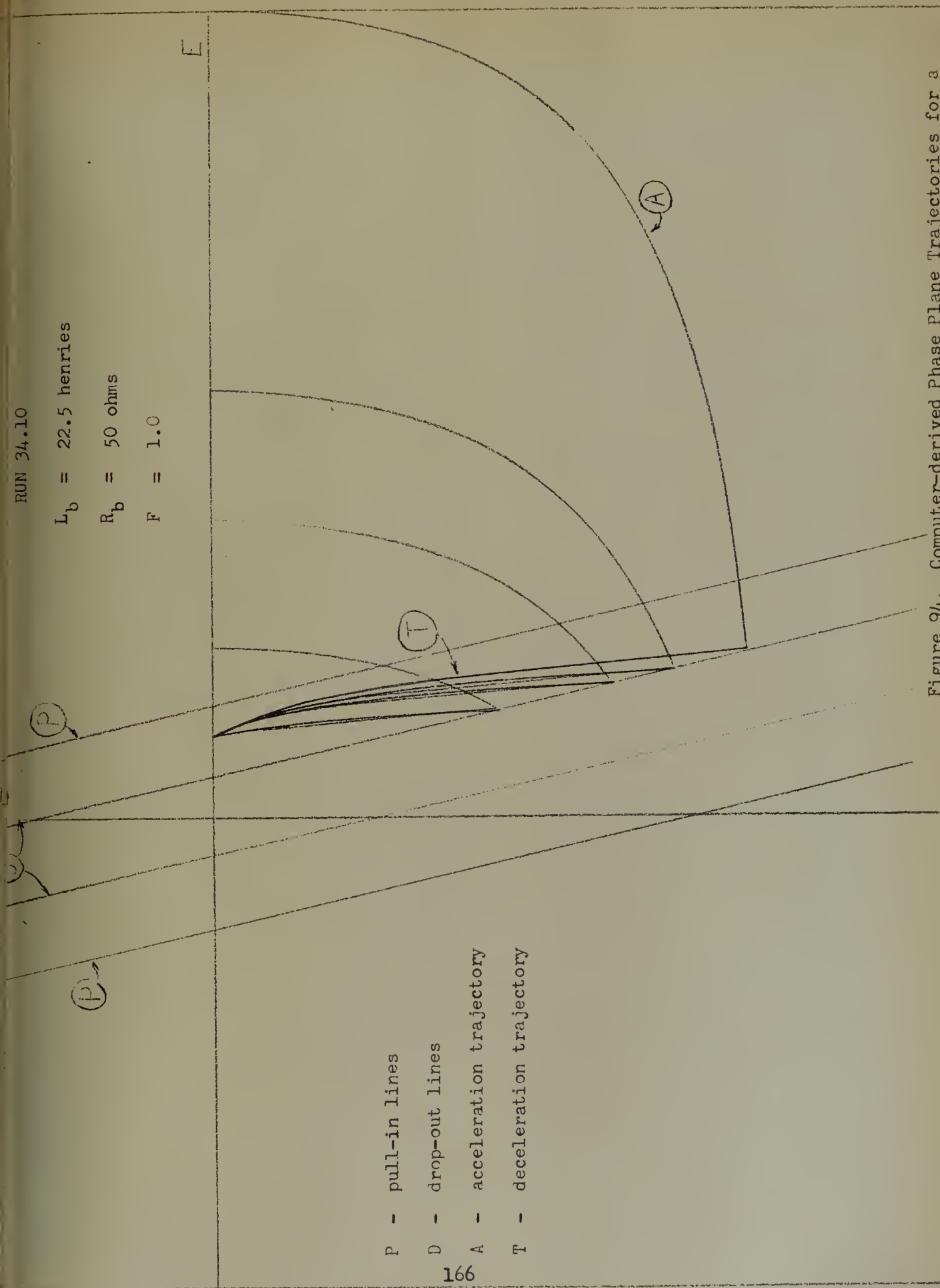
F = 1.0

P — pull-in lines

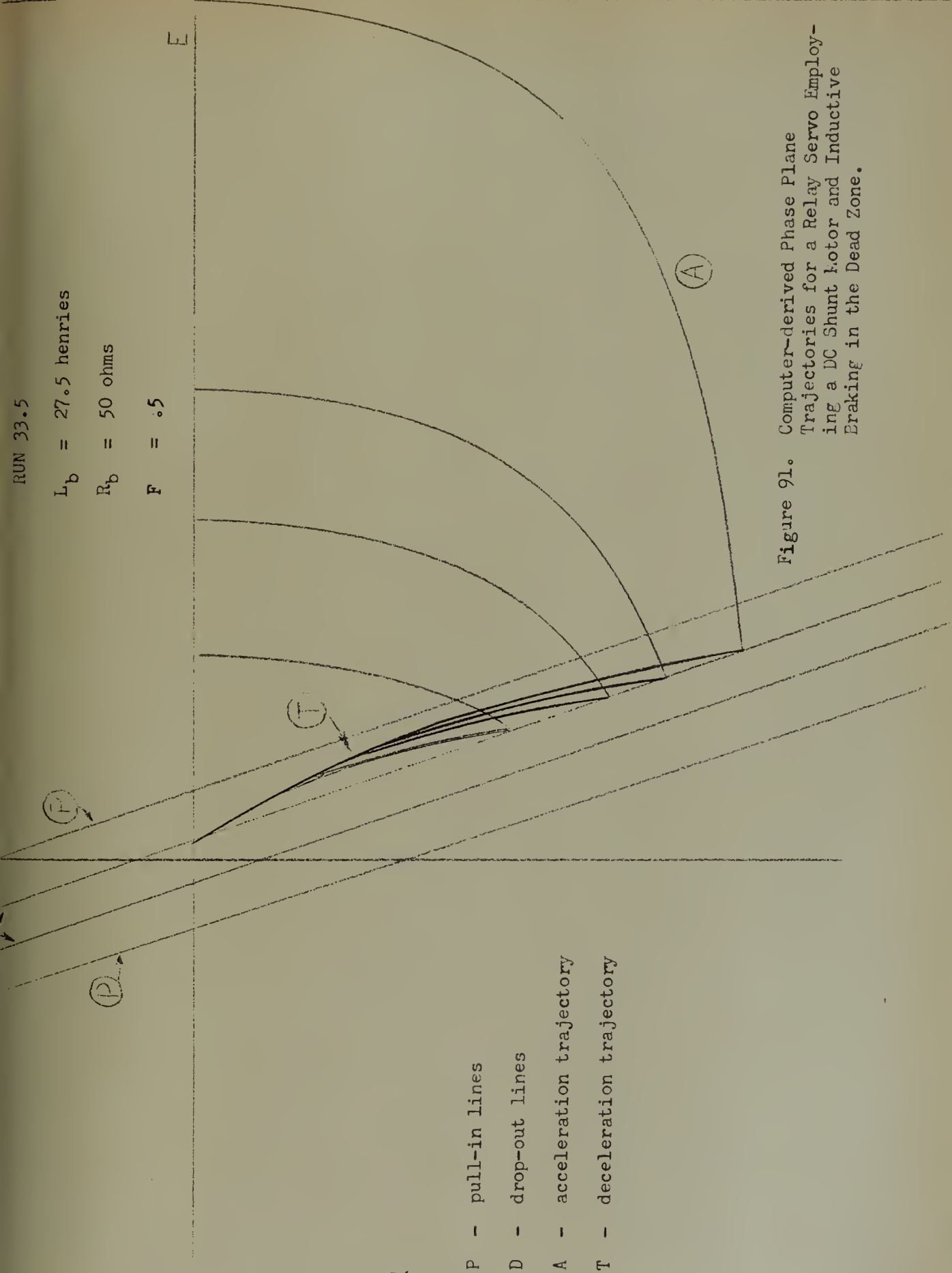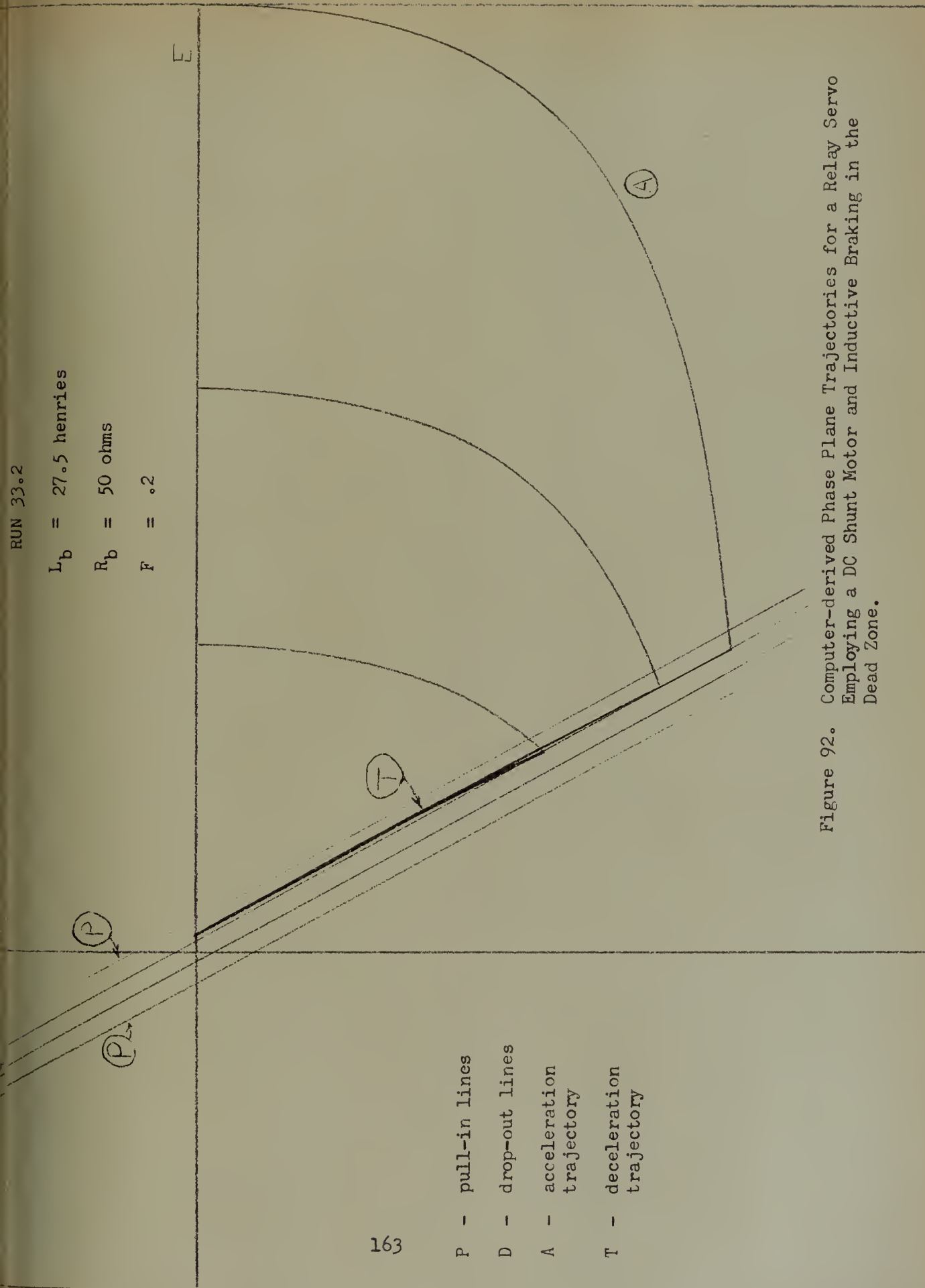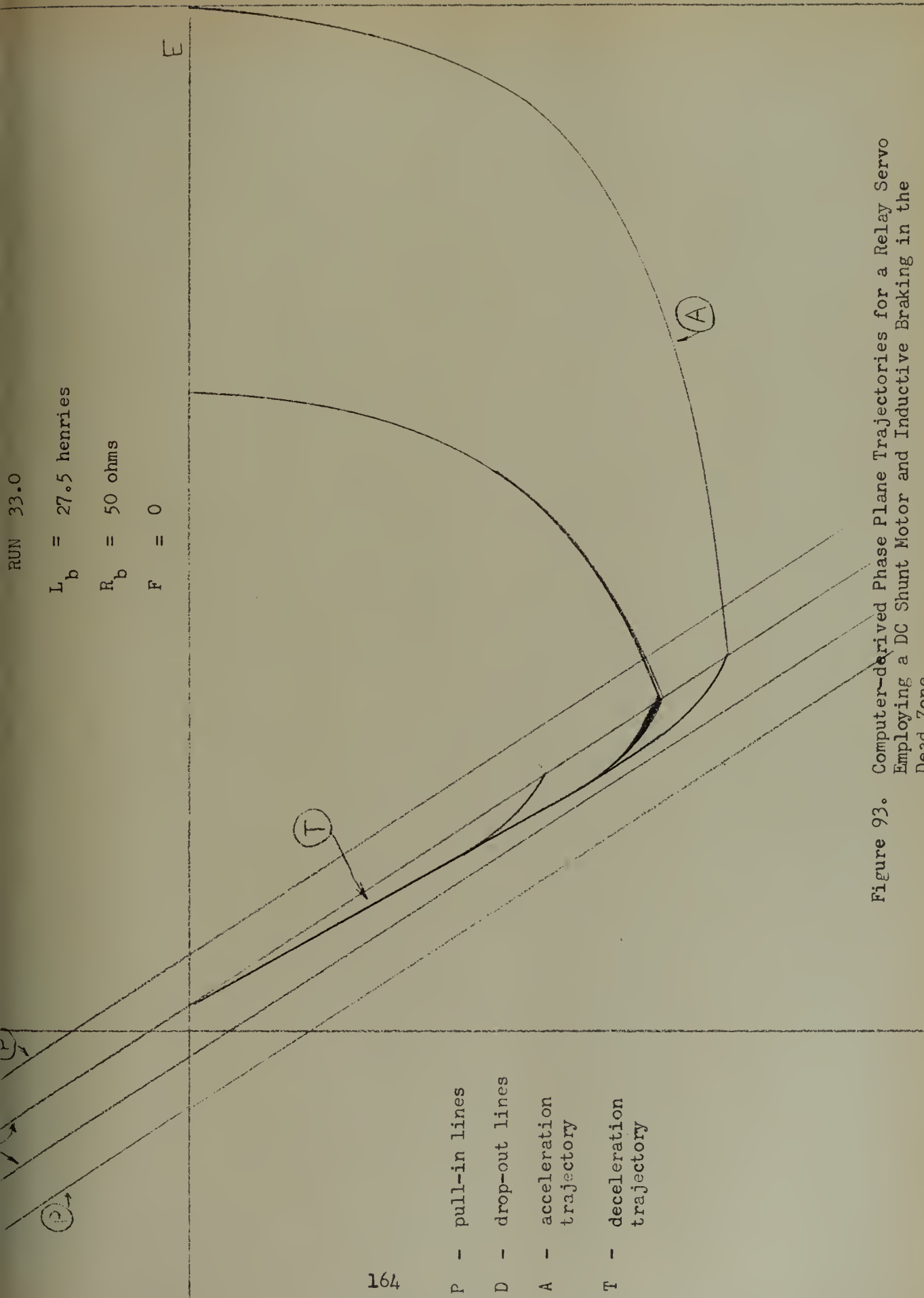D — drop-out lines

A — acceleration trajectory

T — deceleration trajectory

Figure 94. Computer-derived Phase Plane Trajectories for a Relay Servo Employing a DC Shunt Motor and -njuctive Braking in the Dead Zone.

166

RUN 34.9

L_b = 22.5 henries

R_b = 50 ohms

F = .9

Figure 95. Computer-derived Phase Plane Trajectories for a Relay Servo Employing a DC Shunt Motor and Inductive Braking in the Dead Zone.

P — pull-in lines
D — drop-out lines
A — acceleration trajectory
T — deceleration trajectory

RUN 34.75

L_b = 22.5 henries

R_b = 50 ohms

F = .75

Figure 96. Computer-derived Phase Plane Trajectories for a Relay
Servo Employing a DC Shunt Motor and Inductive Braking
in the Dead Zone.

P – pull-in lines

D – drop-out lines

A – acceleration trajectory

T – deceleration trajectory

168

RUN 34.5

L_b = 22.5 henries

R_b = 50 ohms

F = .5

Figure 97. Computer-derived Phase Plane Trajectories for a Relay Servo Employing a DC Shunt Motor and Inductive Braking in the Dead Zone.

P — pull-in lines

D — drop-out lines

A — acceleration trajectory

T — deceleration trajectory

169

L_b = 22.5 henries

R_b = 50 ohms

F = .2

Figure 98. Computer-derived Phase Plane Trajectories for a Relay Servo Employing a DC Shunt Motor and Inductive Braking in the Dead Zone.

P - pull-in lines

D - drop-out lines

A - acceleration trajectory

T - deceleration trajectory

170

RUN 34.0

L_b = 22.5 henries

R_b = 50 ohms

F = 0

Figure 99. Computer-derived Phase Plane Trajectories for a Relay Servo Employing a DC Shunt Motor and Inductive Braking in the Dead Zone.

P – pull-in lines

D – drop-out lines

A – acceleration trajectory

T – deceleration trajectory

171

Figure 100. Computer-derived Phase Plane Trajectories for a Relay Servo Employing a DC Shunt Motor and Inductive Braking in the Dead Zone.

RUN 35.10

L_b = 20 henries

R_b = 50 ohms

F = 1.0

P - pull-in lines

D - drop-out lines

A - acceleration trajectory

T - deceleration trajectory

172

RUN 35.9

L_b = 20 henries

R_b = 50 ohms

F = .9

Figure 101. Computer-derived Phase Plane Trajectories for a Relay Servo Employing a DC Shunt Motor and Inductive Braking in the Dead Zone.

P - pull-in lines

D - drop-out lines

A - acceleration trajectory

T - deceleration trajectory

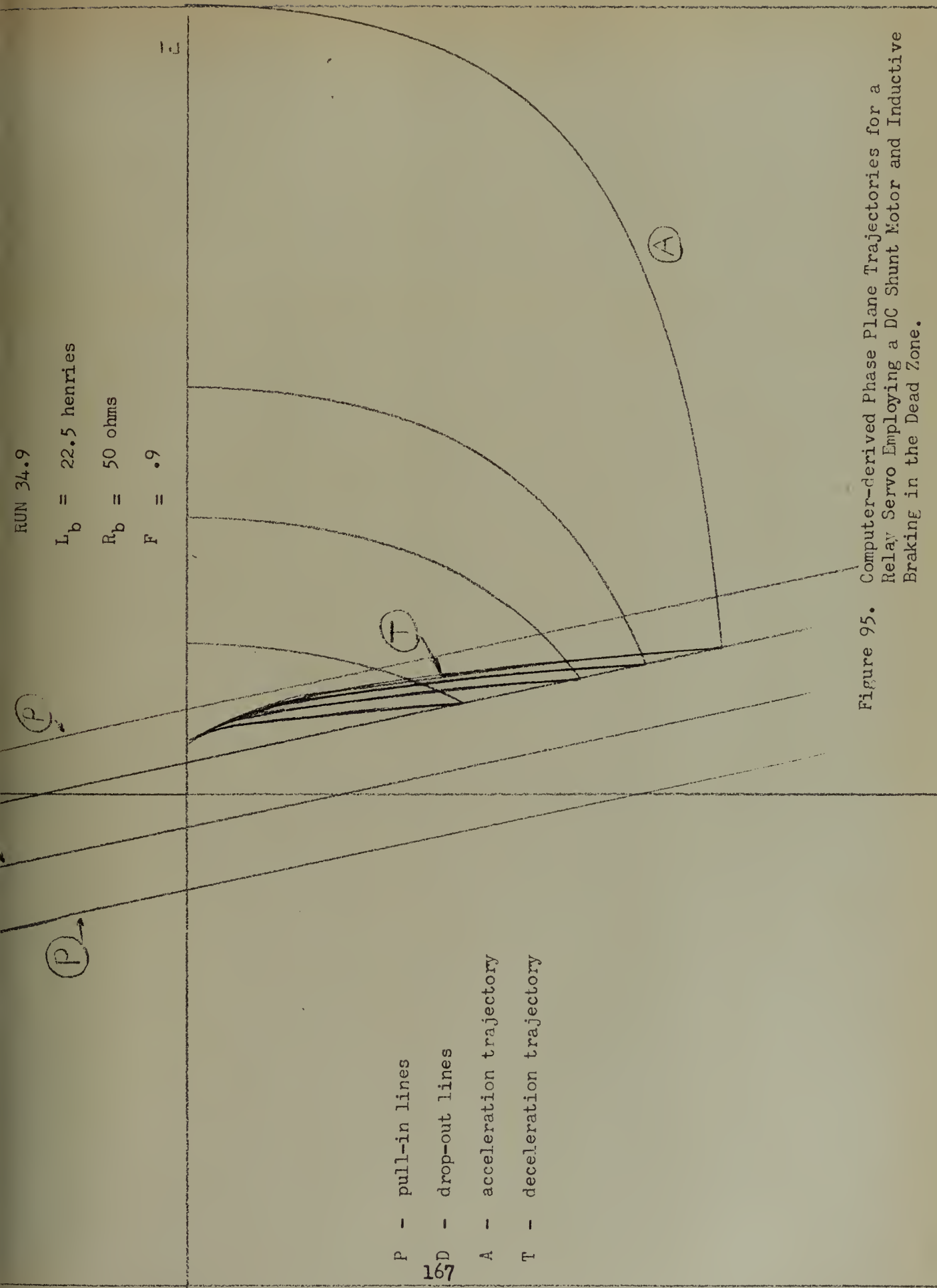173

RUN 35.75

L_b = 20 henries

R_b = 50 ohms

F = .75

Figure 102. Computer-derived Phase Plane Trajectories for a Relay Servo Employing a DC Shunt Motor and Inductive Braking in the Dead Zone.
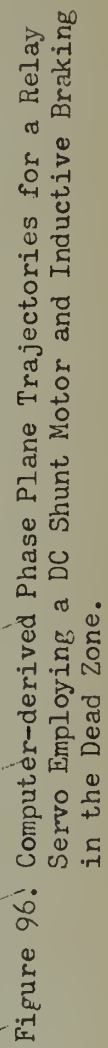
P - pull-in lines

D -- drop-out lines

A - acceleration trajectory

T - deceleration trajectory

174

RUN 35.5

L_b = 20 henries

R_b = 50 ohms

F = .5
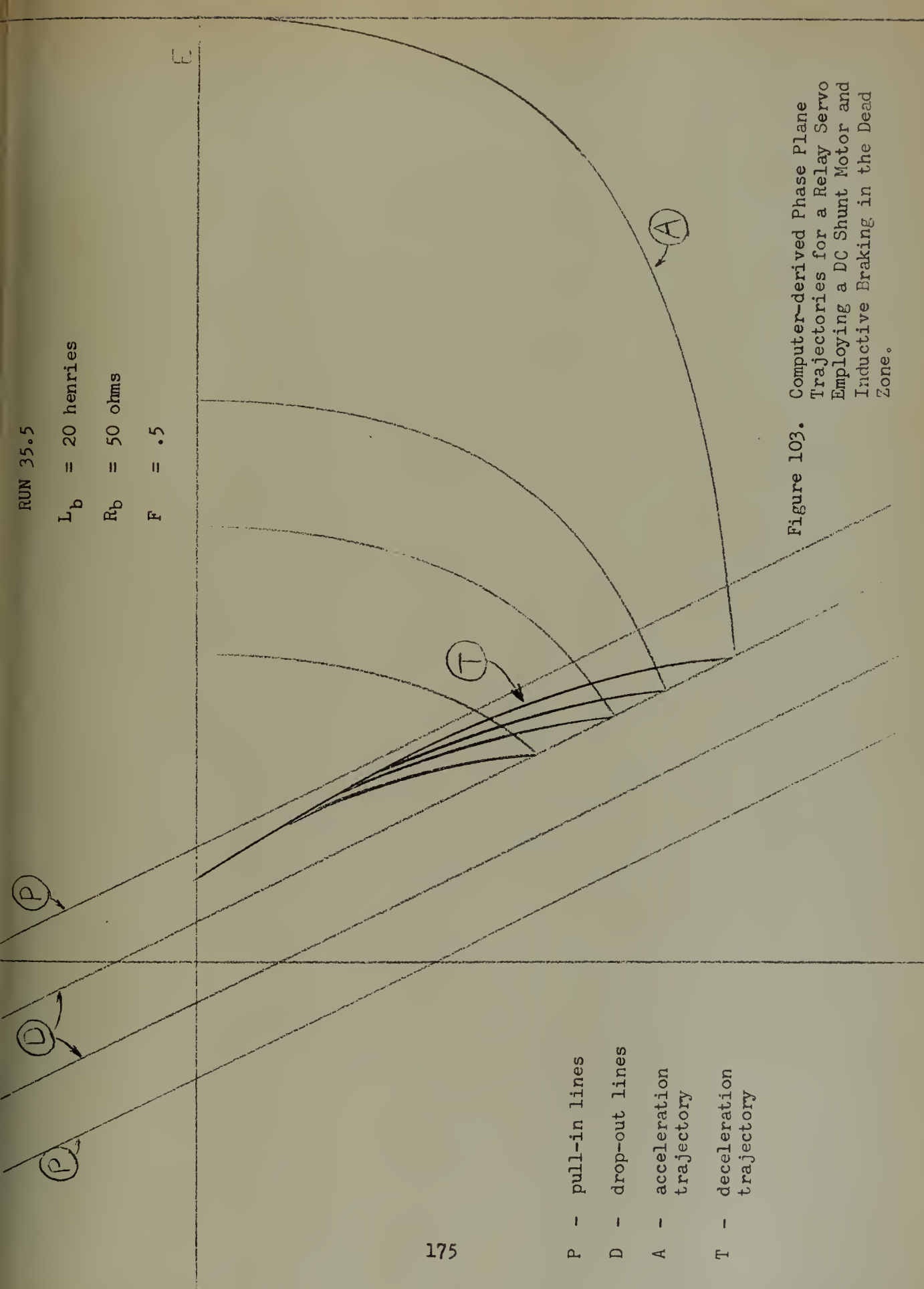
Figure 103. Computer-derived Phase Plane
Trajectories for a Relay Servo
Employing a DC Shunt Motor and
Inductive Braking in the Dead
Zone.

P - pull-in lines

D - drop-out lines

A - acceleration
trajectory

T - deceleration
trajectory

175
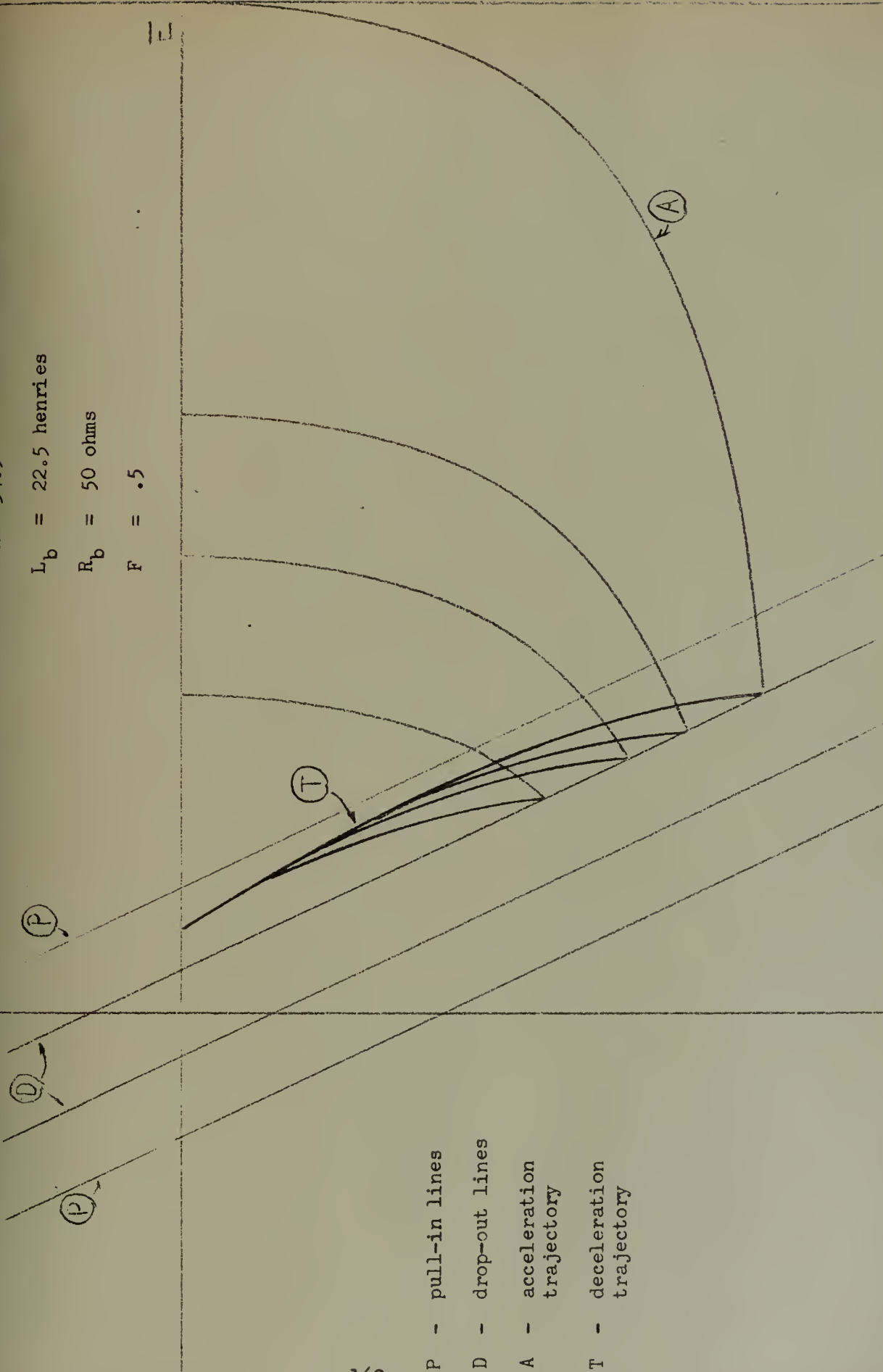
RUN 35.2

L_b = 20 henries

R_b = 50 ohms

F = .2

Figure 104. Computer-derived Phase Plane Trajectories for a Relay Servo Employing a DC Shunt Motor and Inductive Braking in the Dead Zone.

P - pull-in lines

D - drop-out lines
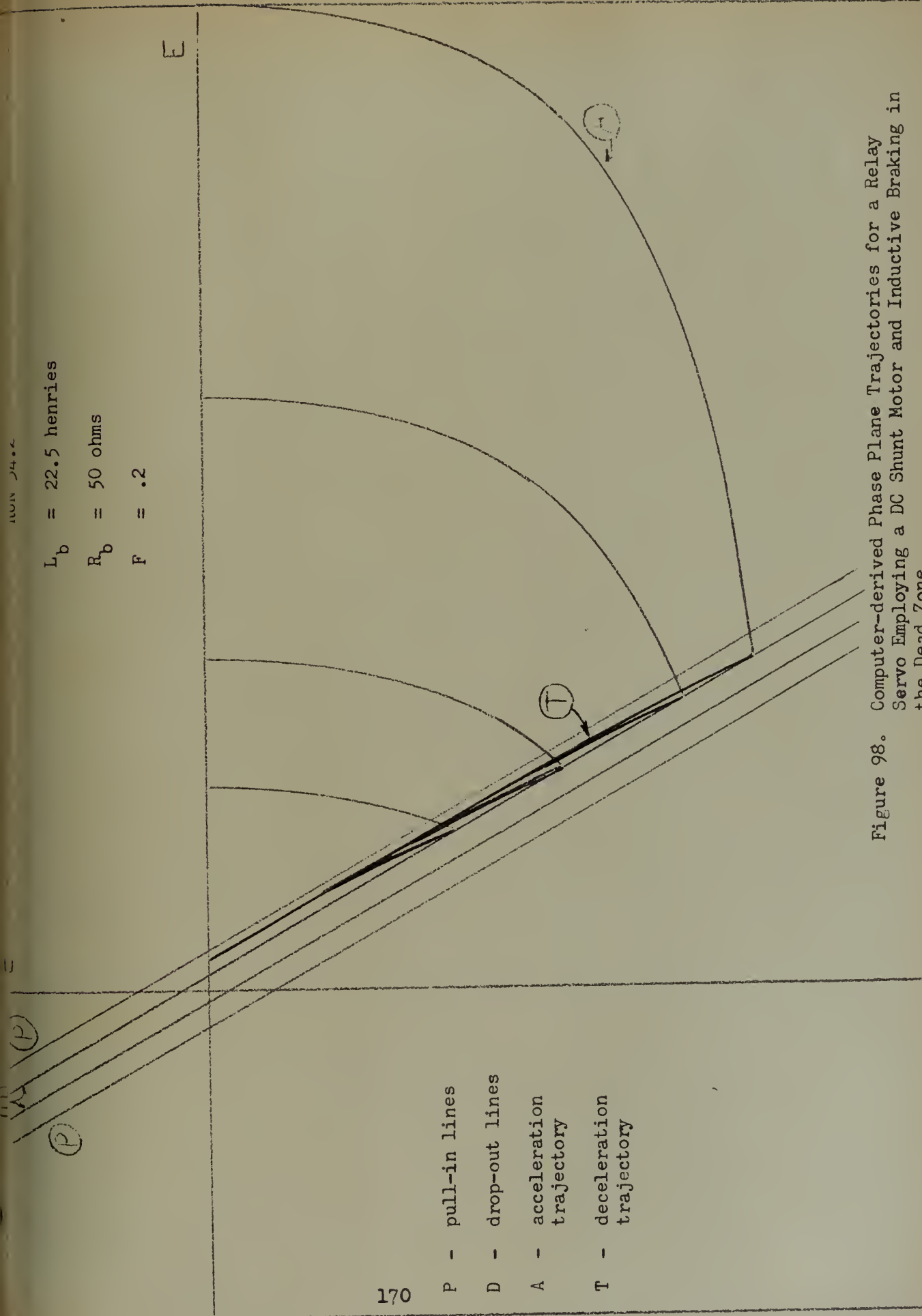
A - acceleration trajectory

T - deceleration trajectory

176
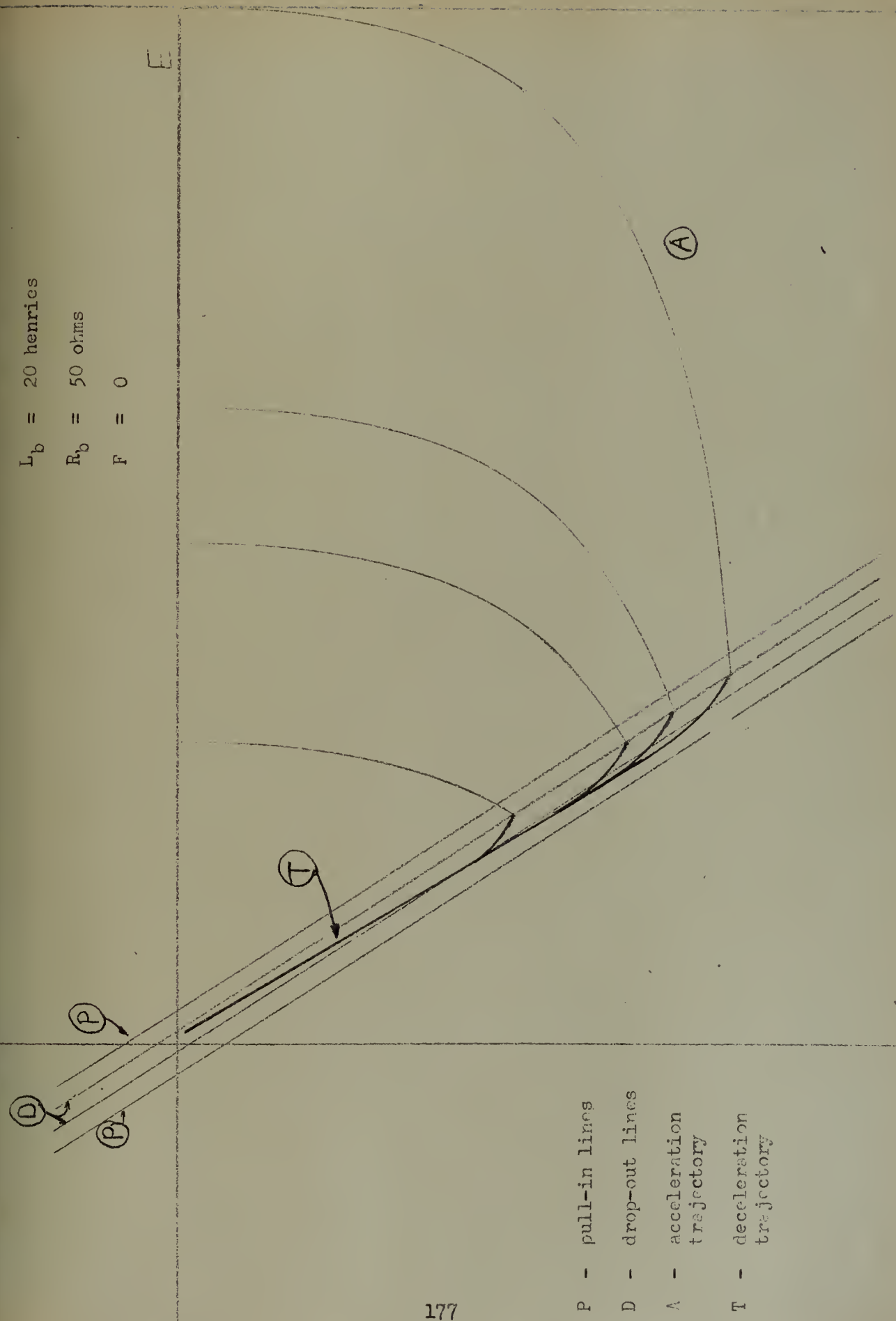
Figure 105. Computer-derived Phase Plane Trajectories for a Relay Servo Employing a DC Shunt Motor and Inductive Braking in the Dead Zone.
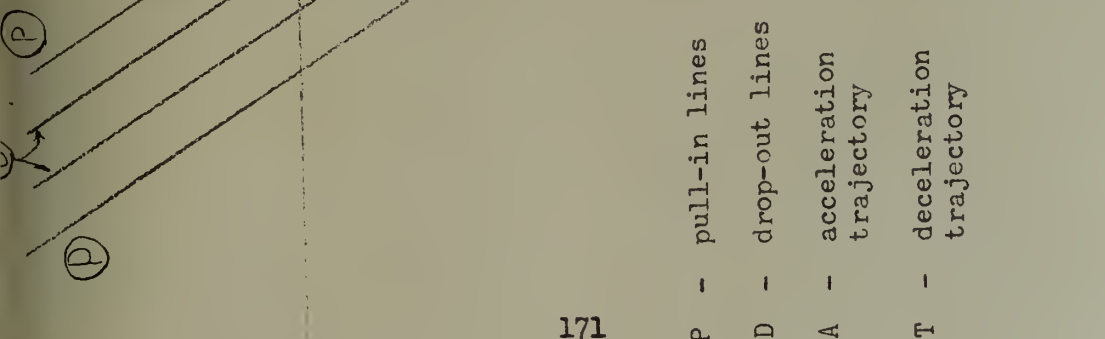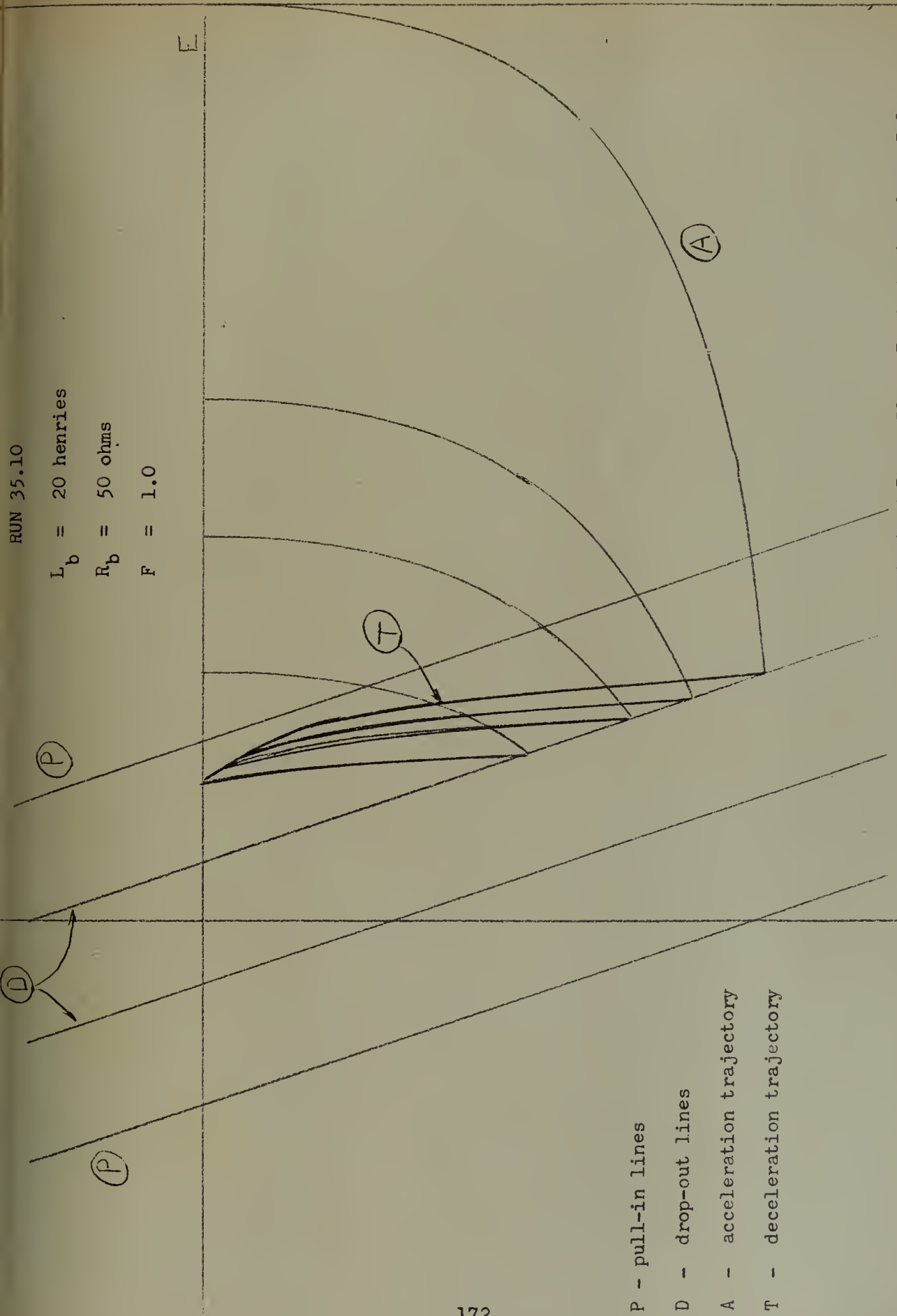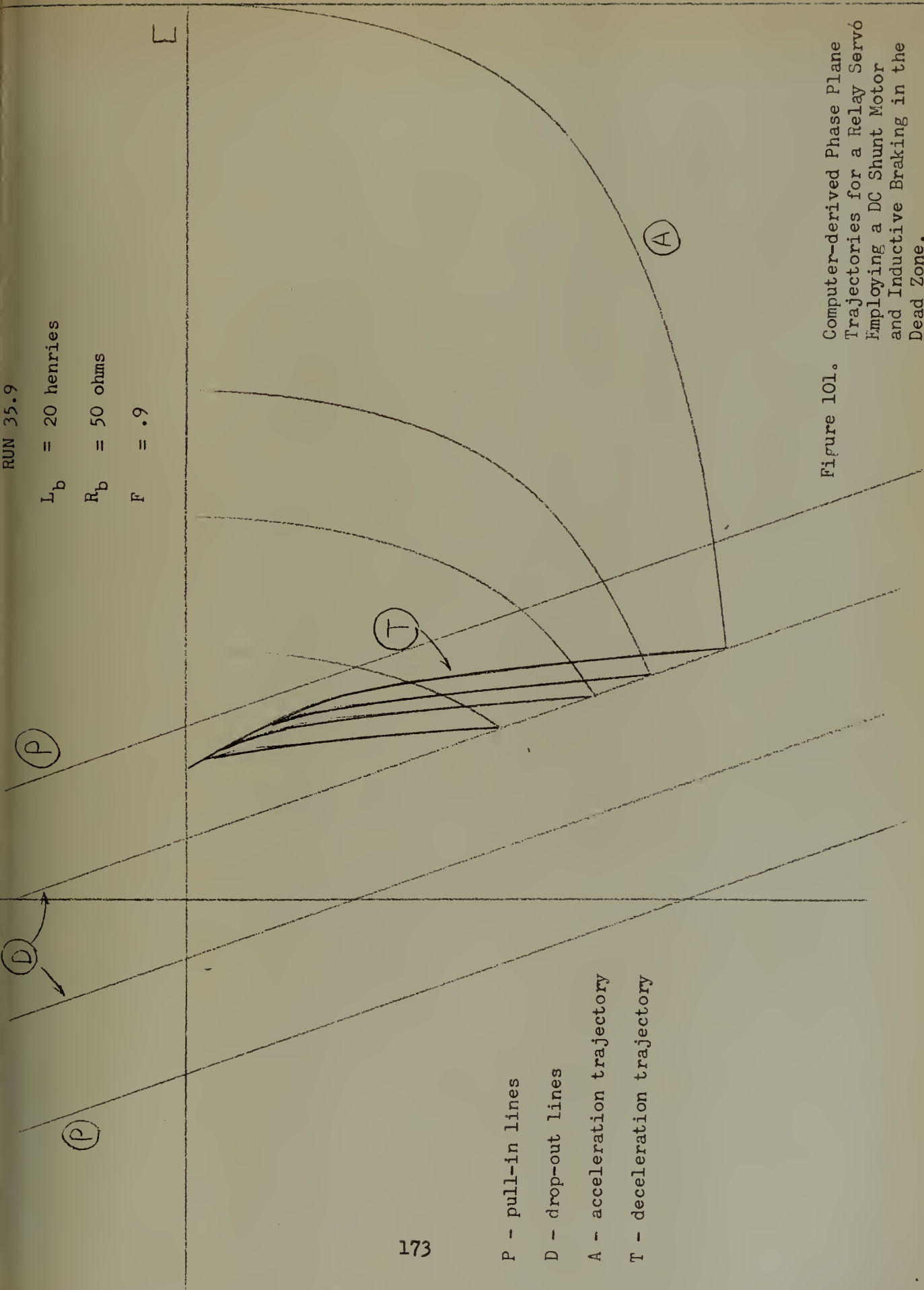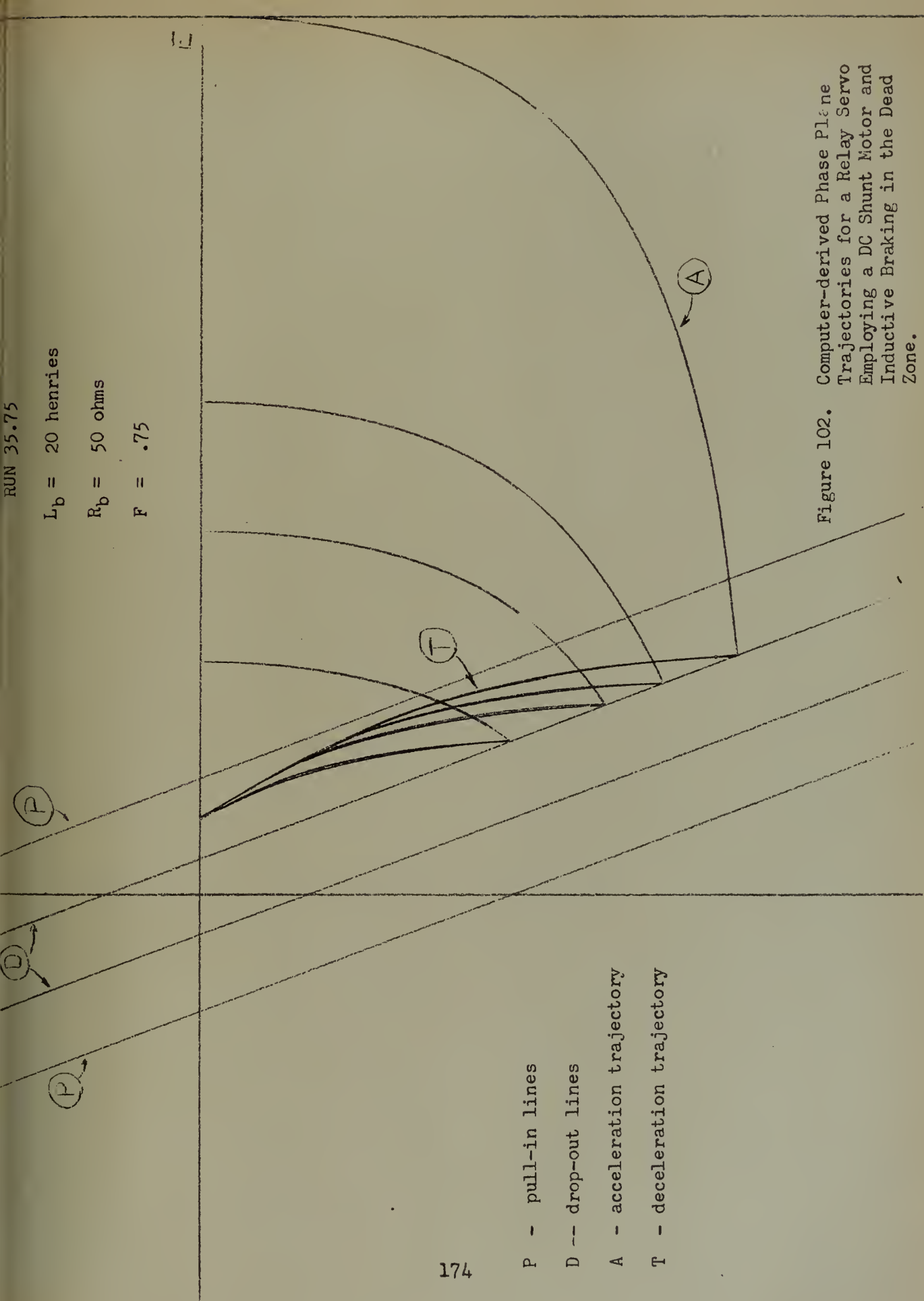
Run 35.0

L_b = 20 henries

R_b = 50 ohms

F = 0

P — pull-in lines

D — drop-out lines

A — acceleration trajectory

T — deceleration trajectory

177

approximation to a straight line is obtained for both case 34.2 and 35.2 just as it is obtained in cases 31.2, 32.2, and 33.2.

TRANSIENT RESPONSE

Transient response curves are shown in Figures 106, 107, 108, and 109. In Figure 106 is shown the effect of varying R_b and L_b in the correct ratio. Notice that the overall time of response is much greater when $L_b = 150$ henries, $R_b = 300$ ohms than it is when $R_b = 50$ ohms, $L_b = 25$ henries. However, even the latter case is preferable to the case when $L_b = 0$, $R_b = 50$ ohms. Notice that the time of response for the case when $L_b = 25$ henries, $R_b = 50$ ohms compares very favorably with the time of response for the optimum relay servo system. Indeed, if the effect of coulomb friction were to exist at all, it is believed that the time of response for the inductive braking case would be less than the time of response for the optimum system.

In Figure 107 is shown the effect of varying the L_b/R_b ratio over a wide range. Notice that where $L_b = 50$ henries and $R_b = 50$ ohms, the response curve is completely unacceptable as was the dead zone trajectory. In the case where $L_b = 12.5$ henries and $R_b = 50$ ohms, the time of response characteristic is much poorer than for the ideal case when $L_b = 25$ henries and $R_b = 50$ ohms.

Figure 108 shows the effect of varying L_b/R_b over a small range. Notice that without coulomb friction a change of time constant from .5 to .6 or .4 almost doubles the time of response. Notice, therefore, that in order to obtain a minimum time of response, rather close adherence to the

(1) Run 19 $R_b = 50$ $L_b = 0$

(2) Run 1 $R_b = 300$ $L_b = 150$

(3) Run 21.10 $R_b = 50$ $L_b = 25$

(4) Run 29 Optimum Case

Figure 106. Transient Response Curves Showing the Effect of Varying R_b and L_b, but Maintaining the Ratio of L_b/R_b Constant.

time (sec)

E (rad)

100

179

50
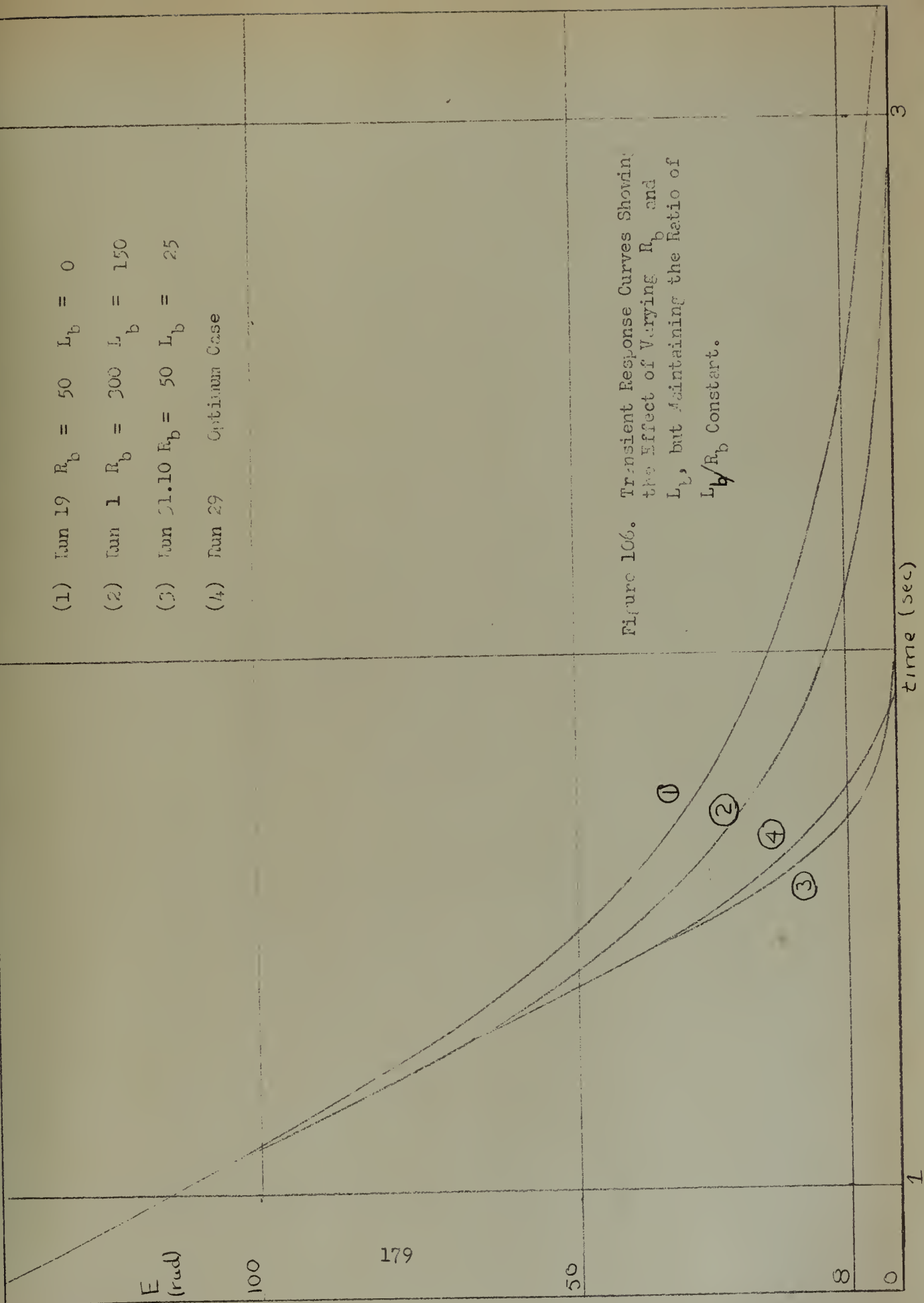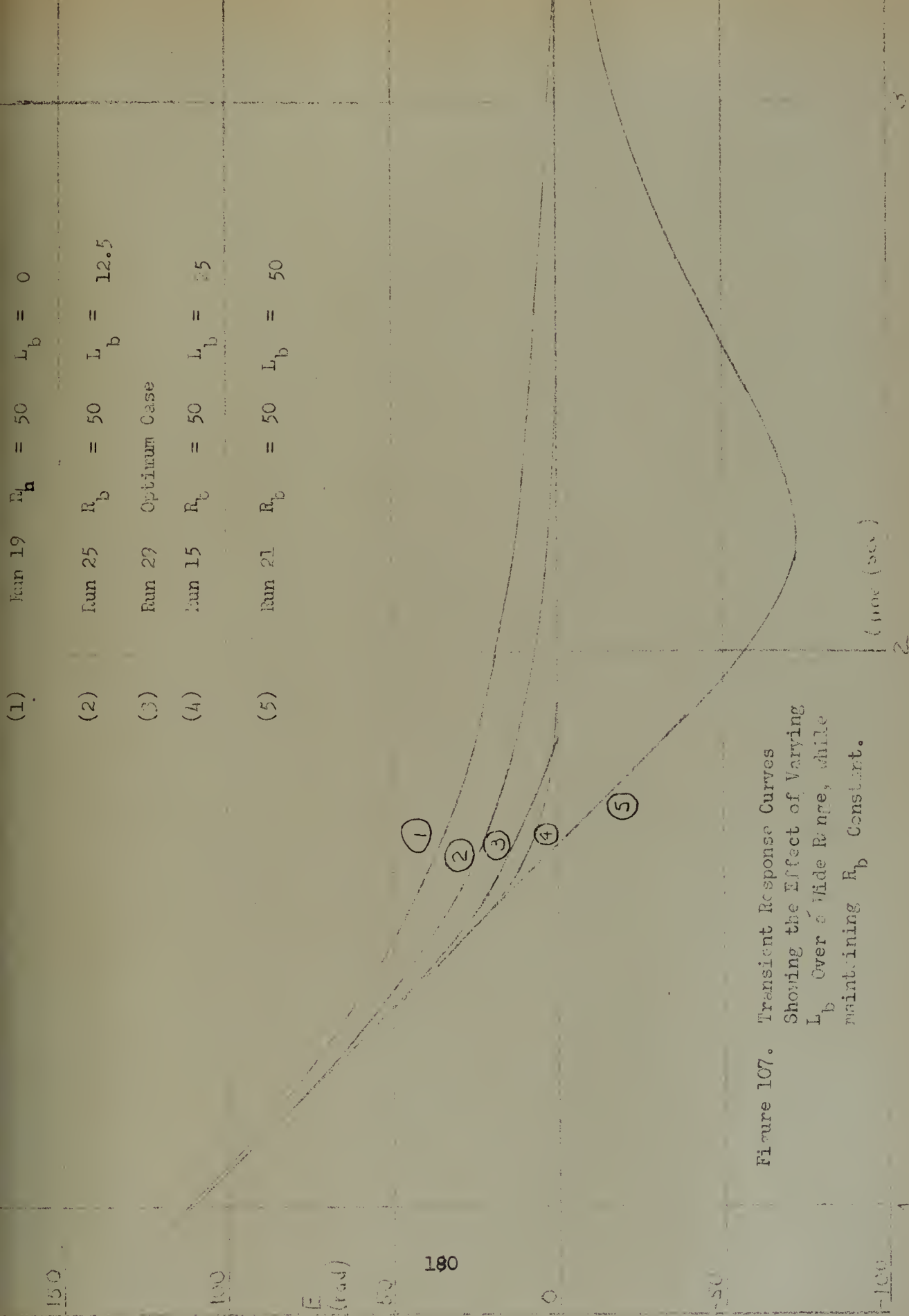
Figure 107. Transient Response Curves Showing the Effect of Varying L_b Over a Wide Range, while maintaining R_b Constant.

(1)   Run 19 $R_b = 50$ $L_b = 0$

(2)   Run 25 $R_b = 50$ $L_b = 12.5$

(3)   Run 27   Optimum Case

(4)   Run 15 $R_b = 50$ $L_b = 75$

(5)   Run 21 $R_b = 50$ $L_b = 50$

Figure 106. Transient Response Curves Showing
the Effect of Varying L_b over
a narrow range while maintaining
R_b constant.

(1) Run 19. R_b = 50 ohms, L_b = 0.

(2) Run 35.10 R_b = 50 ohms, L_b = 20 henries

(3) Run 31.10 R_b = 50 ohms, L_b = 25 henries

(4) Run 29   Optimum Relay Servo

(5) Run 32.10 R_b = 50 ohms, L_b = 20 henries

181

correct L_b/R_b ratio is required. However, even though the actual L_b/R_b ratio varies considerably from the theoretical ideal value, the time of response is still less than what it would be if no inductance at all was included in the braking circuit.

In Figure 109 is shown the effect of F on the time of response. In general, it may be safely stated that as F decreases, the time of response increases. For F = .167 the time of response is almost double that for F = 1.0 even though straight line trajectories are obtained in both cases. Also, it may be stated that if a straight line is obtained for a dead zone trajectory, the time of response varies somewhat inversely as the absolute value of the slope of the dead zone trajectory.

(1) Run 19 R_b = 50 ohms, L_b = 0.

(2) Run 31.167 R_b = 50 ohms, L_b = 25 henries, F = .167

(3) Run 31.75 R_b = 50 ohms, L_b = 25 henries, F = .75

(4) Run 29   Optimum Relay Servo

(5) Run 31.10 R_b = 50 ohms, L_b = 25 henries, F = 1.0

Figure 109. Transient Response Curves

Showing the effect of Varying F.

183

GENERAL DISCUSSION

The complete analysis is subject to the following conditions:

(1) f, C = 0

(2) $L_a << L_b$

(3) $L_a i_1^2 << L_b i_2^2$ for all t during the acceleration phase.

(4) F is a constant for a motor relay combination and is equal to

$\sqrt{1-C_2^2}$

where $C_2^2 = \dfrac{E_R}{L_b i_2^2 - L_a i_1^2}$

(5) $\tau_{e_2} = p \tau_m$

One of the basic requirements of the braking circuit and the motor is that the inductance and resistance shall not take on value which would lead to oscillations in the dead zone. In order to meet this requirement –

$$x^2 + 2x(1 - 2p) + 1 \geqslant \frac{4\tau_{e_1}}{\tau_m}$$

(6) Many times it is a valid assumption that

$$p \cong 1 \quad \text{and} \quad \tau_{e_1} << \tau_m$$

Under this assumption –

$$(x - 1)^2 \geqslant 4 \frac{\tau_{e_1}}{\tau_m}$$

Furthermore, straight lines with identical slopes will be obtained for a dead zone trajectory for all sizes of step inputs under the following conditions:

(1) If F = 1 the trajectory will have a slope equal to $-\dfrac{1}{\tau_m x}$.

(2) If F = x, the trajectory will have a slope equal to $-\dfrac{1}{\tau_m}$.

184

(3) If the restriction that $\tau_m = \tau_{e_2}$ is relaxed somewhat, a straight line will still be obtained for the dead zone trajectory if $F = x$, the slope still being $-\dfrac{1}{\tau_m}$ as in (2) above.

(4) If τ_{e_2} is slightly greater than τ_m a straight line will be obtained for a dead zone trajectory if F is slightly less than one.

The best overall transient response characteristics are provided when $F = 1.0$ and $\tau_{e_2} = \tau_m$ and x is made small. Generally speaking, as F decreases, the overall time of response increases. The time of response for a situation in which the dead zone trajectory is a straight line decreases as the slope of the dead zone trajectory increases (negatively). Under certain conditions the overall time of response for a relay servo employing inductive braking may be made smaller than the time of response for the optimum relay servo, and the dead zone trajectory will be a straight line. This, of course, would mean a linear switching criteria could be adopted which could be provided simply by incorporating derivative feedback into the system.

In the actual construction of a relay servo using inductive braking, the first requirement would be to arrive at a value of F which would be a close approximation of the actual F for any size of step input. The next requirement would be to ascertain the range of values that R_b could take on without having oscillations occur in the dead zone. Then the smallest possible R_b should be obtained consistent with the current-carrying capacity. Next, L_b would be obtained such that $L_b = \tau_m \bar{R}_b$. For a value of F, say, between .5 and 1.0, the value of L_b should be increased to a value of approximately $\dfrac{1}{F}$ times the ideal in order to obtain inductance that would provide suitable characteristics. If F was between

185

0 and .5, x should be made equal to F, and from $x (R_b/R_a)$, R_b and L_b could be determined. In this case the straight line of a lesser slope than possible would have to be accepted for the dead zone trajectory, but, nonetheless, it would be an improvement over simple resistance braking.

CONCLUSIONS:

1. The use of an electrical inductance and resistance as a means of discontinuous damping for a relay servo appears to possess many advantages.

2. If a combination of a properly-chosen relay, inductance, and resistance is used in a relay servo, it is possible to obtain straight lines with identical slopes for dead zone trajectories for any size step input.

3. Reasonable variation from the mathematical solution for R_b, L_b, and F will in general still produce excellent characteristics.

4. The time of response for a relay servo using inductive braking in the dead zone may be made comparable to the time of response of the so-called optimum relay servo.
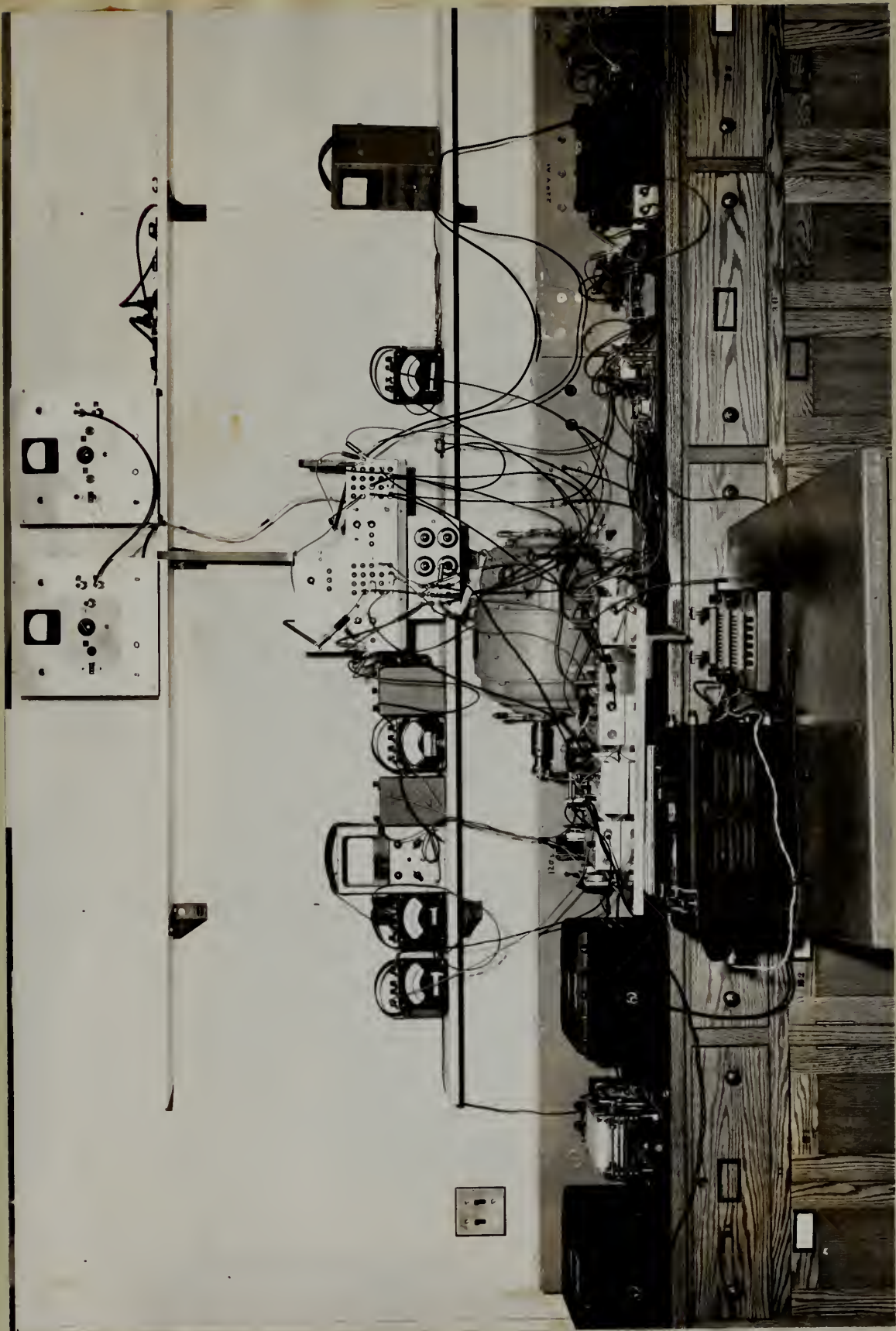
Figure 110. Photograph of Laboratory Equipment

188

THE DERIVATION OF THE ISOCLINE EQUATIONS FOR THE PHASE PLANE
ANALYSIS OF THE DEAD ZONE TRAJECTORY OF A RELAY SERVO USING A
DC SHUNT MOTOR AND A BRAKING RESISTANCE ACROSS THE MOTOR
ARMATURE TERMINALS

The differential equations that describe the behavior of the motor in
the dead zone are as follows:

if flux is a constant –

(1) $\quad K_v \dot{\Theta}_o + i(R_a + R_b) + L_a \dot{i} = 0$

(2) $\quad K_t i = J \ddot{\Theta}_c + f \dot{\Theta}_c - C$

If it is assumed that L_a is small and can be neglected,

(3) $\quad K_v \dot{\Theta}_c + i(R_a + R_b) = 0$

(4) since $\quad \mathcal{E} = \Theta_R - \Theta_c$

(5) then $\quad \dot{\mathcal{E}} = \dot{\Theta}_R - \dot{\Theta}_c$

(6) and $\quad \ddot{\mathcal{E}} = \ddot{\Theta}_R - \ddot{\Theta}_c$

If a step input has been applied to the system –

(7) $\quad \dot{\mathcal{E}} = -\dot{\Theta}_c$

(8) $\quad \ddot{\mathcal{E}} = -\ddot{\Theta}_c$

Equations (2) and (3) may now be written –

(9) $\quad K_t i = -J \ddot{\mathcal{E}} - f \dot{\mathcal{E}} - C$

(10) $\quad -K_v \dot{\mathcal{E}} + i(R_a + R_b) = 0$

Equations (9) and (10) may be rearranged to become –

(11) $\quad J\ddot{\varepsilon} = -K_t i - f\dot{\varepsilon} - C$

(12) $\quad i = \dfrac{K_v \dot{\varepsilon}}{R_a + R_b}$

By substituting equation (12) in (11) –

(13) $\quad J\ddot{\varepsilon} = -\dfrac{K_t K_v}{R_a + R_b} - f\dot{\varepsilon} - C$

(14) $\quad \ddot{\varepsilon} = \dfrac{-K_t K_v \dot{\varepsilon}}{J(R_a + R_b)} - \dfrac{f}{J}\dot{\varepsilon} - \dfrac{C}{J}$

(15) $\quad \dfrac{\ddot{\varepsilon}}{\dot{\varepsilon}} = \dfrac{d\dot{\varepsilon}}{d\varepsilon} = -\dfrac{K_v K_t}{J(R_a + R_b)} - f/J - \dfrac{C/J}{\dot{\varepsilon}}$

If f/J is small compared to the other terms as is usually the

case,   equation (15) becomes

(16) $\quad \dfrac{d\dot{\varepsilon}}{d\varepsilon} = -\dfrac{K_v K_t}{J(R_a + R_b)} - \dfrac{C/J}{\dot{\varepsilon}}$

190

APPENDIX II

SAMPLE CALCULATIONS FOR AN INVESTIGATION OF THE CHARACTERISTICS
OF A RELAY SERVOMECHANISM USING A DC SHUNT MOTOR, DISCONTINUOUS
DAMPING, DERIVATIVE FEEDBACK AND SUBJECTED TO A STEP INPUT

Referring to Figure 8,

$$\text{Let} \quad \frac{R_1}{R_2} = k_1$$

$$\frac{R_1}{R_3} = k_2$$

$$\frac{R_4}{R_5} = k_3$$

$$\frac{R_4}{R_6} = k_4$$

Designate the particular number of degrees of the potentiometer A
at which it is desired that the relay pull-in as z_1.

This establishes the dead zone width.

Designate the number of volts necessary to make the relay pull-in
as $\left(\frac{P_1}{2} \right)$.

Designate the number of volts necessary to make the relay drop-out
as $\left(\frac{D_1}{2} \right)$.

Designate the number of degrees of the potentiometer at which the relay
will drop-out as z_2.

With the motor running as a DC motor at saturation velocity measure
the voltage output of the tachometer and designate it V_2. Also measure
the angular velocity of the potentiometer A. Designate this ω_2
$\left(\text{in } \text{rad}/_{\text{sec}} \right)$.

Designate the desired step input in degrees as R. Part A. Determine X_1,
the voltage across the potentiometer

$$\frac{X_1 \,(\text{volts})}{360 \,(\text{degs})} \times k_2 \times k_3 \times Z_1 \,(\text{degs}) = \left(\frac{P_1}{2}\right)(\text{volts})$$

$$X_1 = \frac{\left(\frac{P_1}{2}\right)(360)}{k_2\, k_3\, Z_1} \,(\text{volts})$$

The equation of a dividing line with error rate feedback is

$$K_1\, \mathcal{E} + K_2\, \overset{o}{\mathcal{E}} = K_3$$

with K_1 in $\dfrac{\text{volts}}{\text{degree}}$

K_2 in $\dfrac{\text{volts-sec}}{\text{degree}}$

K_3 in volts

Part B Determine K.

$$K_1\, \mathcal{E} + K_2\, \overset{o}{\mathcal{E}} = K_3$$

$$\text{Let } \overset{o}{\mathcal{E}} = 0$$

$$K_1 = \frac{K_3}{\mathcal{E}} = \frac{\left(\frac{P_1}{2}\right)(\text{volts})}{Z\,(\text{degs})} = \frac{X_1\, k_2\, b_3}{360} \left(\text{volts}/_{\text{deg}}\right)$$

Part C

Determine K_2

The measure of error rate is

$$K_2 = \frac{V_2 \ (volts)}{\omega_2 \ (rad/sec)} \ a \ k_4 \ \frac{2\pi \ (rad)}{360 \ (deg)}$$

$$= \frac{2\pi \ V_2 \ a \ k_4}{360 \ \omega_2} \left(\frac{volt - sec}{degree} \right)$$

Part D

Determine the slope of the dividing lines

$$\text{Slope} = - \frac{K_1}{K_2}$$

$$= - \frac{X_1 \ k_2 \ k_3 \ \omega_2}{2\pi \ V_2 \ a \ k_4} \left(\frac{degree}{sec - degree} \right)$$

Part E

What is the $\mathcal{E}_0$ intercept at which the relay will pull-in?

$$\mathcal{E}_0 = \frac{K_3}{K_1} = \frac{\left(\frac{P_1}{2} \right) (volts)}{\frac{X_1}{360} \ k_2 \ k_3 \left(\frac{volts}{degree} \right)}$$

$$\mathcal{E} = \frac{\left(\frac{P_1}{2}\right)(360)}{X_1\, k_2\, k_3} = Z_1\ (\text{degrees})$$

Part F

Determine the setting of the potentiometer (b).

Let the battery voltage used to supply the step input be V_3

$V_3\ b\ k_1\, k_3$ is the voltage at the relay.

It is known that a voltage at the relay of $\left(\frac{P_1}{2}\right)$ corresponds

to Z_1 degrees of rotation of the potentiometer A.

$$V_3\ b\ k_1\, k_3 \left[\frac{Z_1\ (\text{degrees})}{\left(\frac{P_1}{2}\right)(\text{volts})}\right] = R \quad \begin{array}{l}\text{degrees of the} \\ \text{potentiometer shaft.}\end{array}$$

$$b = \frac{R\left(\frac{P_1}{2}\right)}{V_3\, k_1\, k_3\, Z_1}$$

Part G

Determine the setting for the Brush Recorder Measuring Error

$$\frac{volts}{degree\ of\ pot} \text{ at the relay} = \frac{X_1}{360} k_2 k_3$$

$$\frac{volts}{degree\ of\ pot} \text{ at the Recorder} = \frac{X_1 k_2}{360}$$

Let k_5 represent the amplification used in the Brush Recorder. Also designate W spaces of the tape as corresponding to the calibration voltage of 20 volts (gain setting).

The spaces on the tape per degree of potentiometer may be represented

by

$$\frac{\frac{X_1}{360} k_2 k_5 \left(\frac{volts\ at\ the\ pen}{degree\ of\ pot} \right)}{\frac{20\ (volts)}{W\ (spaces)}}$$

$$N_1 = \frac{X_1 W k_2 k_5}{(360)(20)} \left(\frac{spaces}{degree} \right)$$

Let N_1 represent the quantity.

For simplicity set N_1 equal to either an integer or a reciprocal of an integer and solve for $W k_5$.

Part H

Determine the Setting for the Brush Recorder Measuring Error Rate

The angular velocity of the potentiometer in degrees per second may

be represented by

$$\omega_2 \times \frac{360}{2\pi} ,$$

$\omega_2 \left(\frac{360}{2\pi} \right)$ corresponds to V_2 volts

from the tachometer.

Let k_6 be the amplification used in the Brush Recorder measuring

Error Rate and designate W_2 spaces of the tape as corresponding to

the calibration voltage of 20 volts (gain setting).

$\omega_2 \left(\frac{360}{2\pi} \right) \left(\frac{deg}{sec} \text{ of the pot} \right)$ corresponds

to $V_2 \, k_6$ volts to the pen of the Brush Recorder.

$\omega_2 \left(\frac{360}{2\pi} \right) \left(\frac{deg}{sec} \right)$ corresponds to

$$V_2 \, k_6 \, (volts) \left[\frac{W_2 \, (spaces)}{20 \, (volts)} \right] .$$

Therefore

$$N_2 \left(\frac{spaces}{deg/sec} \right) = \frac{V_2 \, k_6 \, W_2 \, 2\pi}{\omega_2 \, (360)(20)}$$

Again for simplicity let N_2 be either an integer or the reciprocal
of an integer and solve for $k_6 W_2$.

The solution of a sample problem would be as shown below.

$$\text{Let } Z_1 = 15 \text{ degrees}$$

$$\left(\frac{P_1}{2}\right) = 6.3 \text{ volts}$$

$$\left(\frac{Q_1}{2}\right) = 1.33 \text{ volts}$$

$$V_2 = 90 \text{ volts}$$

$$W_2 = 8.6 \text{ rad}/\text{sec}$$

$$R = 25 \text{ degrees}$$

Part I

Determine the ξ intercept for the drop-out line or Z_2

$$\frac{\left(\frac{P_1}{2}\right)}{\left(\frac{Q_1}{2}\right)} = \frac{Z_1}{Z_2}$$

$$Z_2 = \frac{\left(\frac{Q_1}{2}\right)}{\left(\frac{P_1}{2}\right)} Z_1$$

$$Z_2 = 15 \frac{(1\,33)}{(6\,3)} = 3\,17 \text{ degrees},$$

.

$$X_1 = \frac{\left(\frac{P_1}{2}\right)(360)}{k_1\, k_3\, z_1}$$

$$k_2\, k_3\, X_1 = \frac{\left(\frac{P_1}{2}\right)(360)}{z_1} = \frac{(6.3)(360)}{15} = 151$$

let $k_2 = 10$

$\quad k_3 = 2.5$

$\quad X_1 = 6.05$ volts

Part B

$$K_1 = \frac{X_1\, k_2\, k_3}{360} = \frac{151}{360} = .42\ \frac{volts}{degree}$$

Part C

$$K_2 = \frac{2\pi\, V_2\, a\, k_4}{360\, \omega_2}$$

$$= \frac{(2\pi)(90)\, a\, k_4}{(360)(8.6)}$$

let $a = .3$

$\quad k_4 = 2.5$

Then $K_2 = .137\ \frac{volts-sec}{deg}$

198

Part D

$$\text{slope} = -K_1/K_2 = -\frac{42}{137} = -307 \frac{deg}{sec\text{-}deg}$$

Part F

$$b = \frac{R\left(\frac{P_1}{2}\right)}{V_3 \, k_1 \, k_3 \, Z_1}$$

let $V_3 = 35$

then $b = \dfrac{(25)(63)}{(35)(10)(25)(15)} = .12$

Part G

Desire 1 space per 2 degrees $\left(N_1 = \frac{1}{2}\right)$

$$\frac{1}{2} = \frac{X_1 \, W \, k_2 \, k_5}{(360)(20)}$$

$$k_5 W = \frac{(360)(20)}{(2) X_1 \, k_2} = \frac{(360)(20)}{(2)(605)(10)} = 595$$

let $k_5 = 10$

$$W = 5.95$$

Part H

$$k_6 W_2 = \frac{\omega_2 (360)(20) N_2}{V_2 (2\pi)}$$

If we desire the maximum speed to be represented by 20 spaces

Then
$$N_2 \left[\frac{spaces}{deg/sec} \right] = \frac{20 (2\pi)}{\omega_2 (360)}$$

then
$$k_6 W_2 = \frac{400}{V_2}$$

for
$$V_2 = 90$$

$$k_6 W_2 = \frac{400}{90} = 4.45$$

$$k_6 = 1$$

$$W_2 = 4.5$$

Part I

$$Z_2 = Z_1 \frac{\left(\frac{D_1}{2} \right)}{\left(\frac{P_1}{2} \right)} = 15 \frac{(1.33)}{(6.3)} = 3.17 \text{ degrees}$$

DERIVATION OF THE SYSTEM PARAMETERS SUBJECT TO THE CONDITION

THAT $\quad \tau_m' = 4\tau_e'$

$$\tau_m' = \frac{J(R_a + R_b)}{K_v K_e} = \frac{J R_a}{K_v K_e}\left[1 + \frac{R_b}{R_a}\right]$$

Let $\dfrac{R_b}{R_a} = x$

Then

$$\tau_m' = \frac{J R_a}{K_v K_e}\left[1 + x\right] = \tau_m(1+x)$$

$$\tau_e' = \frac{L_a + L_b}{R_a + R_b} = \frac{L_a}{R_a\left(1 + \frac{R_b}{R_a}\right)} + \frac{L_b}{R_a\left(1 + \frac{R_b}{R_a}\right)} \qquad (1)$$

Let $\dfrac{L_b}{R_b} = p\tau_n = \tau_{e_2}$

$$\tau_e' = \frac{\tau_{e_1}}{1 + x} + \frac{p\tau_m x}{1 - x}$$

Then substituting for τ_m' and τ_e' in (1)

$$\tau_m (1 + x) = \frac{4 \tau_{e_1}}{1 + x} + \frac{4 p \tau_m x}{1 + x}$$

$$(1 + x)^2 = \frac{4 \tau_{e_1}}{\tau_m} + 4 p x$$

Since $p \cong 1$

$$(x - 1)^2 = \frac{4 \tau_{e_1}}{\tau_m}$$

For $\tau_m = .5$

and $\tau_{e_1} = \frac{.5}{300}$

$x \cong 1$

Then

$$R_b = R_a = 300 \, \Omega$$

and

$$L_b = \tau_m R_b = (.5)(300) = 150 \text{ henries}$$

DERIVATION OF THE SYSTEM PARAMETERS SUBJECT TO THE CONDITIONS

that $\quad \tau_m' = 8\tau_e'$

From appendix $\underline{III}$

$$\tau_m' = \tau_m(1+x)$$

and

$$\tau_e' = \frac{\tau_{e_1}}{1+x} + \frac{p\tau_m x}{1+x}$$

Substituting and for $p \cong 1 -$

$$(1+x)^2 = \frac{8\tau_e}{\tau_m} + 8x$$

$$x^2 - 6x + 1 = \frac{8\tau_{e_1}}{\tau_m}$$

Since

$$\tau_{e_1} = \frac{.5}{300}$$

and

$$\tau_m = .5$$

$X = 5.83$ and $X = .17$

$R_b = 1750$ $R_b = 51$

$L_b = 875$ $L_b = 25.5$

DERIVATION OF THE COMPUTER SET-UP FOR SOLUTION OF THE
ACCELERATION PROBLEM

During the acceleration period, the following equations
should approximately describe the situation if $($ is assumed to be
zero.

(1) $\quad V = K_v \dot{\Theta} + i_1 R_a + L_a \dfrac{di_1}{dt}$

(2) $\quad J \ddot{\Theta} = K_c i$

(3) $\quad V = L_b \dfrac{di_2}{dt} + i_2 R_b$

---

(4) $\quad \dfrac{di_1}{dt} = \dfrac{V}{L_a} - \dfrac{K_v}{L_a} \dfrac{d\Theta}{dt} - \dfrac{R_a}{L_a} i_1$

(5) $\quad \dfrac{d^2\Theta}{dt^2} = \dfrac{K_E}{J} i$

(6) $\quad \dfrac{di_2}{dt} = \dfrac{V}{L_b} - \dfrac{R_b}{L_b} i_2$

For $\quad L_a = .5$

$$L_b = 150$$

$$R_a = 300$$

$$R_b = 300$$

$$V = 50$$

$$K_v = .25$$

$$\frac{V}{L_a} = 100$$

$$\frac{V}{L_b} = .333$$

$$\frac{V}{R_a} = .167 \qquad i_1 \text{ max}$$

$$\frac{V}{R_b} = .167 \qquad i_2 \text{ max}$$

$$\frac{J R_a}{K_v K_t} = \tau_m = .5$$

$$\frac{K_t}{J} = 2400$$

$$\overset{\circ}{\theta}_{max} = 200 \text{ rad}/\text{sec}$$

Var	Est Max.	Comp. Max	Scale Factor	Machine Variable
$\dfrac{di_1}{dt}$	100	90	1.11	$\overline{\dfrac{di_1}{dt}}$
$\dfrac{V}{L_a}$	100	90	1.11	$\overline{\dfrac{V}{L_a}}$
$\dfrac{d\Theta}{dt}$	200	90	2.22	$\overline{\dfrac{d\Theta}{dt}}$
i_1	.167	90	.00185	$\overline{i_1}$
Θ	200	90	2.22	$\overline{\Theta}$
$\dfrac{di_2}{dt}$	.333	90	.00370	$\overline{\dfrac{di_2}{dt}}$
$\dfrac{V}{L_b}$	.333	90	.00370	$\overline{\dfrac{V}{L_b}}$
i_2	.167	90	.00185	$\overline{i_2}$
$\dfrac{d^2\Theta}{dt^2}$	400	90	4.44	$\overline{\dfrac{d^2\Theta}{dt^2}}$

$$\frac{di_1}{dt} = \frac{V}{La} - \frac{K_v}{La}\frac{d\Theta}{dt} - i_1\frac{R_a}{La}$$

$$1.11\frac{\overline{di_1}}{dt} = 1.11\frac{\overline{V}}{La} - \frac{.25}{.5}\left(222\frac{\overline{d\Theta}}{dt}\right) - \overline{i_1}\frac{300}{.5}(.00185)$$

$$1.11\frac{\overline{di_1}}{dt} = 1.11\frac{\overline{V}}{La} - 1.11\frac{\overline{d\Theta}}{dt} - 1.11\overline{i_1}$$

$$\frac{\overline{di_1}}{dt} = \frac{\overline{V}}{La} - \frac{\overline{d\Theta}}{dt} - \overline{i_1}$$

$$.00185\,\overline{i_1} = \int 1.11\frac{\overline{di_1}}{dt}\,dt$$

$$\overline{i_1} = 600\int\frac{\overline{di_1}}{dt}\,dt$$

$$\frac{\overline{d^2\Theta}}{dt^2} = \frac{K_T}{J}i_1$$

$$4.44\frac{\overline{d^2\Theta}}{dt^2} = \frac{300}{.125}(.00185\,\overline{i_1}) = 4.44\,\overline{i_1}$$

$$\frac{\overline{d^2\Theta}}{dt^2} = \overline{i_1}$$

$$\frac{di_2}{dt} = \frac{V}{L_b} - i_2 \frac{R_b}{L_b}$$

$$.00370 \overline{\frac{di_2}{dt}} = .00370 \frac{\overline{V}}{L_b} - \frac{300}{150}(.00185 \overline{i_2})$$

$$\overline{\frac{di_2}{dt}} = \frac{\overline{V}}{L_b} - \overline{i_2}$$

$$2.22 \overline{\frac{d\Theta}{dt}} = \int 4.44 \overline{\frac{d^2\Theta}{dt^2}} \, dt$$

$$\overline{\frac{d\Theta}{dt}} = 2 \int \overline{\frac{d^2\Theta}{dt^2}} \, dt$$

$$2.22 \overline{\Theta} = \int 2.22 \overline{\frac{d\Theta}{dt}} \, dt$$

$$\overline{\Theta} = \int \overline{\frac{d\Theta}{dt}} \, dt$$

$$.00185 \overline{i_2} = \int .00370 \overline{\frac{di_2}{dt}} \, dt$$

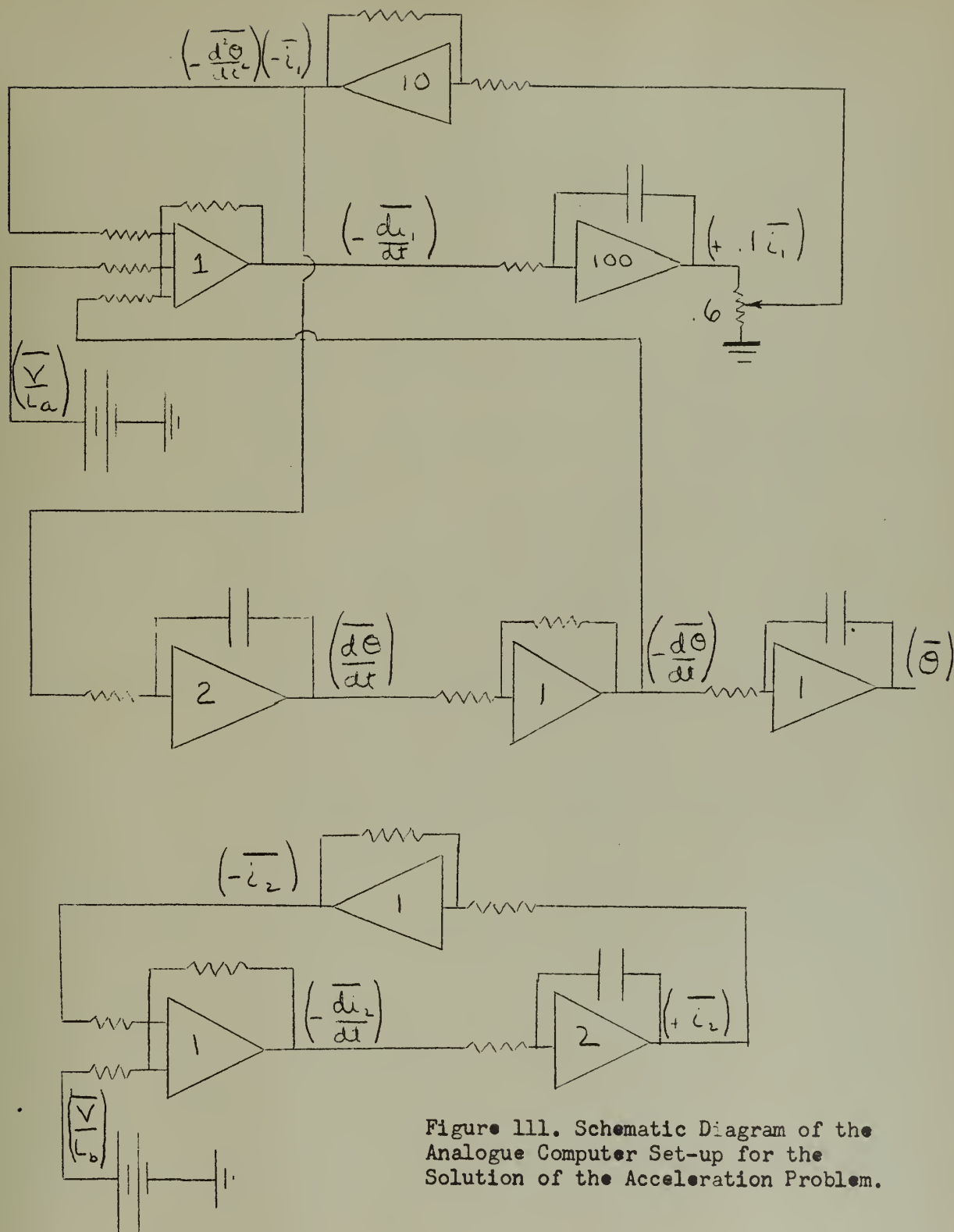$$\overline{i_2} = 2 \int \overline{\frac{di_2}{dt}} \, dt$$

Figure 111. Schematic Diagram of the Analogue Computer Set-up for the Solution of the Acceleration Problem.

209

LIST OF EQUIPMENT

Motors:
1 HP, 230 volts DC, 115 volts shunt field, 1150 RPM, shunt wound; General Electric Co., #1693848, Type B-224-2-1.

1/125 HP, 115 volts DC, shunt wound, 4000 RPM; Electric Indicator Co., #227511, Type FD-163.

Tachometers:
1/75 HP, 110 volts DC, 3400 RPM, #227513, Type FD-38; Electric Indicator Co.

1/75 HP, 110 volts DC, 3400 RPM, #227315, Type FD-38; Electric Indicator Co.

Relays:
Four-pole double-throw; Sigma Instrument Co., Type 6 FX4C - 5000 GD-SIL.

Two-pole single-throw; Leach Relay Co., Type 1127.

Potentiometers:
Linear, continuous turn; Helipot Co., Series G; 10,000 ohms.

Amplifiers, d-c:
From Boeing Electric Analog Computer, Model 7000; operational amplifier used to sum, differentiate, and integrate.

Recorder:
Amplifier; Brush Co., Model BL-932.
Oscillograph; Brush Co., Model BL-202

Computer:
Donner Analogue Computer, Model 30.

BIBLIOGRAPHY

1. Harris, Jr., W. L.   DISCONTINUOUS DAMPING OF RELAY SERVOMECHANISMS.
                          Master's Thesis U. S. N. Postgraduate School.

2. McDonald, D.   NONLINEAR TECHNIQUES FOR IMPROVING SERVO-
                          MECHANISM PERFORMANCE. Proceedings,
                          National Electric Conference, Chicago,
                          Illinois, Vol. 6, 1950, pp. 400-421.

3. Hopkin, M.   A PHASE-PLANE APPROACH TO THE COMPENSATION
                          OF SATURATING SERVOMECHANISMS.
                          American Institute of Electrical Engineers
                          Transactions, Vol. 70, Part I, 1951,
                          pp. 631-639.

4. Thaler, C. J. and Stein,   TRANSFER FUNCTION AND PARAMETER EVALUATION
   W. A.   FOR D.C. SERVOMOTORS. Proceedings of the
                             AIEE, Applications and Industry, January 1956.